bc1352034

HEAT AND MASS TRANSFER WITHIN POROUS BUILDING MATERIALS

By

GRAHAM H. GALBRAITH, BSc MSc

Division of Thermo-Fluids and Environmental Engineering

Department of Mechanical Engineering

University of Strathclyde

Glasgow

A thesis presented for the degree of Doctor of Philosophy in Mechanical Engineering in accordance with the regulations of the University of Strathclyde.

MAY 1992

COPYRIGHT DECLARATION

The copyright of this thesis belongs to the author under the terms of the United Kingdom Copyright Acts as qualified by University of Strathclyde Regulation 3.49. Due acknowledgement must always be made of the use of any material contained in, or derived from, this thesis.

LIST OF CONTENTS

ACKNOWLEDGEMENT

This thesis, and the research studies carried out, could not have been completed without the cooperation of many people, to whom I am most grateful.

I would particularly like to thank my Research Assistant Dr. Zhi Tao, who was a tremendous support to me throughout this work. He provided an excellent 'sounding board' for ideas and patiently performed the many tedious, but highly important, measurements. The typing of this thesis was also carried out by Dr. Tao, who was tolerant of the multitude of re-drafts which were made.

The cooperation of my colleagues, particularly Craig McLean as well as Professor Hugh Simpson is also acknowledged. I value greatly the assistance of Craig McLean who gave much of his time to this work, at the early stages in providing guidance, ideas and encouragement, laterly in reviewing manuscripts. My Head of Division and Project Supervisor Professor Hugh Simpson encouraged me throughout this research and I am grateful for his advice.

The assistance of the Divisional Technicians was also greatly appreciated, most of them being involved in this work at some stage. I would especially like to thank Eric Duncan, the Head Technician of the Division, who was at the receiving end of many urgent calls for help.

The most important support for this work, however, came from my close family. I would like to thank in particular my wife, Caroline, who encouraged me all through my PhD studies, she being positive when I was negative. This thesis would not have been completed without her tolerance and her confidence in my ability.

Finally I would like to express my gratitude to the Science and Engineering Research Council who provided the financial backing to enable this study to be carried out.

ABSTRACT

The thermal and structural performance of building elements can be significantly impaired by the presence of excess moisture. At present, designers have available only simplistic steady-state techniques to predict such effects, for example that presented by Glaser in 1959. These simple models recognise moisture transport in vapour form only and do not allow information on material moisture content to be obtained directly. They are also based on the assumption that the material transport properties are independent of the prevailing environmental conditions, whereas they are in fact complex functions of parameters such as relative humidity.

This research has been carried out to develop a set of model equations which account for both liquid and vapour transfer through porous structures, and which enable material moisture content profiles to be produced. The equations generated in this work are transient and enable the effects of moisture and thermal capacity to be considered. An experimental investigation has also been carried out to produce a methodology which can be used to obtain the required material properties.

These equations and material properties have been combined with realistic boundary conditions to produce a finite difference model which enables simple wall structures to be analysed in terms of temperature, vapour pressure, relative humidity, moisture content and moisture flow rate. The use of this FORTRAN 77 computer code is illustrated by application to traditional and timber-framed wall constructions. The results illustrate the applicability and flexibility of such an approach and confirm the importance of its further development in the future.

LIST OF SYMBOLS

a: volume fraction of air-filled open pore

c: specific heat, kJ/kgK

d: mean pore diameter, m

D: diffusion coefficient, m^2/s

e: specific internal energy, kJ/kg

E: total specific energy, kJ/kg

f: gravitational force, N/kg

F: molecule velocity distribution function, no. of molecules/m^3

g: chemical potential

h: specific enthalpy, kJ/kg

H: heat transfer coefficient, kJ/m^2Ks

i: moment of inertia of unit mass, m^2

I: mass generation rate, kg/m^3s

j: transfer rate, kg/m^2s

k: Boltzmann constant, J/K

L: latent heat of evaporation, kJ/kg

m: mass, kg

M: mole molecular weight

n: number of molecules per unit volume

n_{10}: volumetric concentration of species 1 of a binary mixture

n_{20}: volumetric concentration of species 2 of a binary mixture

p: pressure, N/m^2

q: heat flux, kJ/m^2s

R: gas constant, kJ/kmol K

t: time, s

T: temperature, K

u: moisture content, kg H_2O/kg dry material

v: velocity, m/s

V: wind velocity, m/s

x: coordinate dimension, m

y: ratio of thermal diffusion rate to total diffusion rate

α: transfer coefficient

β: mass transfer coefficient, m/s

δ: boundary layer thickness, m

ϵ: porosity, m^3 void space/m^3 dry material

ζ: length, m

λ: thermal conductivity, kJ/msK

μ: spot or differential permeability, s

$\bar{\mu}$: averaged permeability from cup tests, s

ξ: specific volume, m^3/kg

ρ: density, kg/m^3

σ: stress tensor, kg^2/m^3s^2

τ: effective vapour transfer area factor

υ: tortuosity factor

ϕ: relative humidity, %

χ: volumetric moisture content, kg/m^3

ψ: potential energy, kJ/kg

ω: angular velocity, 1/s

Subscript and Superscript

0: material

1: vapour

2:	liquid water
3:	air
a:	air
D:	diffusion
ei:	environmental
l:	liquid water
p:	filtration
q_cond:	conduction
q_conv:	convection
ri:	radiation
t:	thermal
T:	thermal diffusion
v:	vapour
u:	moisture

LIST OF FIGURES

LIST OF TABLES

LIST OF PLATES

LIST OF APPENDICES

1. INTRODUCTION

For several decades there has been a large volume of research into the physics of moisture movement in porous media. Apart from its significance to many subjects such as petroleum engineering, soil science and microhydrology, etc., it is of great importance in the investigation of heat and moisture transfer within building materials. In building design, a crucial consideration is the prevention of interstitial condensation, which can result in moisture accumulation within building structures. Such an occurrence may cause a deterioration in material performance or even a structural failure of the building fabric[1][2]. This problem has become highlighted with the introduction of non-traditional methods of building, employing materials which are highly sensitive to the presence of moisture.

Since GLASER put forward his interstitial condensation model in 1959[3], many other models have been introduced. They can generally be divided into two categories: a). steady state[1,3,4,5,6];and b). transient (or dynamic)[7,8,9,10].The steady state models are used widely by building technologists and are based on simple FICK's Law theory. They have several important deficiencies as listed below:

- As they are steady state in nature, they are not directly applicable to the non-steady state conditions occurring in the real world.

- They assume moisture transfer in vapour form only and neglect the importance of any form of liquid (or water) transfer.

- The heat flow, and hence the temperature profile, is determined using the simple FOURIER equation, and no coupling between the movement of heat and moisture is included

- They are based on the assumption that condensation will only occur at the point within a composite structure where the actual temperature is below

the local dewpoint temperature. This neglects the process of capillary condensation within materials, which can occur at temperatures above the local dewpoint temperature.

- They assume that a gradient of vapour pressure is the ONLY driving force for moisture transfer, and accordingly apply isothermal material data to non-isothermal conditions.

- They do not enable the moisture content of construction elements to be predicted directly, yet it is the moisture content of materials which affect their thermal and structural performance.

In addition to the above, it has also become clear that although a considerable amount of material data is available for use as input to such models, in most cases the information is confusing or even misleading[11]. This is primarily due to inadequate material specification, insufficient details on material test conditions, and extremely large ranges of values from which to choose[12].

ROWLEY[13] in 1939 was one of the first experimenters to recognize that the use of simple vapour diffusion theory for the transfer of water vapour through porous materials would be inadequate, and suggested that under non-isothermal conditions the flow of heat and mass must be related. It was not until the work of PHILIP & DEVRIES in 1957[14] and DEVRIES in 1958[15] that the inadequacy of applying simple gaseous diffusion, with vapour pressure as the sole driving potential, was clearly demonstrated. Although their efforts were related specifically to soil mechanics, their conclusions are directly applicable to building materials. The transfer equations developed by PHILIP and DEVRIES were obtained by a semi-empirical approach to the problem, and it was not until 1966 that the coupled equations for heat and mass transfer were formalised by LUIKOV[9]. The LUIKOV equations are developed from the basic conservation equations of mass, momentum and energy

and are based on the hydrodynamics and thermodynamics of continuous media. In principal, it is a phenomenological theory in the sense that it employs empirical coefficients to avoid the extreme difficulties in solving the basic conservation equations.

The theory of LUIKOV has been used as the basis of many transient models developed by investigators in this field, some using the theory to its full complexity while others have made many simplifying assumptions.[7][8]

The problem with most of the transient (dynamic) models based on LUIKOV's work, is that although mathematically they appear to adequately handle most moisture transfer problems, there is a lack of experimental data which can be used to validate their accuracy. These published models are generated by theoretical analysis and give little or no experimental results for the empirical coefficients required for their application. This may be due to the extremely long time required for the experiments or be a function of the unreliability of the available experimental techniques which often produce poor results in terms of accuracy and reproducibility. It is also the case that some of the coefficients necessary to apply LUIKOV's theory are impossible to obtain by any of the currently known experimental techniques. Such models are therefore only used by a highly specialised group of researchers, and are in a form which is of little use to a building designer.

As the interstitial condensation problem becomes more widespread, and buildings become more complex, it is clear that the simple FICK's Law models are now inadequate for the needs of Designers.

The aim of this work is to develop a new model which is more accurate than the simple FICK's Law approach, but which is in a form which can be readily used by Designers. This involves the development of a set of equations which account for both vapour and liquid water transport through porous constructions, and which will

enable the actual moisture content of the material elements to be predicted. It is the objective of this work not only to formulate the model itself, but also to develop new experimental procedures which will enable the required material properties to be easily determined.

The generation of this model and associated experimental procedures requires a clear understanding of the moisture transport processes which take place within porous materials. Chapter 2 will develop such an understanding by giving a brief review of the relevant mechanisms of moisture and heat transfer. This leads in Chapter 3 to a review of the mathematical equations and models given in the literature. In Chapter 4 a new set of model equations are developed for application to building constructions, with possible experimental procedures to determine the required transport coefficients presented in Chapter 5. The transport coefficients for a range of seven building materials are determined experimentally in Chapter 6, the results being used to verify the equations. The integrity of the model equations produced is then demonstrated in Chapter 7 by their incorporation into a computer model. The results of this work and recommendations for its further development are then discussed in the concluding Chapter 9 of this thesis.

2. MECHANISMS OF MOISTURE AND HEAT TRANSFER

All building materials are penetrated by a complex pore system which can be filled by air, liquid water and water vapour. To fully describe the movement of moisture it is necessary, therefore, to consider not just the movement of water vapour, but also that of condensed water. Water vapour transfer may occur as a result of molecular diffusion or by filtration motion of the whole moist-air mixture within the pores under a gradient of total pressure. Similarly for liquid transfer, the driving force may be the result of diffusion, capillary absorption and filtration motion within the material as a result of a hydrostatic pressure gradient.

ROSE in 1963[16][17] carried out an experimental investigation to validate the basic ideas of PHILIP & DEVRIES[14], and established the existence of four distinct stages in the wetting of a porous system. These stages can be described in terms of Figure 2.1 as follows:

Stage 1 - Absorption

At very low relative humidities (~0.6%) vapour arriving from the left is not transmitted but absorbed to form a complete absorbed monolayer. Surface diffusion may take place under a two-dimensional spreading pressure.

Stage 2 - Vapour Transfer

This stage involves unimpeded vapour transfer where the vapour behaves as an inert gas. Gaseous molecular diffusion and filtration by pressure gradient are the mechanisms of the transfer process.

Stage 3 - Vapour and Liquid Transfer

This relates to the onset of capillary condensation when vapour will begin to condense within the pores, some of which will eventually fill with water. Consequently, moisture transmission through the material is then possible as a liquid-type flow under the influence of the capillary pressure gradient. This will correspond to a wide range of relative humidities between stage 2 and 3. As most materials will have a broad distribution of pore sizes, the liquid phase will usually be discontinuous and vapour transfer will coexist with liquid transfer. It has been found that at this stage vapour transfer is enhanced by the existence of the liquid phase. This is because the molecules absorbed on the surfaces of the matrix of the medium form bridges or 'islands' between the isolated pores[14][17]. These islands act as short circuits for vapour transfer: vapour condenses on one meniscus of the island and the same amount of liquid (water) evaporates from the other.

Stage 4 - Liquid Transfer

Eventually under high relative humidity conditions the liquid inside the porous media forms a continuous phase. This hydraulic flow may be either fully saturated, or unsaturated, where small air pockets may still be present in the material pores. The transfer process is governed by liquid molecular diffusion, capillary absorption, and filtration by pressure or gravity.

The first stage as described above is generally disregarded in research of this kind as it occurs at relative humidities below those of interest in building studies[18]. Stage three is clearly a highly complex series-parallel system, which cannot be

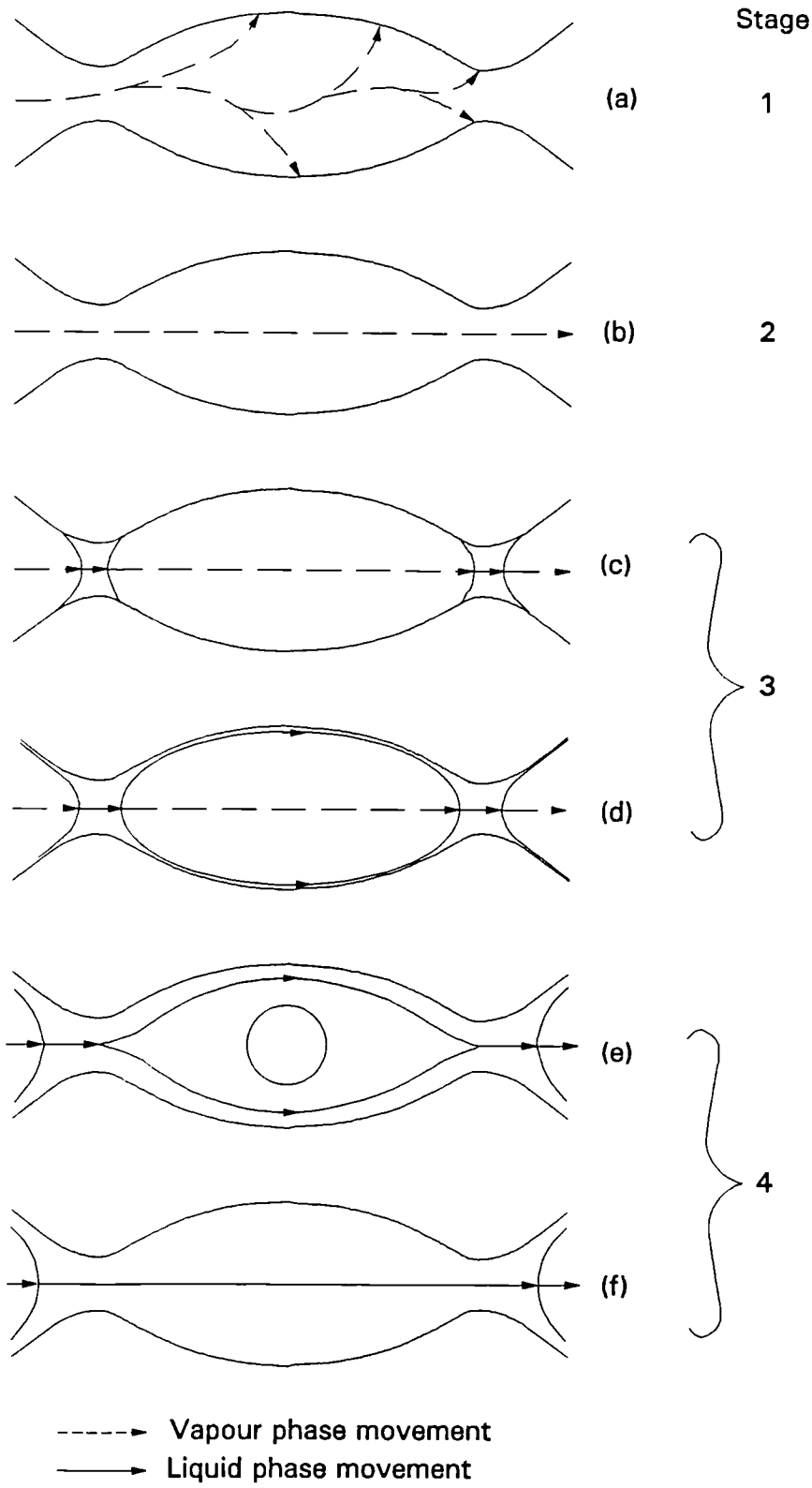

FIGURE 2.1 VARIOUS STAGES IN THE WETTING OF A POROUS MATERIAL

accurately described as either 'liquid' or 'vapour' transfer. This question of terminology is generally handled by using the term 'liquid transfer' to describe the transfer which occurs exclusively in the liquid phase (i.e. stage four); all transfer which involves vapour flow (i.e. stages two and three) is generally designated in literature as 'vapour transfer'. Thus in the absence of liquid continuity, all transfer is regarded as vapour transfer[14].

The liquid phase within the pores of many building materials may also contain salts, and this will further compound an already complex problem[18]. In addition, the possibility of phase change to ice should be included, if the analysis is to be considered as completely rigorous[8]. The influence of dissolved salts and the possibility of freezing is generally neglected as such an analysis would be too complex and would introduce only limited enhancement to the validity of the model.

2.1 Vapour Transfer

2.1.1 Molecular (Concentration) Diffusion

Under isothermal conditions, diffusion of vapour is a process which is governed by concentration gradient and can be described as a type of mixing and balancing process between particles, manifesting itself as an orderly mass transfer.

The diffusion of vapour in air is described by Fick's law as:

$$j_v^D = -D \nabla \rho_v \qquad (2.1)$$

where j_v^D : density of vapour flow rate (kg/m^2s)

D: diffusion coefficient of vapour in air (m^2/s).

ρ_v: vapour concentration (kg/m^3)

In building physics the partial pressure of water vapour in the moist air is often adopted as the basic transport potential. Since water vapour behaves almost as an ideal gas[18] it is possible to apply the relationship:

$$p_v V = m R_v T \quad \text{or} \quad \rho_v = \frac{p_v}{R_v T} \qquad (2.2)$$

Substituting equation (2.2) into equation (2.1) gives:

$$j_v^D = -\frac{D}{R_v T} \nabla p_v + \frac{D p_v}{R_v T^2} \nabla T \qquad (2.3)$$

For isothermal conditions, we may write from equation (2.3) the conventional equation for water vapour diffusion:

$$j_v^D = -\frac{D}{R_v T} \nabla p_v \qquad (2.4)$$

where p_v: water vapour partial pressure (N/m^2)

R_v: gas constant for water vapour, 461.52(J/kgK)

T: absolute temperature (K)

Many empirical expressions for the diffusion coefficient of water vapour in air are given in literature, some examples being given below:

SCHIRMER[19]
$$D = 2.305 x 10^{-5} \left(\frac{T}{273.15} \right)^{1.81} \left(\frac{101323}{p} \right) \qquad (2.5)$$

SHERWOOD[20]
$$D = \frac{0.926 x 10^{-3}}{p} \left(\frac{T^{2.5}}{T + 245} \right) \qquad (2.6)$$

DE VRIES[21]
$$D = 2.17 x 10^{-5} \left(\frac{T}{273.15} \right)^{1.88} \left(\frac{101323}{p} \right) \qquad (2.7)$$

KRISCHER[8]
$$D = 2.39 x 10^{-5} \left(\frac{T}{273.15} \right)^{2.3} \left(\frac{101323}{p} \right) \qquad (2.8)$$

where p is the total barometric pressure (N/m^2)

From the above it is clear that D is dependent both on temperature and total pressure. For the normal range of conditions encountered in building physics, the resulting difference between these expressions is small, and a value for D of 0.000025 m^2/s is generally acceptable[22][23].

Diffusion through a porous material can be considered in a similar fashion to the above, with modifications applied to equation (2.4) to account for the reduced flow area and the tortuosity of the flow path[8][14][15]. Equation (2.4) can therefore be re-written as:

$$j_v^D = -\upsilon a \frac{D}{R_v T} \nabla p_v \qquad (2.9)$$

where υ: tortuosity factor.

a: volume fraction of air-filled open pores

Equation (2.9) is often written as:

$$j_v^D = -D_v \nabla p_v \qquad (2.10)$$

where D_v is the vapour permeability coefficient (kgm/Ns).

The coefficient D_v will not be a constant, but will depend on the moisture content of the porous material, as already outlined. As the amount of liquid water present increases with an increase in moisture content, the space available for pure vapour transfer will decrease, as will D_v. D_v will also be dependent on total pressure and temperature, although this influence will be minimal for normal building studies as previously indicated.

It is important to emphasize that equation (2.10) applies strictly to isothermal conditions. In fact, it is this equation which is the basis of the FICK's Law models, even although they are applied to situations in which a temperature gradient exists. This is clearly incorrect, and where temperature varies through a structure, a modified form of equation (2.3) should be applied as given below:

$$j_v^D = -D_v \nabla p_v + \frac{D_v p_v}{T} \nabla T \qquad (2.11)$$

The temperature gradient term in this equation (2.11) results from the fact that density gradient is the fundamental driving potential for the diffusion process.

2.1.2 Thermal Diffusion

Thermal diffusion is conceptualized as diffusion which is not the result of a density gradient, but which is caused solely by the non-uniformity of the temperature field. The possibility of gas thermal diffusion was discovered in the course of the extension of the kinetic theory to non-equilibrium gases. Kinetic theory uses the famous Maxwell equation to describe the molecule velocity distribution[24]:

$$F = n\left(\frac{M}{2\pi kT}\right)^{\frac{3}{2}} \exp\left[-\frac{MC^2}{2kT}\right] \qquad (2.12)$$

where n: molecule number density, no./m^3

M: molecular mass

C: molecular thermal velocity, m/s

k: Boltzmann constant, J/K

F: the number of molecules per unit volume which have velocity, C, no./m^3.

Because the Maxwell distribution function is for the equilibrium state only, the assumption has been made that equilibrium exists everywhere locally. The above equation clearly indicates that the velocity distribution will not only be affected by the density or concentration n, but also by the temperature T.

Kinetic theory gives the diffusion transfer under a temperature gradient for a binary mixture as[24]:

$$j_1 = -\frac{1}{n_{10} n_{20}} \left[D_{12} \nabla n_{10} + D_T \frac{1}{T} \nabla T \right] \qquad (2.13)$$

where D_{12}: normal concentration diffusion coefficient, kg/ms. (Subscripts 12 means gas 1 diffuses in gas 2.)

D_T: thermal diffusion coefficient, kg/ms

n_{10}, n_{20}: mole fraction or concentrations of the two species. (if n_1, n_2 are the number densities, and $n = n_1 + n_2$, then $n_{10} = n_1 / n$, $n_{20} = n_2 / n$)

In above equation, the first term of the RHS is the normal concentration diffusion and the second term is the contribution of temperature non-uniformity. The thermal diffusion coefficient, D_T, is strongly concentration dependent and is generally considered as temperature independent[25].

For moisture diffusion through porous bodies, if this thermal effect exists at all, a similar equation is expected:

$$j_v^T = -\alpha_v^T \nabla T \qquad (2.14)$$

where α_v^T: vapour thermal diffusivity (kg/msK).

However, there has been little research on the effect of vapour thermal diffusion in building materials. Tests carried out on Glass-Fibre by KUMARAN[26] indicate

that thermal diffusion does have some effect. However, the tests involved temperature differences of around 40^0C across a layer of Glass-Fibre of only 8.55cm thick. Such a high temperature gradient situation is unlikely to be encountered in building applications. The methods currently used by Building Service Engineers for predicting moisture transfer through building structures simply ignore this effect. Some of the existing theoretical models also neglect its effect without giving any clear explanation[8].

2.1.3 Filtration Flow

Under a total pressure gradient, a bulk flow of vapour (or vapour filtration flow) occurs. This will be a dominant flow when the total pressure difference is significant. Due to the extreme complexity of the matrix structure within porous materials, a classical fluid mechanics approach is impossible and instead a vapour filtration coefficient α_v^p is introduced and the flow rate expressed as:

$$J_v^p = -\alpha_v^p \nabla p \qquad (2.15)$$

where α_v^p: filtration coefficient (s).

In building applications, the total pressure difference is often taken as negligible. This is an acceptable assumption, except in cases where severe wind conditions prevail. Vapour filtration flow will therefore be neglected in this work.

2.2 Liquid Transfer

2.2.1 Molecular Diffusion

Liquid transfer through saturated porous media can be expressed using the DARCY law[27] in the form:

$$j_l^D = -\rho_l K \nabla \phi \qquad (2.16)$$

where j_l^D: liquid flux density (kg/m^2s)

ρ_l: water density (kg/m^3)

K: hydraulic conductivity of the medium (m/s)

ϕ: total hydraulic potential (m).

However, for building materials the flow is often unsaturated. It has long been assumed[28], and was confirmed by CHILDS and COLLIS-GEORGE[29], that a modified form of DARCY's law may also hold for the unsaturated flow of liquid water:

$$j_l^D = -\rho_l D_l \nabla \psi \qquad (2.17)$$

In the above equation, the constant K has been replaced by a liquid permeability D_l, which has units of seconds and is a function of the volumetric moisture content of the material. D_l has been found to decrease very rapidly as the moisture content decreases from its saturation value[27]. The hydraulic potential, ψ, in equation (2.17), is expressed in units of m^2/s^2, and is composed of two elements - the gravity potential ψ_g and the matrix potential ψ_m, which is related to the pore water pressure caused by capillary effects. Thus:

$$\psi = \psi_g + \psi_m \qquad (2.18)$$

The matrix potential, ψ_m, can be expressed as:

$$\psi_m = \frac{p_l}{\rho_l} \tag{2.19}$$

where p_l: pore water pressure (N/m^2), proportional to the surface tension of a liquid.

By substituting equations (2.18) and (2.19) into equation (2.17), and applying the relationship $\psi_g = g \cdot z$, then:

$$j_l^D = -D_l \nabla p_l - D_l \rho_l z g \vec{k} \tag{2.20}$$

where g: gravitational constant (m/s^2).

z: height over a reference plane (m).

$\vec{k}$: unit vector in the positive z direction.

2.2.2 Thermal Diffusion

The thermal diffusion effect for liquid, usually called the SORET effect, is generally small compared with that for gas. A salt solution under temperature gradient takes days or months to be balanced while a gas mixture under the same situation would only take a few hours at most. There is no well developed theories for liquid thermal diffusion, and most investigations of this process have been performed using salt solutions combined with salt concentration monitoring. For building applications under normal temperatures, the liquid water thermal diffusion is generally negligible. The equation to express this diffusion in porous bodies can nevertheless be written as:

$$j_l^T = -\alpha_l^T \nabla T \tag{2.21}$$

where α_l^T: liquid thermal diffusivity (kg/msK).

2.2.3 Filtration Flow

In a similar manner to vapour filtration movement, a bulk viscous flow of liquid (or liquid filtration flow) occurs when a total pressure gradient is applied. The flow rate can be obtained by utilizing an experimental liquid filtration coefficient, α_l^p:

$$j_l^p = -\alpha_l^p \nabla p \qquad (2.22)$$

where α_l^p has unit of seconds.

If the total pressure difference is either zero or negligible, the liquid filtration movement is not considered, which is the case for most building applications.

2.3 Total Transfer of Vapour and Liquid

The total moisture transfer as a result of both liquid and vapour flow will clearly be found by simple addition:

$$\begin{aligned} j_{tot} &= j_v + j_l \\ &= (j_v^D + j_v^T + j_v^p) + (j_l^D + j_l^T + j_l^p) \end{aligned} \tag{2.23}$$

For building materials in normal atmospheric conditions, this equation can be simplified by neglecting the thermal diffusion for liquid water and filtration transport, such that:

$$\begin{aligned} j_{tot} &= j_v^D + j_v^T + j_l^D \\ &= -D_v\left[\nabla p_v - \frac{p_v}{T}\nabla T\right] - \alpha_v^T \nabla T - D_l \nabla p_l \end{aligned} \tag{2.24}$$

In this equation D_v, α_v^T and D_l will be functions of the material moisture content and the temperature. For simplicity, the effect of gravity has been omitted, although it is recognized that its influence may not in all cases be negligible[30].

When the vapour thermal diffusion component can be considered small the above equation simplifies to:

$$\begin{aligned} j_{tot} &= j_v^D + j_l^D \\ &= -D_v\left[\nabla p_v - \frac{p_v}{T}\nabla T\right] - D_l \nabla p_l \end{aligned} \tag{2.25}$$

2.4 Heat Transfer

In capillary-porous bodies, the mechanisms of heat transfer are conduction, convection, radiation and phase conversion. Within building materials, radiation heat transfer can be neglected due to the generally low temperature gradients encountered. The importance of heat convection depends on the rate of moisture filtration movement. For the majority of building applications, the Reynolds numbers are considerably less than unity, and the convective heat transfer is thus small in comparison with the conductive component. In consequence, for capillary-porous bodies used as building materials in which temperature differences are small, the transfer of heat is predominantly by heat conduction through the matrix of the media and the multi-phase fluids occupying the pore voids. According to Fourier's law, the rate of heat transfer is expressible as:

$$q_{q\_cond} = -\lambda \nabla T \tag{2.26}$$

where λ is the conductivity of the porous materials, (kw/mK). It is clearly a function of the type of material, its pore distribution and porosity, and also moisture content. As the moisture content increases, the thermal energy storage capacity of the material will also increase.

For dry porous bodies, an increase in porosity ϵ will correspond to a decrease in the thermal conductivity λ. The values of $\lambda = f(\epsilon)$ lie between the conductivity of a pure monolithic (zero porosity) body and that of air.

As mentioned previously, the moisture absorbed by materials will increase the thermal conductivity. KAUFMAN[31], by analysing a large quantity of experimental data on the thermal conductivity of building materials, proposed the following empirical formula:

$$\lambda = \lambda_o \left(1 + \frac{\chi \Delta}{100} \right) \qquad (2.27)$$

where λ_o: thermal conductivity of the perfectly dry material (kJ/msK).

χ: volumetric moisture concentration (kg H_2O / m^3dry material).

Δ: rise in thermal conductivity per one percent of volumetric moisture concentration (m^4/s^2K).

This factor Δ is a function of material density and pore diameter:

$$\Delta = 8.0(1 + \rho^{-0.3}5.7^{-\rho}) + 7.12(d - 0.14)^{0.8}0.05\rho$$

where ρ is the density of the material, g/cm^3 and d is the mean pore diameter (mm).

Temperature is another factor which influences thermal conductivity. DUBNITSKY obtained the following expression for insulating materials, which takes account of the temperature effect[32]:

$$\lambda = \lambda_o + ATue^{-bu} \qquad (2.28)$$

where λ_o: thermal conductivity of the perfectly dry body at 0^0C (kJ/msK).

A, b: constants determined experimentally

u: moisture content (kg H_2O/kg dry material).

As previously mentioned, convective heat transfer is often neglected for building applications due to its small magnitude compared with heat conduction. However, for hygroscopic materials, where a considerable quantity of liquid filtration movement may take place at high moisture contents, there can be a large contribution from capillary suction. Convection will then become a significant factor in heat transfer. Designating h_i as the enthalpy of the $i-th$ component (kJ/kg), the convective heat transfer q_{q_conv} can be expressed as:

$$q_{q\_conv} = \sum_{i=1}^{n} j_i h_i \tag{2.29}$$

If liquid water, water vapour and air are present inside the material, then the above equation becomes:

$$q_{q\_conv} = j_v h_v + j_l h_l + j_a h_a \tag{2.30}$$

Combining equation (2.26) and equation (2.30) gives the total heat transferred j_q as:

$$\begin{aligned} q &= q_{q\_cond} + q_{q\_conv} \\ &= -\lambda \nabla T + j_v h_v + j_l h_l + j_a h_a \end{aligned} \tag{2.31}$$

3. A REVIEW OF COMBINED EQUATIONS FOR HEAT AND MASS TRANSFER

3.1 Heat and Mass Flux

In the previous chapter, the transfers of liquid and vapour within a porous material were classically analysed as separate processes. However, in the real world mass transfer of both liquid and vapour will be inter-related to each other, and also to the energy transfer taking place. Mass flow will convect thermal energy, liquid/vapour phase change will involve latent heat, and the temperature gradient may induce mass flow (thermal diffusion). To describe mathematically this problem, LUIKOV[9][10] and others have used the theory of irreversible thermodynamics[8][33]. Unlike the classical theory of molecular transfer, this states that any single flux component, j_i, is not determined solely by the action of one corresponding thermodynamic force or potential, but by the action of all of the potentials involved.

Assuming uniformity of total pressure and neglecting gravity effects, the process of combined heat and mass transfer in porous materials can be described in terms of a flux of heat, of water vapour and of liquid water. ONSAGER's theory[34] assumes that these three fluxes must correspond to three generalised driving potentials, and that each flux must be a linear combination of the three potentials. The most logical potentials to choose in this case must therefore be:

temperature, T, for heat transfer

water vapour pressure, p_v, for vapour transfer

capillary water pressure, p_l, for liquid transfer

In the above it is assumed that the temperature will be identical for each phase at any given time and location.

The flux can therefore be described by phenomenological equations of the form:

$$\begin{aligned} j_q &= \alpha_{11}\nabla T + \alpha_{12}\nabla p_l + \alpha_{13}\nabla p_v \\ j_v &= \alpha_{21}\nabla T + \alpha_{22}\nabla p_l + \alpha_{23}\nabla p_v \\ j_l &= \alpha_{31}\nabla T + \alpha_{32}\nabla p_l + \alpha_{33}\nabla p_v \end{aligned} \qquad (3.1)$$

In the terminology of irreversible thermodynamics the "α" coefficients are called kinetic coefficients.

If it is assumed that local thermodynamic equilibrium exists between liquid and vapour, then the variables p_v and p_l will be thermodynamically dependent on each other. Application of the fundamental laws of thermodynamics leads to the formulation of the well-known Kelvin equation (Appendix One):

$$p_l - p = \frac{RT}{\gamma_l}\ln\left(\frac{p_v}{p_{vs}(T)}\right) = \frac{RT}{\gamma_l}\ln\phi \qquad (3.2)$$

where p: total pressure (N/m^2).

p_{vs}: saturation vapour pressure (N/m^2).

R: general gas constant (kJ/kmol K).

γ_l: molar volume of water (18×10^{-6} m^3/mol).

ϕ: relative humidity.

Using this equation, p_l can be re-expressed in terms of p_v and vice-versa. The number of independent potentials describing the fluxes can therefore be reduced to two, in this case temperature and either vapour or capillary pressure. This leads to the description of liquid and vapour flux by the same potential, the total flux of moisture, j, being the sum of j_v and j_l. The system of equations can now be given as:

$$j_q = \alpha_{11} \nabla T + \alpha'_{12} \nabla p_v$$

$$j = (\alpha_{21} + \alpha_{31}) \nabla T + \alpha'_{22} \nabla p_v \qquad (3.3)$$

or

$$j_q = \alpha_{11} \nabla T + \bar{\alpha}_{12} \nabla p_l$$

$$j = (\alpha_{21} + \alpha_{31}) \nabla T + \bar{\alpha}_{22} \nabla p_l \qquad (3.4)$$

As there is an absence of experimental techniques which can be used to measure the pore capillary pressure p_l, equation (3.3) is a more practical form of description.

It is also possible to relate vapour pressure, p_v, to material moisture content, u, by the use of the moisture retention curve, or sorption isotherm. This relationship can be experimentally obtained by allowing samples to reach equilibrium for a range of known atmospheric conditions of temperature and relative humidity (or vapour pressure). In this situation the moist air within the unfilled pore space must have a partial vapour pressure equal to that of the surrounding air.

The shape of the sorption isotherm relating u to p_v or ϕ, can vary depending on the type of vapour (adsorbate) and for different solids (adsorbent). BRUNAUER, EMMETT, and TELLER[35] have grouped sorption isotherms into five different classes as shown in Figure 3.1.For moisture flow within porous hygroscopic building materials there is some disagreement concerning the type of sorption isotherm which should be formed. GREGG and SING[36] predicted theoretically that a type IV isotherm should be produced, while HANSEN[37] stated that S-shaped type II isotherms were almost always formed for porous building materials. Experimental evidence[35][36][37[38][39]suggests that Hansen's observations are correct and building materials will exhibit a sigmoid type II shape. Figure 3.2 show a typical sorption isotherm for a porous hygroscopic building material, with the relevant sorption effects

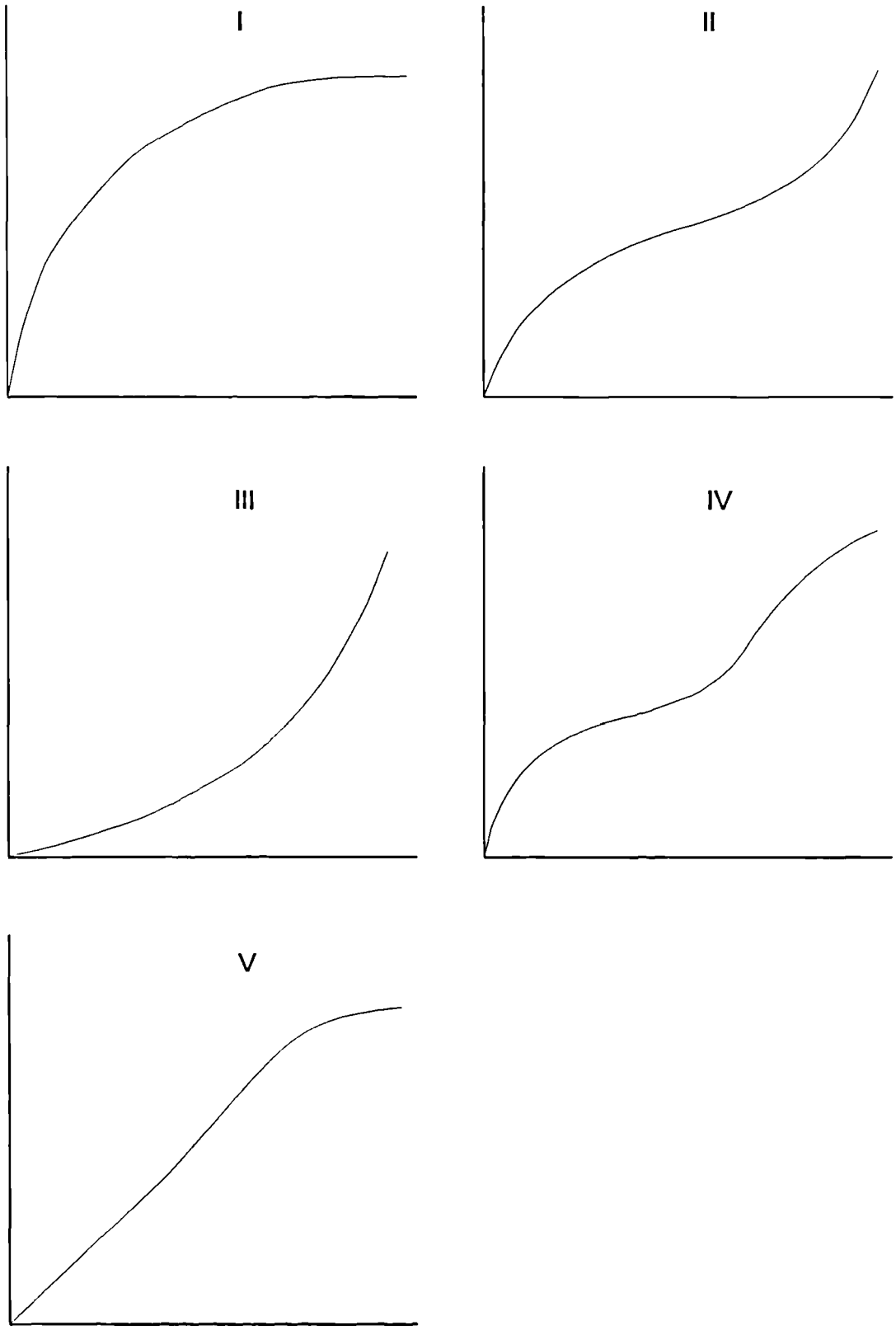

FIGURE 3.1 SHAPES OF THE SORPTION ISOTHERMS

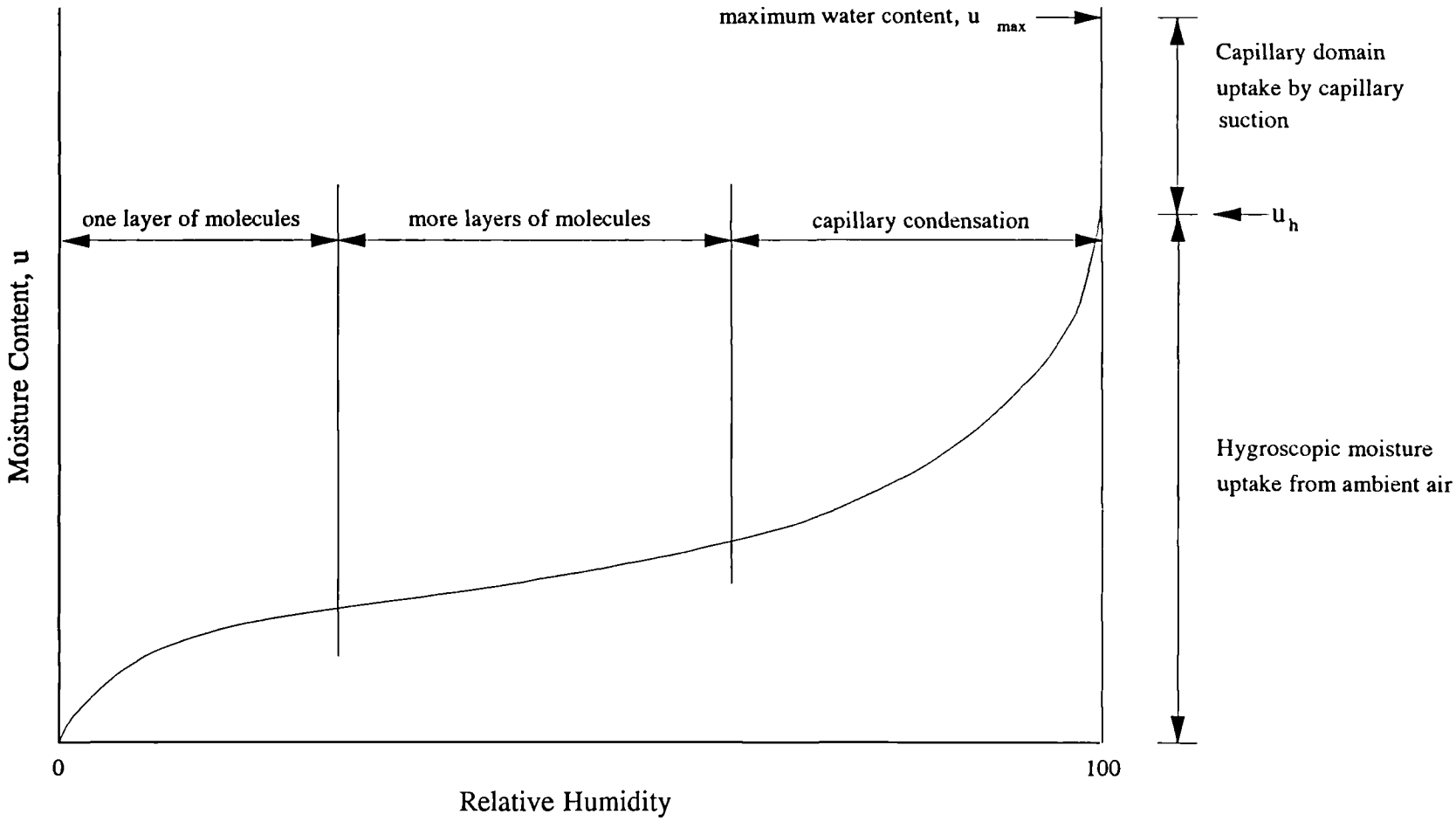

Fig.3.2 Typical Sorption Isotherm Curve

indicated. At 100% relative humidity, the curve shows a vertical rise to full water saturation, u_{max}, the maximum moisture content that a material can acquire in suction, i.e. in contact with liquid water.

Associated with the sorption isotherm there is a hysteresis phenomena between the process of *"wetting"* (absorption) and *"drying"* (desorption)[36][37][38][39]. This effect can be significant and many different theories have been proposed to explain its occurrence. Certain authors have suggested that it may not be an actual hysteresis effect, but instead may be a consequence of the time and measurement boundary conditions applied[40]. Nevertheless, for practical calculations, the averaged values between the absorption and desorption will give sufficiently accurate results[41]. If the average values are used, the sorption isotherm can be represented by a mathematical function such that

$$u = f(p_v, T) \tag{3.5}$$

By application of this equation, as well as the Kelvin equation, the flux expressions for moisture transfer can be re-expressed using any of the variables below:

T : temperature u : moisture content

p_v : partial vapour pressure p_l : capillary pressure

This represents six possibilities as follows:

$$(p_v, T);\ (p_v, u);\ (p_v, p_l);\ (u, T);\ (p_l, T);\ (u, p_l)$$

The heat and moisture flux equations can be formulated as a linear combination involving any of the above couples. The coefficients of the equations in each case will be different, and it is therefore important to know which model was used for measurement when using data in a calculation.

3.2 Conservation Equation

The equations for the conservation of liquid and vapour mass can be expressed as:

$$\frac{\partial \rho_0 u_l}{\partial t} = -\nabla \cdot j_l + I_l \qquad (3.6)$$

$$\frac{\partial \rho_0 u_v}{\partial t} = -\nabla \cdot j_v + I_v \qquad (3.7)$$

where ρ_0: material dry density, kg/m^3.

u_l: liquid content (kg H_2O/kg dry material).

u_v: vapour content (units as u_l).

I_l: liquid water source term, kg/m^{3}s.

I_v: vapour source term, kg/m^{3}s.

I_l describes the increase of water content by condensation, I_v describes the increase in vapour content by evaporation.

$$I_l + I_v = 0 \qquad (3.8)$$

and by addition of equations (3.6) and (3.7)

$$\frac{\partial \rho_0 u}{\partial t} = -\nabla \cdot j \qquad (3.9)$$

In equation (3.9), u is the overall moisture content per unit mass of material, and j is the moisture flux as before.

In a similar manner for energy conservation

$$\frac{\partial \rho_0 ue}{\partial t} = -\nabla \cdot \dot{q} \qquad (3.10)$$

where u: moisture content (liquid+vapour), kg moisture/kg dry material

e: internal energy, kJ/kg

q: heat flux, kw/m^2

The combination of equations (3.10) and (3.9) represent the complete conservation laws for moisture and heat flow in porous building materials. While these equations themselves are simple, the difficulty lies in the expression of the fluxes j and q. Many different formulations have been proposed for j and q involving a variety of driving potentials (see previous section). This has led to equations in the literature which, although identical in structure, appear very different. This has created considerable confusion and often renders material data obtained by one researcher of no direct value as input to a model proposed by another. It is this fact more than any other which has hindered progress towards an accurate model which can be passed from the research community into building design practice.

3.3 Review of Relevant Equations in Literature

Constantly monitoring the process of mass and heat transfer inside a wall structure is very difficult due to the extreme complexity in material microscopic-level structure and the interactions between vapour, gas, liquid (water), capillaries, and solid matrix. In order to overcome these difficulties in the theoretical analysis of moisture transfer, porous bodies are often taken as isotropic, homogeneous and continuous, i.e., the actual porous medium is replaced by an ideal continuum which is a structureless substance. Kinematic and dynamic variables, and the state parameters which are continuous functions of spatial coordinates and time, can be assigned to any point. With this simplification the classical conservation equations of mass, momentum and energy can then be constructed. Luikov[9][10] proposed a set of conservation equations for each phase inside the porous media but the equations were difficult to solve as they required a detailed quantitative description of the interaction between components in each phase and between phases.

Simplification of such equations is therefore required. Because the process of transfer in porous bodies is very slow, the momentum equation can be simplified as Darcy's equation (see Section 2.2). Also by neglecting the gravitational force, all terms related to gravity and inertia in the energy equation can be ignored. Luikov in his work relates the flow rate j with three driving forces as $j = \alpha_u \nabla \cdot u + \alpha_T \nabla \cdot T + \alpha_p \nabla \cdot p$, where u is moisture content of the porous media; T is the temperature and p the total pressure. α_u is moisture mass diffusivity, α_T is the thermal mass diffusivity and α_p is the filtration motion (or the so-called viscous flow) diffusion coefficient. The basic conservation equations are then developed by Luikov to become:

$$\frac{\partial T}{\partial t} = \alpha \nabla^2 T + \epsilon_{12} \frac{L}{c} \frac{\partial u}{\partial t} \qquad (3.11)$$

$$\frac{\partial u}{\partial t} = \alpha_m \nabla^2 u + \alpha_T \nabla^2 T + \alpha_{pp} \nabla^2 p \qquad (3.12)$$

$$\frac{\partial p}{\partial t} = \alpha_p \nabla^2 p - \epsilon_{12} \frac{1}{C_\alpha} \frac{\partial u}{\partial t} + \alpha_p \frac{p}{T} \frac{\partial T}{\partial t} \qquad (3.13)$$

where α is the thermal diffusivity; L is the latent heat of evaporation; ϵ_{12} is the phase conversion factor; c is the specific heat of the porous body; C_α is a coefficient describing the properties of air in the process of transfer of a vapour-gas mixture.

In the energy equation (3.11), the viscous flow convection term has been neglected as in the majority of cases moisture transfer in capillary-porous bodies is associated with a Reynolds number which is considerably less than unity, though no definition for Reynolds number is specified.

Solutions are obtainable for this set of equations using numerical analysis, if all the coefficients are known from experiment.

At the same period of time as Luikov's work, similar equations were derived by Philip and De Vries[14] and De Vries[15].

In Luikov's theory, every coefficient has a definite physical meaning. However, they are not always easy to determine and, in fact, some are impossible to obtain. The first difficulty is the phase conversion factor ϵ_{12}. According to Luikov's definition, ϵ_{12} is:

$$\epsilon_{12} = \frac{\alpha_{uv}}{\alpha_u} = \frac{\text{vapour diffusivity}}{\text{total diffusivity of vapour \& liquid}} \qquad (3.14)$$

That is to say, ϵ_{12} is the ratio of vapour transfer rate over the total moisture transfer rate including vapour and liquid in the porous body. It cannot be defined

without a knowledge of individual vapour and liquid flow coefficients. However, in reality, it is very difficult to distinguish vapour transfer from the total moisture transfer, and for the hygroscopic region the moisture transfer is always coupled with vapour and liquid transfer. Some confusion may have arisen here as many authors simply take the total moisture transfer (RH $<98\%$) as the vapour flow[7][8][41]. This assumes a unit phase conversion factor. Thus a method for the determination of individual vapour and liquid water flow coefficients needs to be developed if the phase conversion factor is to be used.

The second difficulty is the coefficient C_α. Luikov defines C_α as:

$$C_\alpha = \frac{\epsilon a_t M}{R \rho_0} \tag{3.15}$$

where ϵ: porosity of the porous medium, (m^3/m^3)

a_t: portion of the void space in porous medium occupied by the vapour-air mixture,

M: mean molar molecular weight of the vapour-air mixture.

This coefficient is clearly a function of the phase conversion factor due to the presence of the term a_t in its definition.

Despite all of these difficulties, Luikov's approach has been the fundamental theory for the investigation of heat and mass transfer in a capillary-porous body. Over the years it has been constantly used and modified. Some authors have complicated Luikov's theory by considering more influencing factors in the basic conservation

equation, e.g. often the viscous flow heat convection term is included in the energy conservation equation. Others have made additional assumptions to simplify Luikov's theory and have produced solutions which are less accurate but more easily handled.

Kohonen[7] presents a complete theory to predict moisture and heat movement in wall structures. Based on Luikov's fundamental theory, Kohonen introduced the following major modifications:

1) utilization of volume averaging theorem.

In Luikov's theory, porous media are considered as isotropic, homogeneous and continuous, i.e.,the actual multi-phase porous medium is replaced by an ideal continuum which is a structureless substance. This means that kinematic and dynamic variables, and the state parameters that are continuous functions of the spatial coordinates and time, can be assigned to any point. This, however, is not an accurate physical assumption because of the complex matrix structure of porous media. BEAR[42] introduces the concept of REV (Representative Elementary Volume) associated with every point of porous media. According to the volume averaging theorem, the values of any kinematic and dynamic variables assigned to any point are not the values at that point but rather average values of variables over REV. Kohonen in his model applies basic volume averaging theorems to all three classic conservation equations and thus every term in the equations is an averaged value rather than local point value as in Luikov's theory.

2) viscous flow convection included in the energy equation.

In developing his theory, Luikov states that this convection term is small in comparison with the conductive term, provided the Reynolds number is less than 20 when there is an absence of filtration motion. For most cases of moisture transfer, the Reynolds numbers are less than unity, although no clear definition for Reynolds number is specified.

Kohonen includes the convection term, and this leads to an extra term in the energy equation, $\sum \nabla \cdot < h_k j_k >$, where <> indicates volume averaging and j_k is the so-called viscous flow. As indicated by Darcy's equation this flow is directly proportion to total pressure gradient. This suggests that where there is either no total pressure gradient or a small total pressure gradient the convection term can be ignored, while for other cases it is necessary to add the term to the energy equation.

Kohonen's complete model is naturally much more complicated than Luikov's and it requires many experimental coefficients before there is any hope of a solution, which in turn involves a great deal of experimental work and an extremely long experimental period. In Kohonen's presentation, however, there is little experimental data given, except some rather schematic drawings. Moreover, the phase conversion factor is used in this model. Kononen merely mentioned the name for the experimental technique as the wet or dry cup method, without either presenting any experimentation or experimental data (see section 6.1.1.for a description of the 'cup' method).

While Luikov, Kohonen and several others have described moisture transfer using temperature and moisture content as the driving forces, others researches have chosen different potentials (see Section 3.1).

One of the simplest models was presented by Ann-Charlotte Anderson[8]. In this model, the total pressure influence is neglected which is equivalent to neglecting filtration movement, i.e. no viscous flow, and the temperature field is also assumed steady state and linear. The solution thus involves only the moisture transport equation. The driving forces have been chosen to be the vapour and liquid capillary pressure.

$$\frac{\partial u}{\partial t} = \frac{\partial}{\partial x}\left(D_{vp} \frac{\partial p_v}{\partial x} \right) + \frac{\partial}{\partial x}\left(D_{lp} \frac{\partial p_l}{\partial x} \right) \qquad (3.16)$$

where p_v: vapour pressure,

p_l: liquid pressure,

D_{vp}: vapour diffusivity in porous medium,

D_{lp}: liquid diffusivity in porous medium.

The two pressures are related by Kelvin's equation. Therefore with knowledge of D_{vp} and D_{lp} together with boundary conditions of either p_v or p_l, this partial differential equation is simple to solve.

However the vapour diffusivity D_{vp} is evaluated in this model by the standard cup method and the vapour diffusivity thus obtained is actually the moisture diffusivity.

Although only a limited number of models have been reviewed, many more papers have been published over the decades to predict moisture and heat transfer in porous media and building structures. Ignoring all the differences in techniques used, they all involve application of the conservation equations combined with experimental coefficients. In this way it is possible to eliminate consideration of the microscopic level complexity of porous media. Setting up a theoretical model is

comparatively easy. The difficulty arises with the description of the vapour, liquid water and energy flux terms and the determination of the required experimental coefficients. It is well known that obtaining building material properties requires an extremely long time period, and results may differ from material to material, reproducibility being not always possible even for the same kind of material. This is the main reason why there is little data available on the experimental coefficients used in the models, although there is a great deal of literature on the subject. It is clear that the number of coefficients used and the complexity of obtaining them have to be the crucial factor for consideration when developing a new model for use by designers.

In the next chapter, the conservation equations which will be used in this work are formulated. These equations are similar to those given by other authors such as Luikov. The main difference lies in the simplifying assumptions which are made to avoid the use of indeterminate coefficients. In these equations the liquid and vapour flux terms are not combined to give a total moisture flux, but are retained as individual transfer rates. To solve these equations will require individual liquid and vapour transfer coefficients to be determined experimentally for materials, which up till now has not been achieved. The mathematical description of the individual mass fluxes, and the experimental methods used to obtain values for the transfer coefficients are the subject of Chapter 5.

4. DEVELOPMENT OF APPROPRIATE HEAT AND MASS CONSERVATION EQUATIONS

In the following analysis, consideration will be given to a capillary-porous body in which all temperatures are above freezing point with the bound substances being only in the form of water, vapour and inert gas (air). Within the equations developed, the suffix 1 will be used to denote moisture in vapour form, suffix 2 for liquid water, suffix 3 for inert gas and suffix 0 will refer to the properties of a perfectly dry porous body.

4.1 Continuity Equation

For a fixed control volume, the mass conservation equation can be expressed as:

$$\frac{\partial(\rho_0 u_i)}{\partial t} = -\nabla \cdot j_i + I_i \qquad (4.1)$$

where u: substance content, kg/kg dry material

ρ: density, kg/m^3

j: transfer rate, kg/m^{2}s

I: generation rate, kg/m^{3}s.

In equation (4.1) and all subsequent equations, the summation convention is applied, e.g. $j_i = \sum_{k=0}^{3} j_k$.

If no chemical reaction exists, $I_3 = 0$, u_0 is unity and j_0 is zero. Because only temperature above freezing point is considered, $I_1 = -I_2$.

Equation (4.1) can be summed to give:

$$\frac{\partial(\rho_0 u)}{\partial t} = -\nabla \cdot j \qquad (4.2)$$

where $u = u_i, j = j_i$

4.2 Energy Equation

The energy conservation equation is often written in a form similar to that for mass conservation (4.1) as[9]:

$$\frac{\partial(\rho_0 u_i h_i)}{\partial t} = -\nabla \cdot (q_{q\_cond} + h_i j_i) = -\nabla \cdot (q_{q\_cond} + q_{q\_conv}) \qquad (4.3)$$

In developing the above equation (4.3), it has been assumed that momentum and gravitational effects are negligible. The LHS of equation (4.3) is the rate of change of the enthalpy within a control volume including material matrix, and all components in every phase. The RHS of equation (4.3) expresses the exchange rate of energy on the surfaces of the control volume. The first term is the heat conduction while the second is the enthalpy exchange caused by actual molecular displacement under diffusion.

Designating c_i as the isobaric specific heat,

$$c_i = \left(\frac{\partial h_i}{\partial T}\right)_{p_i} \qquad (4.4)$$

$$\text{or} \quad h_i = \int_{T_0}^{T} c_i dT \qquad (4.5)$$

Equation (4.3) then becomes:

$$(c_i \rho_0 u_i)\frac{\partial T}{\partial t} + h_i \frac{\partial(\rho_0 u_i)}{\partial t} = -\nabla \cdot q_{q\_cond} - j_i c_i \nabla T - h_i \nabla \cdot j_i \qquad (4.6)$$

Utilizing equation (4.1) for i=3, and $c = c_i u_i$

$$c\rho_0\frac{\partial T}{\partial t}+h_1\frac{\partial(\rho_0 u_1)}{\partial t}+h_2\frac{\partial(\rho_0 u_2)}{\partial t}$$

$$=-\nabla\cdot q_{q\_cond}-j_i c_i\nabla T-\sum_{i=1}^{2}h_i\nabla\cdot j_i \qquad (4.7)$$

Equation (4.7) is the basic form of the energy conservation equation. The difficulty in solving it comes from the terms of density variation with time, because it is necessary to know the rate of change of individual substance concentrations and the rate of phase conversion. Assumptions have to be made to make this equation solvable. This leads to the energy equation being re-written into the following two forms, depending upon the situation under consideration.

4.2.1 Hygroscopic Materials

For hygroscopic materials, the moisture within porous materials will be mainly in the form of liquid water at medium or high relative humidities. That is to say, $u_2 \gg u_1$ and $u_2 \cong u = u_2 + u_1$.

From the continuity equation (4.1) we may write:

$$\frac{\partial(\rho_0 u_1)}{\partial t}=-\nabla\cdot j_1+I_1 \qquad (4.8)$$

$$\frac{\partial(\rho_0 u_2)}{\partial t}=-\nabla\cdot j_2+I_2 \qquad (4.9)$$

Subtracting equation (4.9) from (4.8) and rearranging gives:

$$I_1=\frac{1}{2}\left[\frac{\partial(\rho_0 u_1)}{\partial t}-\frac{\partial(\rho_0 u_2)}{\partial t}+\nabla\cdot j_1-\nabla\cdot j_2\right]$$

$$=\frac{1}{2}\left[\frac{\partial[\rho_0(u_1-u_2)]}{\partial t}+\nabla\cdot(j_1-j_2)\right] \qquad (4.10)$$

Given that $u_2 \gg u_1$, then

$$\rho_0(u_1 - u_2) \cong -\rho_0 u_2 = -\rho_0 u$$

Equation (4.10) can thus be simplified as:

$$I_1 = \frac{1}{2}\left[-\frac{\partial(\rho_0 u_2)}{\partial t} + \nabla \cdot (j_1 - j_2) \right]$$

$$= \frac{1}{2}\left[-\frac{\partial(\rho_0 u)}{\partial t} + \nabla \cdot (j_1 - j_2) \right] \qquad (4.11)$$

From equation (4.2) given that:

$$-\frac{\partial(\rho_0 u)}{\partial t} = \nabla \cdot j = \nabla \cdot j_1 + \nabla \cdot j_2$$

then equation (4.11) is simplified as:

$$I_1 = \nabla \cdot j_1 \qquad (4.12)$$

The above relationship will introduce a substantial error when the vapour content is of the same order of magnitude to that of liquid water. This will be the situation when the relative humidity is low or the materials are highly non-hygroscopic. Another case may be where the moisture transfer is solely due to the temperature gradient.

The energy equation (4.7) can be modified by application of the equations of continuity to give:

$$c\rho_0 \frac{\partial T}{\partial t} = -\nabla \cdot q_{q\_cond} - j_i c_i \nabla T + L I_1 \qquad (4.13)$$

where L: latent heat of liquid water vaporization, kJ/kg

Substituting equation (4.12) into the energy equation (4.13) gives:

$$c\rho_0 \frac{\partial T}{\partial t} = -\nabla \cdot q_{q\_cond} - j_i c_i \nabla T + L \nabla \cdot j_l \qquad (4.14)$$

The above equation presents no great difficulty in analysis if it is possible to separate experimentally liquid and vapour flow rates. Thus the final set of governing equations are:

$$\frac{\partial(\rho_0 u)}{\partial t} = -\nabla \cdot j \qquad (4.2)$$

$$c\rho_0 \frac{\partial T}{\partial t} = -\nabla \cdot q_{q\_cond} - j_i c_i \nabla T + L \nabla \cdot j_l \qquad (4.14)$$

$$j = j_i = j_i(p_l, T) \qquad (4.15)$$

$$q_{q\_cond} = \lambda \nabla T \qquad (4.16)$$

$$u = u(p_l, T) \qquad (4.17)$$

The above equations (4.14) to (4.17) are similar to those developed by Luikov and applied in his work.

4.2.2 Non-Hygroscopic Materials

For highly non-hygroscopic materials, the content of vapour and liquid water will be comparable and thus the assumption of (4.12) will be not valid. However, an alternative assumption can be made related to $\rho_0 u_l$, the mass of vapour per unit volume of material. The volume of the gaseous phase will be far greater than that of liquid water, i.e.,the whole void of the materials are mainly occupied by vapour. If ϵ is the porosity of the material then $\rho_0 u_l = \epsilon \rho_l$, thus:

$$\frac{\partial(\rho_0 u_1)}{\partial t} = \epsilon \frac{\partial \rho_1}{\partial t} \tag{4.18}$$

If the perfect gas law is applicable to vapour, then

$$\frac{\partial \rho_1}{\partial t} = \frac{M_1}{RT}\frac{\partial p_1}{\partial t} - \frac{M_1 p_1}{RT^2}\frac{\partial T}{\partial t} \tag{4.19}$$

For the above assumption, u_2 must equal the total moisture content minus the vapour content, $u_2 = u - u_1$. Thus:

$$\frac{\partial(\rho_0 u_2)}{\partial t} = \frac{\partial(\rho_0 u)}{\partial t} - \frac{\partial(\rho_0 u_1)}{\partial t} \tag{4.20}$$

In above equation, u is a function of vapour pressure and temperature:

$$\frac{\partial u}{\partial t} = \left(a_u^T \right) \left(\frac{\partial p_1}{\partial t} \right) + \left(a_u^{p_1} \right) \left(\frac{\partial T}{\partial t} \right) \tag{4.21}$$

where $a_u^T = (\partial u / \partial p_1)_T$: the slope of the sorption isotherm curve.

$a_u^{p_1} = (\partial u / \partial T)_{p_1}$: obtainable with isotherms of different temperatures.

Substituting equations (4.18), (4.19) and (4.20) into equation (4.7) gives:

$$a_k^T \frac{\partial T}{\partial t} + a_k^{p_1} \frac{\partial p_1}{\partial t} = -\nabla \cdot q_{q\_cond} - j_i c_i \nabla T + \sum_{i=1}^{2} h_i \nabla \cdot j_i \tag{4.22}$$

where $a_k^T = c\rho_0 - L\epsilon\frac{M_1 p_1}{RT^2} + h_2\rho_0 a_u^{p_1}$ (4.23)

$$a_k^{p_1} = L\epsilon\frac{M_1}{RT} + h_2\rho_0 a_u^T \quad (4.24)$$

Then the system of conservation equations are:

$$\frac{\partial(\rho_0 u)}{\partial t} = -\nabla \cdot j \quad (4.2)$$

$$a_k^T\frac{\partial T}{\partial t} + a_k^{p_1}\frac{\partial p_1}{\partial t} = -\nabla \cdot q_{q\_cond} - j_i c_i \nabla T + \sum_{i=1}^{2} h_i \nabla \cdot j_i \quad (4.22)$$

$$j = j_i = j_i(p_1, T) \quad (4.15)$$

$$q_{q\_cond} = \lambda \nabla T \quad (4.16)$$

$$u = u(p_1, T) \quad (4.17)$$

This completes the set of partial differential equations for the situation where the mass of vapour is comparable with that of liquid water.

Equations (4.2), (4.14), (4.15), (4.16), (4.17) and (4.22) will be used in the computer simulation of the phenomenon of moisture transfer within building structures.

The main difficulty with the application of these equations becomes the experimental determination of the values for the vapour and liquid transfer coefficients. This problem, which is the main factor which renders most models unusable, is discussed in the following chapter.

5. DETERMINATION OF THE MASS FLUX FOR INDIVIDUAL COMPONENTS

Solution of the set of governing equations outlined in Chapter 4 involves the determination of the transport flux of vapour, liquid water and inert gas individually. This introduces considerable experimental difficulties as liquid water flow and vapour flow are always coupled, and conventional techniques allow only the total moisture transfer to be measured. New theories are therefore required to develop a way to separate liquid water and vapour flows.

5.1 Vapour and Liquid Water Flux

If the total pressure field is uniform, and the effect of thermal diffusion is neglected, then the diffusion flux for moisture transfer through a material, j, can be expressed as:

$$\begin{aligned} j &= j_1 + j_2 \\ &= -D_1 \nabla \rho_1 - D_2 \nabla p_2 \end{aligned} \tag{5.1}$$

If vapour is assumed to behave as an ideal gas, then the vapour transfer rate, j_1 of equation (5.1) becomes (see equation (2.3)):

$$j_1 = -D_1 \nabla \rho_1 = -\frac{D_1}{R_v T} \nabla p_1 + \frac{p_1 D_1}{R_v T^2} \nabla T \tag{5.2}$$

By utilizing the Kelvin's equation,

$$p_2 = p + R_v T \rho_2 \ln \frac{p_1}{p_s} \tag{5.3}$$

along with the Clausius Clapeyron equation[43]:

$$\frac{dp_1}{dT} = \frac{L}{T[\xi_1 - \xi_2]} \tag{5.4}$$

the gradient of p_2 becomes:

$$\nabla p_2 = \frac{R_v T \rho_2}{p_1} \nabla p_1 + R_v \rho_2 \left[\ln \phi - \frac{L}{R_v T} \right] \nabla T \tag{5.5}$$

where $\phi = p_1 / p_s$: the relative humidity.

L: the latent heat of liquid water vaporization, kJ/kg.

Thus equation (5.1) is changed to be:

$$\begin{aligned} J &= J_1 + J_2 \\ &= -\left(\frac{D_1}{R_v T} + \frac{D_2 R_v T \rho_2}{p_1} \right) \nabla p_1 - \left[D_2 R_v \rho_2 \left(\ln \phi - \frac{L}{R_v T} \right) - \frac{p_1 D_1}{R_v T^2} \right] \nabla T \end{aligned} \tag{5.6}$$

Under isothermal conditions, the above equation is simplified to become:

$$J = -\left(\frac{D_1}{R_v T} + \frac{D_2 R_v T \rho_2}{p_1} \right) \nabla p_1 \tag{5.7}$$

From isothermal permeability values, the moisture flux could be expressed as:

$$j = -\mu \nabla p_1 \tag{5.8}$$

where μ: spot or differentail permeability, (s).[12][23][46]

Equations (5.7) and (5.8) give:

$$\mu = \frac{D_1}{R_v T} + \frac{D_2 R_v T \rho_2}{p_1}$$

$$= \frac{D_1}{R_v T} + \frac{D_2 R_v T \rho_2}{\phi p_s} \qquad (5.9)$$

In equation (5.9), μ, D_1 and D_2 are all functions of temperature and vapour pressure or relative humidity.

The vapour transfer coefficient in the above equation, D_1, differs from that of vapour transfer in bulk air, D, due to the space confinement for transfer and the complex structure of the capillaries. D is a function of temperature and total pressure and so is constant for isothermal conditions under a constant total pressure (see Section 2.1.1). D_1 and D are related to each other by the tortuosity and air content as[14][44]:

$$D_1 = D \upsilon a \qquad (5.10)$$

where υ: tortuosity of the material

a: air content of material, m^3/m^3.

For a certain volume of material, as the relative humidity increases, the formation of liquid water within the pores will reduce the tortuosity and the air content. This reduction however is a very complex phenomenon related to capillary structure and the moisture content. Considering a cross-section, A, of the material, with area A_1 free of liquid water, then within A_1 the tortuosity υ and air content a can be considered unchanged, if the material is assumed uniform. Outwith A_1, the vapour transfer is zero due to the total blockage caused by the presence of liquid water. If an effective vapour transfer area factor, τ, is introduced into (5.10) as:

$$D_1 = \tau D \upsilon a \qquad (5.11)$$

where $D\upsilon\alpha$ now remains constant.

Let $D'_1 = D\upsilon\alpha$, then:

$$D_1 = D'_1\tau \tag{5.12}$$

If the material porosity is $\epsilon(m^3/m^3)$ and the sorption isotherm moisture content is u_s (kg/kg), then the effective vapour transfer area factor could be evaluated approximately as:

$$\tau \cong 1 - \frac{\rho_0 u_s}{\rho_2 \epsilon} \tag{5.13}$$

Considering that the liquid flow will be diminished when the relative humidity approaches zero, $\phi \to 0$, the influence of the relative humidity on the liquid transfer coefficient, D_2, could be explicitly expressed as $D_2 = D'_2\phi^n$. This functional relationship with relative humidity is proposed by the author based on previous work which he has carried out in this field, and the experimental results on material behaviour obtained during this work (see Chapter 6). The second term of equation (5.9) then becomes:

$$\frac{D_2 R_v T \rho_2}{\phi p_s} = \frac{D'_2 R_v T \rho_2}{p_s}\phi^{n-1} = \frac{D'_2 R_v T \rho_2}{p_s}\phi^m \tag{5.14}$$

where the n or m coefficients must be determined by experiment.

Equation (5.9) combined with (5.12) and (5.14) can then be simplified as:

$$\mu = \frac{D'_1}{R_v T}\tau + \frac{D'_2 R_v T \rho_2}{p_s}\phi^m \tag{5.15}$$

letting $D_1^* = \frac{D'_1}{R_v T}$, $D_2^* = \frac{D'_2 R_v T \rho_2}{p_s}$, (5.15) then becomes:

$$\mu = D_1^* \tau + D_2^* \phi^m$$

$$= D_1^* \left(1 - \frac{\rho_0 u_s}{\rho_2 \epsilon} \right) + D_2^* \phi^m \qquad (5.16)$$

The above equation separates the vapour and liquid water flux. The first part of the equation, $D_1^* \tau$, will relate to the vapour transfer while the second part, $D_2^* \phi^m$ will relate to the liquid water transfer.

The values of D_1^*, D_2^* and m of equation (5.16) can then be determined experimentally with three or more standard 'cup' tests over the a range of relative humidity conditions, the accuracy increasing with the number of data points used (see Chapter 6).

The vapour transfer coefficient could be simplified by considering the following observations based on Figure 5.1:

1) For building materials, a typical sorption isotherm curve is the S-shaped type II (see Chapter 3). From 0%~3%, the diffusion process could be discarded because the dominant process is molecular monolayer absorption. The moisture content of the sorption isotherm increases slowly at low relative humidity and when the RH reaches 60%~70%, it starts to increase sharply.

2) the vapour transfer coefficient, $D_1^* (1 - \rho_0 u_s / \rho_2 \epsilon)$, will follow a reversed pattern. It starts to decrease slowly at low RH and then when the sorption isotherm begins to increase sharply it decreases faster.

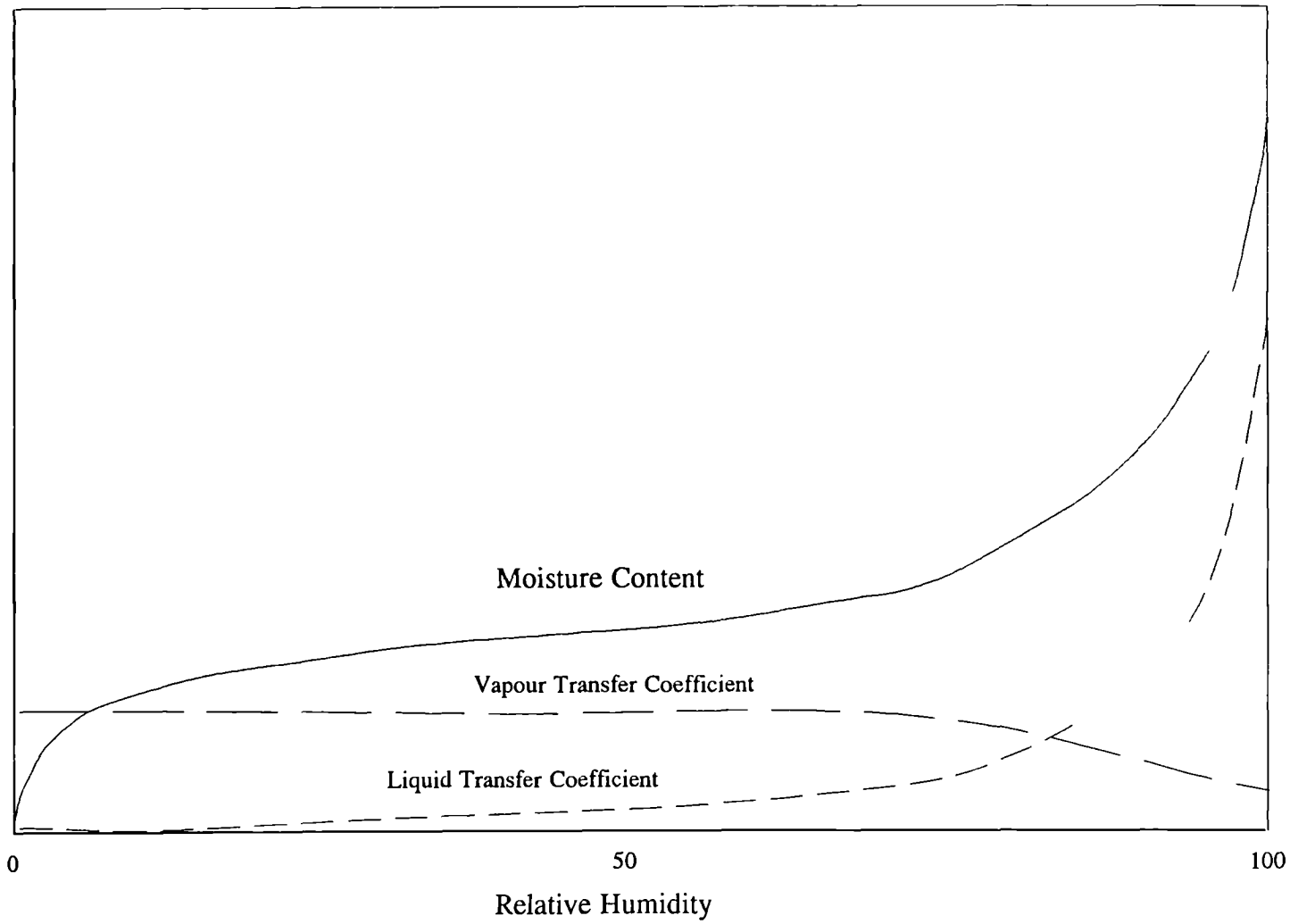

Fig.5.1 Typical Curves of Sorption Isotherm And Transfer Coefficients

3) even at 100% relative humidity, the void space free for vapour transfer is still considerable, e.g., for the highly hygroscopic material PARTICLE BOARD the void space not occupied by liquid water calculated with equation (5.13), using the experimental data of Chapter 6, is over 70% at 100% relative humidity.

4) when the vapour transfer coefficient starts to decrease, the liquid water transfer begins to be predominant, and the contribution to the total mass transfer by vapour movement becomes proportionally small.

From the above a conclusion can be drawn that no great error will be introduced if the vapour transfer coefficient is considered to be a constant. This leads to further simplification of equation (5.16) as:

$$\mu = D_1^* + D_2^* \phi^m \qquad (5.17)$$

To illustrate the effect of this simplification the results of applying equation (5.16) and equation (5.17) to the same set of three normal cup experiments for particle board are plotted in Figure 5.2. The particle board has a measured dry density of 589.1 kg/m^3 and a measured porosity of 62.7%.

equation (5.16) predicts:

$$\mu = 3.77 x 10^{-12}(1 - 0.941 u_s) + 1.24 x 10^{-11} \phi^{8.38} \qquad (5.18)$$

equation (5.17) predicts:

$$\mu = 3.55 x 10^{-12} + 1.20 x 10^{-11} \phi^{8.91} \qquad (5.19)$$

From Fig.5.2 it is clear that the permeabilities predicted by the two methods are nearly the same; the liquid flow coefficients and the vapor flow coefficients obtained by each method results in minimal differences at high relative humidity.

Fig.5.2 Comparison of Two Equations for the Prediction of Permeability

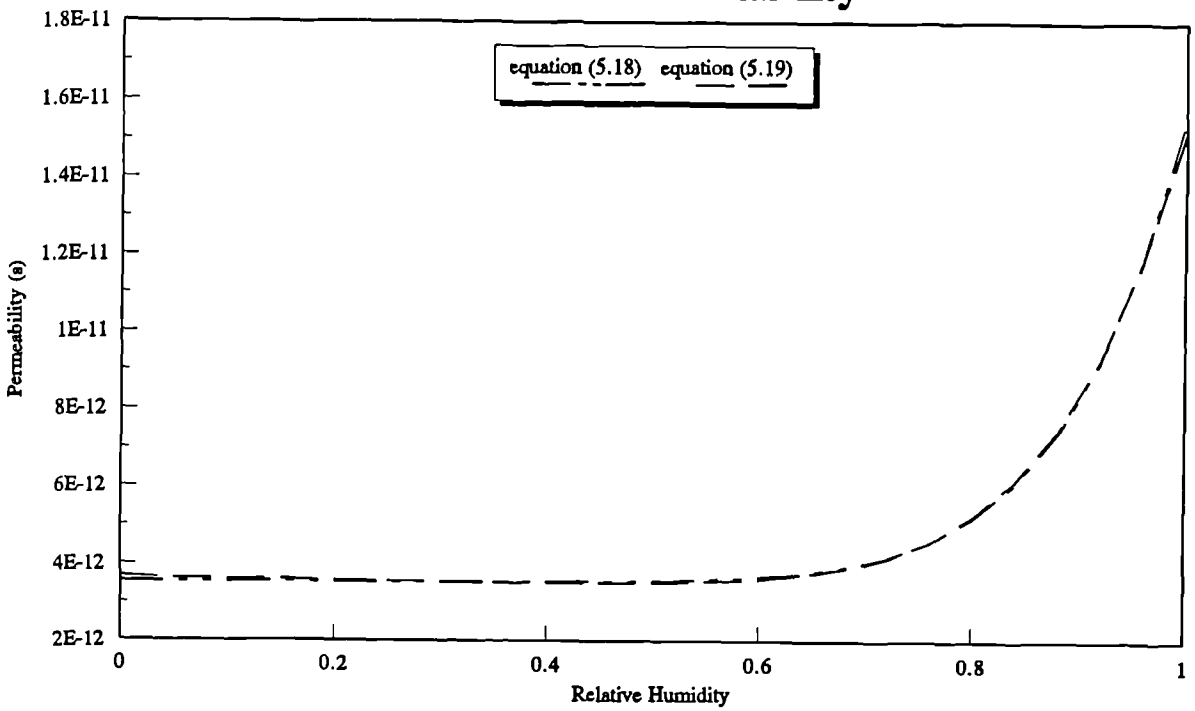

Thierry Duforestel[33] of the CSTB in France, in discussion with the author, has recently proposed an alternative method to separate the vapour and liquid flow by the assumption that the total pressure change will only influence the vapour transfer coefficient by $1/p$ (see equations (2.5) to (2.8)), the liquid water transfer being independent of total pressure, p. Equation (5.7), developed for isothermal conditions, could be re-expressed as:

$$j = j_1 + j_2 = -\mu \nabla p_1$$
$$= -\left(\frac{D''_1}{p} + D''_2 \right) \nabla p_1 \qquad (5.20)$$

where D''_1: vapour transfer coefficient, Ns/m^2.

$D''_2 = D_2 \rho_2 R_v T / p_1$, the liquid transfer coefficient, s.

Isothermal experiments carried out under the same relative humidity conditions, but varying barometric pressures, can then be used to determine these coefficients. A graph plotted of μ against $1/p$ should produce a straight line with gradient D''_1 and intercept D''_2.

The difficulty with this method is that it involves experimental operation under pressure and/or vacuum in a completely sealed chamber. This leads to many practical problems.

In theory all of the above methods should give results which are comparable. In Chapter 6 the pressure vessel method is used on only one material (particle board) to show the comparability between this technique and the data obtained using the assumptions contained in either equation (5.16) or (5.17).

5.2 Inert Gas

The flow of inert gas (air) is a complex function of vapour flow, water flow and vapour condensation rate. This interdependence is the result of the gas flux being constrained to maintain the total pressure constant and uniform. If the total pressure is p, then:

$$\begin{aligned} p &= p_1 + p_3 \\ &= \rho_3 R_3 T + \rho_1 R_1 T \end{aligned} \tag{5.21}$$

Differentiating the above equation with respect to time gives:

$$\frac{\partial p}{\partial t} = R_3 T \frac{\partial \rho_3}{\partial t} + R_1 T \frac{\partial \rho_1}{\partial t} + (\rho_3 R_3 + \rho_1 R_1) \frac{\partial T}{\partial t} \tag{5.22}$$

Because barometric pressure is assumed constant, equation (5.22) can be rearranged as:

$$R_3 T \frac{\partial \rho_3}{\partial t} = -R_1 T \frac{\partial \rho_1}{\partial t} - (\rho_3 R_3 + \rho_1 R_1) \frac{\partial T}{\partial t} \tag{5.23}$$

Multiplying equation (5.23) by the porosity of the porous body, ϵ, gives:

$$R_3 T \epsilon \frac{\partial \rho_3}{\partial t} = -R_1 T \epsilon \frac{\partial \rho_1}{\partial t} - \epsilon (\rho_3 R_3 + \rho_1 R_1) \frac{\partial T}{\partial t} \tag{5.24}$$

Assuming that the void occupied by liquid water is negligible compared to the gaseous phase, then $\epsilon \rho_1$ and $\epsilon \rho_3$ are approximately equivalent to the volumetric contents of vapour and inert gas respectively, i.e. $\epsilon \rho_1 = \rho_0 u_1$ and $\epsilon \rho_3 = \rho_0 u_3$. Substituting this into equation (5.24) leads to:

$$R_3 T \frac{\partial \rho_0 u_3}{\partial t} = -R_1 T \frac{\partial \rho_0 u_1}{\partial t} - \epsilon (\rho_3 R_3 + \rho_1 R_1) \frac{\partial T}{\partial t} \tag{5.25}$$

Utilising the continuity equation (4.1),and given that no chemical reactions exist ($I_3 = 0$), equation (5.25) becomes:

$$\nabla \cdot j_3 = -\frac{R_1}{R_3}\nabla \cdot j_1 + \frac{R_1}{R_3} I_1 + \frac{\epsilon}{R_3 T}(\rho_3 R_3 + \rho_1 R_1)\frac{\partial T}{\partial t} \quad (5.26)$$

Equation (5.26) states that the flux of inert gas must be such that it compensates the pressure loss due to the vapour net flow and condensation and the temperature variation. If $I_1 = 0$ and $\partial T / \partial t = 0$, then:

$$j_3 = -\frac{R_1}{R_3} j_1 \quad (5.27)$$

which is the situation of steady state vapour transfer in air.

In order to estimate j_3 numerically, however, equation (5.26) has to take another form. In equation (5.24), ρ_1 is a function of vapour pressure and temperature, i.e. $p_1 = \rho_1 R_1 T$. Substituting this relationship into equation (5.24) together with the continuity equation (4.1), j_3 could be expressed as:

$$\nabla \cdot j_3 = \frac{\epsilon}{R_3 T}\left(\frac{\partial p_1}{\partial t} + \rho_3 R_3 \frac{\partial T}{\partial t}\right) \quad (5.28)$$

The above equation could be used to estimate j_3 in a numerical analysis of the problem by utilizing the values of $\partial p_1 / \partial t$ and $\partial T / \partial t$ of the previous time step together with the boundary condition for air flow.

6. EXPERIMENTAL EVALUATION OF MATERIAL MOISTURE PROPERTIES

The model equations outlined in Chapter 4 are only of practical value if the material data required for their application can be determined. It must be possible for this data to be measured experimentally using techniques which can be performed in any standard building laboratory.

In this section the ideas presented in Chapter 5 will be investigated and an experimental procedure developed to allow determination of the required material moisture properties.

To achieve this, a range of experiments have been carried out on seven common building materials, details of which are given in Table 6.1.The thickness values quoted in this table are nominal values obtained from the manufacturers. The porosity was obtained by measurement on five samples of each material using a helium gas porosimeter on site at Heriot-Watt University. The material conductivities and specific heats were extracted or calculated from manufacturers information and standard reference sources. The dry densities were measured by the author with circular samples dried at 70^0C in the oven until equilibrium was reached. The values quoted in each case for Table 6.1 are average values for the samples investigated.

The bulk of the experiments have involved the hygroscopic Particle Board and the non-hygroscopic Extruded Polystyrene. The experiments have been designed to allow the following properties to be evaluated:

(i) vapour and liquid water transfer coefficients

(ii) sorption isotherms

In addition, a range of experiments were performed to investigate the importance of thermal diffusion effects. Thermal diffusion has attracted little

Table 6.1 Building Materials Used in Experiments

Material	Detailed Description	General Information				
		L (mm)	ρ_0 (kg/m^3)	c_0 (J/kgK)	λ_0 (W/mK)	ϵ (m^3/m^3)
Particle Board	BS5669 Type 1 general purpose for building applications	12	589	1298[b] 1880[c]	0.078[b] 0.099[c]	62.7%
Extruded Polystyrene	Styrofoam SP extruded polystyrene plastic foam	24	36	1470[c]	0.027[d] 0.024[c]	69.4%
Plywood	Malaysian Morranti wood with WBP formaldahyde glue	12	561	1214[b] 1880[c]	0.14[a] 0.115[b] 0.114[c]	79%
Wood	Norwegian Spruce variety "picea abies"	14	388	1382[b]	0.13[a] 0.12[b]	76.5%
Plasterboard	Gyproc Gypsum	12 9	846 881	840[c]	0.16[a] 0.263[c]	71.5% 71.7%
Expanded Polystyrene	Insulation material	25	16.6	1400[a] 1470[c]	0.035[a] 0.038[b] 0.037[c]	92.5%
Brick	Facing brick	-	1500	840[c]	0.72[b] 0.65[c]	23.7%

[a]: CIBSE Guide[45]
[b]: ASHRAE Handbook 1981 Fundamental[46]
[c]: Catalogue of Material Properties[47]
[d]: Manufacturer suggested value

Values quoted from [b] are for 24^{0}C.
Values quoted from [c] are for 20^{0}C except for that of extruded polystyrene which is at 10^{0}C.

attention from investigators and there is little relevant information available. It could, however, be important under certain circumstances.

This chapter is divided into three sections, covering each of the above topics.

6.1 Vapour and Liquid Water Transfer Coefficients

In Chapter 5 two possible methods of evaluating the vapour and liquid water transfer coefficients were outlined.

The first, based on the standard isothermal cup test method combined with a calculation procedure, involved making assumptions about the form of mathematical relationship between the coefficients and the test relative humidity. This is the preferred method as only standard equipment is required and the technique is easily applied. All of the seven materials quoted in Table 6.1 have been tested using this approach and the transfer coefficients evaluated.

The second technique assumes that a reciprocal relationship exists between the vapour diffusion coefficient and the total pressure when diffusion takes place within porous materials. That reciprocal relationship has been shown to be valid by many investigators for vapour diffusion in bulk air (see Section 2.1.1 of Chapter 2). This method involves carrying out vapour flow experiments under a range of barometric pressures. It can be cumbersome and has many practical difficulties associated with the test equipment. Tests with this technique were only carried out for Particle Board. These tests provide a comparison with the results from the isothermal cup test procedure, and validate the form of mathematical relationship assumed by the author for the liquid transfer coefficient D_2.

6.1.1 The Standard Isothermal Cup Tests

Test Procedure

The isothermal cup test used complies with the British Standard 4370 part 2, 1973[48]. In the test, a 250 ml beaker of glass is used. It has a 65mm internal diameter and a belled mouth to facilitate sealing (Plate 6.1). The test specimen is cut to fit

tightly into the beaker, with a specified clearance between specimen and beaker of 0.25 mm. The sealant is a mixture of microcrystalline wax (90%) and soft yellow paraffin (10%). A circular metal template with a chamfered edge is fabricated to provide an accurately defined test area during the sealing process (Plate 6.2).

A diagram of the test cup arrangement is shown in Figure 6.1. A layer of melted wax is brushed on to the curved surface of the specimen. The upper part of the cup is then warmed and the waxed sample pushed into place so that its upper surface is just below the top edge of the beaker. The metal template is positioned centrally on the top surface of the specimen and melted wax poured along its circumference to complete the seal (Plate 6.3).

The vapour pressure inside the cup is regulated with water ('wet' cup, 100% RH), dessicant ('dry' cup, 0% RH) or a saturated salt solution. The salt solutions used during the research are given in Table 6.2 along with the relative humidities they can regulate within the cups. Values of relative humidity of salt solutions were extracted from *THE INTERNATIONAL CRITICAL TABLES*[49]. The cup is then position in an environmental chamber (Plate 6.4), where the outside surface of the sample is exposed to a controlled atmosphere. A sketch of the chamber is shown in Figure 6.2. This arrangement enables a constant vapour pressure difference to be maintained across the sample and the vapour flow rate can be found from the steady increase or decrease in the weight of the cup measured with a PRECISA 500M balance (Plate 6.5). The chamber environmental conditions were monitored using a PROTIMETER dewpoint meter DP989M connected to a GOERZ SE120 flatbed chart recorder (Plate 6.6). The sensor was hung directly above the test area within the chamber. Velocities measured directly above the test cups for all tests ranged from 1.4 to 2.5 m/s. The thickness of each sample was measured using a calibrated

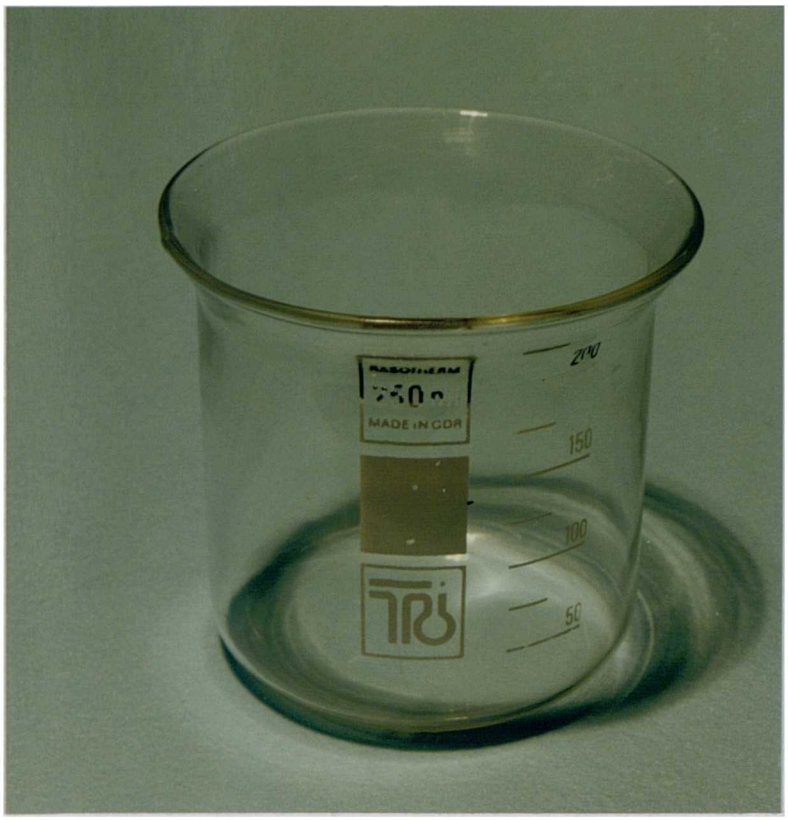

Plate 6.1 BS4370 Standard Test Cup

Plate 6.2 Circular Template For Sealing Cups

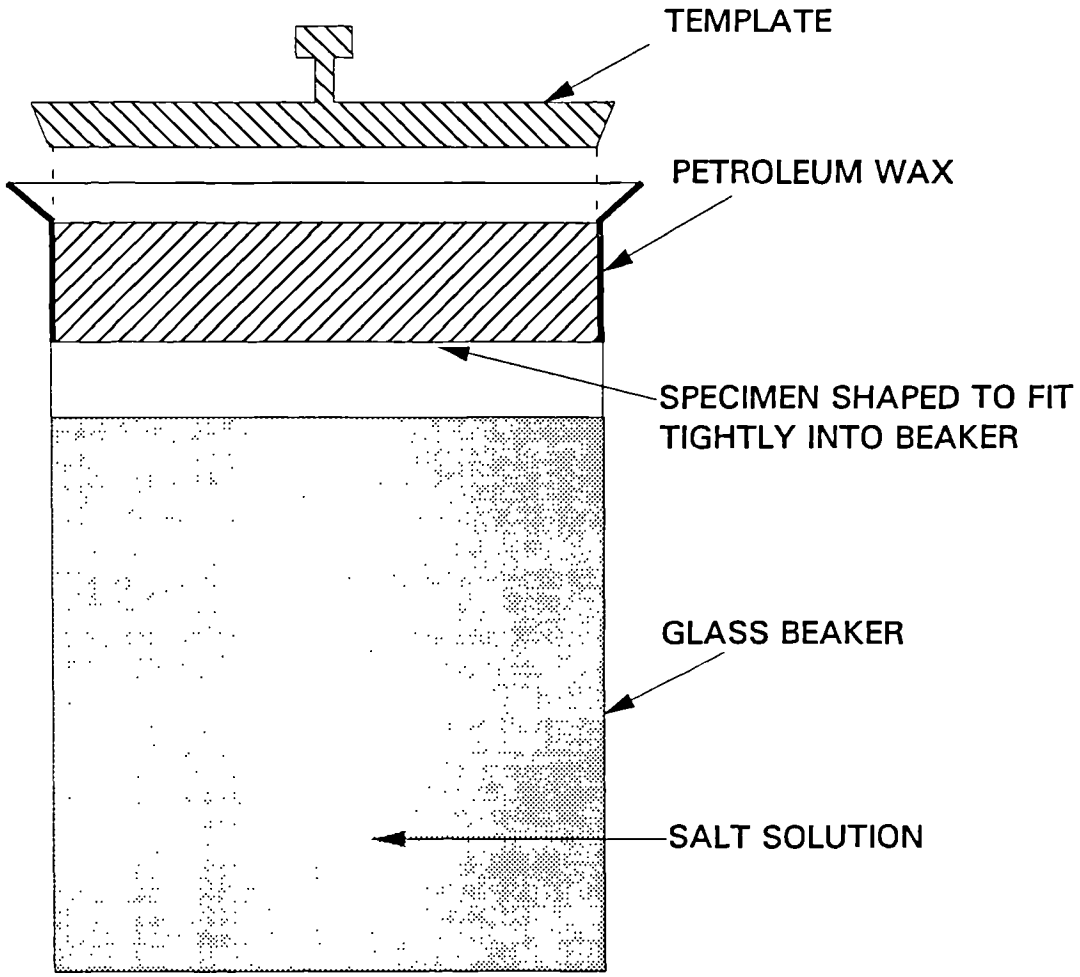

FIGURE 6.1 BRITISH STANDARD ISOTHERMAL CUP

Plate 6.3 Sealing of Specimen in Test Cup

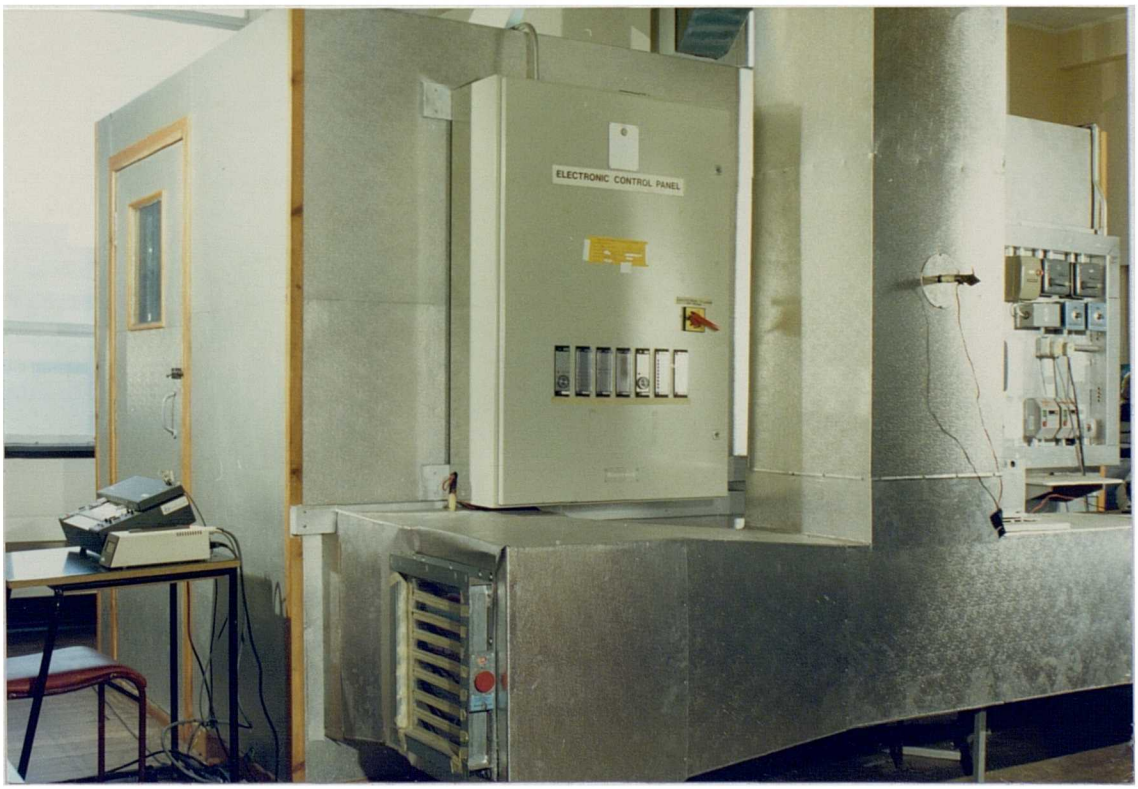

Plate 6.4 Environmental Test Chamber

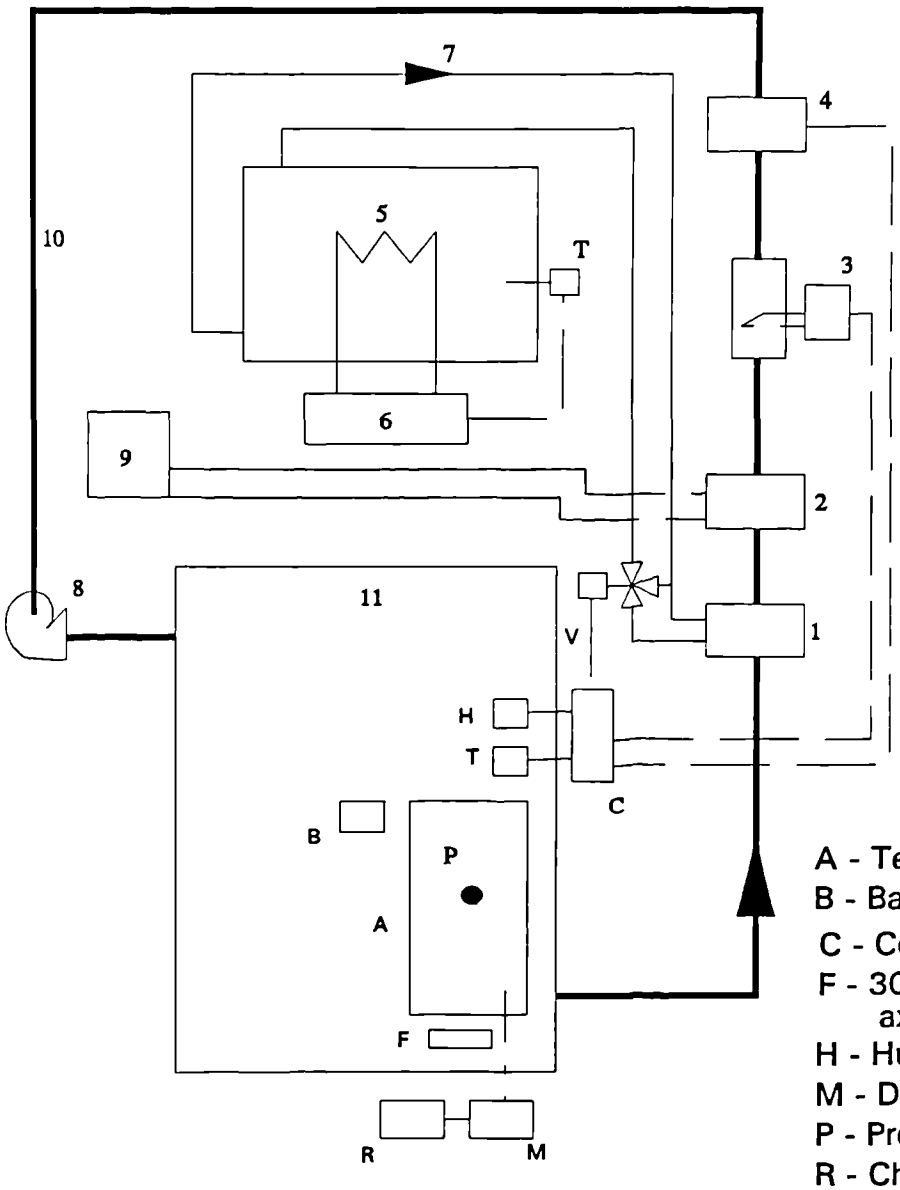

A - Test area
B - Balance
C - Control panel
F - 300mm dia. axial-flow fan
H - Humidistat
M - Dew-point meter
P - Protimeter probe
R - Chart recorder
T - Thermostat
V - 3-Port motorised valve

1 - 300x300mm chilled-water coil, 4 row, finned.
2 - 300x300mm direct-expansion coil, 4 row, finned.
3 - Calomax SP6 steam humidifier, 5.5kW, 6.75 kg/h, 6 stage.
4 - 300x300mm electric reheating coil, 4 kW, 4 stage.
5 - 1.5x1.2x1m chilled-water tank, with evaporator coil and agitator
6 - Semi-hermetic refrigeration compressor (R12), 2 cyl., 2.2kW/water-cooled condenser
7 - Chilled-water pump.
8 - 400mm dia. centrifugal fan, variable speed
9 - Hermetic refrigeration compressor (R12)/air-cooled condenser
10- 300x300mm ducting, insulated.
11- Environmental chamber

FIGURE 6.2 DIAGRAMMATIC LAYOUT OF EXPERIMENTAL TEST FACILITY

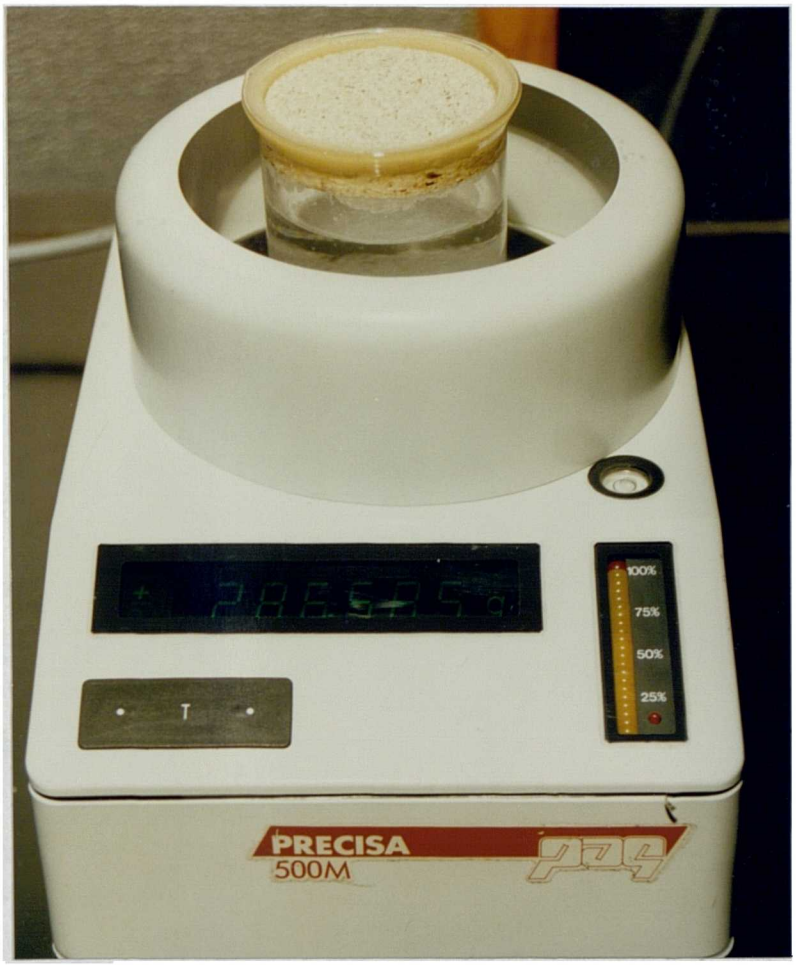

Plate 6.5 Precisa 500M Balance Used for Cup Weight Measurements

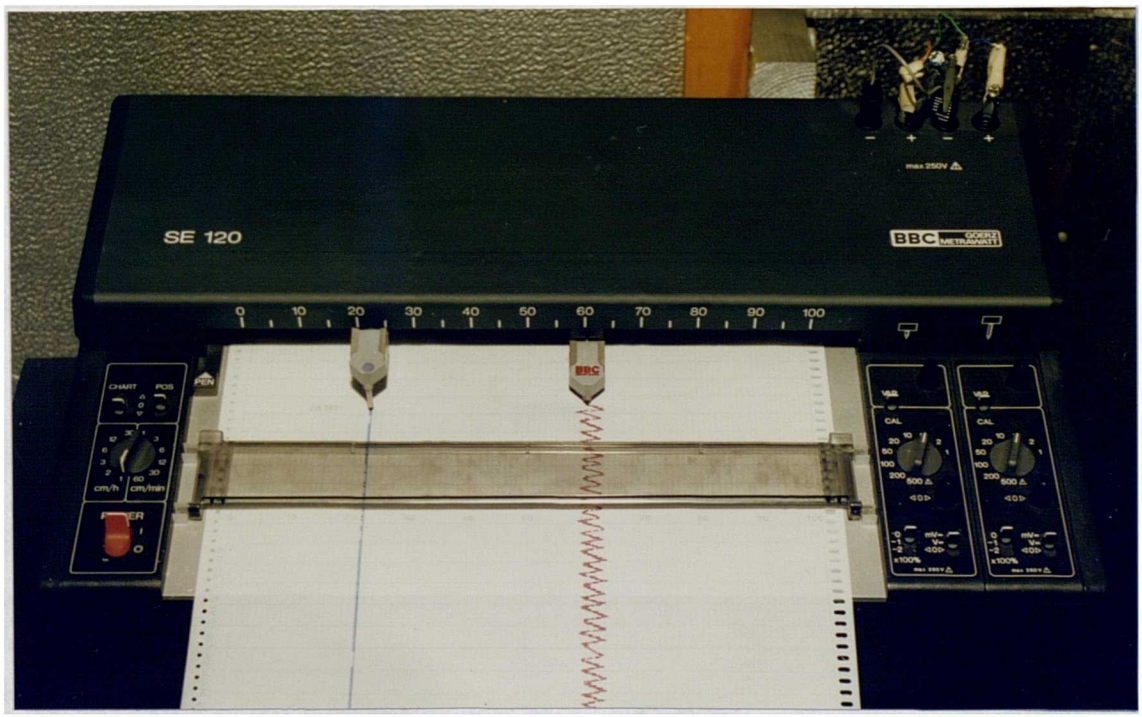

Plate 6.6 Flatbed Chart Recorder Showing Chamber Environmental Conditions

Table 6.2 Salt Solutions Used and Their Relative Humidities

Salt Solution	15^{0}C	20^{0}C	25^{0}C
$CaCl_2$	35.0	32.0	31.0
$K_2CO_3.2H_2O$	44.0	44.0	43.0
$NaBr.2H_2O$	-	58.0	57.0
NaCl	77.5	76.5	76.5
NH_4Cl	80.0	80.0	79.0
KNO_3	96.2	93.0	93.0
$NH_4H_2PO_4$	-	93.1	93.0
$CaSO_4.5H_2O$	-	98.0	-

Table 6.3 Test Conditions for Particle Board and Extruded Polystyrene

Test Temperature: 23^{0}C	
Relative Humidity Conditions	
Test Cup	Environmental Chamber
0%	60%
80%	60%
93%	60%
100%	60%

Table 6.4 Test Conditions for Other Materials

Test Temperature: 20^{0}C, 25^{0}C	
Relative Humidity Conditions	
Test Cup	Environmental Chamber
0%	60%
90%	60%
100%	60%
100%	80%

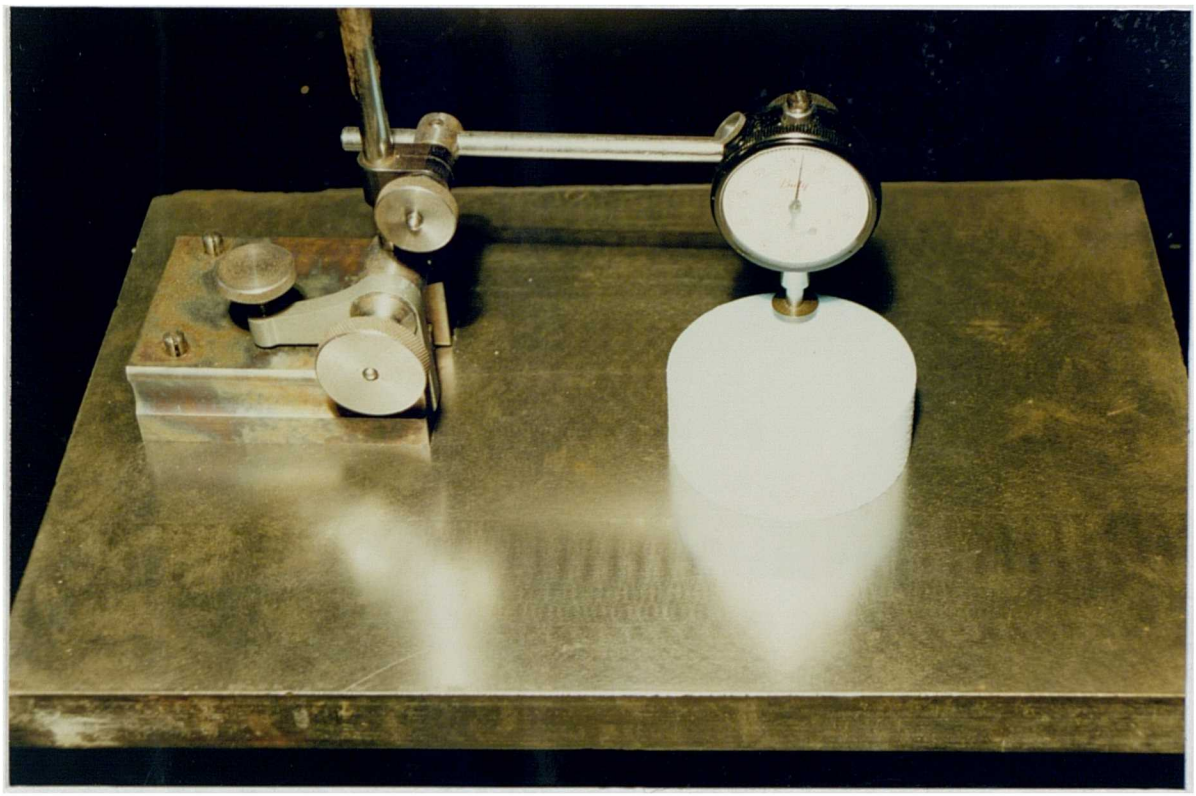

Plate 6.7 BATY Dial Gauge and Block for Sample Thickness Measurements

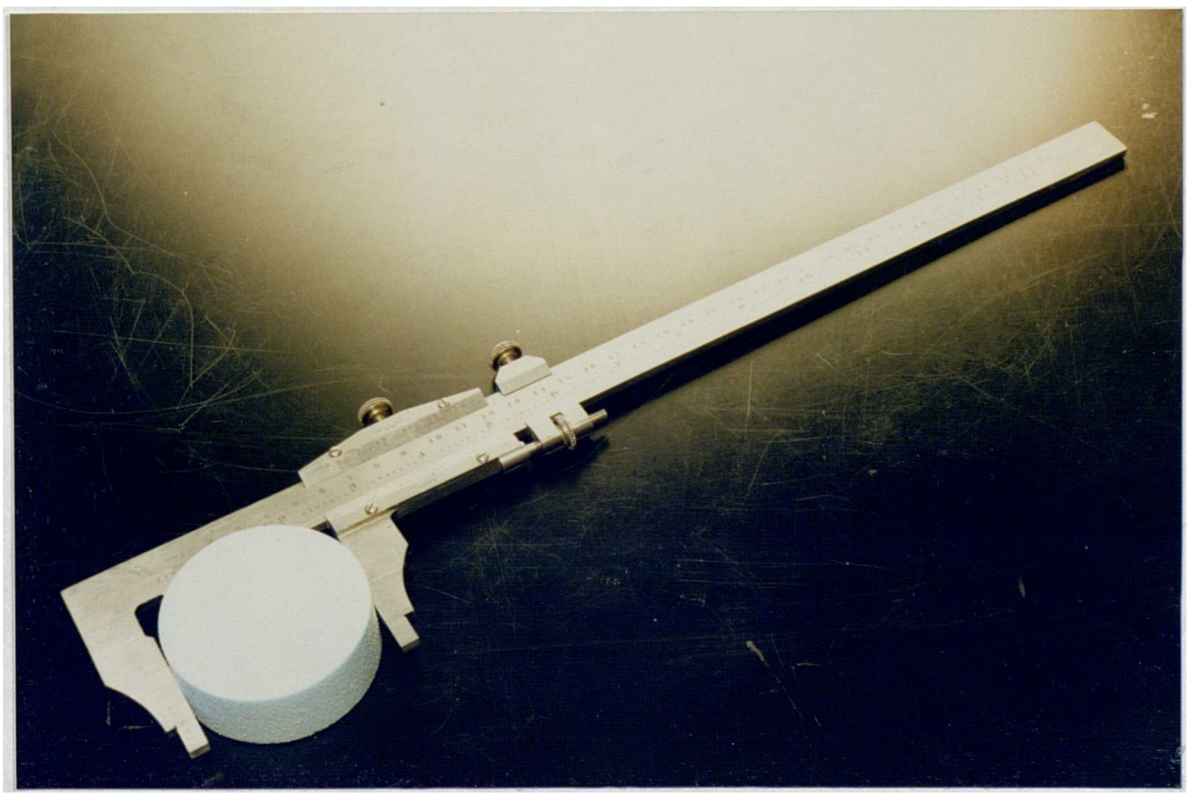

Plate 6.8 VERNIER Caliper Gauge for Diameter Measurements

BATY dial gauge and block with an accuracy of 0.01mm (Plate 6.7) before the sample was mounted in the cup, and sample diameters were determined using a Vernier caliper gauge accurate to 0.02mm (Plate 6.8). This will only introduce around 0.2% error for the determination of the volume of the sample with a thickness of 12mm and a diameter of 64.5mm.

For each individual cup test, generally six samples were selected with a pre-conditioned density variation not exceeding 5%, which guarantees the sample uniformity. The number of samples used allow material variations to be averaged out and enables badly sealed samples to be identified. The weight change with time was measured for each cup on a daily basis until equilibrium was reached and enough points were collected to allow regression analysis. A graph of weight change against time could then be produced and the gradient calculated and used to determine the total moisture flow rate. This flow rate relates to the boundary conditions between the inside of the cup and the environmental chamber. Application of equation (5.8) allows the calculation of an averaged permeability for the experiment as:

$$\bar{\mu} = \frac{1}{\Delta\phi}\int_{\phi_1}^{\phi_2} \mu \, d\phi \qquad (6.1)$$

where $\quad j = \mu \nabla p_1, \quad \mu = \mu(\phi) \quad \text{and} \quad \Delta\phi = \phi_2 - \phi_1$

It has been demonstrated in previous research investigations by the author[11][50], that by carrying out at least four experiments on each material covering a range of relative humidities, a relationship between μ, the spot or differential permeability and relative humidity can be determined. This can be done either by hand drawing a curve to fit the data or by mathematical curve fitting procedures.

In Chapter 5 it was shown that this spot permeability could also be expressed in terms of the vapour and liquid water transfer coefficients using equation (5.16) or

(5.17). In these equations a form of mathematical relationship between each coefficient and relative humidity has been assumed by the author. From equation (5.16) we may write:

$$\bar{\mu} = \frac{1}{\Delta\phi}\int_{\phi_1}^{\phi_2} D_1^*\left(1 - \frac{\rho_0 u_s}{\rho_1 \epsilon}\right)d\phi + \frac{1}{\Delta\phi}\int_{\phi_1}^{\phi_2} D_2^*\phi^m d\phi$$

$$\therefore \quad \bar{\mu} = D_1^*\left(1 - \frac{\rho_0 \overline{u_s}}{\rho_1 \epsilon}\right) + \frac{D_2^*}{\Delta\phi[m+1]}[\phi_2^{m+1} - \phi_1^{m+1}] \qquad (6.2)$$

or $$\bar{\mu} = \overline{D_1^*} + \overline{D_2^*}$$

And similarly, using equation (5.17):

$$\bar{\mu} = \frac{1}{\Delta\phi}\int_{\phi_1}^{\phi_2} [D_1^* + D_2^*\phi^m]d\phi$$

$$\therefore \quad \bar{\mu} = D_1^* + \frac{D_2^*}{\Delta\phi[m+1]}[\phi_2^{m+1} - \phi_1^{m+1}] \qquad (6.3)$$

or $$\bar{\mu} = \overline{D_1^*} + \overline{D_2^*}$$

By carrying out at least three permeability tests over a range of relative humidity conditions either equation may be solved to determine the values of D_1^*, D_2^* and exponent m.

Experimental Conditions and Test Results

The test conditions for the Particle Board and the Extruded Polystyrene are listed in Table 6.3. The temperature of 23^0C was chosen to be in line with the

requirement of most current European test standards for isothermal permeability tests. This presents a suitable range of experimental conditions which can be used to give results which, in the experience of the author, can be considered reliable.

For the remaining samples, tests were carried out at temperatures of 20^0C and 25^0C, the full range of experimental conditions being listed in Table 6.4.

The materials were tested in general using a total of six individual isothermal cups for each test condition. A mean test permeability was then calculated to enable the effects of material variations to be minimised. The individual isothermal test cup results are given in Appendix Two, along with the calculated mean and standard deviations of permeability.

The mean permeabilities calculated for each test condition were then used to determine for each material and test temperature the vapour and liquid water transfer coefficients.

In Table 6.5 these coefficients are presented both for the varying vapour flow model (model 1) as presented in equation (5.15) and for the constant vapour flow model (model 2) of equation (5.17).

In the calculation of the coefficients using model 1 it is necessary to have available the absorption isotherms for each material measured at the given test temperature. In this work the material absorption isotherms were measured only at temperatures of 20^0C or 23^0C due to constraints of time (see Section 6.2). Although absorption isotherms are influenced by temperature this influence is generally small[37], and for the purpose of this work, the data for 20^0C has been used for model 1 when calculating the coefficients corresponding to a test temperature of 25^0C.

Table 6.5. Calculated Transfer Coefficients from Isothermal Cup Tests

Set No.	Test Material	Test Temp.	Transfer Coefficient					
			Varying Vapour MODEL 1			Constant Vapour MODEL 2		
		^0C	$D_1^* x 10^{12}$	$D_2^* x 10^{12}$	m	$D_1^* x 10^{12}$	$D_2^* x 10^{12}$	m
1	Particle Board	23	3.77	12.4	8.38	3.55	12.0	8.91
2	Plywood	20	1.15	17.8	8.96	1.02	17.7	9.20
3	Plywood	25	1.16	17.7	9.04	1.04	17.6	9.29
4	Wood	20	1.58	37.0	5.65	1.44	36.8	5.68
5	Wood	25	1.54	35.7	6.46	1.40	35.5	6.51
6	Brick	20	0.77	6.78	11.80	0.76	6.79	11.92
7	Plasterboard (thin)	20	22.2	23.3	9.49	21.3	22.2	10.18
8	Plasterboard (thin)	25	21.4	14.2	5.62	20.5	12.7	5.68
9	Plasterboard (thick)	20	24.5	22.3	5.27	23.6	20.9	5.33
10	Plasterboard (thick)	25	24.0	20.6	5.66	23.1	19.1	5.71
11	Extruded Polystyrene	23	2.28	0.00	1.0	2.28	0.00	1.0
12	Expanded Polystyrene	20	6.39	0.16	1.0	6.39	0.16	1.0
13	Expanded Polystyrene	25	6.08	0.60	1.0	6.08	0.60	1.0

TEST MATERIAL	TEST TEMP. ^0C	TEST RH RANGE %	MEASURED PERMEABILITY $\bar{\mu}x10^{12}$	MODEL1 PREDICTION $\bar{\mu}x10^{12}$	MODEL1 PREDICTION % difference	MODEL2 PREDICTION $\bar{\mu}x10^{12}$	MODEL2 PREDICTION % difference
Particle Board	23	0 - 60	3.66	3.57	-2.5	3.56	-2.7
		80 - 60	3.89	4.15	6.7	4.17	7.2
		93 - 60	5.59	5.32	-4.8	5.30	-5.2
		100 - 60	6.43	6.54	1.7	6.54	1.7
Plywood	20	0 - 60	1.04	1.04	0.0	1.04	0.0
		80 - 60	2.97	2.97	0.0	2.97	0.0
		93 - 60	5.34	5.34	0.0	5.34	0.0
		100 - 60	8.82	8.82	0.0	8.82	0.0
	25	0 - 60	1.06	1.05	-0.9	1.05	-0.9
		90 - 60	2.81	2.79	-0.7	2.79	-0.7
		100 - 60	5.24	5.29	1.0	5.30	1.1
		100 - 80	8.77	8.75	-0.2	8.74	-0.3
Wood	20	0 - 60	1.8	1.8	0.0	1.8	0.0
		90 - 60	11.5	11.2	-2.6	11.2	-2.6
		100 - 60	14.2	14.8	4.2	14.8	4.2
		100 - 80	23.0	22.8	-0.9	22.8	-0.9
	25	0 - 60	1.6	1.6	0.0	1.6	0.0
		90 - 60	9.5	9.41	-0.9	9.41	-0.9
		100 - 60	12.8	13.0	1.6	13.0	1.6
		100 - 80	20.7	20.6	-0.5	20.6	-0.5
MEAN % DIFFERENCE					0.06		0.06

Table 6.6 Comparison Between Measured And Predicted Average Permeabilities

TEST MATERIAL	TEST TEMP. ^0C	TEST RH RANGE %	MEASURED PERMEABILITY $\bar{\mu}x10^{12}$	MODEL1 PREDICTION $\bar{\mu}x10^{12}$	MODEL1 PREDICTION % difference	MODEL2 PREDICTION $\bar{\mu}x10^{12}$	MODEL2 PREDICTION % difference
Brick	20	0 - 60	0.73	0.73	0.0	0.76	4.1
		60 - 93	1.34	1.38	2.9	1.38	2.9
		60 - 100	2.21	2.07	-6.3	2.07	-6.3
		80 - 100	3.18	3.24	1.9	3.24	1.9
Plaster Board (Thin)	20	0 - 60	21.3	21.1	-0.94	21.3	0.0
		60 - 90	23.3	23.3	0.0	23.3	0.0
		60 - 100	26.3	26.2	-0.38	26.3	0.0
		80 - 100	30.4	30.4	0.0	30.4	0.0
	25	0 - 60	20.7	20.7	0.0	20.7	0.0
		60 - 89	23.7	23.3	-1.7	23.3	-1.7
		60 - 100	24.4	25.1	2.9	25.1	2.9
		80 - 100	28.2	27.9	-1.1	27.9	-1.1
Plaster Board (Thick)	20	0 - 60	23.8	23.9	0.42	23.9	0.42
		60 - 93	28.9	29.6	2.4	29.6	2.4
		60 - 100	32.7	31.5	-3.7	31.6	-3.4
		80 - 100	35.7	36.1	1.1	36.1	1.1
	25	0 - 60	23.3	23.3	0.0	23.3	0.0
		60 - 93	28.2	28.2	0.0	28.1	-0.28
		60 - 100	29.9	30.0	0.3	30.0	0.3
		80 - 100	34.2	34.2	0.0	34.2	0.0
MEAN % DIFFERENCE					-0.11		0.16

Table 6.6 (continue)

TEST MATERIAL	TEST TEMP. ^{o}C	TEST RH RANGE %	MEASURED PERMEABILITY $\bar{\mu}x10^{12}$	MODEL1 PREDICTION $\bar{\mu}x10^{12}$	MODEL1 PREDICTION % difference	MODEL2 PREDICTION $\bar{\mu}x10^{12}$	MODEL2 PREDICTION % difference
Extruded Polystyrene	23	0 - 50	2.28	2.28	0.0	2.28	0.0
		80 - 60	2.11	2.28	0.81	2.28	0.81
		93 - 60	2.50	2.28	-8.8	2.28	-8.8
		100 - 60	2.12	2.28	7.5	2.28	7.5
Expanded Polystyrene	20	0 - 60	6.4	6.44	0.6	6.44	0.6
		60 - 93	6.7	6.51	-2.8	6.51	-2.8
		60 - 100	6.5	6.52	0.3	6.52	0.3
		80 - 100	6.4	6.53	2.0	6.53	2.0
	25	0 - 60	6.2	6.27	1.1	6.27	1.1
		60 - 93	6.9	6.54	-5.2	6.54	-5.2
		60 - 100	6.5	6.56	0.9	6.56	0.9
		80 - 100	6.4	6.62	3.4	6.62	3.4
MEAN % DIFFERENCE					0.6		0.6

Table 6.6 (continue)

A computer routine was written to enable the coefficients D_1^*, D_2^* and m to be determined directly by input of the relevant material data, test conditions and average permeability results. The program itself, with sample output for the particle board, is given in Appendix Four.

The suitability of the mathematical relationships assumed for Model 1 and Model 2 have been investigated, and the results are given as Table 6.6 In this table predicted average permeabilities have been calculated using the coefficients of Table 6.5, for environmental conditions corresponding to those used in the original experiments. In Table 6.6 the Predicted values from each model are shown alongside the actual test results with the percentage difference between them also shown. It is clear from this that there is little difference between the two models. The maximum difference for both models is 8.8% which occurs for the non-hygroscopic material, Extruded Polystyrene. This 8.8% difference is small and it can be concluded that both models produce good results.

The relative merits of Model 1 and Model 2 can be investigated further by analysing in more detail the results for Particle Board. This material was chosen as it exhibits characteristics typical of a hygroscopic building material.

Table 6.5 gives the relationship between vapour and liquid water transfer coefficients and relative humidity for particle board as:

$$\text{model 1:} \quad D_1^*\tau = 3.77 \times 10^{-12}(1 - 0.941\, u_s), \quad D_2^*\phi^m = 1.24 \times 10^{-11}\phi^{8.38} \tag{6.4}$$

$$\text{model 2:} \quad D_1^* = 3.55 \times 10^{-12}, \quad D_2^*\phi^m = 1.20 \times 10^{-11}\phi^{8.91} \tag{6.5}$$

Figure 6.3 and Figure 6.4 present the above equations in graphical form. In both cases, the liquid transfer coefficients start from zero when no liquid is present at the dry condition and all the void space is occupied by the gaseous phase. At the

Fig.6.3. Transfer Coefficients Using Model 1

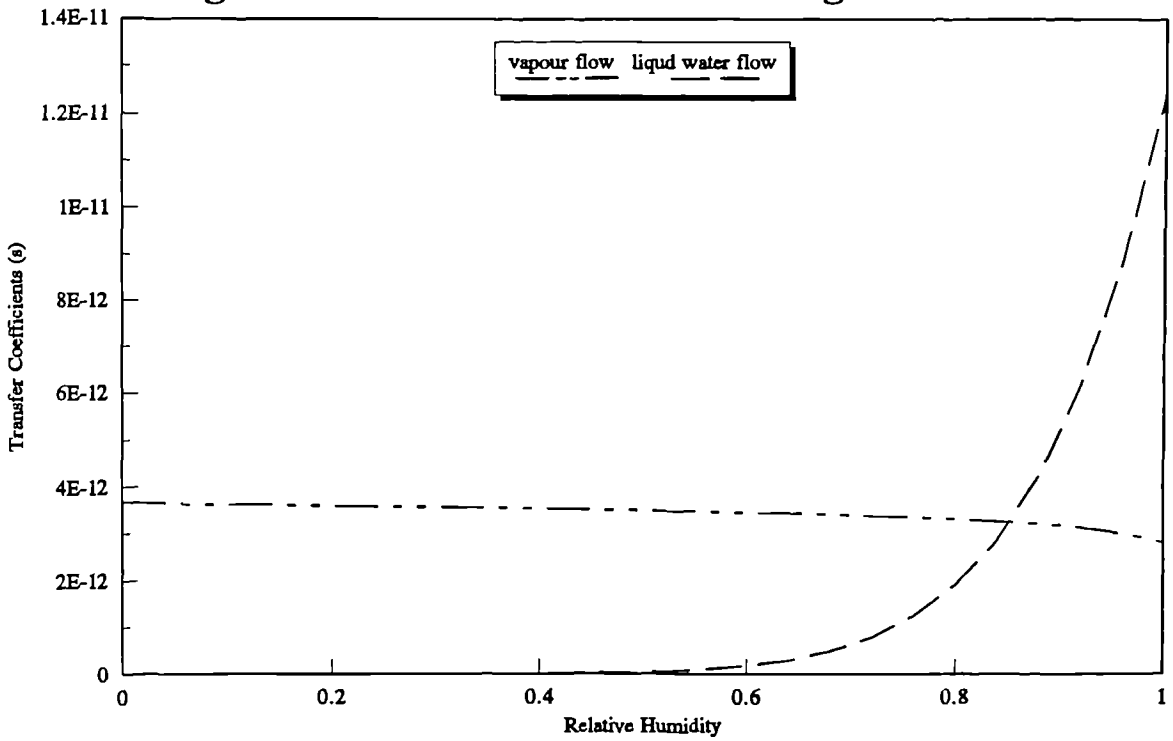

Fig.6.4. Transfer Coefficients Using Model 2

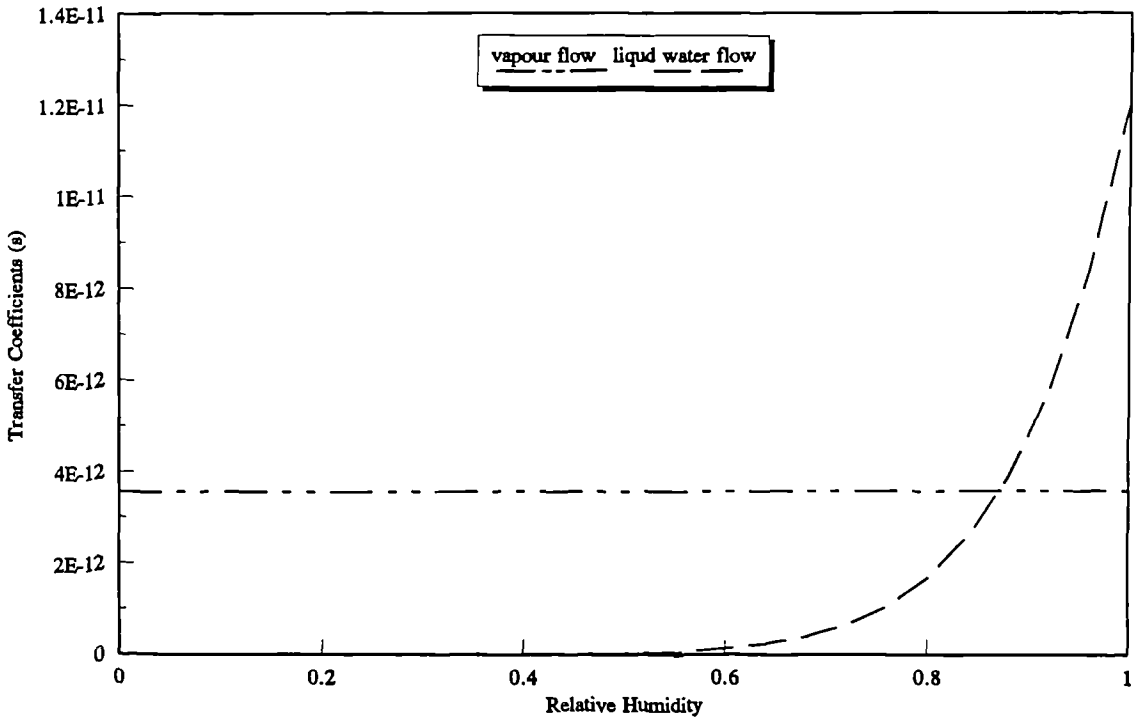

low relative humidity range, below 60-70%, because capillary condensation has not started and the predominant process is the absorption of multi-layer molecules, the liquid water transfer increases rather slowly. Over the high relative humidity range, when capillary condensation is predominant, the amount of liquid water present in the material increases sharply with any increase of relative humidity and the '*short circuit*' effects of the '*water islands*' within the pores of the material greatly enhances the water transfer rate (see chapter 2). The vapour transfer coefficient in model 1 gradually decreases as the liquid water transfer coefficient increases with more and more void space occupied by the liquid. On the other hand, model 2 assumes a constant vapour transfer coefficient.

The two models should in theory predict the same total amount of moisture transfer regardless of the differences in individual transfer rates. The largest discrepancies between the individual component transfer rates for the two models lie over the high relative humidity condition. This can be shown, by comparing the ratio of the flow rate of liquid water to vapour, predicted by each model. The ratio of transfer coefficients is given from the above two equations for particle board as:

$$\text{model 1:} \quad \frac{\text{Liquid Water}}{\text{Vapour}} = 3.29 \frac{\phi^{8.38}}{1 - 0.941 u_s}$$

$$\text{model 2:} \quad \frac{\text{Liquid Water}}{\text{Vapour}} = 3.38 \phi^{8.91}$$

The above equations are shown plotted as Figure 6.5. At relative humidities approaching 100%, model 1 predicts a ratio of 4.40 while model 2 predicts 3.38. Model 2, when compared with model 1, over-predicts the vapour transfer rate by 23% and under-predicts the liquid transfer rate by 5%. This will affect the energy equation (4.7) accordingly. A rough estimation, under the assumption that all other variables other than the individual transfer rates are kept the same for the two models, indicates

that model 2 will underestimate the convection term $j_i c_i \nabla T$ by 2% and over-estimate the net enthalpy increase term $h_i \nabla \cdot j_i$ by 19%. However these discrepancies will be considerably reduced when the relative humidity departs from 100%.

The vapour and liquid water transfer coefficients enable the permeability for particle board over the complete range of relative humidity at a temperature of 23^{0}C to be described mathematically as:

$$\text{model 1:} \qquad \mu = 3.77x10^{-12}(1-0.941u_s) + 1.24x10^{-11}\phi^{8.38} \qquad (6.6)$$

$$\text{model 2:} \qquad \mu = 3.55x10^{-12} + 1.20x10^{-11}\phi^{8.91} \qquad (6.7)$$

Based on experimental results, Galbraith and McLean[50] put forward the concept of differential permeability and proposed an exponential form of curve fit for permeability values over the whole relative humidity range:

$$\mu = Ae^{B\phi} + C \qquad (6.8)$$

In this equation ϕ is the relative humidity and A, B and C are constants to be determined from experimental data. They were calculated using this procedure for the same particle board as used above as: $A = 1.35x10^{-14}$, $B = 6.49$ and $C = 3.26x10^{-12}$ for a test temperature of 23^{0}C.

Figure 6.6 is a graphical comparison of the permeability curves predicted by equation (6.6), (6.7) and (6.8). It is clear that the two models developed during this research give permeability curves in close agreement with the curve obtained during previous investigations.

As the equation for model 2 is less complex than for model 1, and the determination of the constants does not require absorption isotherms or material porosities, it seems logical than model 2 is the most suitable standard method to adopt.

Fig. 6.5 Ratio of Transfer Coefficients

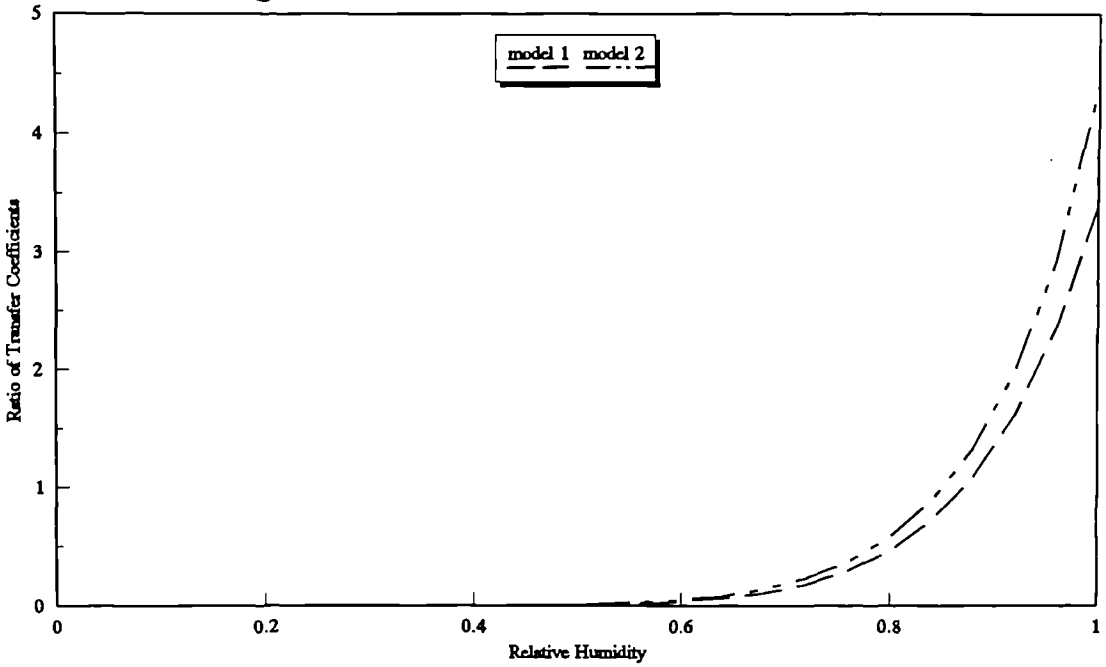

Fig.6.6 Comparison of Prediction Equations

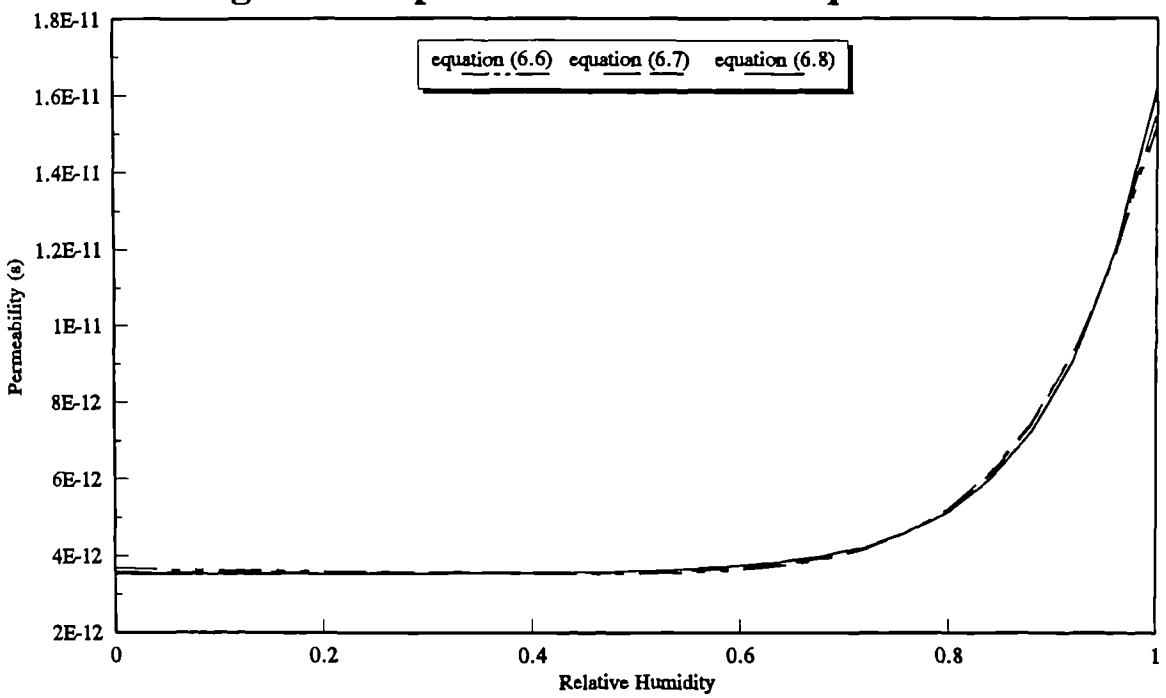

6.1.2 The Pressure Chamber Tests

Test Procedure

The method using different barometric pressures outlined in Chapter 5 requires a pressure chamber arrangement. The chamber should be extremely air tight and maintain a constant pressure. Figure 6.7 is a sketch of the pressure chamber designed. It was made of 12" diameter of steel pipe and consisted of two sub-chambers and a sample mounting panel. The left sub-chamber was 20" long and had a balance sitting on the platform within and a tray of salt solution on top of the balance (Plate 6.9). The right sub-chamber was 10" long and had a tray of salt solution on the platform (Plate 6.10). Both of the sub-chambers had cradles bolted to large platforms to reduce the level of vibration during operation. In between the two sub-chambers, there was a sample mounting panel made of perspex of 6.4mm thick. It contained up to six 64.5mm samples (Plate 6.11). A sketch of the panel is shown in Figure 6.8. The method of mounting the samples was the same as that for the standard isothermal cup. The two sub-chambers and the sample panel were then bolted together. The pressure of the whole chamber was adjusted by the use of a vacuum or compressing pump. Once the pre-determined pressure was reached, the valve leading to the pump was closed with the other two valves left open until the pressures of the two sub-chambers were balanced. Those two valves were then firmly closed. The pressure difference of the two sub-chambers was constantly monitored using a manometer. The signals from the balance and the pressure transducer monitoring the left sub-chamber pressure were fed to a computer. The whole arrangement (Plate 6.12) was located within the environmental chamber with a constant temperature maintained.

When one test was finished, the curve of weight change against time was produced and its gradient used to calculate the average permeability over the

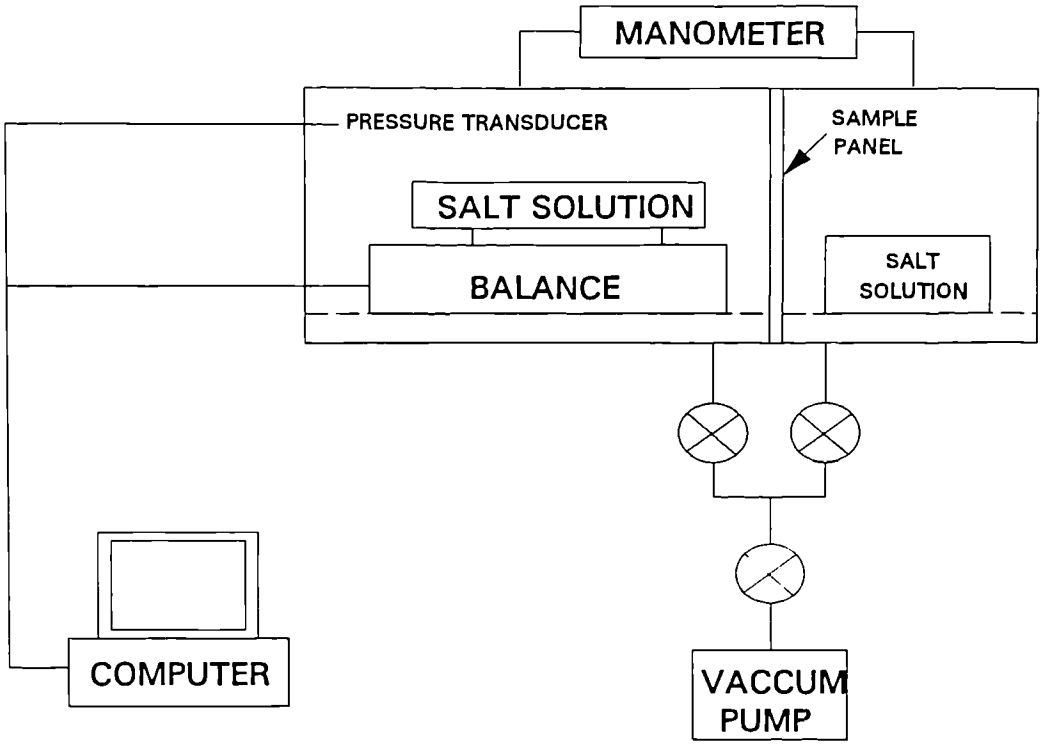

FIGURE 6.7 SKETCH OF THE PRESSURE CHAMBER

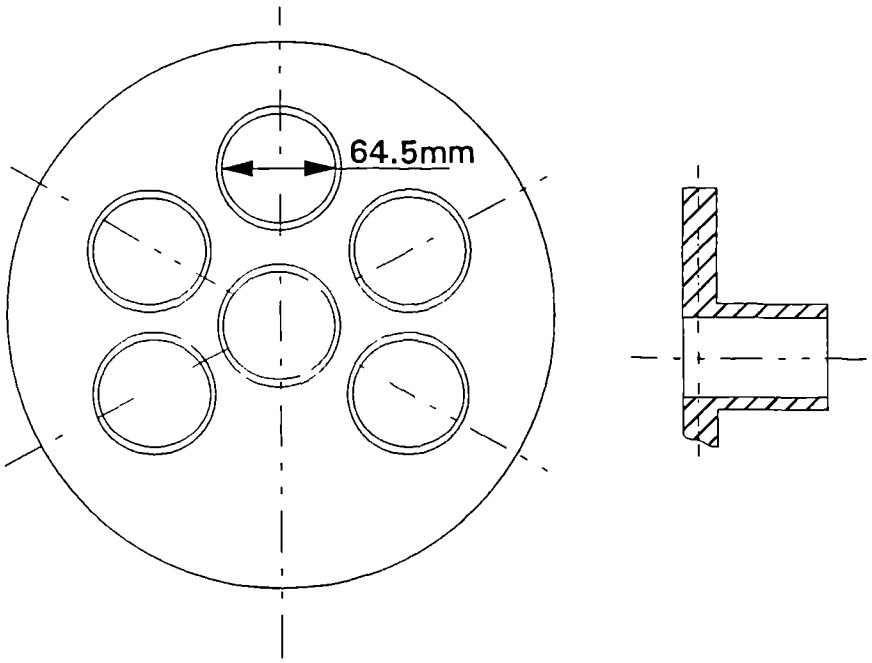

FIGURE 6.8 SAMPLE MOUNTING PANEL

Plate 6.9 Left Sub-chamber of Pressure Chamber

Plate 6.10 Right Sub-chamber of pressure Chamber

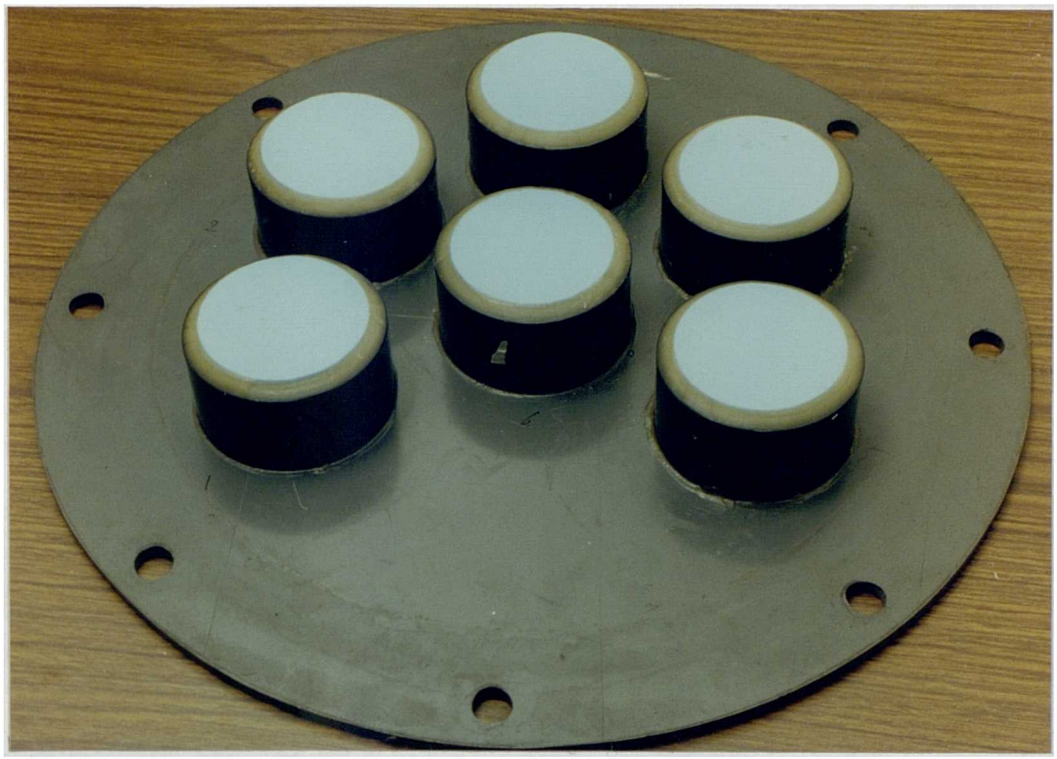

Plate 6.11 Sample Mounting Panel

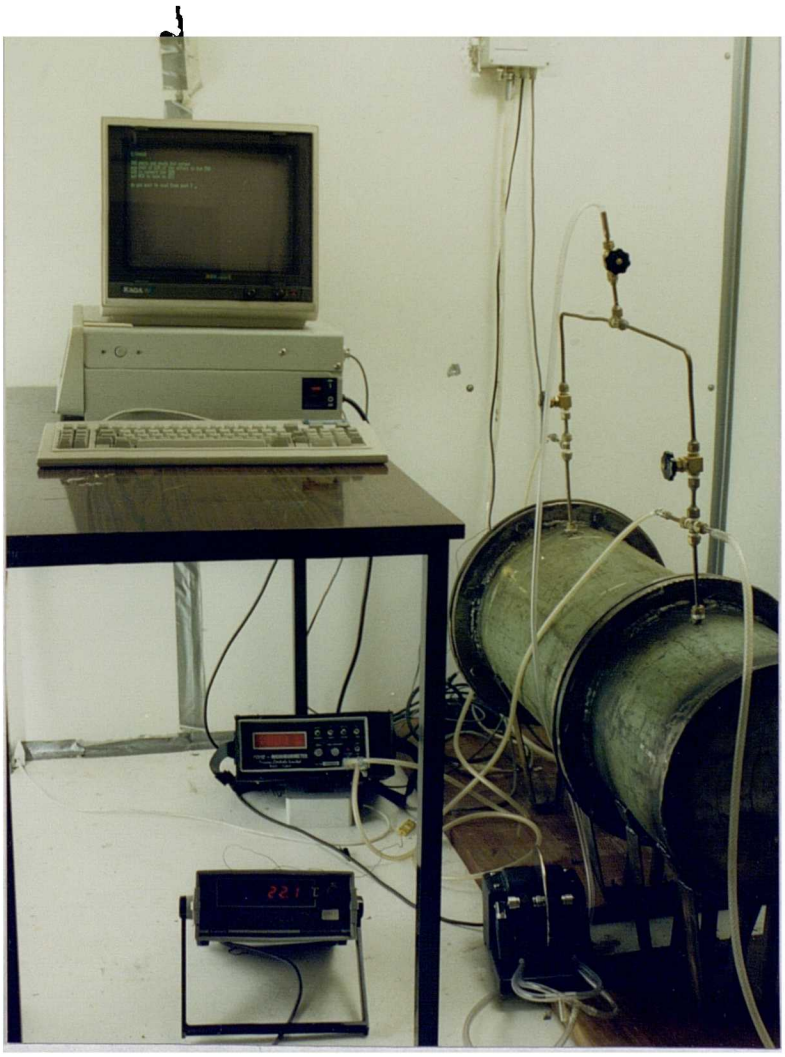

Plate 6.12 Complete Pressure Chamber Arrangement with Associated Equipment

relative humidity range of the test. The pressure chamber was then set to a new pressure. Results of several tests under the same hygroscopic conditions with different pressure were then collected to produce average permeability $\bar{\mu}$ against $1/p$. A straight line should then be obtained, its gradient being the average vapour transfer coefficient $\overline{D''_1}$, the intercept being the average liquid transfer coefficient $\overline{D''_2}$ (see equation (5.20)).

Experimental Conditions and Results

The tests with different barometric pressures were carried out for the hygroscopic Particle Board only. The purpose of the test was to allow further validation of the isothermal cup test method. The practical difficulties associated with this procedure made testing of other materials impossible within the time available. The test conditions used alongside the average permeabilities measured are listed in Table 6.7. The test data is also shown in graphical form as Figure 6.9.

Figure 6.9 clearly indicates the validity of assuming that for Particle Board an inverse relationship exists between permeability and barometric pressure. It would be expected that similar results would have been obtained for other materials. Table 6.8 gives the average vapour transfer coefficient $\overline{D''_1}$ and the average combined liquid transfer coefficient $\overline{D''_2}$ calculated from the experimental results plotted in Figure 6.9.

6.1.3 Comparison of Results

In order to compare the normal cup test method and the pressure chamber method the transfer coefficients of D_1^* and D_2^* of equation (5.16) and (5.17) have to be converted into the average coefficients $\overline{D''_1}$ and $\overline{D''_2}$ corresponding to the relative

Table 6.7 Particle Board Pressure Chamber Test Results

Test Temperature: 23^{0}C		
Relative Humidity Conditions (%)	Test Pressure (bar)	Measured Peameability $\bar{\mu} x 10^{12}$
3 - 58	0.667 0.811 1.009 1.272	4.90 4.016 3.276 2.592
58 - 93	0.701 0.814 1.266	5.911 5.370 4.538

Table 6.8 Calculated Transfer Coefficients For Particle Board Determined From The Pressure Chamber Tests

Test Temperature: 23^{0}C			
Set No.	Test Relative Humidity Conditions (5)	Transfer Coefficients	
		$\overline{D''_1} x 10^{12}$	$\overline{D''_2} x 10^{12}$
1 2	3 - 58 58 - 93	3.22 2.11	0.064 2.85

FIGURE 6.9 PRESSURE CHAMBER TEST RESULTS FOR PARTICLE BOARD

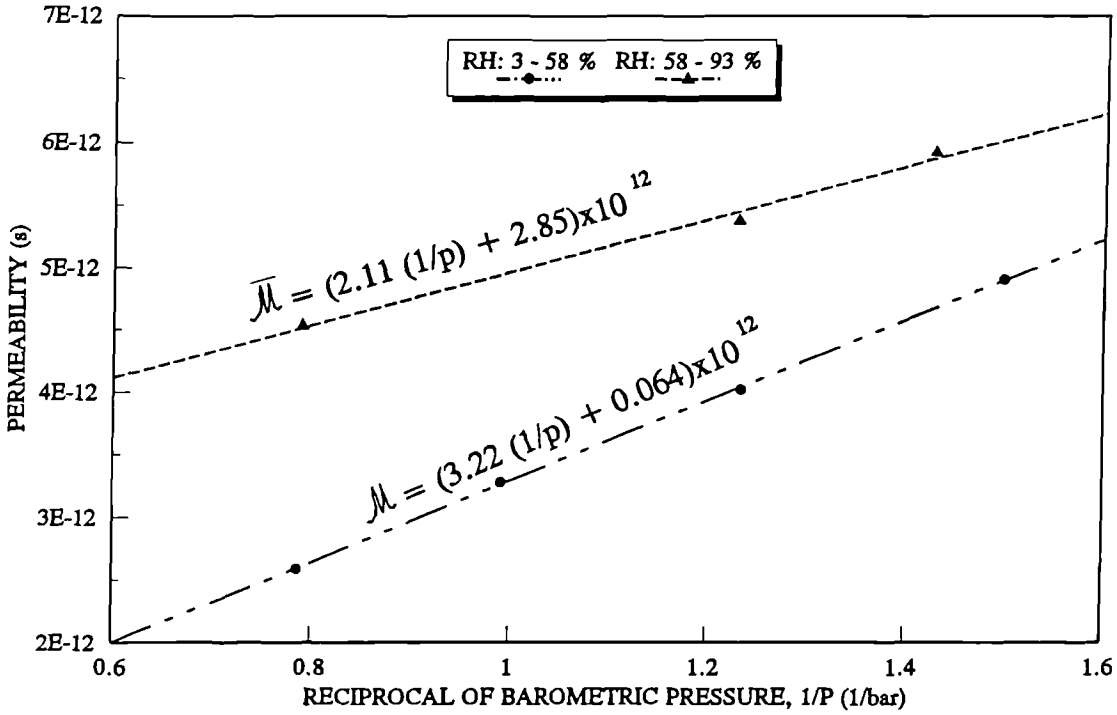

humidity ranges used in the test. This averaging procedure is carried out using equations (6.2) and (6.3) as before. $\overline{D^*_1}$ multiplied by standard barometric pressure should then equate to the measured coefficient $\overline{D''_1}$, and $\overline{D^*_2}$ should equate to the measured coefficient $\overline{D''_2}$.

Table 6.9 lists the predicted average transfer coefficients for particle board determined using both models 1 and 2, alongside the test results from the pressure chamber method. The coefficients are in good agreement, with minimal discrepancy between them considering the experimental error involved and the fact that different sets of samples were used for the tests. The varying vapour flow equation of Model 1 and the pressure chamber method both predict a drop of vapour transfer rate with increased relative humidity, and vice versa for the liquid transfer.

For particle board over the range of relative humidity between 3 - 58%, the liquid flow accounts for 1.9% of the total flow predicted by the pressure chamber method, in comparison with 0.4% for Model 1 and 0.3% for Model 2. At relative humidities between 58 - 93%, the pressure chamber method predicted 57.5% liquid flow while Model 1 and Model 2 predicted 36.2% and 31.9% respectively.

It is important to recognise that although the same materials were used in each set of experiments, there may have existed differences between the sample structures and hence their behaviour. Considering the inherent experimental inaccuracies associated with testing of this nature, the results for the pressure chamber investigation appear to be reasonably consistent with the data from Model 1 or Model 2.

Table 6.9 Comparison of Different Methods for the Determination of Transfer Coefficients For Particle Board

Models	Transfer Coefficients			
	RH: 3 - 58		RH: 58 - 93	
	Vapour $\frac{}{D''_1 x 10^{12}}$	Water $\frac{}{D''_2 x 10^{12}}$	Vapour $\frac{}{D''_1 x 10^{12}}$	Water $\frac{}{D''_2 x 10^{12}}$
Constant Vapour Model with Normal Cup Tests	3.55	0.010	3.55	1.67
Varying Vapour Model with Normal Cup Tests	3.55	0.015	3.33	1.89
Pressure Test	3.22	0.064	2.11	2.85

Table 6.10 Constants for Sorption Isotherm Correlations

Test Material	Temperature (^{0}C)	u_h	A	n
Particle Board	23	0.2683	7.32×10^{-2}	1.90
Plywood	20	0.3984	0.309	1.66
Wood	20	0.4198	0.453	1.59
Brick	20	7.73×10^{-3}	0.107	1.91
Thin Plasterboard	20	0.26	2.32×10^{-4}	4.02
Thick Plasterboard	20	0.19	7.5×10^{-4}	4.00
Extruded polystyrene	23	0.0184	2.63×10^{-3}	10.65
Expanded Polystyrene	20	0.0508	1.31×10^{-3}	2.10

6.2 Material Sorption Isotherms

Material sorption isotherms are required by the governing equations of the transfer process outlined in Chapter 4, to relate the vapour pressure with the level of the material moisture content. This information is also necessary for the evaluation of the effective vapour transfer area for the varying vapour transfer coefficient model (equation (5.15)). Figure 6.11 shows a typical sorption isotherm. The upper curve represents the desorption process, with materials drying out and releasing moisture; the lower curve represents the absorption process with materials wetting and intaking moisture. The transition from one equilibrium state to another follows an intermediate scanning curve which lies within the two boundary curves. The reason for the discrepancy between the absorption and desorption process and the 'hysteresis effect', as it called, is not clearly understood, though a variety of theories have been presented (see Chapter 3).

6.2.1 Experimental Procedure

Sorption isotherms were constructed for both the absorption and desorption processes. The absorption isotherms were obtained by firstly equilibriating material samples with dry dessicant and then moving them to environments of higher relative humidity. The desorption processes were carried out by equilibriating material samples with 100% relative humidity and then shifting them to environments of lower relative humidity. Weight changes of samples were then monitored until they reached equilibrium. All procedures were carried out under the same temperature. In general a total of six samples were used at each test condition, the samples themselves being only small cubes of materials to reduce the amount of time required for equilibrium. Each individual relative humidity required was maintained by a suitable salt solution

contained in a plastic box sealed by aluminium tape (Plate 6.13). The equilibriated samples were dried in an oven at 70^0C to determine their moisture content (Plate 6.14).

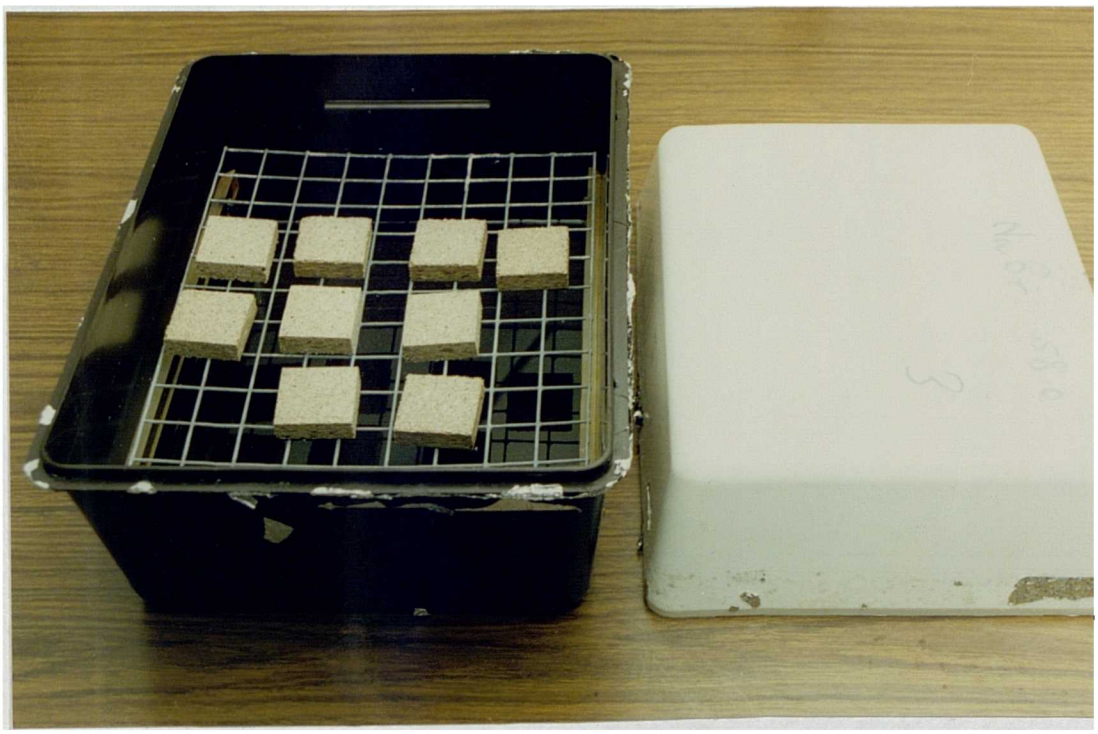

Plate 6.13 Containers Used for Sample Equilibrium

Plate 6.14 Oven for Sample Drying at 70°C

Fig.6.10 Typical Sorption Isotherm

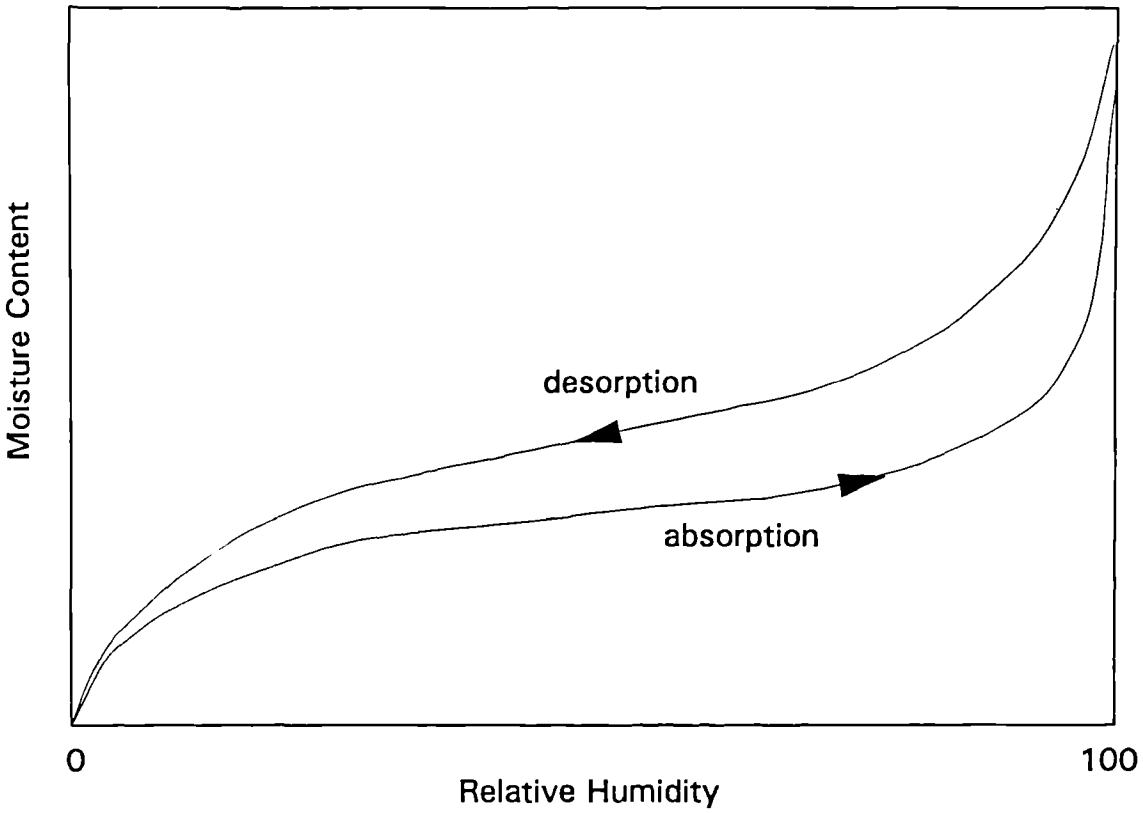

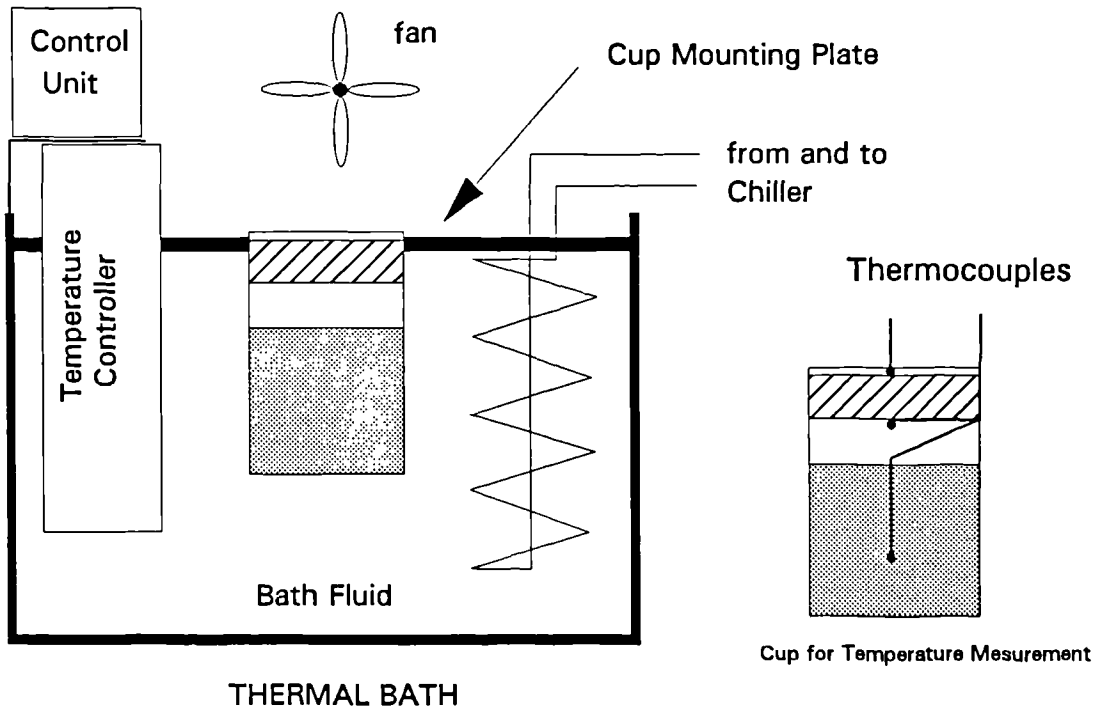

Fig.6.11 Experimental Arrangement for Thermal Diffusion Test

6.2.2 Results and Their Interpretation

The equilibrium moisture contents obtained over a range of relative humidity conditions are given for each of the materials investigated in Appendix Two. In theory, for each material the mean values of the absorption and desorption process could be used to produce a single correlation which approximates the sorption isotherm. There are several correlations proposed in the literature[35][51][52], the one most commonly used is that suggested by Hansen[37]:

$$u = u_h\left(1 - \frac{\ln \phi}{A}\right)^{-\frac{1}{n}} \qquad (6.9)$$

where u: the moisture content, kg/kg.

u_h, A and n are experimentally determined constants.

In practice it was found that the time periods required for material equilibrium were very long (over ten weeks for some hygroscopic materials). As a result of this, absorption and desorption curves were determined for extruded polystyrene only, a single curve being measured for the remaining materials. For the same reason, the test were carried out at one temperature, namely 23°C for extruded polystyrene and particle board, and 20°C for the other materials.

Table 6.10presents the three constants for the above correlation, equation (6.9), applied to all of the materials given in Table 6.1.

6.3 Investigation of Thermal Diffusion Effects

The magnitude and importance of moisture thermal diffusion effects within building materials, or more generally through any porous body, has not been clearly established by researchers. Although this effect has been neglected in most of the theoretical investigations documented in literature, experimental results are not available in the literature to justify this action. It is therefore necessary to clarify its role in the process of moisture transfer through porous materials.

6.3.1 Experimental Procedure

Figure 6.11 is a schematic drawing of the experimental arrangement used in this investigation. The environmental chamber was operated at conditions of 23^0C and 60% relative humidity. The thermal bath was set to a constant temperature of 15^0C. The materials used in this test were the hygroscopic particle board and the non-hygroscopic extruded polystyrene. Six samples of 64.5mm diameter of each material were mounted into glass beakers using the procedure outlined in Section 6.1.1. Salt solutions were used to maintain a constant vapour pressure within the beakers. These beakers were then placed into the thermal bath with only one sample surface exposed to the environmental chamber (Plate 6.15). In order to prevent contamination of the beaker surface by the fluid of the thermal bath, each beaker was enclosed by a thin plastic sheath before being placed in the cup mounting plate (Plate 6.16). This enabled a temperature gradient as well as a vapour concentration gradient to be introduced across the samples. The weights of these beakers were measured daily until the moisture transfer reached the stage of equilibrium. An additional 'dummy' cup was used to monitor the temperature variation of the sample surfaces and of the salt solution. Three thermocouples were used, one on each sample surface, and one within the salt solution (Figure 6.11 and Plate 6.17).

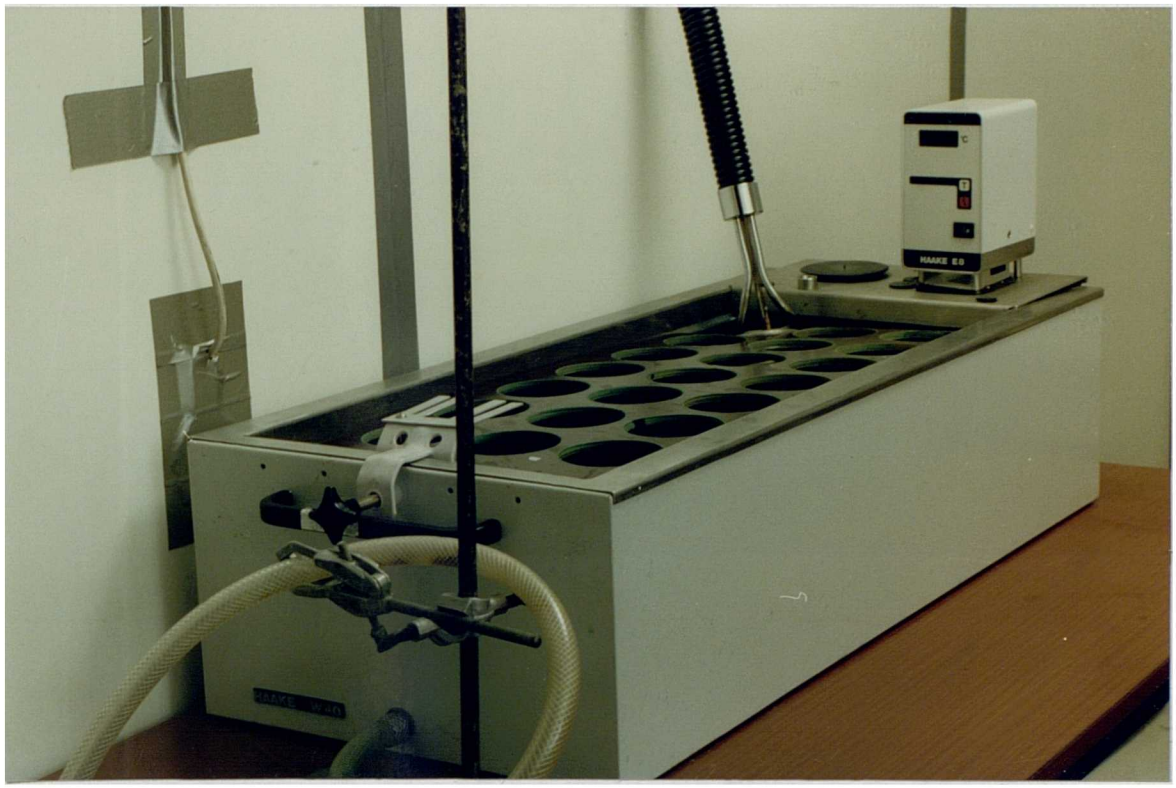

Plate 6.15 Thermal Bath Used for Thermal Diffusion Experiments

6.3.2 Experimental Results and Analysis

If it is assumed that the thermal diffusion effects for moisture transfer can be neglected, then the diffusion equation could be written as:

$$j_{diff} = -D_v \nabla \rho_v \qquad (6.10)$$

where j_{diff}: normal moisture diffusion rate, kg/m^{2}s

D_v: diffusion coefficient, m^2/s

ρ_v: vapour concentration or density, kg/m^3.

When the cups reach equilibrium, the vapour density gradient could be simplified as:

$$\begin{aligned} \nabla \rho_v &= \frac{\Delta \rho_v}{\zeta} = -\frac{\rho_{v1} - \rho_{v2}}{\zeta} \\ &= -\left(\frac{p_{v1}}{T_1} - \frac{p_{v2}}{T_2} \right) / \zeta R \\ &= -\left(\frac{p_{s1}\phi_1}{T_1} - \frac{p_{s2}\phi_2}{T_2} \right) / \zeta R \end{aligned} \qquad (6.11)$$

where ζ: sample thickness, m

ϕ: relative humidity

p_s: saturated vapour pressure, N/m^2

subscript 1 and 2 denote the sample inner and outer surface respectively.

The diffusion coefficient, D_v, is a function of temperature and relative humidity. For simplicity, an arithmetic average value across the sample is used, so that:

Plate 6.16 Thin Plastic Sheath Used to Avoid Cup Contamination

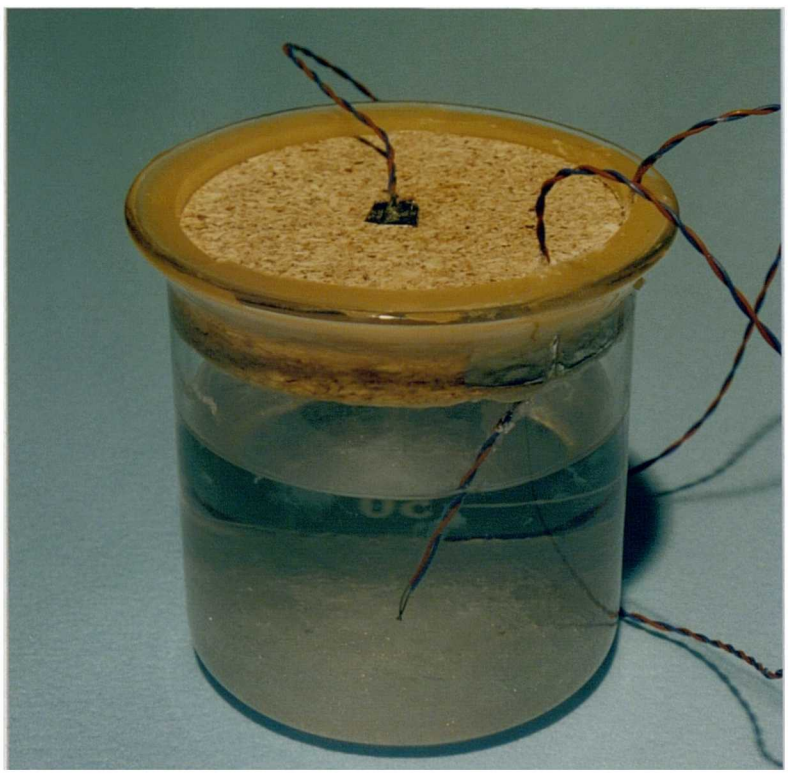

Plate 6.17 'Dummy' Test Cup with Thermocouples Attached

$$\overline{D}_v = \frac{(D_{v1} + D_{v2})}{2} \qquad (6.12)$$

where $\overline{D}_v$: average diffusion coefficient over the temperature and relative humidity difference, m^2/s

Applying the perfect gas law to equation (6.10):

$$j_{diff} = -D_v \rho_v \left[\frac{1}{p_v} \nabla p_v - \frac{1}{T} \nabla T \right]$$

$$= -\frac{\rho_v}{p_v} D_v \nabla p_v + \frac{\rho_v}{T} D_v \nabla T \qquad (6.13)$$

For isothermal conditions, equation (6.13) becomes:

$$j_{diff} = -\frac{\rho_v}{p_v} D_v \nabla p_v = -\mu \nabla p_v \qquad (6.14)$$

which is the standard diffusion equation used for building applications, with μ as the isothermal permeability.

The diffusion coefficient D_v in this case is therefore:

$$D_v = \mu \frac{p_v}{\rho_v} = \mu R_v T \qquad (6.15)$$

where R_v: gas constant for vapour, 461.5 J/kgK

Substituting equation (6.15) into equation (6.12) gives:

$$\overline{D_v} = \frac{(D_1 + D_2)}{2}$$

$$= \frac{(\mu_1 T_1 + \mu_2 T_2) R_v}{2} \qquad (6.16)$$

Substituting equation (6.11) and equation (6.16) into equation (6.10) gives the diffusion rate for cups under equilibrium conditions as:

$$j_{diff} = \frac{1}{2\zeta}[\mu_1 T_1 + \mu_2 T_2]\left[\frac{p_{s1}\phi_1}{T_1} - \frac{p_{s2}\phi_2}{T_2}\right] \qquad (6.17)$$

μ_1: isothermal spot permeablity at position 1.

μ_2: isothermal spot permeablity at position 2.

It has been shown elsewhere by the author[53] that the functional dependence of the isothermal permeability on temperature can be neglected over the range of temperatures found in buildings. The values of permeability in this equation can be given , therefore, as the spot values of isothermal permeability corresponding to the relative humidity conditions ϕ_1 or ϕ_2.

If thermal diffusion does influence the process of moisture transport, the complete equation of moisture transfer would be:

$$j = j_{diff} + j_{therm} \qquad (6.18)$$

where j: total moisture transfer rate, kg/m^{2}s

j_{therm}: moisture thermal diffusion rate, kg/m^{2}s.

It is important to note that j_{therm} is not the second term of equation (6.13), which has already been included in j_{diff}. j_{therm} is the diffusion transfer solely by the temperature gradient when the vapour concentration gradient is zero.

From equation (6.18), it follows:

$$j_{therm} = j - j_{diff} \tag{6.19}$$

And the percentage of the total moisture transfer caused by thermal diffusion can then be expressed as:

$$y = \left(\frac{j_{therm}}{j} \right) x\,100 = \left(1 - \frac{j_{diff}}{j} \right) x\,100 \tag{6.20}$$

Equation (6.17) was used to predict the amount of moisture diffusion which would be expected if no thermal diffusion effects were present. The permeability values μ_1 and μ_2 in this equation were determined using the constants given in Table 6.5 combined with equation (5.16).

These values were then compared with the total moisture transfer rate measured from the thermal diffusion experiments and the proportion of thermal diffusion calculated using equation (6.20). Table 6.11 and 6.12 show the results obtained for both the particle board and the extruded polystyrene.

It would appear from these results that the effects of thermal diffusion are small, and that by neglecting such effects in the governing equations any associated error would be of little significance.

Table 6.11 Thermal Diffusion Effects for Particle Board

No. Of Test	RH_1	RH_2	T_1 ^0C	T_2 ^0C	j kg/m^2s $x10^{-7}$	j_{diff} kg/m^2s $x10^{-7}$	j_{therm} kg/m^2s $x10^{-7}$	y %
1	60	0	22.6	19.5	4.856	4.841	0.015	0.3
2	60	33	22.3	19.3	3.174	3.186	-0.012	-0.4
3	60	44	22.1	18.8	2.997	2.772	0.225	7.5
4	60	76	22.5	18.8	1.286	1.366	-0.080	-6.2

Table 6.12 Thermal Diffusion Effects for Extruded Polystyrene

No. Of Test	RH_1	RH_2	T_1 ^0C	T_2 ^0C	j kg/m^2s $x10^{-7}$	j_{diff} kg/m^2s $x10^{-7}$	j_{therm} kg/m^2s $x10^{-7}$	y %
1	61.5	0	22.4	16.0	1.290	1.400	-0.110	-8.5
2	61.5	77.5	22.4	16.3	0.315	0.299	0.016	5
3	61.5	44.0	22.4	16.4	0.695	0.784	-0.089	-12.8

7. COMPUTER PREDICTION MODEL

The previous chapter presented experimental methods which can be used to measure the material properties required by the equations of mass and energy conservation. These governing equations for heat and mass transfer through porous materials were developed in Chapters 4 and 5, and are summarised for convenience in Table 7.1. Inspection of this table shows that they are all partial differential equations, which will require the use of numerical analysis techniques for their solution. The equations in Table 7.1 are presented in their generalised form, and can be applied to one, two or three dimensional problems.

In this chapter the one dimensional flow problem will be investigated, although the principles involved could equally be applied to multi-dimensional analysis. The one-dimensional situation is much simpler to formulate and is applicable, with little error, to the central areas of building envelopes. A methodology for the solution of the governing equations will be developed and combined with realistic boundary conditions to enable the performance of simple building structures to be investigated.

7.1 The Finite Difference Method

Many textbooks have been produced which outline the principles of applying numerical methods to the solution of partial differential equations[54][55][56][57][58]. The intention here is to provide a brief outline of the discretization method used in this work, rather than a complete description of numerical methods. More detailed information on this subject is widely available to the reader elsewhere.

Numerical methods are, of course, approximate and produce results at discrete time intervals. Of the numerical methods available, those involving finite difference approximations are straight forward, are more frequently used, and are generally

Table 7.1 Governing Equations

Material Type	Governing Equations	Euqation No.
Hygroscopic	Mass Conservation: $\frac{\partial(\rho_o u)}{\partial t} = -\nabla \cdot j$	(4.2)
	Energy Conservation: $c\rho_0 \frac{\partial T}{\partial t} = -\nabla \cdot q_{q\_cond} - j_i c_i \nabla T + L\nabla \cdot j_1$	(4.14)
	Moisture Flow Rate: $j = j_1 + j_2 = -\left(\frac{D_1}{R_v T} + \frac{D_2 R_v T \rho_2}{p_1}\right)\nabla p_1 - \left[D_2 R_v \rho_2 \left(\ln\phi - \frac{L}{R_v T}\right) - \frac{p_1 D_1}{R_v T^2}\right]\nabla T$	(5.6)
	Moisture Content: $u = u_h\left[1 - \frac{1}{A}\ln\phi\right]^{-\frac{1}{n}}$	(6.9)
Non hygroscopic	Mass Conservation: $\frac{\partial(\rho_o u)}{\partial t} = -\nabla \cdot j$	(4.2)
	Energy Conservation: $a_k^T \frac{\partial T}{\partial t} + a_k^{p_1} \frac{\partial p_1}{\partial t} = -\nabla \cdot q_{q\_cond} - j_i c_i \nabla T + \sum_{i=1}^{2} h_i \nabla \cdot j_i$	(4.22)
	Moisture Flow Rate: $j = j_1 + j_2 = -\left(\frac{D_1}{R_v T} + \frac{D_2 R_v T \rho_2}{p_1}\right)\nabla p_1 - \left[D_2 R_v \rho_2 \left(\ln\phi - \frac{L}{R_v T}\right) - \frac{p_1 D_1}{R_v T^2}\right]\nabla T$	(5.6)
	Moisture Content: $u = u_h\left[1 - \frac{1}{A}\ln\phi\right]^{-\frac{1}{n}}$	(6.9)

more applicable than any other[55]. Finite difference methods are concerned with approximating partial derivatives with a truncated Taylor's series expansion[56]. There are a variety of methods available to preform this 'discretization' of partial differential equations, including both explicit and implicit formulations.

Explicit finite difference approximations are used in this case as they are the most straightforward and involve formulas which express one unknown value at a new time step directly in terms of known values at a previous time step. Explicit methods are easier to formulate and solve, as they do not require simultaneous solution of equations. However, their solution is only stable under restrictive conditions. The stability criterion for an explicit finite difference equation is such that the time step for solution cannot be chosen independently of the spatial distance between discrete nodal points. This generally results in smaller time steps being used than are strictly necessary, with the consequence that an excessive amount of computing power may be required to reach a final solution.

Three separate finite difference approximations have been used to represent the derivatives which appear in the governing equations. The equations are discussed with reference to Figure 7.1, superscripts being used to represent the time step being considered, while subscripts relate to the relevant nodal position.

The first order partial derivatives with respect to time are approximated using a two-point forward finite difference as[59]:

$$\frac{\partial y}{\partial t} = \frac{y_i^{k+1} - y_i^k}{\Delta t} \qquad (7.1)$$

where y: variable being considered

t: time, s.

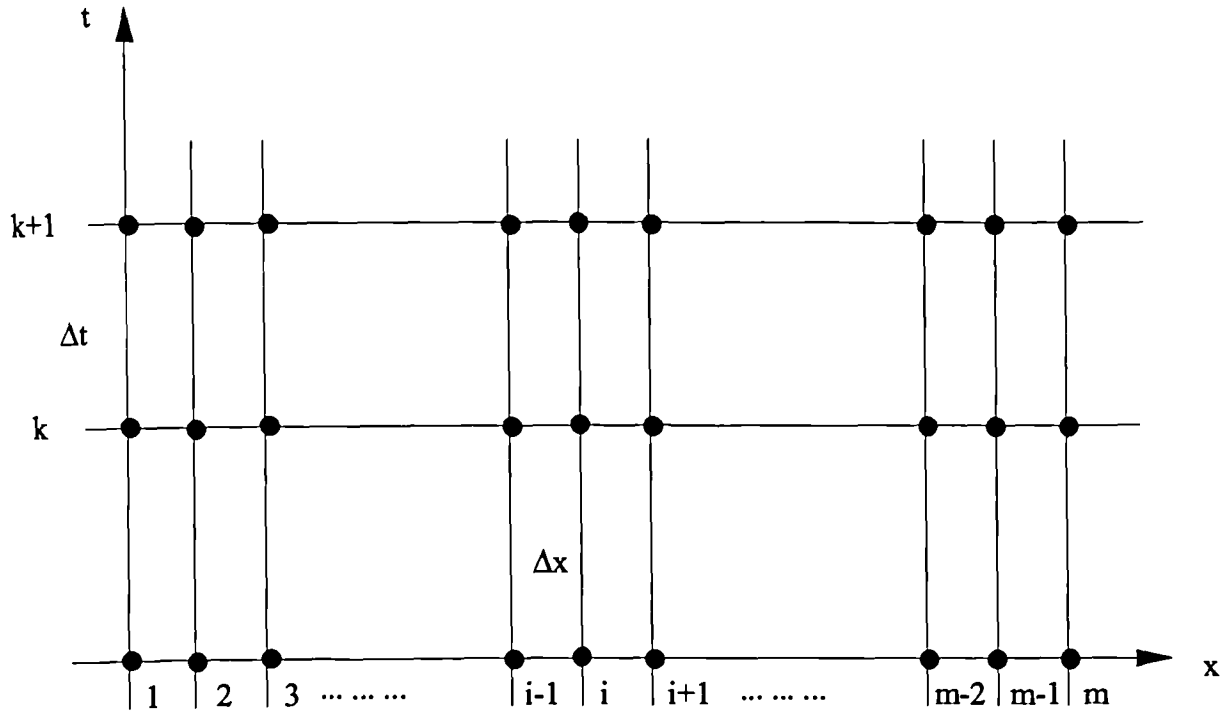

Fig. 7.1 Finite Difference Scheme

Δt: time step, s.

k: kth time step, k=0,1,2,...n

i: ith nodal point, i=1,2,3,...m

For derivatives with respect to the space dimension, x, a central difference approximation is used for first order derivatives, while the standard three point method is used for the second order derivatives[59]. Thus:

$$\frac{\partial y}{\partial x} = \frac{y_{i+1}^k - y_{i-1}^k}{2\Delta x} \tag{7.2}$$

$$\frac{\partial^2 y}{\partial x^2} = \frac{y_{i+1}^k - 2y_i^k + y_{i-1}^k}{(\Delta x)^2} \tag{7.3}$$

where Δx: the step in space dimension between nodal points.

Equations (7.2) and (7.3) can only be applied to points within materials. For derivatives on surfaces, a three point scheme has been employed as[59]:

Left surface $$\left.\frac{\partial y}{\partial x}\right|_{i=1} = \frac{-3y_1^k + 4y_2^k - y_3^k}{2\Delta x} \tag{7.4}$$

Right surface $$\left.\frac{\partial y}{\partial x}\right|_{i=m} = \frac{3y_m^k - 4y_{m-1}^k + y_{m-2}^k}{2\Delta x} \tag{7.5}$$

All of the above equations are approximations in that their derivation involves the truncation of a Taylor's series expression. The truncation error is of the order of (Δt) for equation (7.1) and of the order of $(\Delta x)^2$ for the remaining equations (7.2) to (7.5).

The governing equations of Table 7.1. have been discretized using the above difference representations to allow their solution by computer. The numerical form of these equations has been given for reference in Table 7.2.

Table 7.2 Governing Equations in Numerical Form

Material Type	Governing Equations
Hygroscopic	**Mass Conservation:** $u_i^{k+1} = u_i^k - \frac{\Delta t}{\rho_0} \nabla \cdot j_i^k$ **Energy Conservation:** $T_k^{k+1} = T_i^k - \frac{\Delta t}{c\rho_0}\left[\lambda_i \frac{T_{i+1}^k - 2T_i^k + T_{i-1}^k}{\Delta x^2} - j_i^k c_i \frac{T_{i+1}^k - T_{i-1}^k}{\Delta x} + L\nabla j_{1i}^k\right]$ **Moisture Flow Rate:** $j_i^k = j_{1i}^k + j_{2i}^k$ $= -\left(\frac{D_1}{R_v T_i^k} + \frac{D_2 R_v T_i^k \rho_2}{p_{1i}^k}\right)\frac{p_{1(i+1)}^k - p_{1(i-1)}^k}{\Delta x} - \left[D_2 R_v \rho_2\left(\ln\phi_i^k - \frac{L}{R_v T_i^k}\right) - \frac{p_{1i}^k D_1}{R_v T^{k2}_i}\right]\frac{T_{1(i+1)}^k - T_{1(i-1)}^k}{\Delta x}$ Within Materials: $\nabla \cdot j_i^k = \frac{j_{i+1}^k - j_{i-1}^k}{2\Delta x}$ Left Surfaces: $\nabla \cdot j_i^k = \frac{-3j_i^k + 4j_{i+1}^k - j_{i+2}^k}{2\Delta x}$ Right Surfaces: $\nabla \cdot j_i^k = \frac{3j_i^k - 4j_{i-1}^k + j_{i-2}^k}{2\Delta x}$ **Substituting j_i^k with j_{1i}^k in the above three equations gives expressions for ∇j_{1n}^k**

(continue to next page)

(continued from previous page)

Table 7.2 Governing Equations in Numerical Form

Material Type	Governing Equations
Non-hygroscopic	The same as for hygroscopic materials except for the energy equation which becomes: $$T_i^{k+1} = T_i^k + \frac{1}{\left[a_k^T + a_k^{p_1} \left(\frac{\partial p_s}{\partial T} \right)_i^k e^{\Lambda \left[1 - \left(\frac{u_i^k}{uh} \right)^{-n} \right]} \right]}$$ $$x \left[\lambda_i \frac{T_{i+1}^k - 2T_i^k + T_{i-1}^k}{\Delta x^2} - j_i c_i \frac{T_{i+1}^k - T_{i-1}^k}{2\Delta x} + \sum_{i=1}^{2} h_i \nabla \cdot j_i^k - a_k^{p_1} p_s \frac{An}{u_i^k} \left(\frac{u_i^k}{uh} \right)^{-n} e^{\Lambda \left[1 - \left(\frac{u_i^k}{uh} \right)^{-n} \right]} \left(\frac{\partial u}{\partial t} \right)_i^k \right]$$ where $(\partial u / \partial t)$ is obtained form mass conservation $(\partial p_s / \partial T)$ is readily available from the Clausius Clapeyron Equation

7.2 Boundary Conditions

The solution of the governing equations requires the specification of appropriate boundary conditions. Such boundary conditions must be established for external surfaces, internal surfaces and for the interfaces between different material elements.

The boundary equations applied within this model are analysed in detail within Appendix Three, and involve the application of standard mass and energy flow relationships. In this section a brief description is given of the solution strategy involved when dealing with different boundary types.

There are considered by the author to be five different boundary situations which may be encountered in work of this nature, as follows:

(a) material to air (external & internal environment)
(b) material to material
(c) material to air gap to material
(d) material to vapour barrier to material
(e) material to vapour barrier to air gap to material
(f) material to air gap to vapour barrier to material

The first two items in this list are standard boundary conditions as normally encountered. Items (c) to (f), though not strictly single boundary relationships, can be solved with much greater simplicity if handled using boundary type equations. These items involve an air gap and/or a vapour barrier which will influence the flow process in a manner which can be considered analogous to a boundary resistance. Each of these boundary conditions are illustrated graphically as Figure 7.2.

If the assumption is made that there is no accumulation of mass or energy on surfaces, a simple mass and energy balance can be carried out at each boundary. It is also assumed in this analysis that where air gaps exist, they are unventilated and

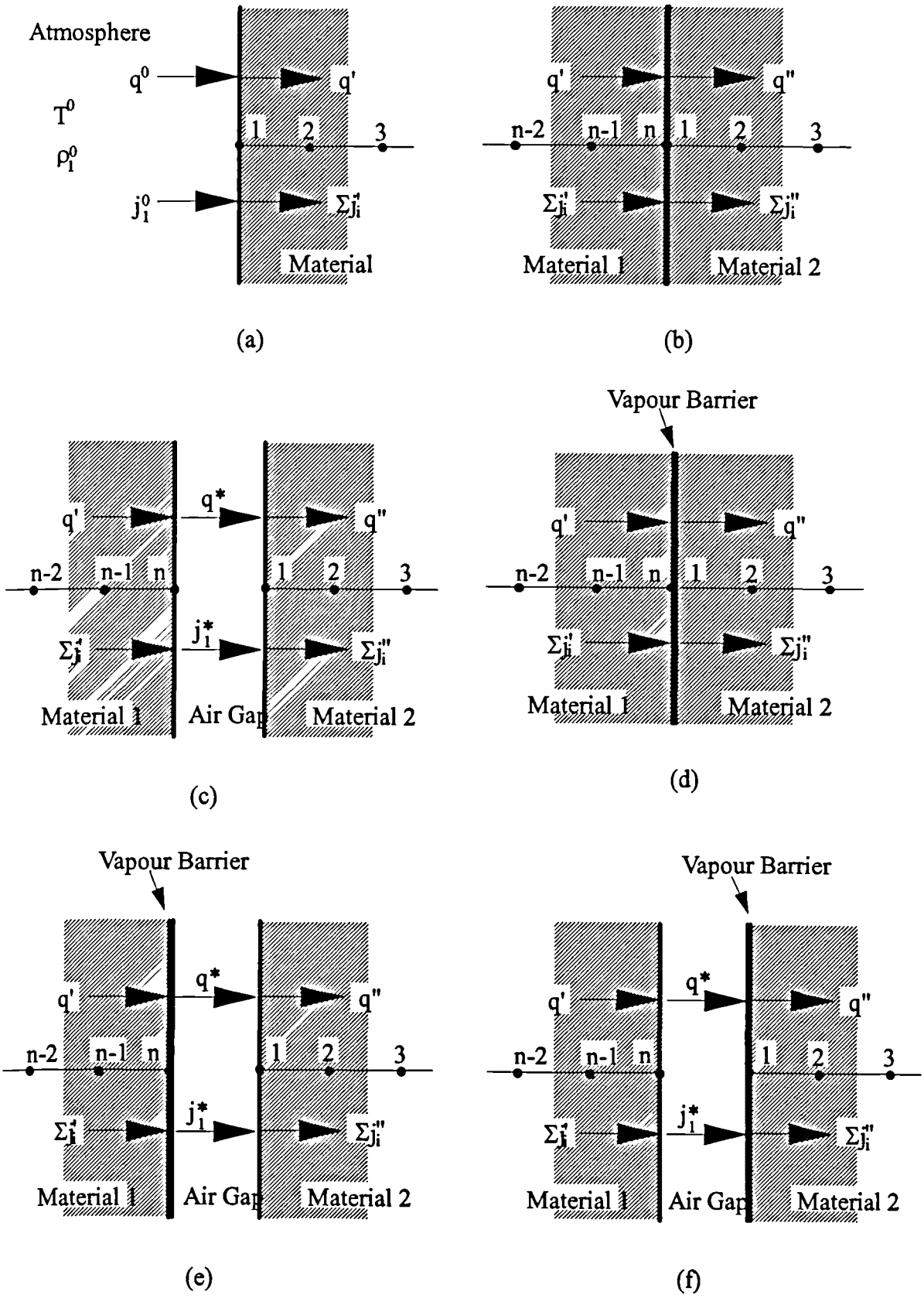

Fig.7.2 Graphical Presentation of Boundary Types

no mass or energy input occurs within the cavity. Vapour barrier elements are handled as if they resist completely the passage of liquid water and permit only small amounts of vapour diffusion depending upon their permeability. The thermal resistance of a vapour barrier is taken to be zero.

The conservation equations applied to each boundary type are presented for reference as Table 7.3. These equations can be applied to known conditions at a previous time step and used to calculate the values of the state variables at the new time step.

Table 7.3 Bounadry Conservation Equations

Boundary Type	Boundary Conservation	
	Mass	Energy
(a)	$j_1^0 = \sum j'_i$	$j_1^0 h_1^0 + H(T^0 - T'_1) = \sum j'_{il} h'_{il} - \lambda'_1 \nabla T'_1$ where H: total heat transfer coefficient
(b)	$\sum j'_{in} = \sum j''_{il}$ $\rho'_{1n} = \rho'_{11}$ $P'_{1n} = P''_{11}$	$\sum j'_{in} h'_{in} - \lambda'_n \nabla T'_n = \sum j''_{il} h''_{il} - \lambda''_1 \nabla T''_1$ $T'_{in} = T''_{11}$
(c)	$\sum j'_{in} = j_1^* = \sum j''_{il}$ $j_1^* = -\frac{1}{\xi^*}(P''_{11} - P''_{1n})$ where ξ^*: vapour resistance	$\sum j'_{in} h'_{in} - \lambda'_n \nabla T'_n = q^* = \sum j''_{il} h''_{il} - \lambda''_1 \nabla T''_1$ $q^* = -(T''_{11} - T'_{in}) H^*$ where H^*: air gap heat transfer coefficient
(d)	$\sum j'_{in} = j_1^* = \sum j''_{il}$ $j_1^* = -\frac{1}{\xi^*}(P''_{11} - P''_{1n})$ where ξ^*: vapour resistance	$\sum j'_{in} h'_{in} - \lambda'_n \nabla T'_n = \sum j''_{il} h''_{il} - \lambda''_1 \nabla T''_1$ $T'_{in} = T''_{11}$
(e)	$\sum j'_{in} = j_1^* = j_1^* = \sum j''_{il}$ $j_1^* = j_1^* = -\frac{1}{\xi^* + \xi^*}(P''_{11} - P''_{1n})$	$\sum j'_{in} h'_{in} - \lambda'_n \nabla T'_n = q^* = q^* = \sum j''_{il} h''_{il} - \lambda''_1 \nabla T''_1$ $q^* = q^* = -(T''_{11} - T'_{in}) H^*$ vapour barrier has no heat resistance
(f)	$\sum j'_{in} = j_1^* = j_1^* = \sum j''_{il}$ $j_1^* = j_1^* = -\frac{1}{\xi^* + \xi^*}(P''_{11} - P''_{1n})$	$\sum j'_{in} h'_{in} - \lambda'_n \nabla T'_n = q^* = q^* = \sum j''_{il} h''_{il} - \lambda''_1 \nabla T''_1$ $q^* = q^* = -(T''_{11} - T'_{in}) H^*$ vapour barrier has no heat resistance

7.3 Stability and Convergence of Numerical Solutions

As stated in Section 7.1, numerical methods produce approximate solutions to physical problems involving partial differential equations. Any differences in result between a non-exact numerical solution and an exact analytical analysis will be caused by two inaccuracies:

(1) the truncation errors caused by discretization of the equations.

(2) the round-off errors occurring during the repetitive arithmetic operations of the computer.

Truncation errors are of concern in terms of numerical convergence and relate to the accuracy of the numerical procedure. Round-off errors are of concern in terms of instability of solution. Instability will exist where any error introduced will be amplified and will grow as the calculation proceeds from one marching time step to the next.

In general the analysis of convergence of a numerical procedure is difficult to carry out. However, Lax's Equivalence Theorem[59] states that given a properly posed initial value problem and a finite difference approximation that satisfies consistency, stability is the necessary and sufficient condition for convergence. This theorem is widely applied in most computational work, although it has never been proven for non-linear partial differential equations. Assuming that Lax's theorem may be applied to the non-linear equations of this work, the existence of a stable solution can be considered an adequate indication that the solution will both be stable and will converge.

While it is very difficult and complicated to carry out a detailed theoretical analysis of stability for individual non-linear partial differential equations, it is almost

impossible to do so for a set of equations, in a way which fully accounts for the influence of boundary conditions. Such an analysis is, in any case, not considered necessary or appropriate for this research work, and only an approximate approach is used. If the computational efficiency of the model requires to be improved in the future, a more detailed analysis may be considered useful.

Examining the governing equations (4.1) and (4.13) and considering that the moisture transfer is a very slow diffusion process, the stability condition required for the mass conservation equation is likely to be less restrictive than that for energy conservation. Therefore, stability of the energy equation is likely to imply stability for the complete set of governing equations.

In the energy equation (4.13), the temperature variation with time is caused by heat conduction, convection and phase conversion. Generally speaking, heat conduction will be dominant while convection and phase conversion will be proportionally small. If an error is generated, it would be expected that the conduction term will bear the biggest influence and its error will be much larger than that of the other two terms. A stability condition estimated on the basis of the conduction term alone should give a reasonable approximation to the true stable criterion. Neglecting the convection and phase conversion, the energy equation is reduced to the standard parabolic equation:

$$\frac{\partial T}{\partial t} = \left(\frac{\lambda}{c\rho_0}\right)\frac{\partial^2 T}{\partial x^2} \tag{7.6}$$

and its stability condition is readily available as[59]:

$$\left(\frac{\lambda}{c\rho_0}\right)\frac{\Delta t}{(\Delta x)^2} \leq \frac{1}{2n} \tag{7.7}$$

where n: is the number of dimensions. For the one dimensional problem, n = 1.

Δt: time step, s.

Δx: the step in space dimension, m.

This implies that there is an upper limit on the time step, Δt, for any given value of Δx. The energy equation (4.21) for non-hygroscopic materials will produce the same condition if all non-important terms are similarly neglected.

The above condition is used in the numerical analysis to establish the solution time step which is considered acceptable for any given mesh distribution.

7.4 Computer Solution Strategy

The finite difference equations have been combined with the boundary conditions to produce a computer program written in FORTRAN[60][61]. The program code follows the standard of MISCROSOFT FORTRAN VERSION 5.1[62].

The program is configured in a modular form with a core program and sixteen modules which are designed to carry out single tasks and are 'called' by the core program. This makes the operation of the program much easier to validate and facilitates future maintenance. Table.7.4 lists the modules by name with a brief description of their functions. The full program code is included in Appendix Four with a more detailed description of the operation of each module. The solution strategy adopted is illustrated by the flowchart given as Fig.7.3.

The input data for the model is provided in the form of an editable data file, an example of which is given in Appendix Four. This file contains all the necessary physical information for the structure being analysed, as well as the relevant initial and boundary conditions. The environmental conditions at either side of the structure are currently provided as single mean values for each month of the year. This, of course, could be refined in the future to include mean daily or hourly values over a summer or winter season, depending on user requirements.

The core program 'reads' this input data file (calls subroutine 'File_Read') and then generates the nodal mesh for the wall structure either automatically or manually (calls either subroutine 'Man_Mesh' or 'Auto_Mesh'). Automatic mesh generation requires as input the total number of mesh points for the complete structure. The program then positions nodes within each layer such that, as far as possible, the vapour and thermal resistance values between each nodal point are balanced. Manual mesh generation requires individual input of the number of nodal points required within each elemental layer making up the structure.

Table 7.4 List of program Modules

Module Name	Purpose
CHMTBS	Main Program which interacts with the user and calls subroutines as required
FILE_READ	Reads the data file and assigns variables
MAN_MESH	Manually generates nodal mesh points
AUTO_MESH	Automatic generation of mesh
PRES_TO_MOI	Converts vapour pressure to moisture content using the sorption isotherm
MOI_TO_PRES	Convert moisture content to vapour pressure using the sorption isotherm
PROPERTY	Calculates properties for local mesh points
FLOW_RATE	Calculates flow rates for each component
HYGRO	Calculates values of state variables for new time step for hygroscopic materials
NON_HYGRO	Calculates values of state variables for new time step for non-hygroscopic materials
OUT_PUT	This module opens file and outputs data
M_A_BOUND	Solves boundary conditions for outside surfaces

(continue to next page)

(continue from previous page)

Table 7.4 List of program Modules

Module Name	Purpose
M_M_BOUND	Solves boundary conditions for material/material interfaces
M_G_M_BOUND	Solves boundary conditions for material/air gap/material interfaces
M_V_M_BOUND	Solves boundary conditions for material/vapour barrier/material interfaces
M_V_G_M_BOUND	Solves boundary conditions for material/vapour barrier/air gap/material interfaces
ERROR_HANDLE	Checks error type should any error happen

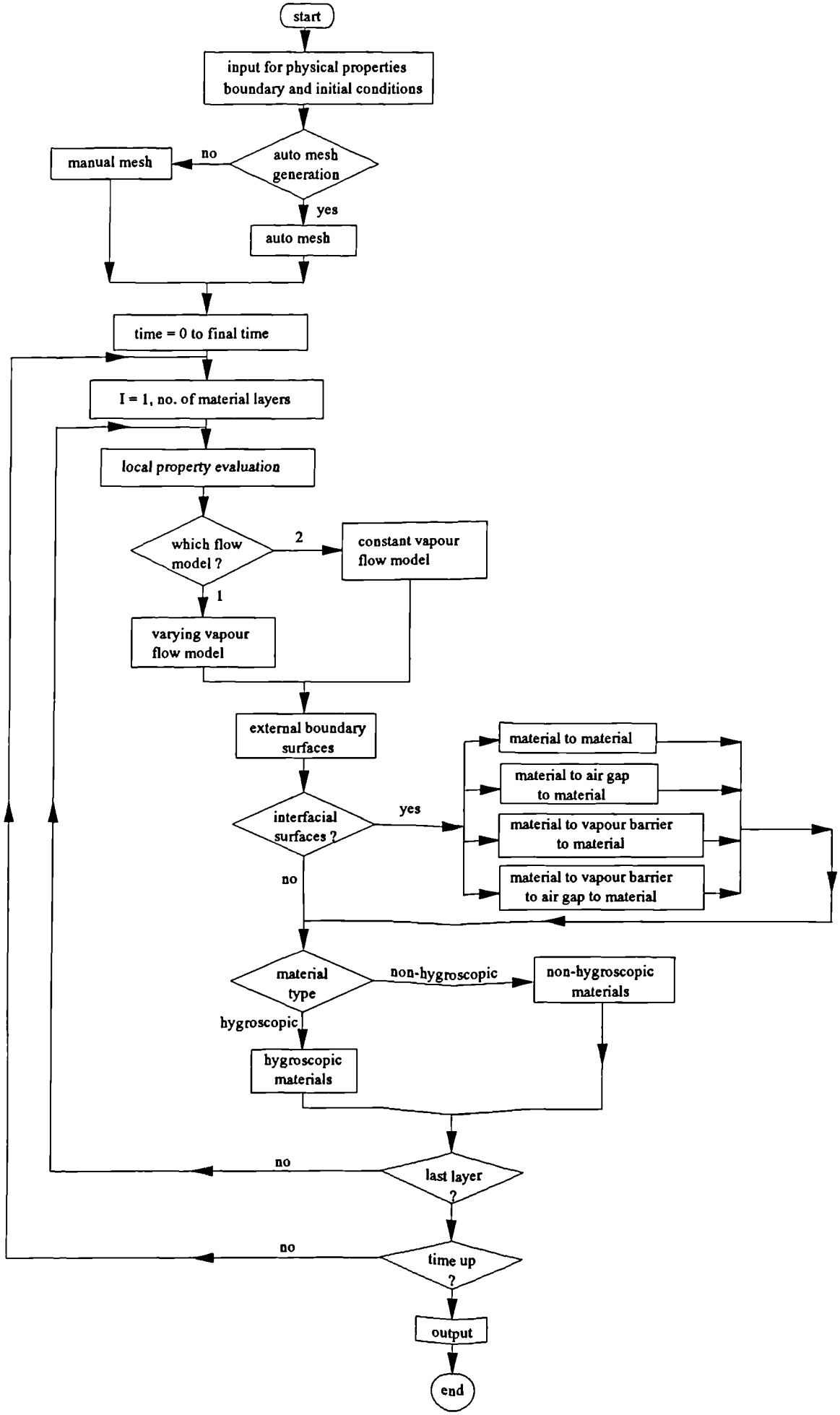

Fig. 7.3 FLOW CHART OF PROGRAM CHMTBS

At this stage the program estimates the time step required by each layer to ensure stability and then chooses the solution time step as the smallest of the values calculated.

The main solution process then begins, by evaluating local values for the transfer coefficients, moisture flow rates and thermal conductivities (calls subroutine 'Property', 'Flow_Rate'). These local properties are calculated based on the initial values given in the data file.

The core program then checks the boundary types of all boundary surfaces involved and calls the corresponding subroutines which calculate property values at the new time step (calls 'M_A_Bound', 'M_M_Bound', 'M_V_M_Bound', 'M_G_M_Bound', 'M_G_V_M_Bound', 'M_V_G_M_Bound'). In the naming of the subroutines, 'm' stands for material, 'v' for vapour barrier, 'g' for air gap and 'bound' refers to the fact that they are boundary condition modules.

The governing equations given in numerical form in Table 7.2 are then solved to give the temperature, vapour pressure, vapour density, relative humidity and moisture content values for the next time step (calls subroutine either 'Hygro' or 'Non_hygro'). The program then repeats the calculations until the final time step is reached. This solution approach is further amplified in Figure 7.4, which is a graphical representation of the program strategy.

The program outputs vapour pressure, vapour density, moisture content and temperature for three points within each layer - one close to each surface, and one at the centre. In addition, data on the total flow rate of moisture at each surface of the construction is given (calls subroutine 'Out_Put').

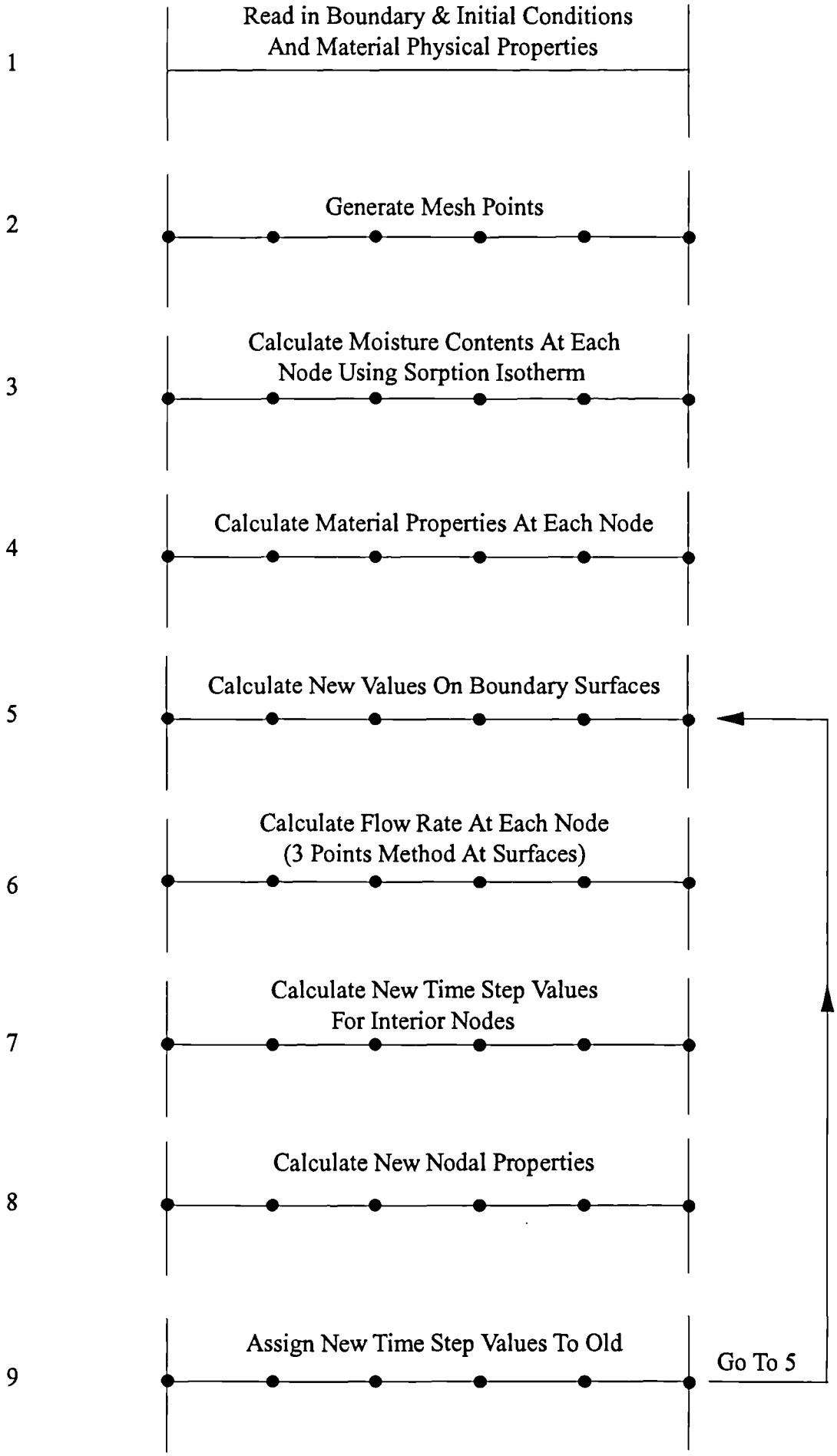

Fig.7.4 Graphical Illustration of Program Strategy

In order to investigate the gradients of the properties through the construction, local nodal values of properties are stored for three time periods - at t=0, at the mid-point of the time period and at the end of the solution period.

All of the above data is stored in numerical data files which can then be interrogated using standard graphical software packages, such as Lotus Freelance Graphics[63].

8. EXAMPLES OF COMPUTER PROGRAM OPERATION

The operation of the computer code has been investigated by application to several structural elements under a range of environmental conditions.

The model integrity was firstly verified through use with single layer partitions, where it is possible to intuitively estimate the type of physical results which would be expected.

The overall capabilities of the computer program were then demonstrated by modelling two standard constructions, namely a timber framed wall and a masonry brick wall.

8.1 Simulation of Single Layer Partitions.

The compatibility of the solution equations and the inside/outside boundary conditions can be illustrated by running the model for single layer partitions where more complicated boundary conditions are avoided (i.e. material interfaces, air gaps, vapour barriers etc.). Two single layer partitions have been investigated comprising of:

a solid wood partition (15mm thick)
a brick wall (103mm thick)

The model has been run for each of the above using environmental conditions which correspond to those recommended in BS5250[64] for steady state calculations. The partitions were assumed to be initially equilibriated at 65% relative humidity and 15^{0}C. The environmental conditions of the air in contact with surface two were then changed to become 95% relative humidity and 5^{0}C at t=0 and all times thereafter. The conditions of the air at surface one were maintained at 65% relative

humidity and 15^{0}C. This produced a transient situation in which there existed a temperature, relative humidity and vapour pressure gradient across the partitions (Figure 8.1). At equilibrium this will produce results which should correspond to the standard recommended environmental conditions for the assessment of condensation risk[64].

The program was then set to simulate the moisture and thermal conditions within the partitions over a period of 30 days.

8.1.1 Wood Partition Results.

The predicted flow rates of moisture, as well as the moisture contents, vapour pressures and temperatures, are shown plotted against time in days as Figure 8.2.

Figure 8.2(a) presents the flow rates of moisture at both surfaces of the wood. From this it is clear that, after about 20 days, moisture equilibrium is reached, and a steady flow of moisture takes place from surface one to surface two.

The predicted moisture content, vapour pressure and temperature variations against time are shown in Figures 8.2 (b), (c) and (d) respectively. The data in each graph is shown for three locations, namely the mid-point and at each surface. In all cases the results are as might be expected, all tending towards steady values at equilibrium. It is interesting to note the speed with which the temperature profiles reach equilibrium in comparison with the moisture content and vapour pressure profiles. This reflects the very large difference in time constants between the processes of energy and mass exchange.

The moisture content and temperature profiles are given for days 0, 1, 10 and 30 as Figure 8.3. Figure 8.3(a) illustrates the way in which the moisture content

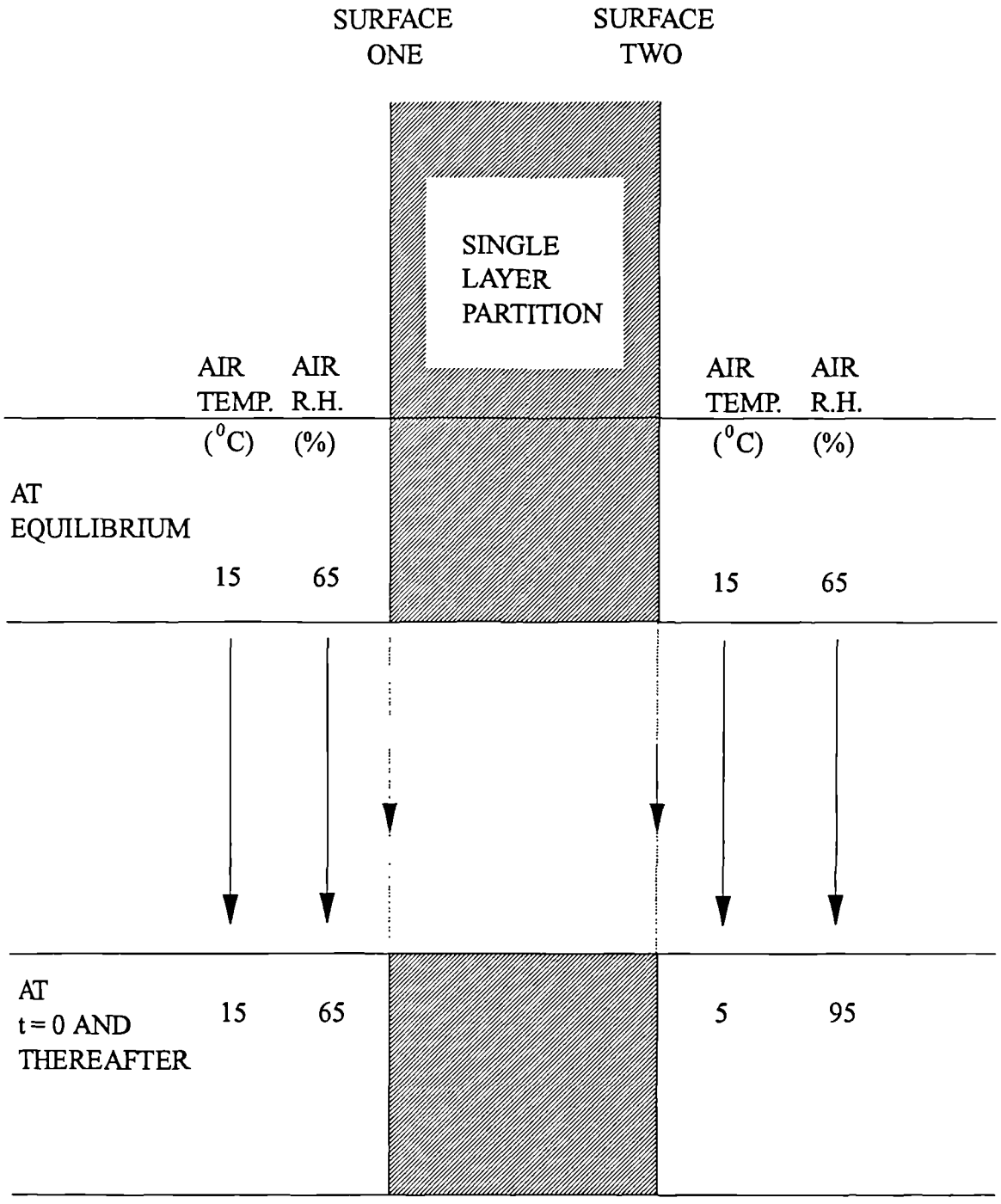

Figure 8.1 Model Environmental Conditions Used in the Simulations

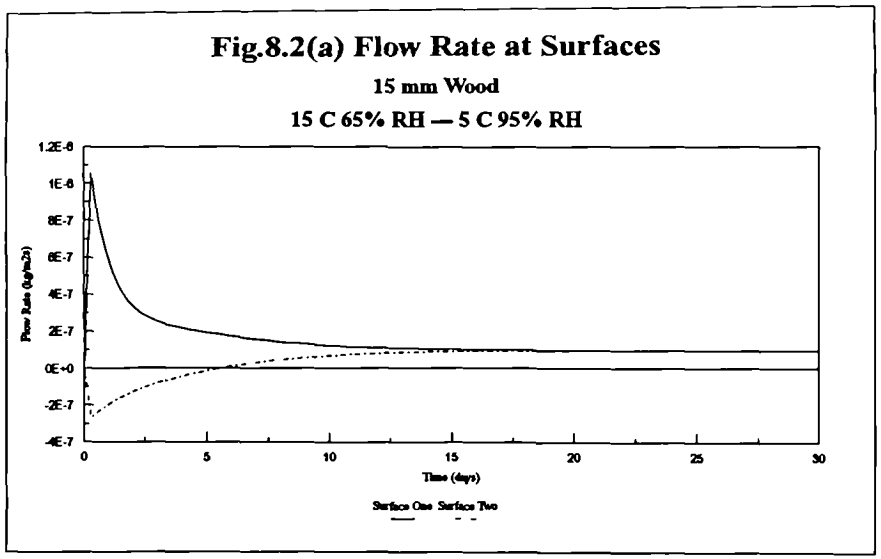

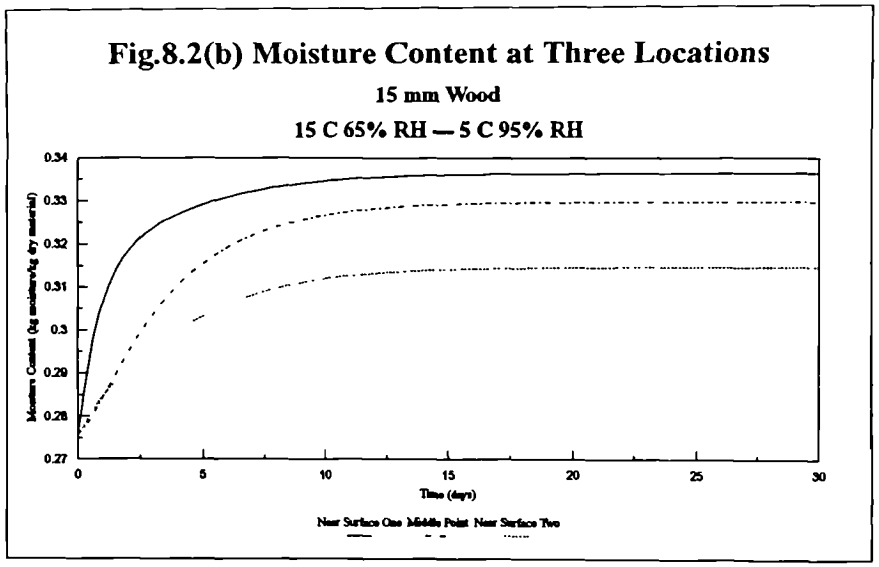

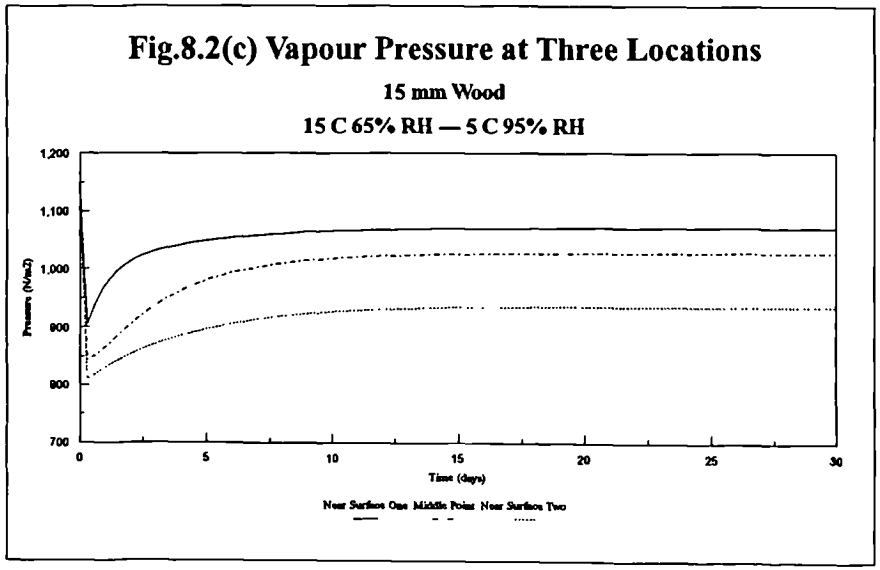

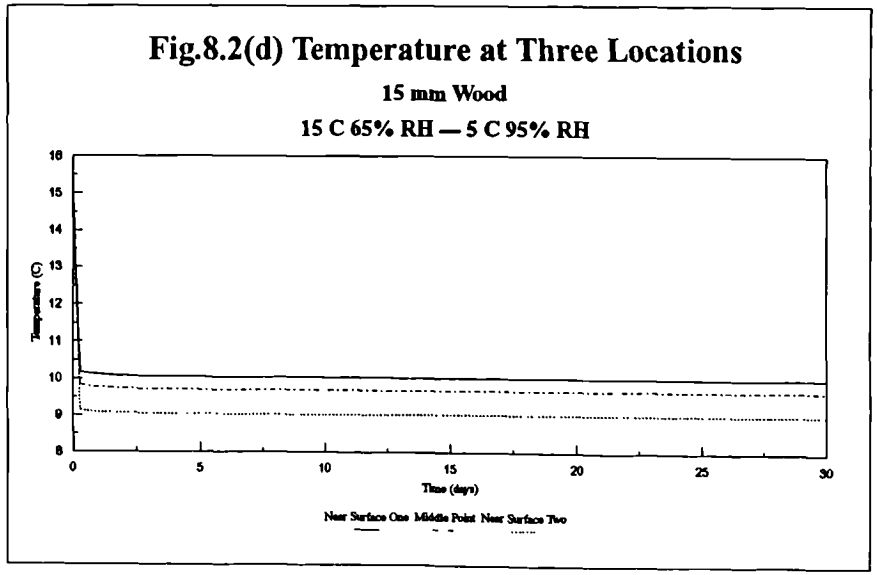

Figure 8.2 Wood Partition Results: data plotted against time for different locations

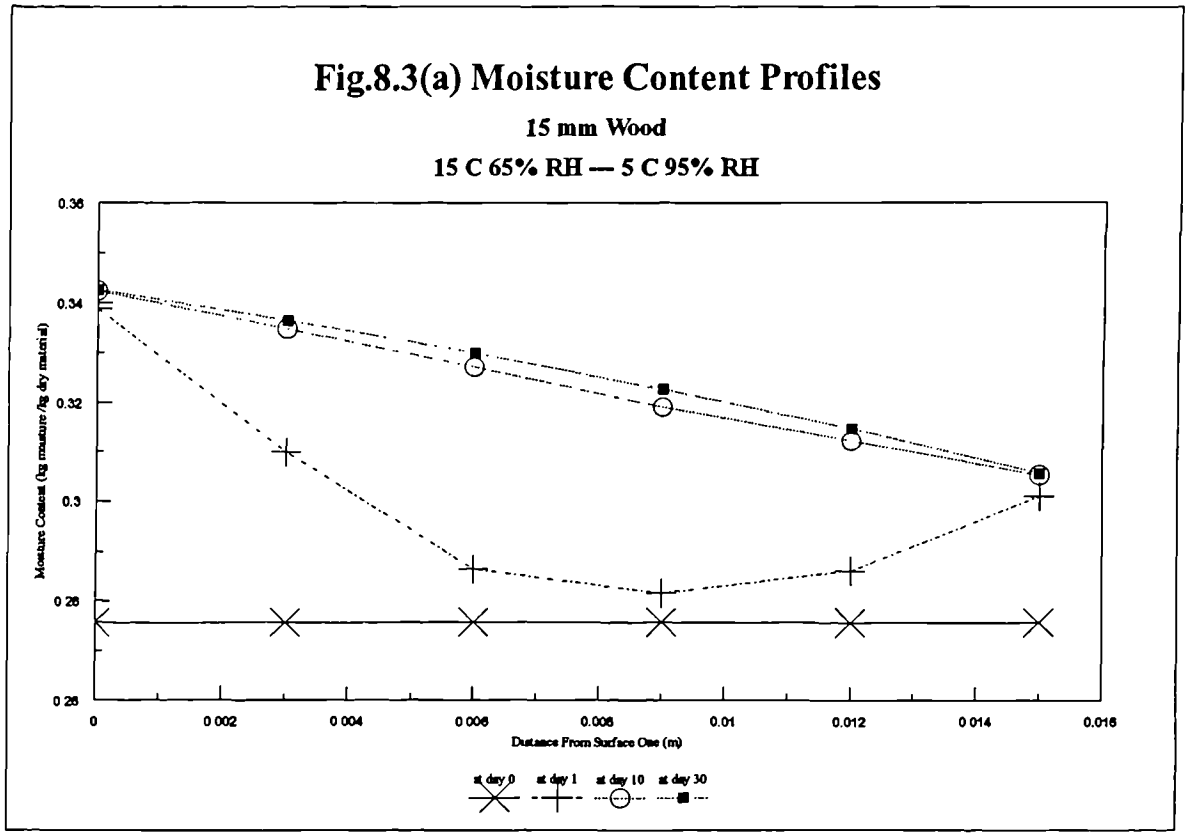

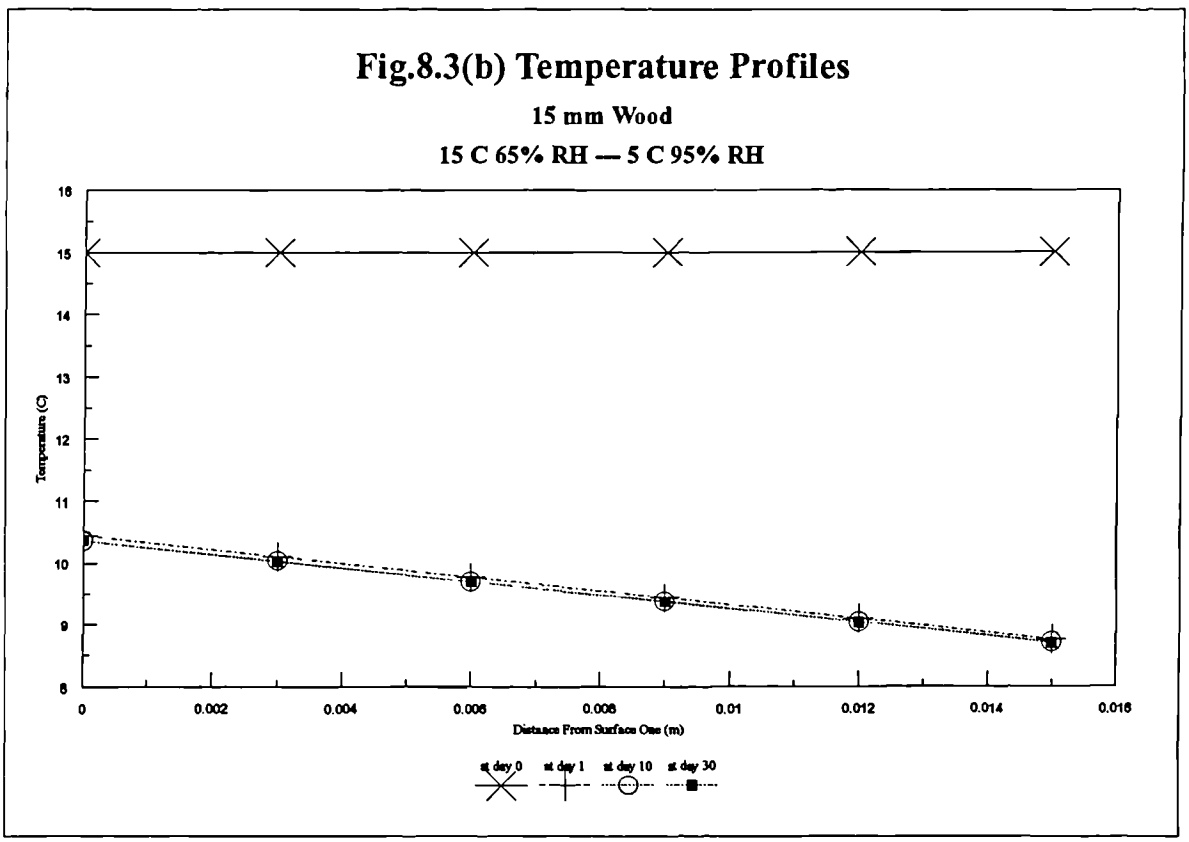

Figure 8.3 Wood Partition Results: data profiles plotted against distance for four time steps

has changed towards equilibrium during the simulation. A similar variation for temperature is shown in Figure 8.3(b), but in this case steady state is almost reached by day 10, with a linear profile being produced.

8.1.2 Brick Partition Results.

The results of this simulation have been produced in exactly the same form as above, namely

-Figure 8.4 showing the variation of flow rate, moisture content, vapour pressure and temperature against time.

-Figure 8.5 showing the moisture content and temperature profiles through the brick at days 0, 1, 10 and 30.

The results obtained are once again as may be expected, showing a gradual change towards equilibrium. It is, however, clear from these graphs that, in this case, steady state has not yet been reached for the mass exchange process, even after 30 days. The moisture content variations in Figures 8.4(b) and 8.5(a) clearly show that enough time has not yet elapsed for the centre of the partition to respond to surface changes. As with the wood partition, the temperature response is rapid, with steady state conditions occurring within the first day.

To investigate further the equilibrium of the brick, the same simulation was re-run, but in this case for a period of 365 days. The graphs of Figure 8.6 show that, even after this length of time, the flow rates have not fully reached steady values, the flows not yet being equal at both surfaces. These graphs demonstrate clearly the very large time scales associated with moisture movement, particularly for dense materials.

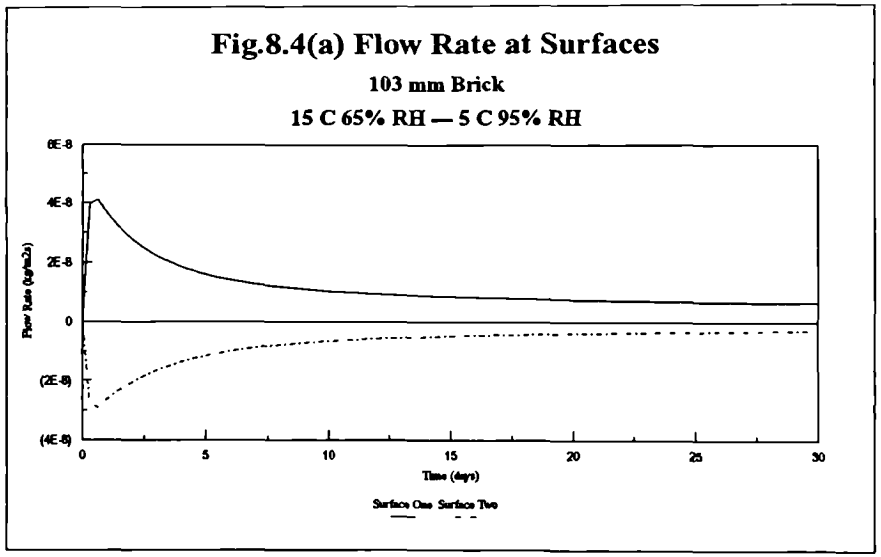

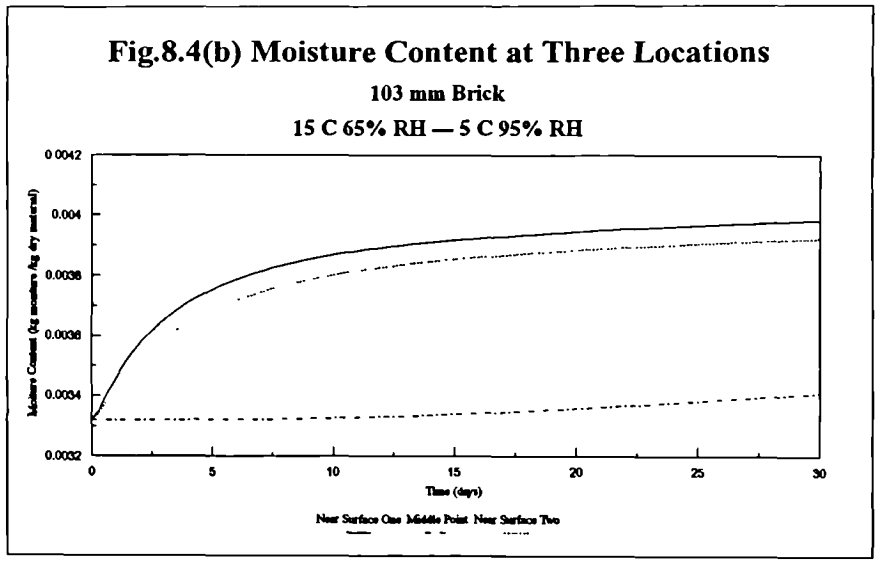

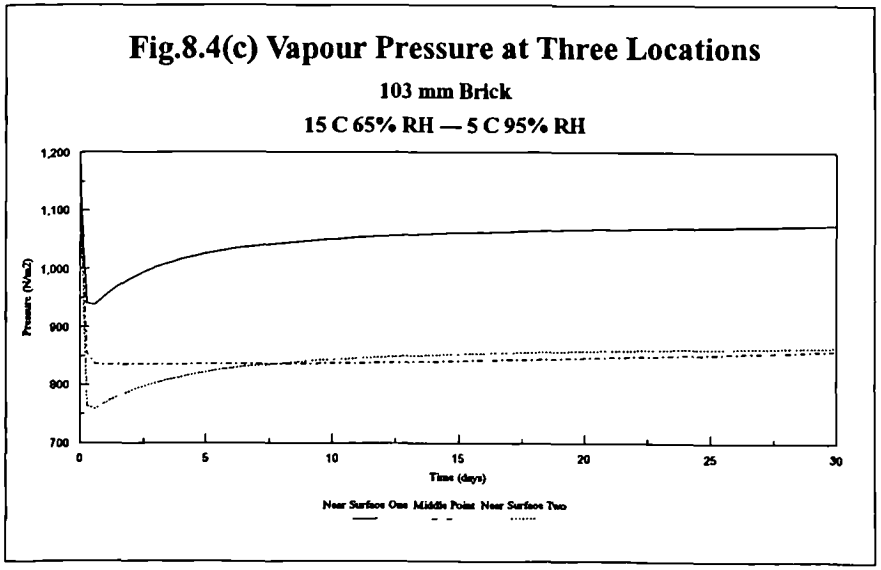

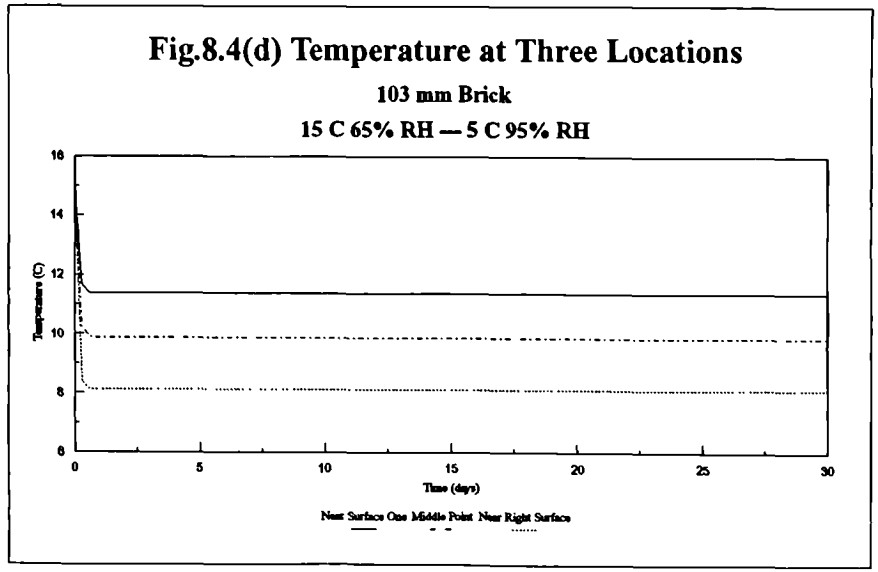

Figure 8.4 Brick Partition Results: data plotted against time for different locations

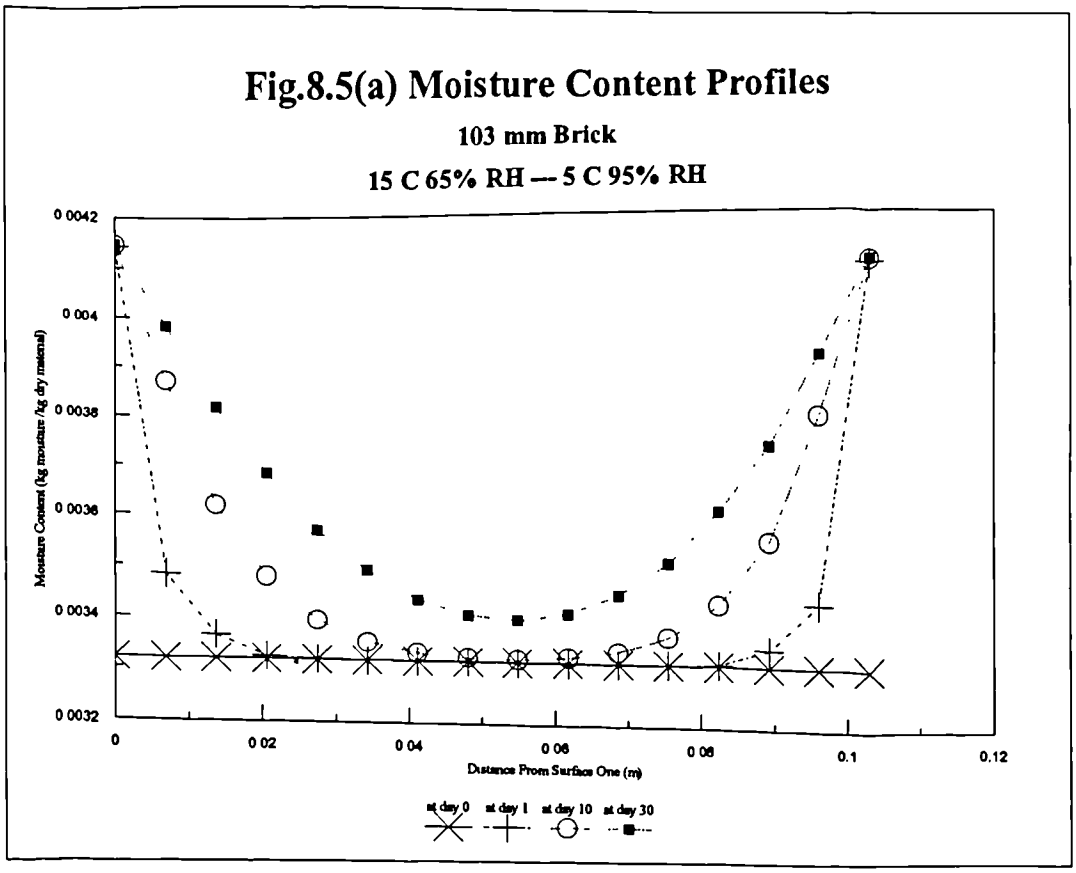

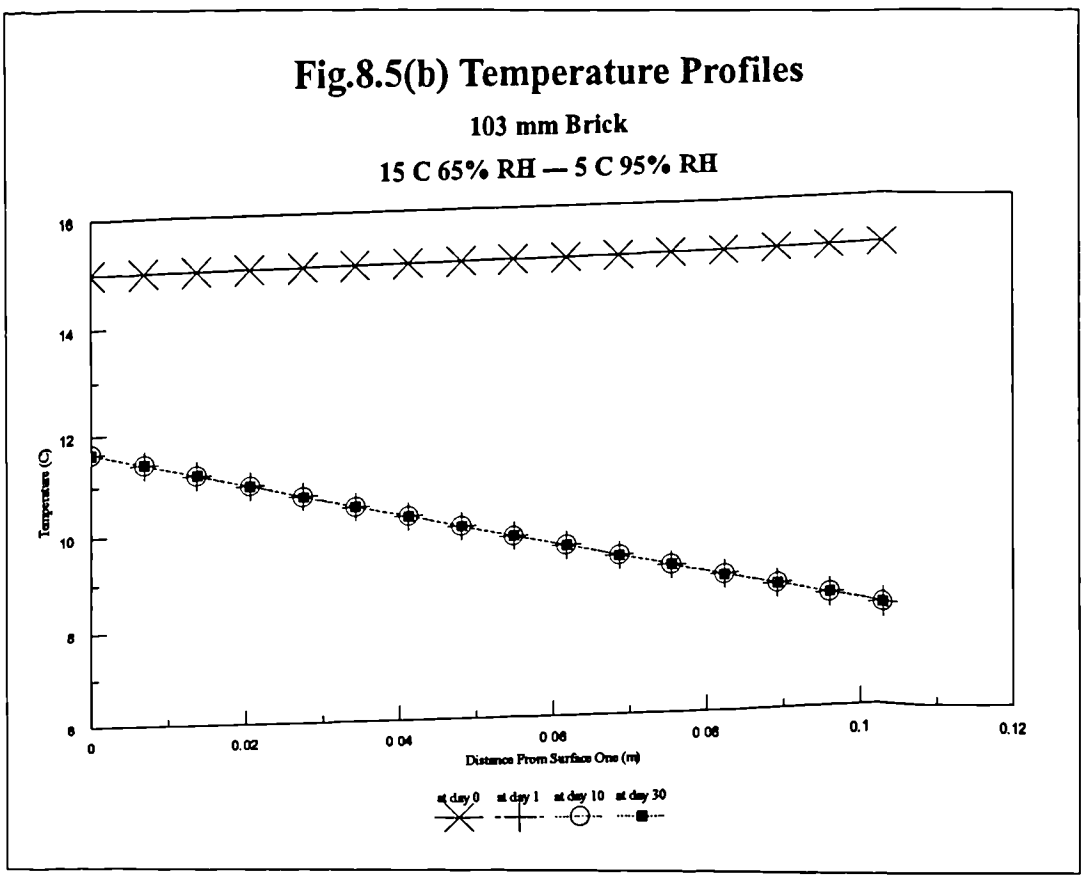

Figure 8.5 Brick Partition Results: data profiles plotted against distance for four time steps

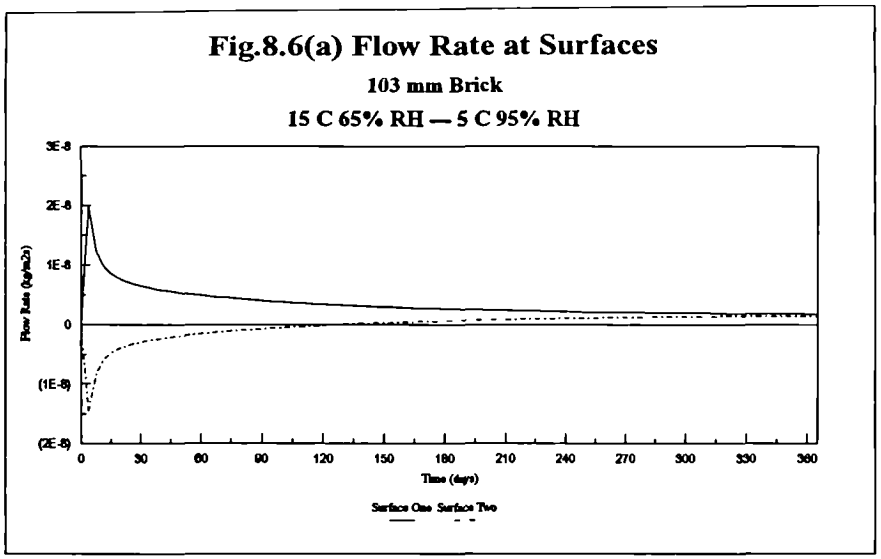

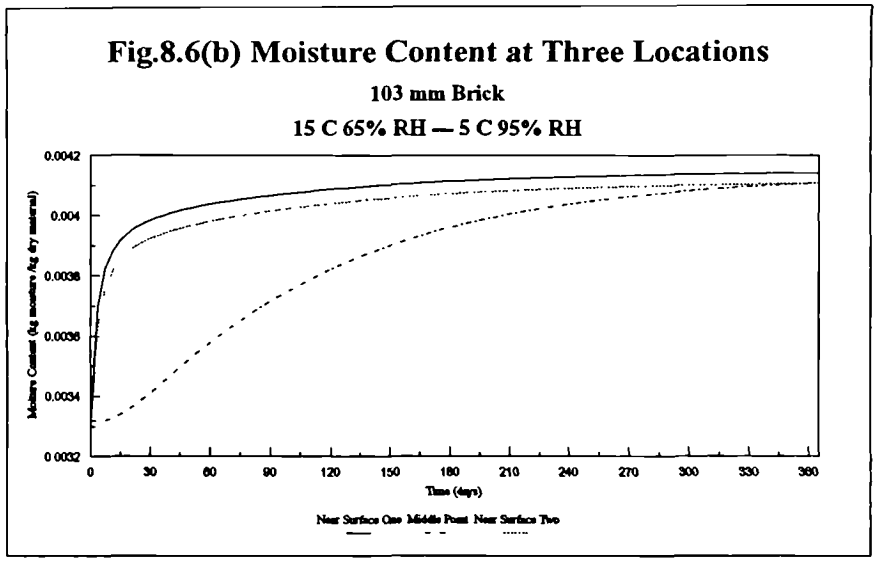

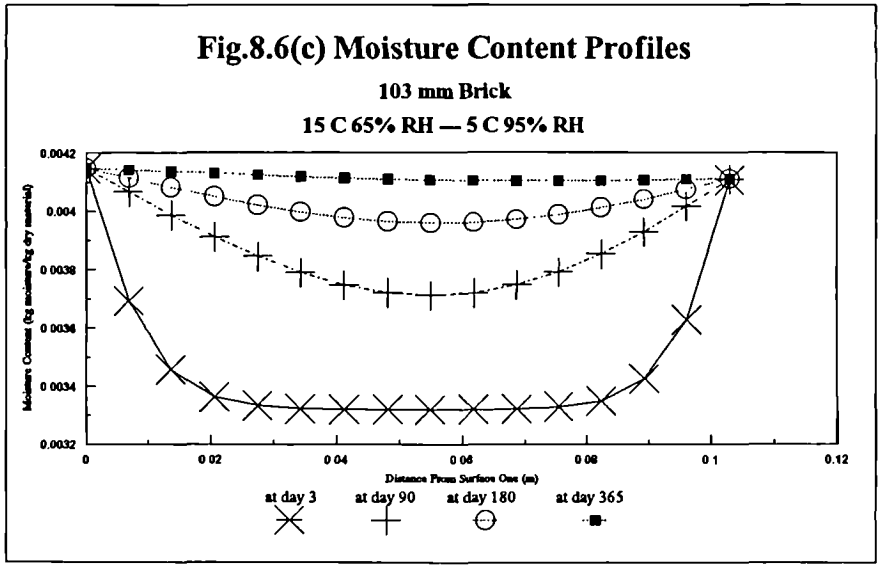

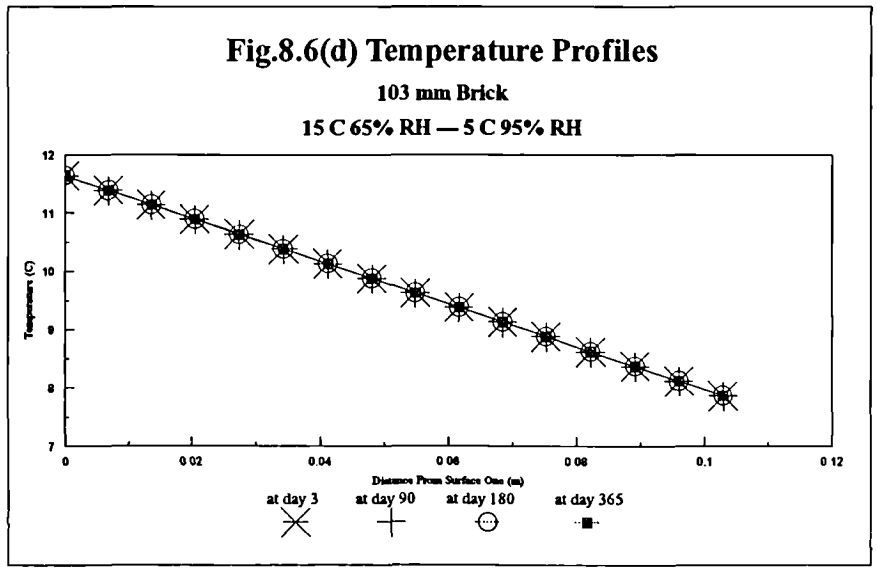

Figure 8.6 Brick Partition Results For 365 Day Simulation

8.2 Simulation of a Standard Timber Framed Wall.

The model has been tested using a standard design of timber framed wall as described in BS5250[64]. This design consists of an outer brick layer, an air gap, a plywood lined timber frame with insulation, and an internal plasterboard lining. The wall configuration is shown schematically, along with the thermal and moisture properties used in the simulation, as Figure 8.7.The vapour check incorporated within the structure is assumed to resist completely the passage of water, and to offer a large vapour resistance of 500×10^9 Ns/kg. This follows values suggested within BS5250[64].

The environmental conditions have been taken to be constant after t=0 and are identical to those used in Section 8.1 and recommended in BS5250[64] for steady state calculations. Again this produces a transient simulation, which at equilibrium should give results corresponding to the standard recommended environmental conditions for the assessment of condensation risk. The model in this case has been run for a period of three months (90 days), the typical winter period used for such calculations.

8.2.1 Moisture Content and Temperature Transients.

The predicted variations of moisture content with time are shown in Figure 8.8 for each material layer. In this figure a graph is given for each material layer, showing the transients at surface one, the mid-point and surface two. For both the plasterboard and polystyrene elements, moisture equilibrium takes place rapidly, while for the brick and plywood, equilibrium is not reached even after 90 days. In fact, at day 90 the plywood continues to show an increasing trend towards moisture accumulation, although the absolute quantities involved are small. This slow response to moisture movement is as would be expected for the brick, being a dense material with large moisture capacity and a relatively high moisture transfer resistance. The results

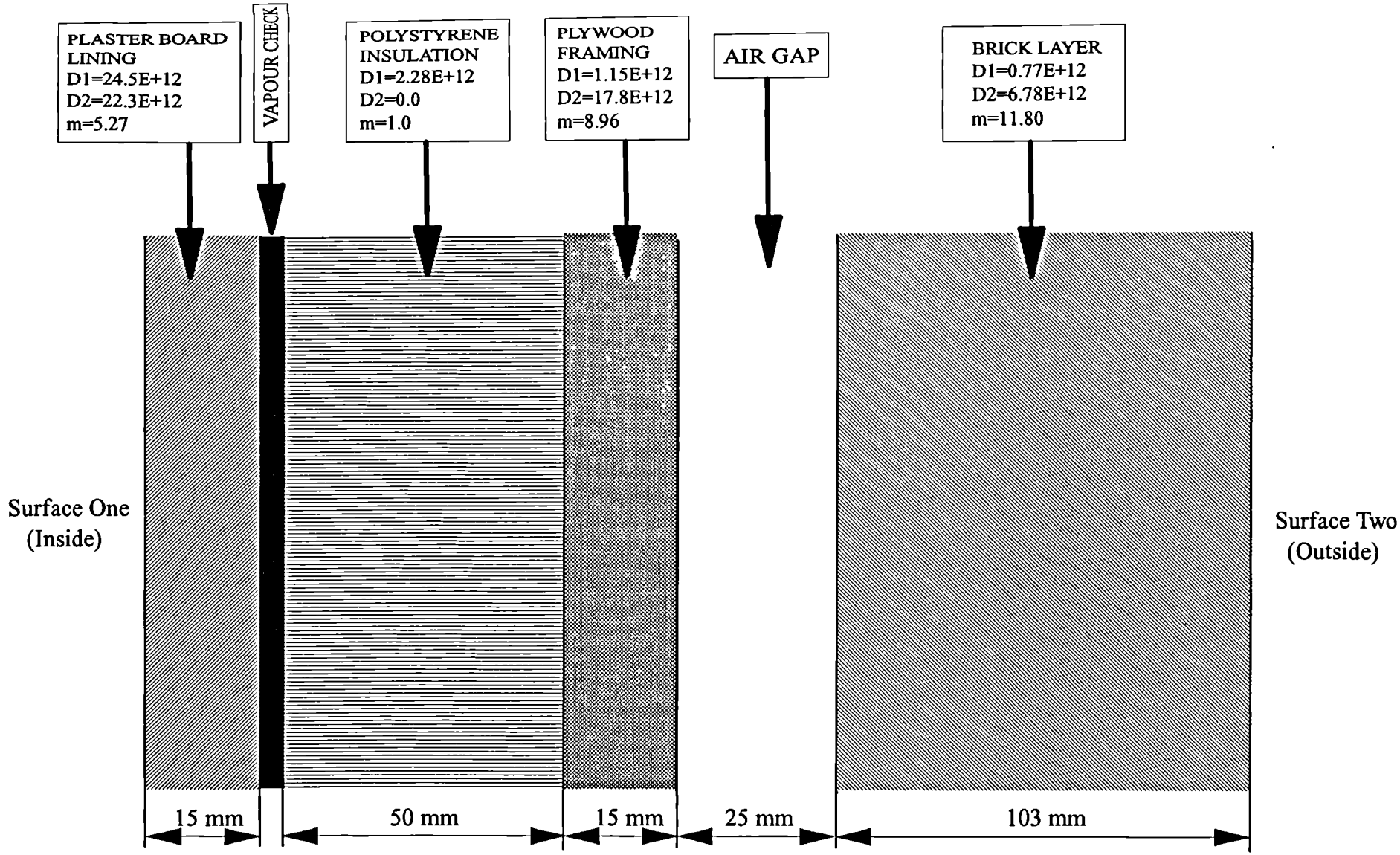

Figure 8.7 Timber Frame Wall Configuration

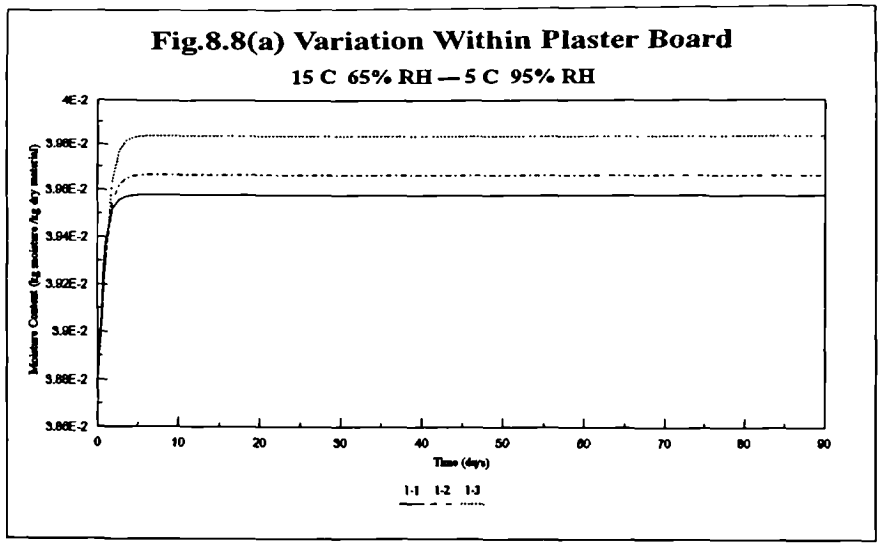

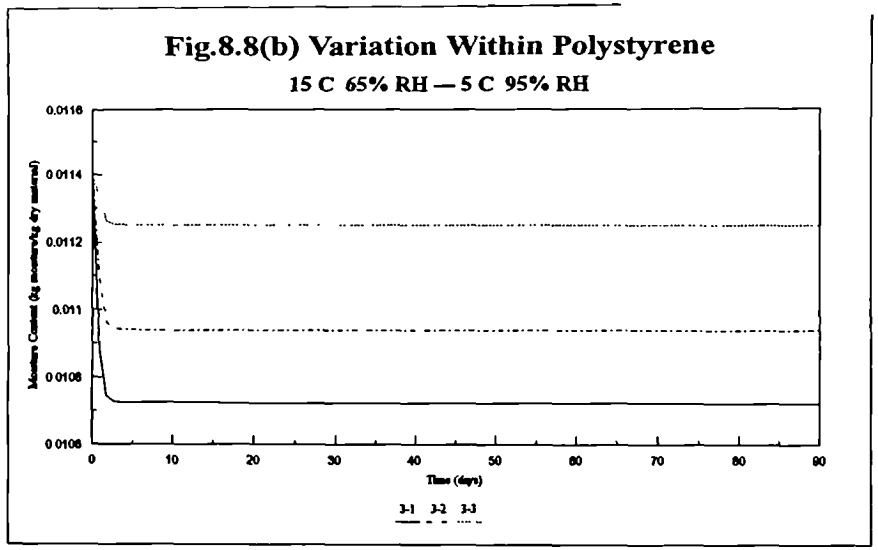

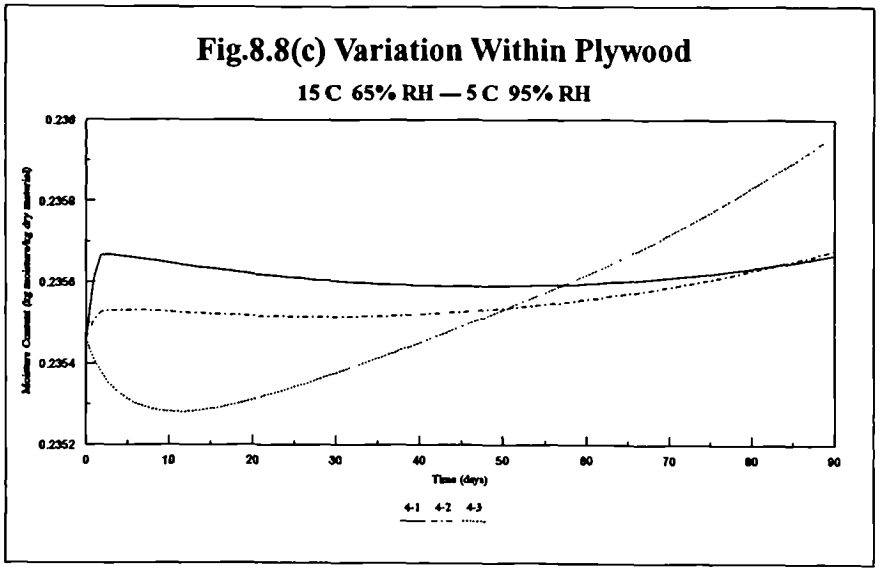

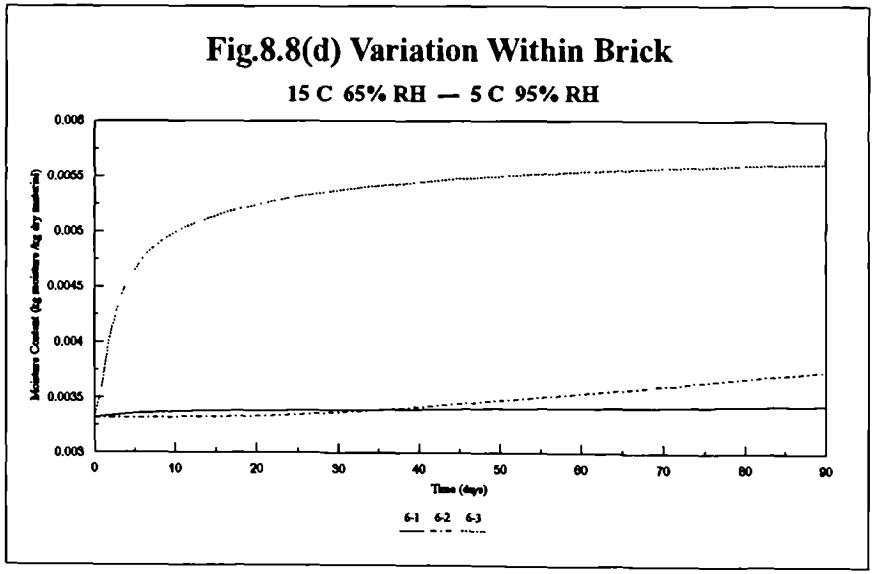

Figure 8.8 Timber Frame Wall Results: moisture content data plotted against time at three locations for each layer of material

for plywood would indicate a problem of continued moisture accumulation. The model was re-run for a period of 365 days to investigate further this effect. The plywood indicated an averaged moisture content of 24% by mass after this period of time, although the structure had still not reached equilibrium. In Figure 8.9 the temperature transients show equilibrium occurring much more rapidly, in all cases within a few days.

8.2.2 Moisture Content and Temperature Profiles.

Figure 8.10 shows the moisture content profile through the construction at day 90, while Figure 8.11 shows the temperature profile. Both results are once again as may be expected. To check the risk of moisture damage to the construction, it would be necessary to compare the moisture contents of each material with appropriate limiting values. In this case the plywood has the highest predicted moisture content, which corresponds in percentage terms to 24% by mass. For wood-based materials, risk of deterioration is thought to be high for percentage moisture contents greater than 20%[46][65]. The plywood in this case is therefore under severe risk.

8.2.3 Moisture Flow Rates.

The flow rates of moisture at both surfaces of the construction are plotted in Figure 8.12. After initial transient effects, the values begin to converge. It is clear, however, that equilibrium is not yet reached even after 90 days, with flow taking place into the wall from both surfaces. A profile of the flow rates at day 90 is given in Figure 8.13. This diagram shows the changing flow rate values and clearly demonstrates the

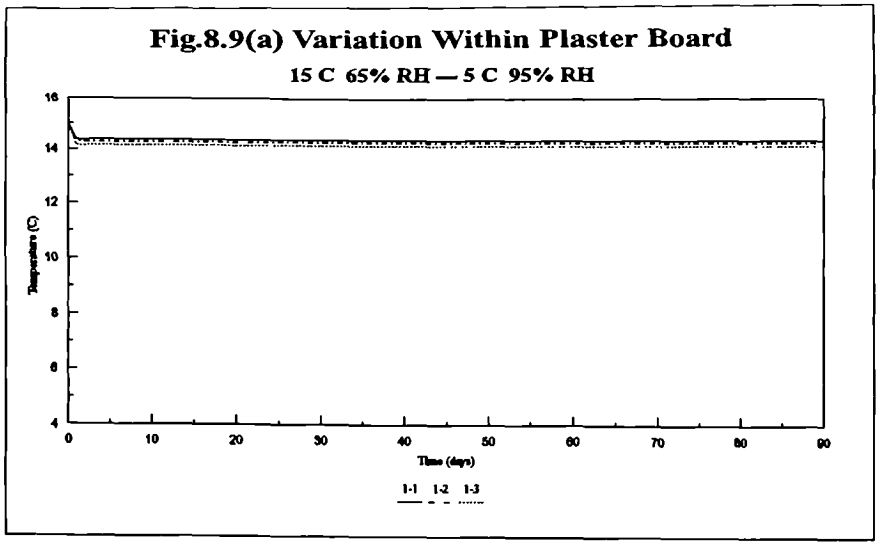

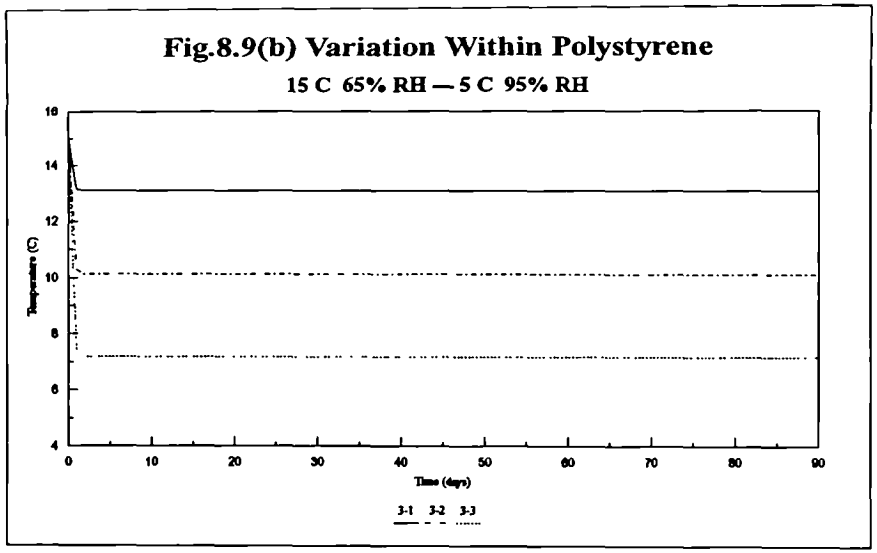

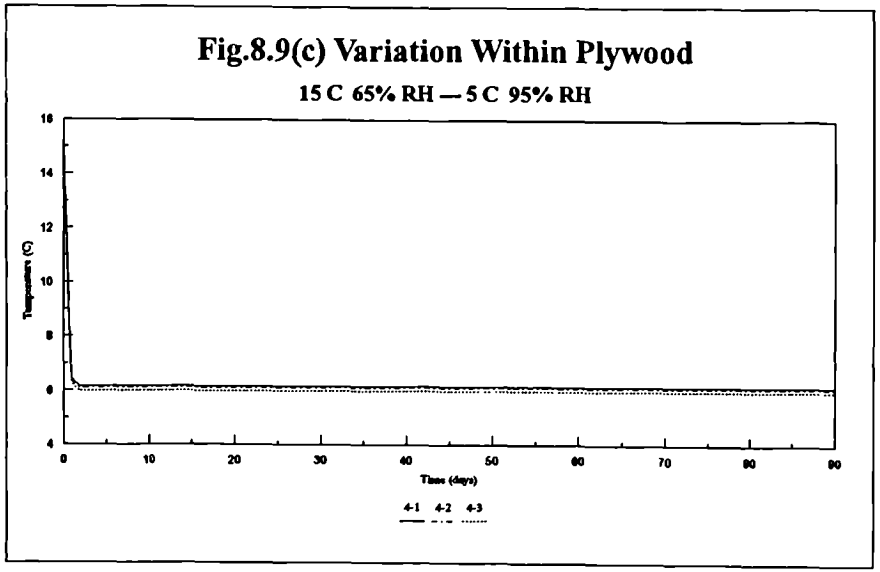

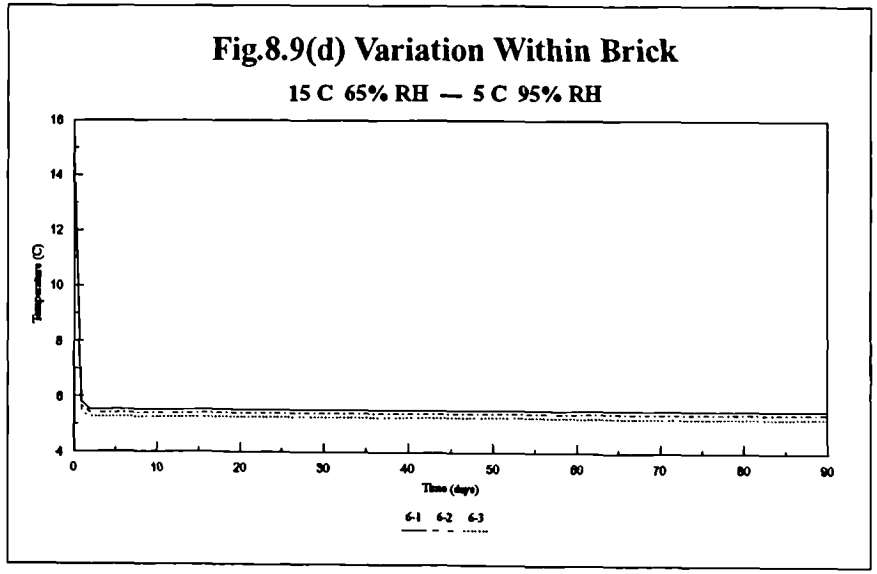

Figure 8.9 Timber Frame Wall Results: temperature data plotted against time at three locations for each layer of material

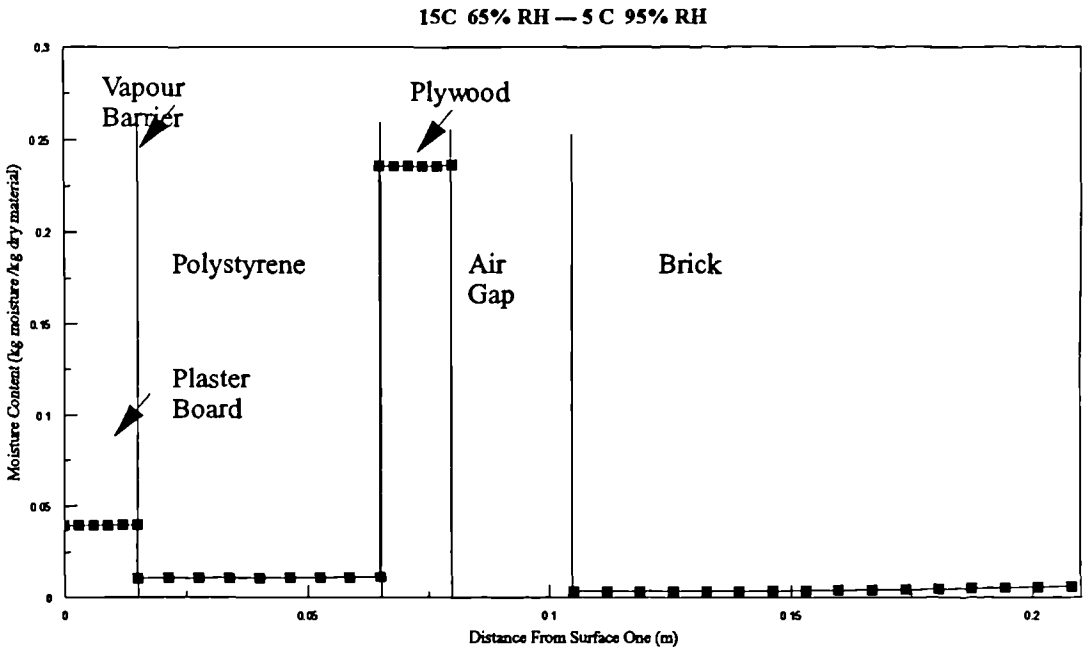

Figure 8.10 Timber Frame Wall Results: moisture content profiles

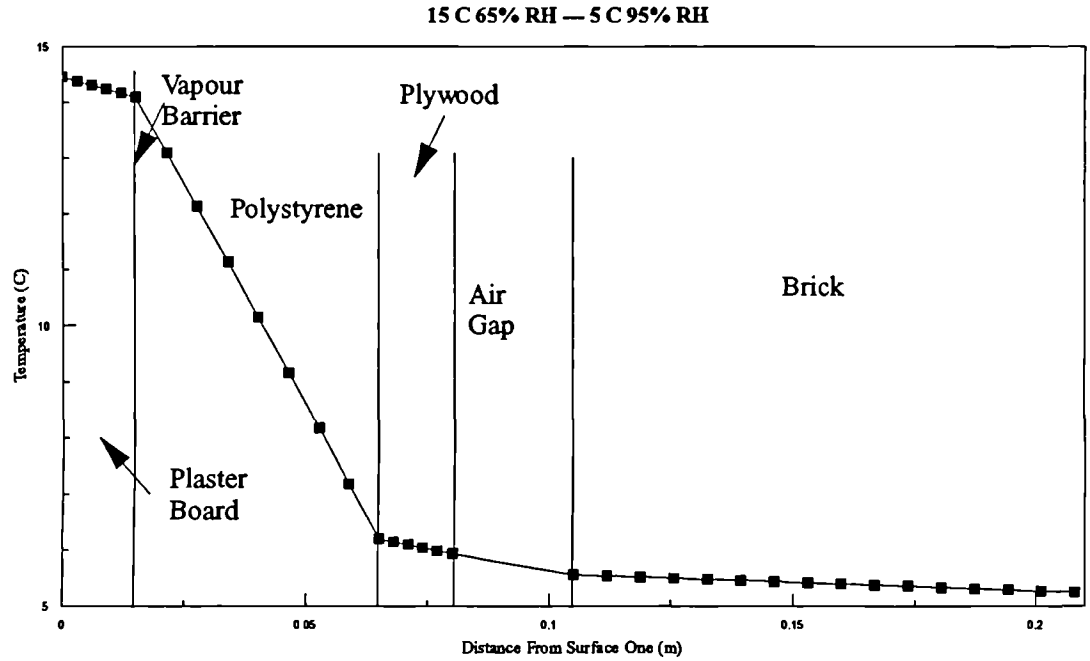

Figure 8.11 Timber Frame Wall Results: temperature profiles

Figure 8.12 Timber Frame Wall

Flow Rate At Surfaces

15 C 65% RH --- 5 C 95% RH

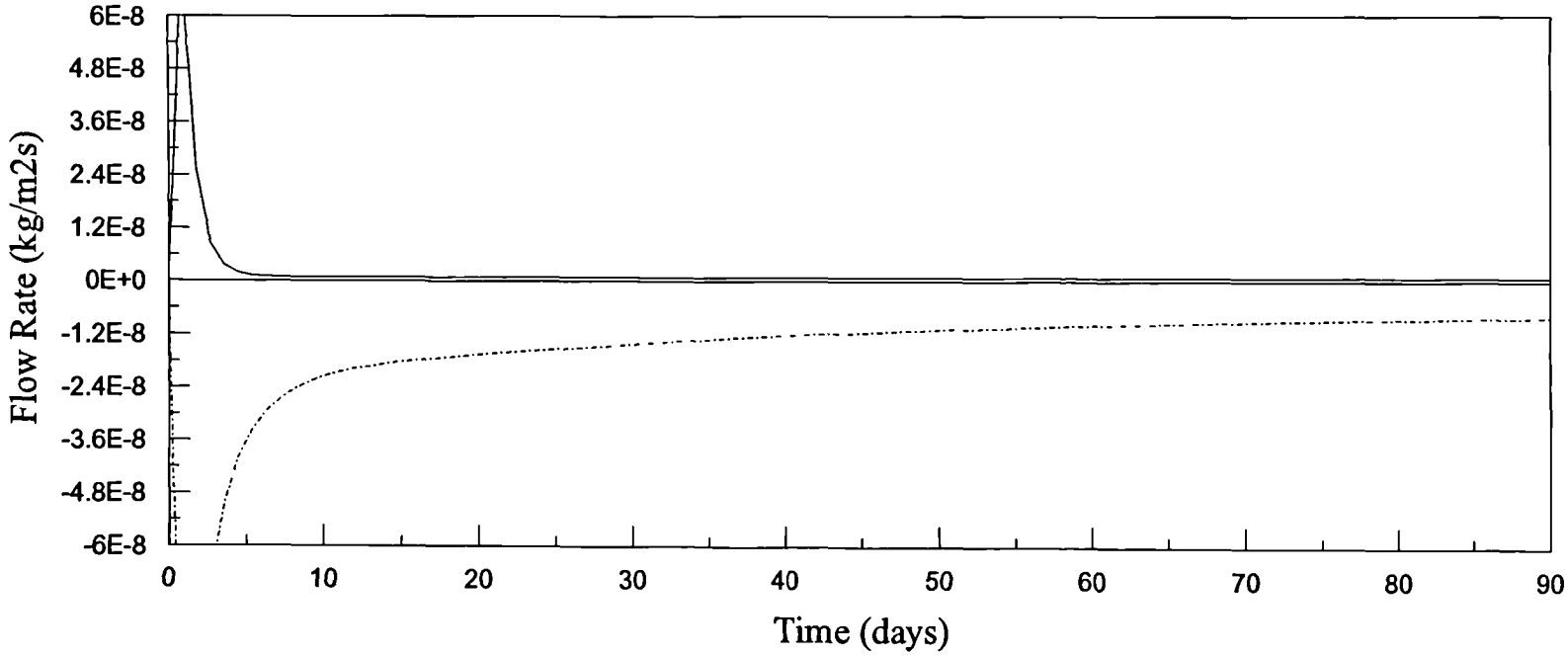

Plaster Board Surface 1 Brick Surface 2

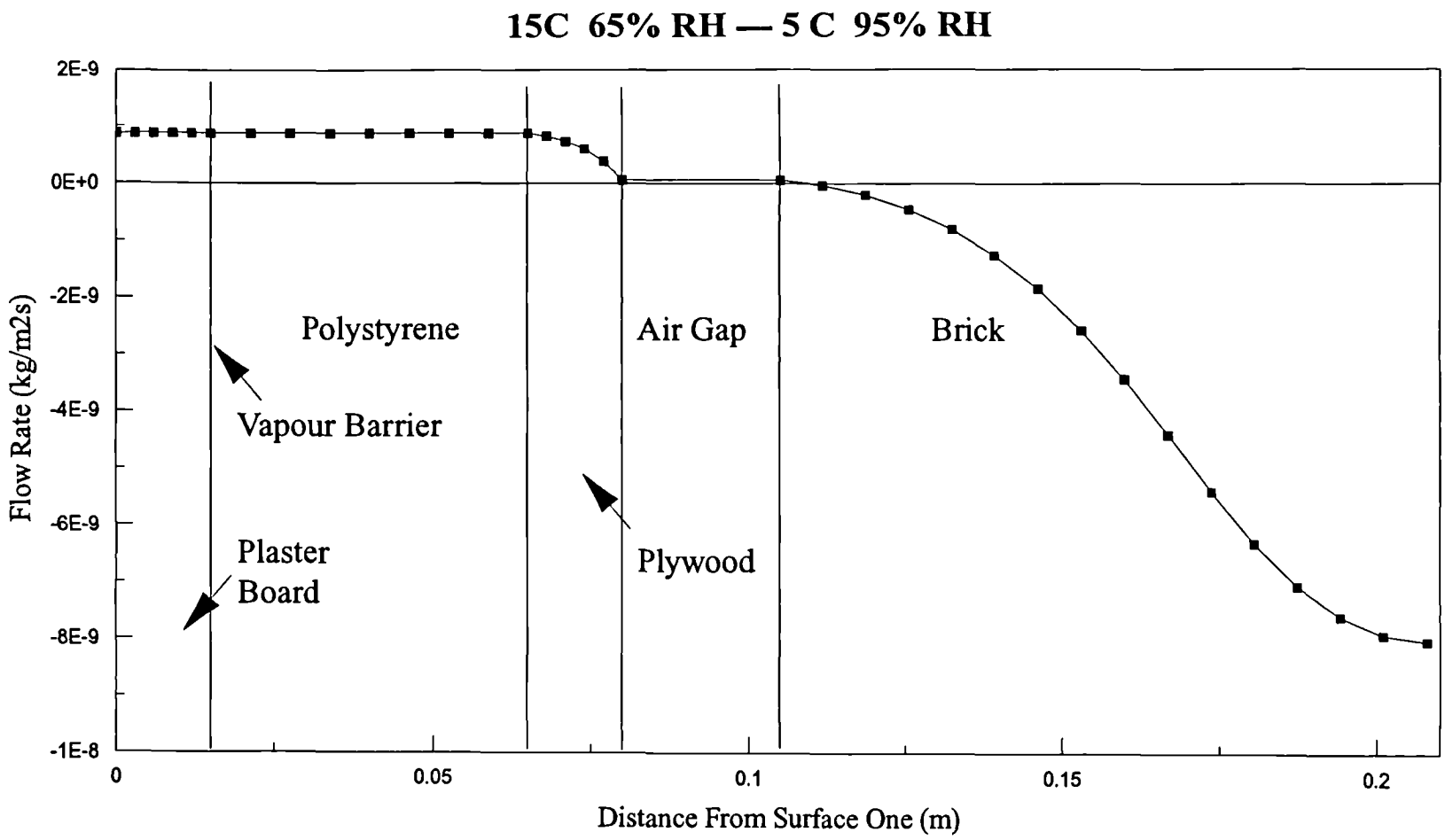

Figure 8.13 Timber Frame Wall Results: flow rate profile

fact that equilibrium has not yet been reached, with the plywood accumulating moisture from the warm side, while the brick is accumulating moisture from the cold side. This again emphasises the large time scales associated with moisture movements.

8.3 Simulation of a Standard Masonary Wall.

The wall structure modelled in this case consists of an outer and inner layer of brick enclosing polystyrene insulation, with an internal lining of plasterboard. The details of this wall are shown schematically as Figure 8.14, the design following the suggested practice of BS5250[64].

The environmental conditions used in this simulation are identical to those used for the timber framed wall. The model has also been run for the same time period, namely 90 days.

8.3.1 Moisture Content and Temperature Variation with Time.

Figures 8.15 and 8.16 show the moisture contents and temperature transients plotted against time for three locations within each material layer. As before, temperature equilibrium is rapid, while the moisture contents, particularly for the brick, require many days before equilibrium is reached. In fact, it seems unlikely from the graphs that mass flow equilibrium has been reached even after 90 days.

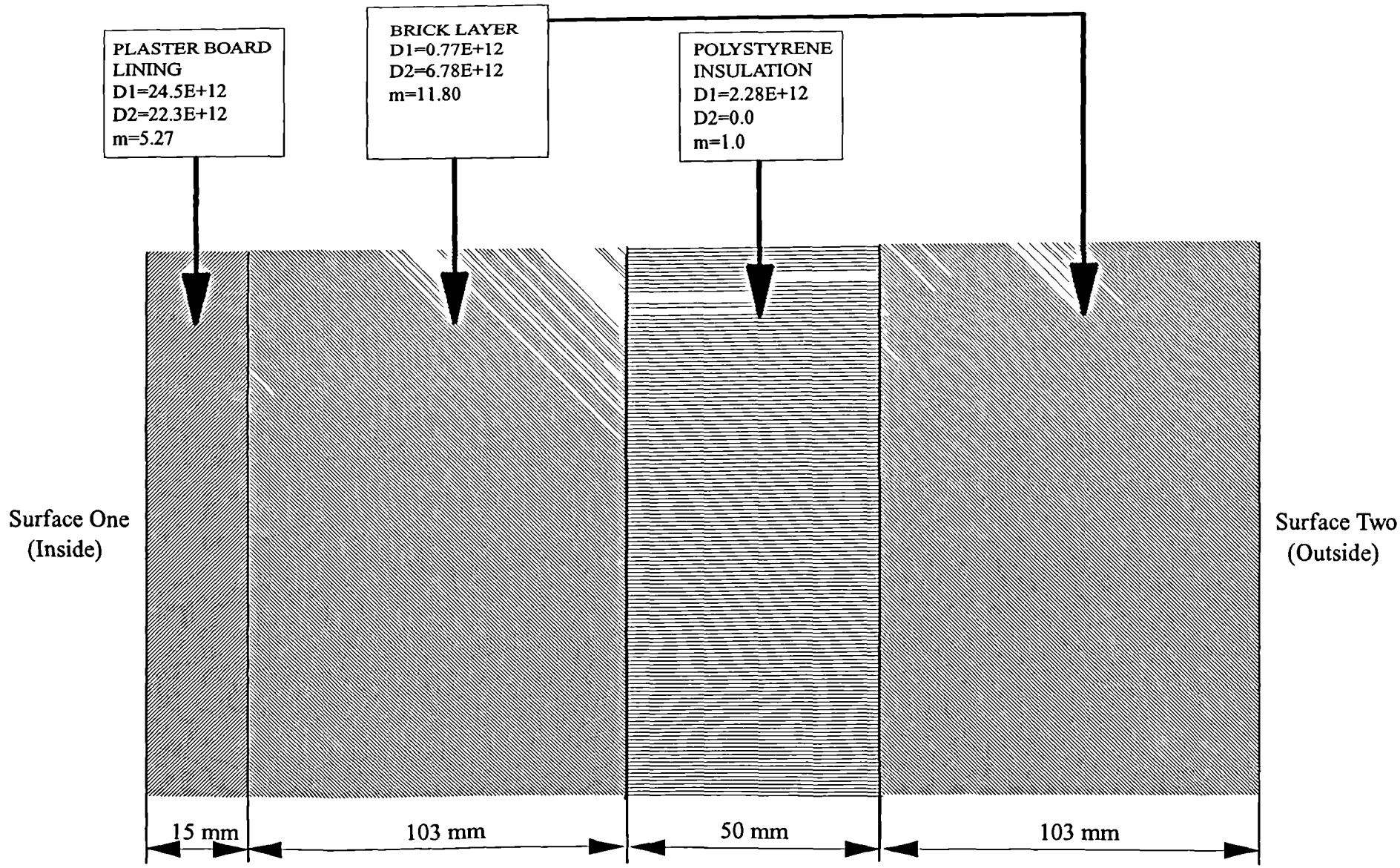

Figure 8.14 Masonary Wall Configuration

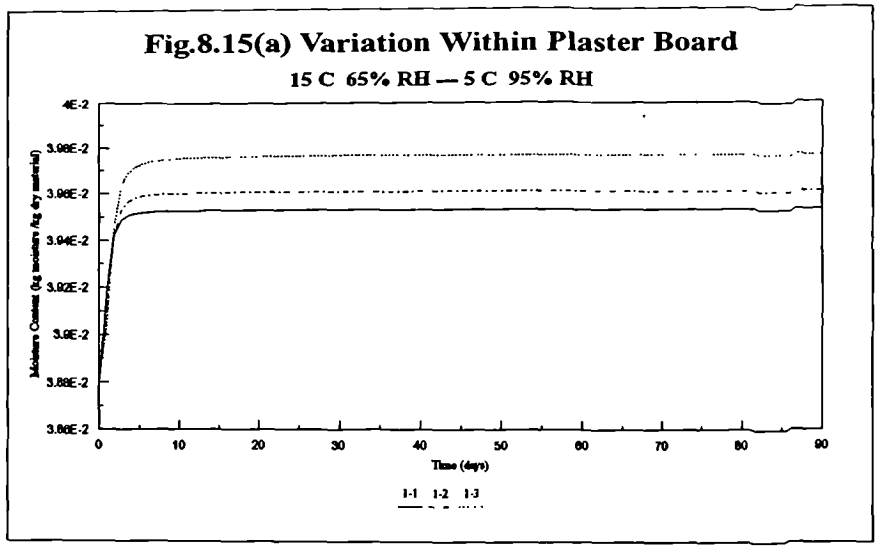

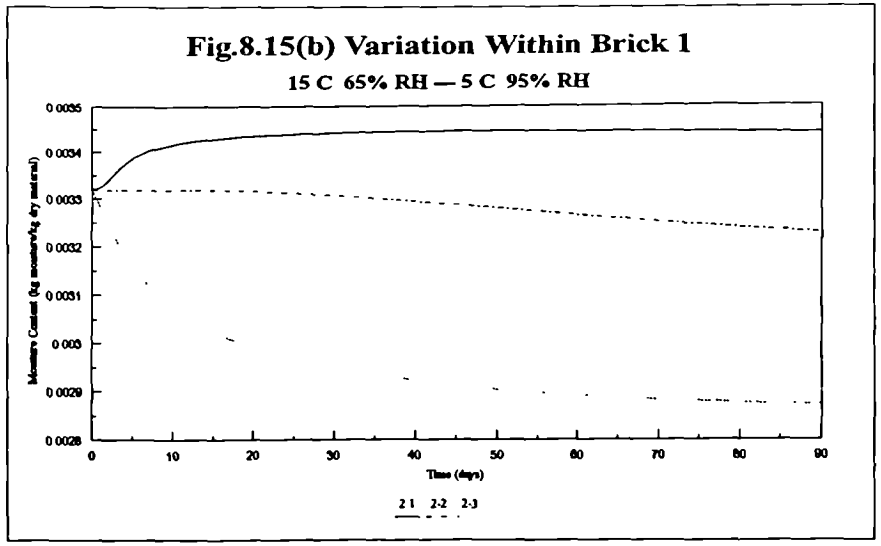

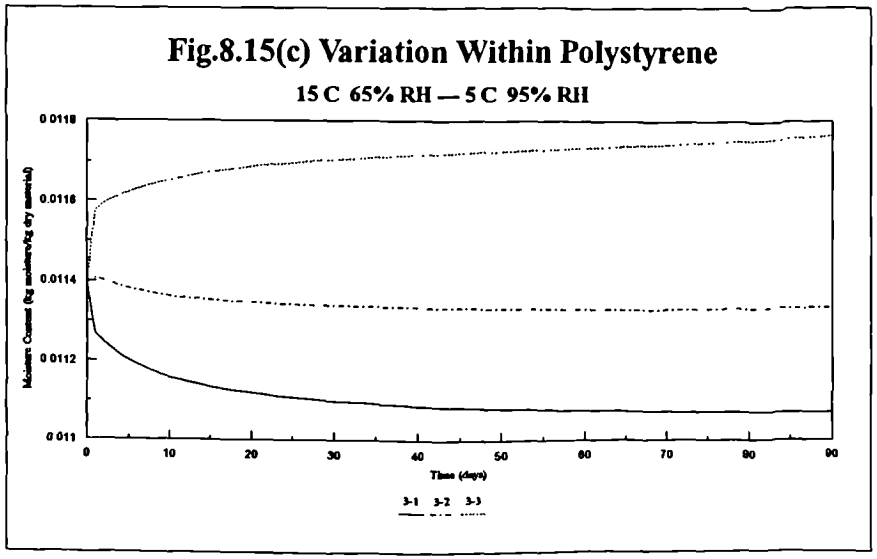

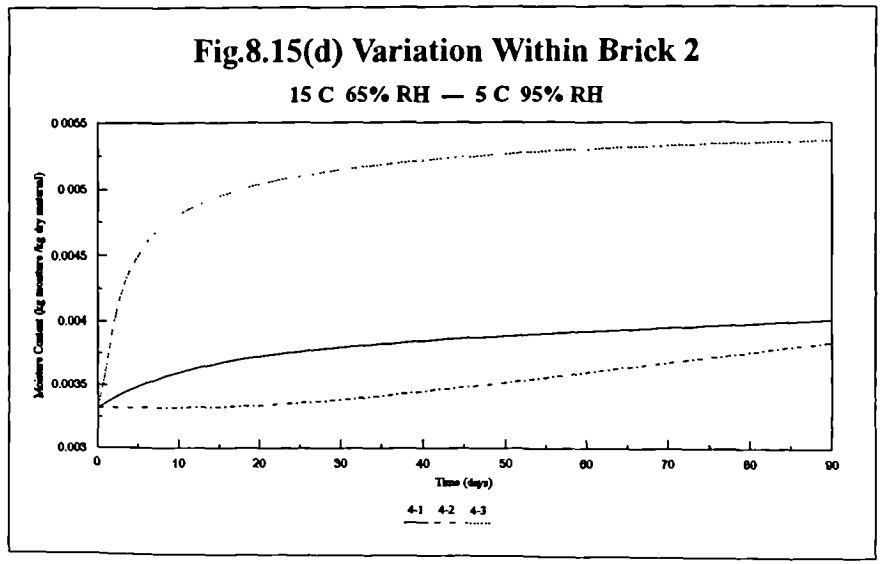

Figure 8.15 Brick Wall Results: moisture content data plotted against time at three locations for each layer of material

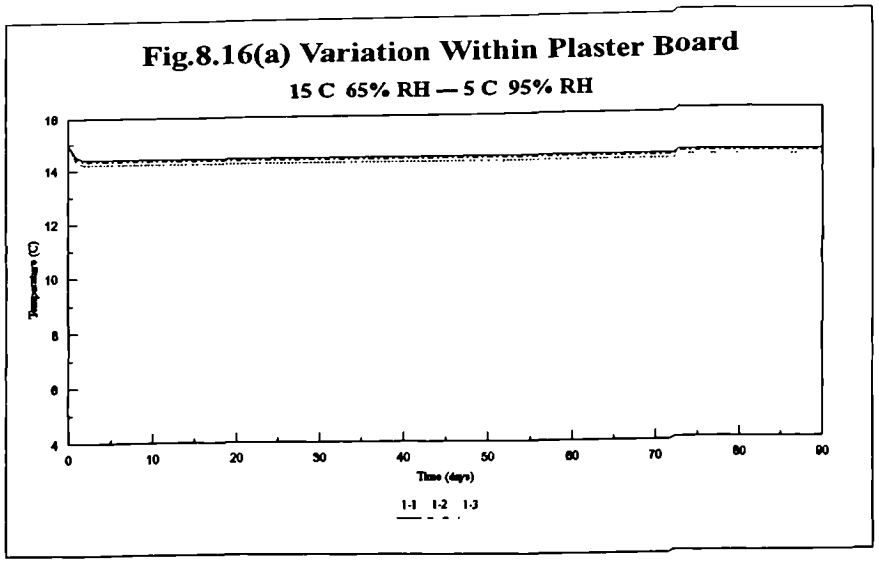

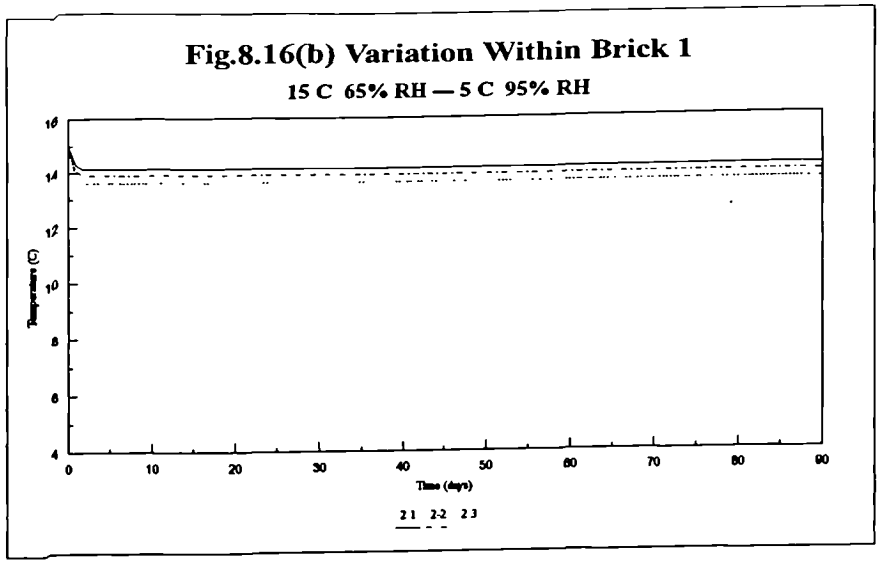

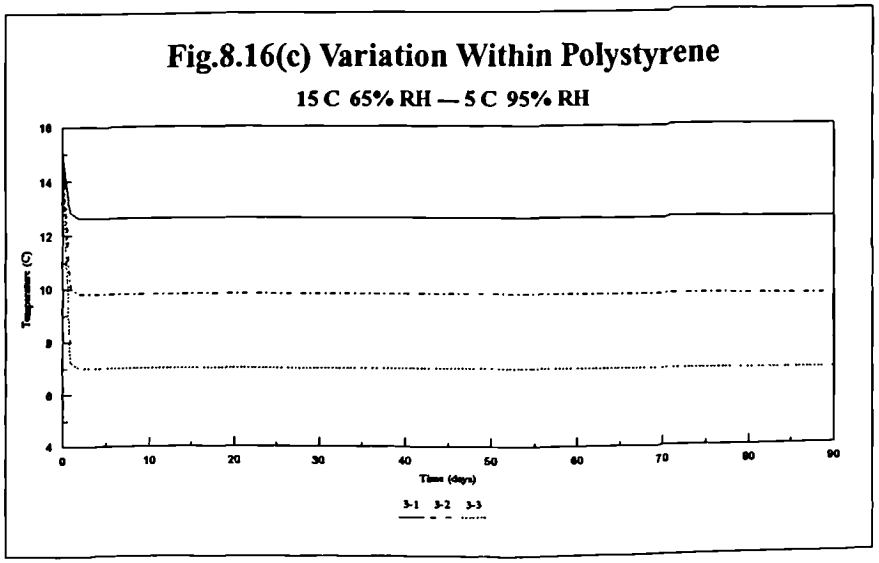

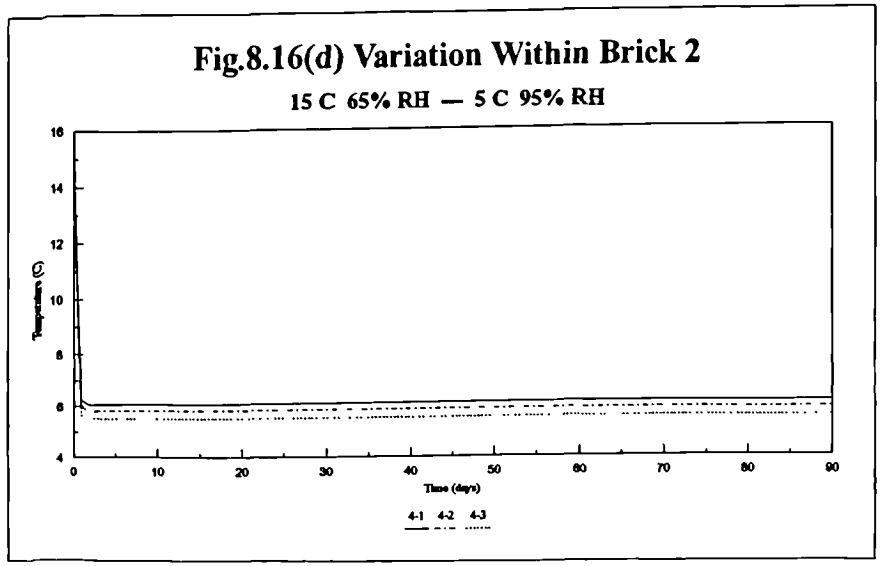

Figure 8.16 Brick Wall Results: temperature data plotted against time at three locations for each layer of material

8.3.2 Moisture Content and Temperature Profiles.

The moisture content and temperature profiles are given as Figure 8.17and 8.18 respectively. The absolute moisture contents of the plasterboard and insulation at day 90 can be re-expressed as 4% and 1% by mass respectively. If 20% by mass is used as the danger level, it would seem that neither will be under risk of moisture damage.

8.3.3 Moisture Flow Rates.

The flow rates of moisture at both surfaces of the structure are given in Figure 8.19, while Figure 8.20 shows a profile of the flow rates throughout the wall at day 90. These graphs indicate that equilibrium is not yet reached with moisture accumulating due to flow into the construction from both surfaces.

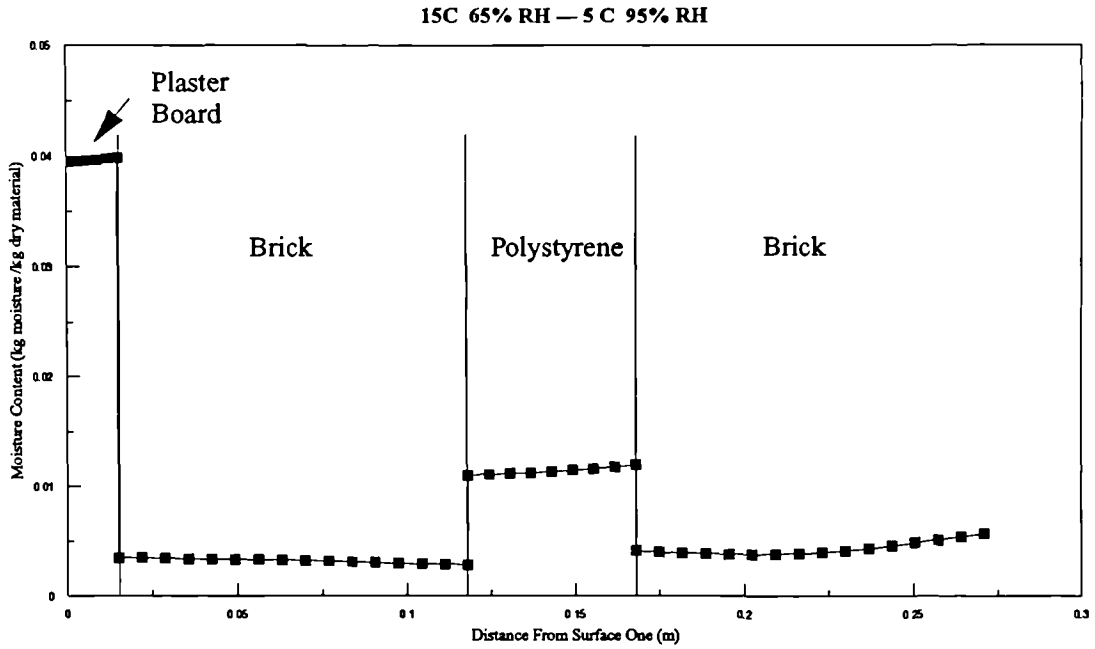

Figure 8.17 Brick Wall Results: moisture content profiles

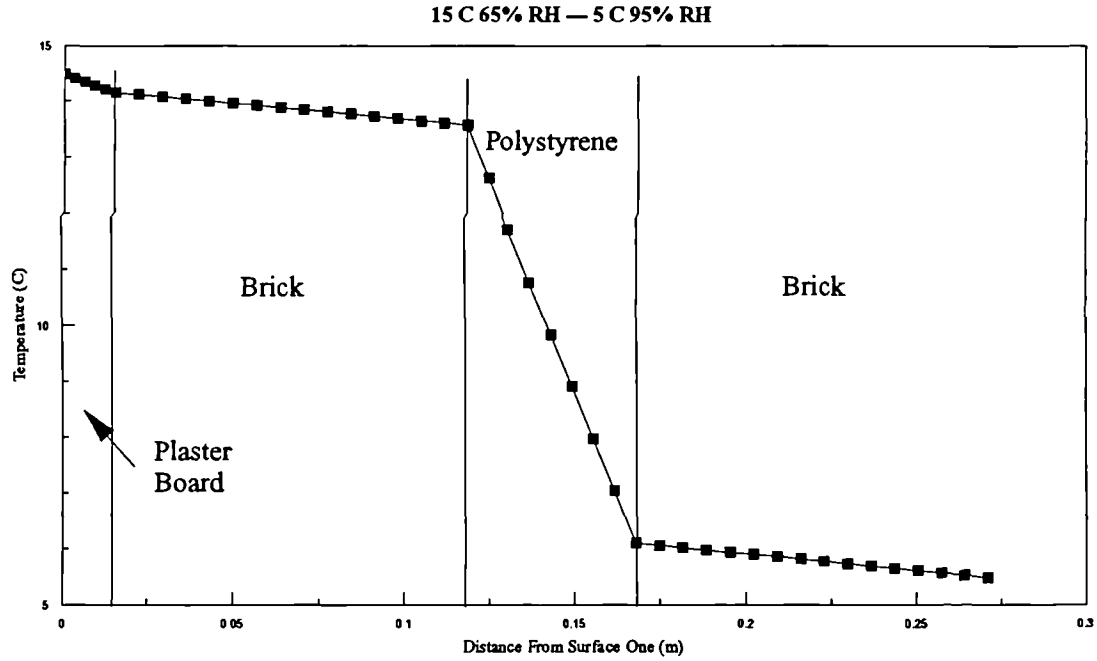

Figure 8.18 Brick Wall Results: temperature profiles

Figure 8.19 Brick Wall

Flow Rate At Surfaces

15 C 65% RH --- 5 C 95% RH

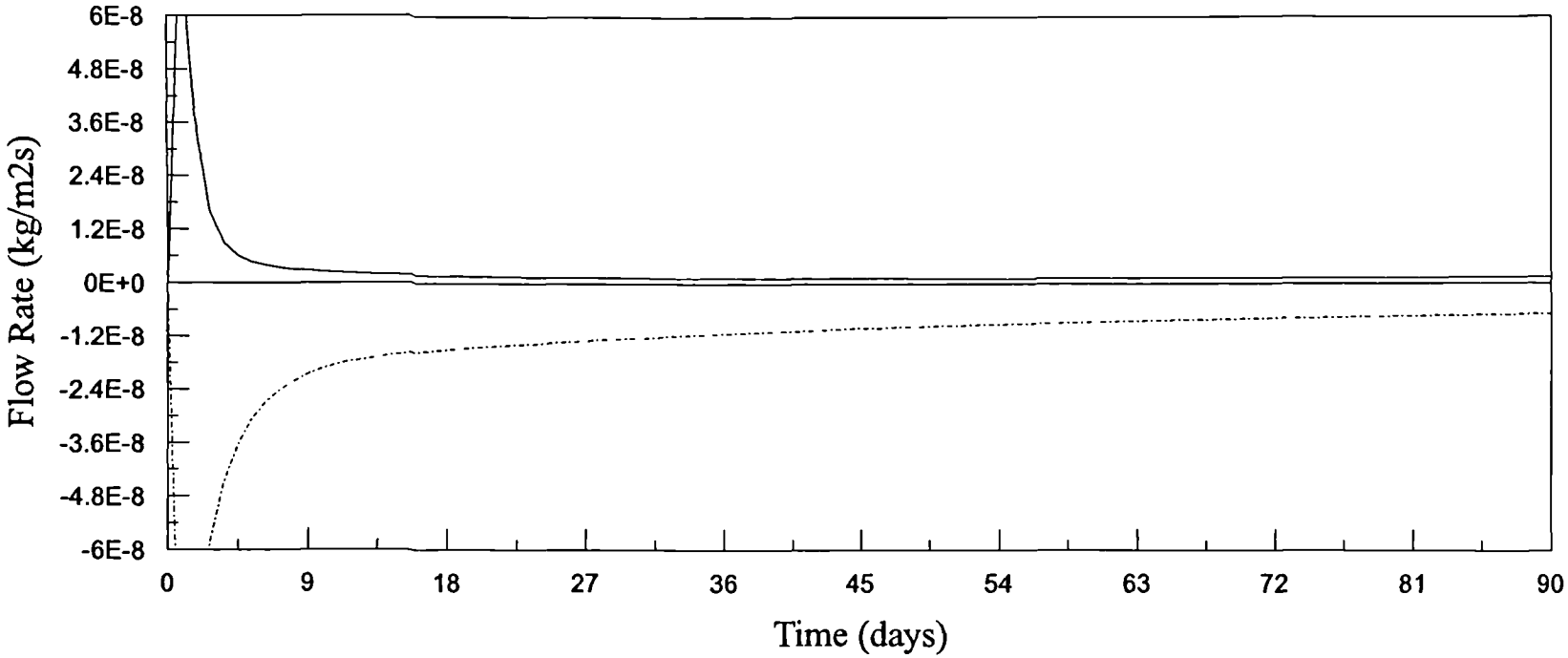

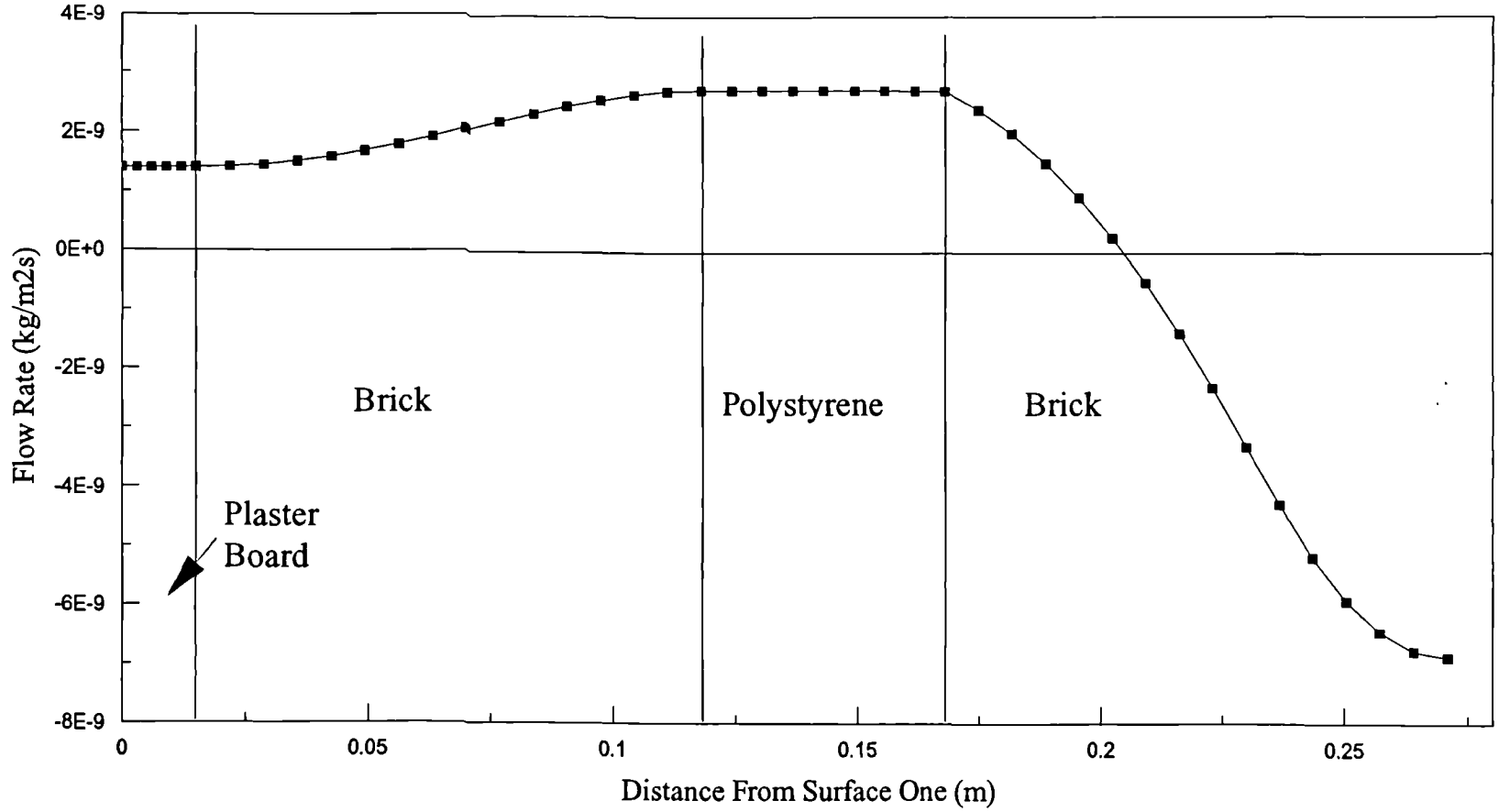

Figure 8.20 Brick Wall Results: flow rate profile

9. CONCLUSIONS AND RECOMMENDATIONS.

Moisture transfer through porous building materials is a complex process which, up until recently, has been treated in a simplistic manner by many researchers. The majority of models in use today are steady state, with vapour pressure used as the sole driving potential. These models only account for moisture movement in the form of water vapour.

Experimental results obtained during this research have demonstrated that, for hygroscopic building materials, the transfer of liquid water within pores is of great importance at high relative humidities. Investigation of the transfer mechanisms involved has highlighted the complexity of this process, and the coupled effect between heat and mass transfer.

While several researchers have attempted to formulate combined heat and mass transfer equations (notably Luikov[9][10]), these models, in almost all cases, require the input of parameters which are indeterminate. One of the main difficulties lies in the experimental separation of the liquid and vapour transfer coefficients. It is also the case that in the literature much uncertainty exists as to the role of so called 'thermal diffusion' in the moisture transfer process, and that no authoritative view has been postulated on the correct set of driving potentials to be adopted.

In this work a set of combined heat and mass transfer equations have been developed, based on the premise that the fundamental potential for mass transfer will be concentration gradient. This premise involves the use of vapour density and

liquid pressure as the only credible driving potentials, which by manipulation leads to the use of vapour pressure and temperature within the governing equations. It is possible to re-arrange these equations using other parameters, but these represent the most suitable for measurement and experimental purposes. Some researchers have attempted to use material moisture content as a potential, but this is clearly incorrect as, unlike temperature and vapour pressure, this will not be a continuous function throughout a multi-layer construction.

The solution of the equations developed require the experimental evaluation of the vapour and liquid transfer coefficients, as well as material sorption isotherms. In this research it has been demonstrated that these parameters can be obtained using experimental techniques which are an extension of existing test methods, and which do not involve unrealistic facilities. This experimental approach combined with the heat and mass transfer equations, has produced a model which is fully transient in nature, accurately describes all of the significant transport mechanisms, and does not require the use of indeterminate data.

A subsidiary set of experiments has shown that when the equations are properly formulated, there is no 'thermal diffusion' effect of any significance. The temperature coefficient within the governing equations, as developed, is a function only of the mathematical manipulation from the actual driving potentials of vapour density and liquid pressure to the more usable potentials of vapour pressure and temperature. This temperature coefficient is not a true 'thermal diffusion' effect, such an effect being defined as occurring as a function of temperature gradient alone. No 'thermal gradient' coefficient is therefore included in the final model equations produced in this work.

The value of this more accurate approach to the modelling of moisture movement through building structures has been demonstrated by coding the equations into a one dimensional finite difference computer model. While this computer model could be considered crude in terms of input/output and inefficient in terms of the solution algorithm, it has been used successfully in the analysis of simple structures. The results produced illustrate the immense importance of transient effects in the modelling of moisture transfer and the very large difference in time constant between the process of thermal and moisture equilibrium. This further highlights the inadequacy of simple steady state models, when equilibrium times of up to and beyond one year may be expected for masonary materials.

The model in its current form is, however, limited in the following respects:

(i) the solution time for a relatively simple construction is of the order of seven hours for a 90 day simulation, when run on a standard model 386 personal computer.

(ii) the output data is generated as a numerical data file and requires to be interrogated using other commercial software packages.

(iii) *the model requires input of external and internal* parameters for any selected month. At present no account can be taken of diurnal, weekly or monthly variations.

(iv) the range of building structures which can be analysed is limited to the restricted data base of material properties currently available. Reliable data on only eight materials has been determined during this work.

It is also the case that in this research no consideration has been given to the possibility of water existing in the form of ice within materials, the effects of salt depositions, or the influence of surface wetting from rain. These effects have been regarded at this stage as being of secondary importance. The model is also limited in its handling of certain boundary conditions, notably in terms of air cavities. At present, air cavities can only be treated as unventilated. It is recognised by the author that ventilation to and from air cavities could significantly affect the mass and energy balance, but a lack of data on such effects makes their inclusion uncertain. A similar difficulty exists in handling the influence of bulk air movement through structures due to wind induced total pressure differences.

The model as it stands is clearly a significant step forward in terms of understanding, and provides a more accurate tool for use by researchers in this field. The greatest potential for this work in the short term lies in improving the computing aspects and data base to make it accessible to designers. In order to enhance the model in this way, improvements would be recommended as given below:

(i) **User Interface**: At present the user must supply the necessary material properties and relevant weather parameters. A complete data base of material properties and weather information should be incorporated into the code. The user should be able to select the structural components by name.

(ii) **Program Output**: The output capability of the model should be enhanced to give directly profiles of temperature and material moisture content as graphical output. There should also be identification of the locations where 'critical' values of material moisture content have been exceeded.

(iii) **Weather Conditions**: Weather input based on the use of a 'standard weather year' should be compiled (e.g. utilising Kew 1967 standard weather file covering a complete year, or a three month winter climate period).

(iv) **Solution Algorithms**: Development work is needed to improve the efficiency of computation and hence to reduce the run time required. This necessitates an investigation of the solution algorithm, perhaps involving implicit finite differencing. It is probable that an alternative language to Fortran would be more suitable.

(v) **Data Base Enhancement**: A reliable set of data is required on at least a further twenty commonly used building components to enable an acceptable range of wall structures to be analysed. This could be achieved partly by measurement and partly by re-analysis of results from experiments carried out by other researchers. It will also be necessary to establish 'safe limits' on the maximum moisture contents considered acceptable for each material to avoid adverse thermal or structural degradation

In the longer term, research is clearly required on the effect and magnitude of air movements both through structures and within cavities. Only when such information is available can the theoretical basis of this model be improved to include such influences.

REFERENCE

1. BRITISH STANDARD 5250, 1975. 'Code of basic data for the design of buildings: The control of condensation in dwellings'.

2. SANDERS, CHRIS 'Condensation Effects on Structure Durability', Building Service Journal, Nov. 1988.

3. GLASER, H. 'Graphical method for investigation of diffusional process'. Kaltetechnik, 11, 1959.

4. SILCOCK, G.W.H. and SHIELDS, T.J. 'Predicting condensation: an alternative approach'. Energy in Buildings. January/February 1985.

5. JOHNSON K. A., 'Interstitial Condensation', Building Technical File, Number 8, Jan. 1985.

6. KEIPER, G., CAMMERER, W., WAGNER, A. 'A New Diagram for Technical Assessment of Moisture protection of Building constructions'. Geshundheits-Ingenieun, 95, 1974.

7. KOHONEN R. 'A Method to Analyze the Transient Hygrothermal Behaviour of Building Materials and Components'. PhD Thesis, Helsinki University of Technology, Otaniemi, Finland, October 1984.

8. ANN-CHARLOTTE ANDERSSON 'Verification of Calculation Method for Moisture Transport in Porous Building Materials'. D6:1985, Swedish Council for Building Research.

9. LUIKOV, A. V. 'Heat and Mass Transfer in Capillary-porous Bodies'. Pergamon Press, 1966.

10. LUIKOV, A. V. 'System of Differential Equations of Heat and Mass Transfer in Capillary-Porous Bodies', Int. J. Heat Mass Transfer, Vol. 18,1975

11. GALBRAITH, G.H. and McLEAN, R.C. 'Realistic Vapour Permeability Values', Building Research and Practice, vol.14, No.2, 1986.

12. McLEAN, R.C. and GALBRAITH, G.H. 'Interstitial Condensation - the Applicability of Conventional Vapour Permeability Values', Building Services Engineering Research & Technology.

13. ROWLEY, F. B. 'A Theory Covering the Transfer of Vapour through Materials', ASME Transaction, Vol.45, 1939.

14. PHILIP J. R., and DE VRIES D. A. 'Moisture Movement in Porous Materials under Temperature Gradients'. Transactions, American Geophysical Union, Vol. 38, No.2, April 1957.

15. DE VRIES D. A. 'Simultaneous Transfer of Heat and Moisture in Porous Media.' Transactions, American Geophysical Union, vol.39, No.5, October 1958.

16. ROSE, D. A. 'Water Movement in Porous Materials: Part I - Isothermal Vapour Transfer', British J. of Applied Physics, vol.14, 1963,pp256-262.

17. ROSE, D. A. 'Water Movement in Porous Materials: Part II - the Separation of the Components of Water Movement', British J. of Applied Physics, vol.14, 1963,pp491-496.

18. CLAESSON, JOHAN 'Fundamentals of Moisture and Energy Flow in Capillary-Porous Building Materials' Univ. of Lund, Sweden (1977).

19. SCHIRMER, R. 'Diffusionszahl von Wasserdampt-Luft-gemischen und dis Verdampfungsgeschwindigkait', Z. VOI, Beil. Verfahr, Techn. 1938.

20. SHERWOOD, T.K., PIGFORD, R.L. 'Absorption and Extraction', McGraw-Hill Book Company, New York, 1958.

21. DE VRIES D. A. 'Some remarks on gaseous diffusion in soils', Trans. 4th Intern. Cong. Soil Sci., 2, 1950.

22. KOTHANDARAMAN, C.P., SUBRAMANYAN, S. 'Heat and Mass Transfer Data Book', 3rd Edition, Wiley Eastern Ltd., 1977.

23. McLEAN, R.C. 'Interstitial Condensation and the Vapour Transmission Performance of Building Materials', MPhil Thesis, Univ. of Strathclyde, 1988.

24. GREW, K.E., IBBS, T.L. 'Thermal Diffusion in Gases' Cambrigde University Press, 1952.

25. VAN GONGEN, M.E.H. 'Thermal Diffusion Effects in Shock Tube Boundary Layer', Technische Hogeschool Eindhoven, 1978.

26 KUMARAN, M.K. 'Moisture Transport Through Glass-Fibre Insulation in the Presence of a Thermal Gradient', Journal of Thermal Insulation, Vol.10, 1987.

27. PHILIP, J.R. 'Theory of Infiltration', Advances in Hydroscience, vol.5, pp215-296,1969.

28. RICHARDS, L.A. 'Capillary Conduction of Liquid through Porous Mediums', Physics 1, pp328-333, 1931.

29. CHILDS, E.C., COLLIS-GEORGE, N. 'The Permeability of Porous Materials', Proc. Roy. Soc. A201, pp392-405, 1950.

30. VOS, B.H. 'Moisture Transport in Porous Materials', TNO, Delfl, 1966.

31. KAUFMAN, B.N. 'Thermal Conductivity of Building Materials', Gosstroiizdat, 1955.

32. DUBNITSKY, V.I. Izv VTI No.10, 1952

33. THIERRY DUFORESTEL, Personal Communication.

34. DE GROOT, S.R. 'Thermodynamics of Irreversible Process', Interscience, New York, 1952.

35. BRUNAVER S., EMMETT P.H, TELLER E. 'Adsorption of gases in Multimolecular Layer' Jornal of American Chemical Society, Vol.60, 1938.

36. CREGG S.J, SING K.S.W 'Adsorption, Surface Area & Porosity' Academic Press, 1967.

37. HANSEN, KURT KIEWGAARD 'Sorption Isotherm, A Catalogue' *Technical* Report 162/86, Building Materials Laboratory, The Technical University of Denmark, 1986.

38. TVEIT, ANNANIAS 'Measurement of Moisture sorption and moisture Permeability of Porous Materials', Norwegion Building Research Institute, Report 45, OSLO, 1966.

39. BRAND, R.S. 'Sorption Isotherms for Building Materials' BEng Thesis, Strathclyde University, 1989.

40. KURT KIE [illegible], 'Kapillarer und dampfformiger Feuchtetransport in mehrschichtigen bauteilen' Dissertation zur Erlangung des Grades, Doktor-Ingenier des Fachbereiches, bauwesen der Universitat-Gasamthochschele-Essen, essen, 1983

41. PEDERSEN, C.R. 'Combined Heat and Mass Transfer in Building Construction', Report no.214, Tech. Univ. of Denmark, 1990.

42. JACOB BEAR 'Dynamics of Fluids in Porous Media.' American Elsevier Publishing Company, inc. 1972.

43. HOLMAN, J.P. 'Thermodynamics', McGraw-Hill Book Company, 1980.

44. PENMAN, H.L. 'Gas and Vapour Movement in Soil'. I. J. Agr. Sci., 30, 437-462, 1940.

45. CHARTERED INSTITUTE OF BUILDING SERVICES ENGINEERS, GUILDE BOOK A, 1986.

46. AMERICAN SOCIETY OF HEATING, REFRIGERATION AND AIR CONDITIONING ENGINEERS, HANDBOOK OF FUNDAMENTALS 1985

47. INTERNATIONAL ENERGY AGENCY, 'Catalogue of Material Properties' Report Annex XIV, Vol.3, 1991.

48. BRITISH STANDARD 4270, 1973, Part 2, 'Methods of Test for Rigid Cellular Materials'.

49. 'International Critical Tables', McGraw-Hill Book Company, New York, 1930

50. GALBRAITH, G.H., McLEAN, R.C. 'Interstitial Condensation And The Vapour Permeability of Building Materials', Energy in Buildings, 14, 1990.

51. LANGMUIR, I. Journal of the American Chemical Society, Vol.40, 1918.

52. LYKOW, A.W. 'Transporterscheinungen in Kapillarporosen Korpern', Akademie-Veriag, Berlin, 1958.

53. McLEAN, R.C., GALBRAITH, G.H., SANDERS 'Moisture Transmission Testing of Building Materials and the Presentation of Vapour Permeability Values', Building Research and Practice, No.2, 1990.

54. SMITH, G.D. 'Numerical Solution of Partial Differential Equations: Finite Difference Methods', Oxford University Press, 1978.

55. BAYLEY, OWEN & TURNER 'Heat Transfer', Nelson, 1972.

56. CLARKE, J.A. 'Energy Simulation in Building Design', Adam Hilger, 1985.

57. INCROPERA, DE WITT 'Fundamentals of Heat and Mass Transfer', 3rd Edition, Wiley, 1990

58. SHIH, T.M. 'Numerical Heat Transfer', Hemisphere Publishing Corporation, 1984.

59. ANDERSON, TANNEHILL, PLETHER 'Computational Fluid Mechanics and Heat Transfer', McGraw-Hill, 1984.

60. BALFOUR & MARWICK 'Programming in Standard FORTRAN 77', Heinemann Educational Books, 1982.

61. MOJENA & AGELOFF 'FORTRAN 77', Wadsworth Publishing Company, 1989.

62. 'Miscosoft FORTRAN V5.1 Reference', Microsoft Corporation, 1991.

63. 'User's Guide: Freelance Graphics for Windows Release 1.0', Lotus Development Corporation, 1991.

64. British Standard 5250:1989 'British Standard Code of Practice for Control of Condensation in Building'

65. R.C. DEGROOT 'Wood Decay Ecosystem in Residential Construction', Proceeding of XVIth IUFRO World Congress, Vancouver, 1976

APPENDIX ONE

DERIVATION OF KELVIN'S EQUATION

APPENDIX ONE DERIVATION OF KELVIN'S EQUATION

In moisture transfer in building materials, Kelvin's equation has been constantly used in order to relate the vapour pressure and liquid water pressure inside capillary pores. The derivation of Kelvin's equation is based on classical thermodynamics. Let g denote the chemical potential and the superscripts α and β the different phases. When the two phases are in equilibrium their chemical potentials have to be equal, i.e. $g^{\alpha} = g^{\beta}$. The chemical potentials are a function of pressure and temperature. With any change in temperature and pressure, the whole system will equilibriate at a new state, which has to satisfy the condition $dg^{\alpha} = dg^{\beta}$. Then:

$$\left(\frac{\partial g^{\alpha}}{\partial T^{\alpha}}\right)_{p^{\alpha}} dT^{\alpha} + \left(\frac{\partial g^{\alpha}}{\partial p^{\alpha}}\right)_{T^{\alpha}} dp^{\alpha} = \left(\frac{\partial g^{\beta}}{\partial T^{\beta}}\right)_{p^{\beta}} dT^{\beta} + \left(\frac{\partial g^{\beta}}{\partial p^{\beta}}\right)_{T^{\beta}} dp^{\beta} \qquad (A1.1)$$

If $dT^{\alpha} = dT^{\beta} = 0$, then

$$\left(\frac{\partial g^{\alpha}}{\partial p^{\alpha}}\right) dp^{\alpha} = \left(\frac{\partial g^{\beta}}{\partial p^{\beta}}\right) dp^{\beta} \qquad (A1.2)$$

From thermodynamic relationships:

$$\frac{\partial g^{\alpha}}{\partial p^{\alpha}} = V^{\alpha} \rightarrow \text{Specific Volume}$$

Equation (A1.2) becomes:

$$V^{\alpha} dp^{\alpha} = V^{\beta} dp^{\beta} \qquad (A1.3)$$

if α: vapour phase.

β: liquid phase

then V^{α}: vapour specific volume (m^3/kg).

p^{α}: vapour pressure above interface (N/m^2).

V^{β}: liquid specific volume (m^3/kg).

p^{β}: liquid pressure below interface (N/m^2).

Integrating equation (A1.3) for pressure changes:

$$\int_{p_o^{\alpha}}^{p_1^{\alpha}} V^{\alpha} dp^{\alpha} = \int_{p_o^{\beta}}^{p_1^{\beta}} V^{\beta} dp^{\beta} \qquad (A1.4)$$

where subscript o, in this situation, specifically refers to the pressures when the interface between the liquid and vapour is flat, and subscript 1 to those when the interface is curved, as inside a capillary.

Taking vapour as a perfect gas and liquid water as incompressible, then $V^{\beta} = \text{constant}$ and $V^{\alpha} = RT/p^{\alpha}$. Equation (A1.4) becomes:

$$RT \int_{p_o^{\alpha}}^{p_1^{\alpha}} \frac{1}{p^{\alpha}} dp^{\alpha} = V^{\beta} \Delta p^{\beta} \qquad (A1.5)$$

$$\therefore \quad RT \ln\left(\frac{p_1^{\alpha}}{p_o^{\alpha}}\right) = V^{\beta} \Delta p^{\beta} \qquad (A1.6)$$

$$\therefore \quad p_1^{\beta} - p_o^{\beta} = \frac{RT}{V^{\beta}} \ln\left(\frac{p_1^{\alpha}}{p_o^{\alpha}}\right) \qquad (A1.7)$$

p_o^{α} and p_o^{β} are pressures applied on the free flat interface, thus $p_o^{\alpha} = p_o^{\beta}$. Equation (A1.7) is:

$$p_1^{\beta} - p_o^{\alpha} = \frac{RT}{V^{\beta}} \ln\left(\frac{p_1^{\alpha}}{p_o^{\alpha}}\right) \qquad (A1.8)$$

Equation (A1.8) is the Kelvin's equation.

APPENDIX TWO

EXPERIMENTAL RESULTS

-- SECTION ONE: ISOTHERMAL CUP TEST RESULTS

-- SECTION TWO: EQUILIBRIUM MOISTURE CONTENT RESULTS

-- SECTION THREE: NON-ISOTHERMAL CUP TEST RESULTS

APPENDIX TWO

SECTION ONE

ISOTHERMAL CUP TEST RESULTS

MATERIAL: Particle Board

TEMPERATURE: 23°C

TEST NO.	TEST PERMEABILITY OVER RH RANGE: (% INSIDE CUP - % OUTSIDE CUP) $\bar{\mu} \times 10^{12}$			
	0-60	80-60	93-60	100-60
1	3.72	4.21	5.66	6.47
2	3.68	3.75	5.72	5.81
3	3.79	3.84	5.53	6.67
4	3.57	3.46	5.87	6.40
5	3.80	4.06	5.25	6.90
6	3.84	4.05	5.48	6.36
AVERAGE VALUE	3.73	3.90	5.59	6.44
ST. DEVIATION	0.10	0.27	0.22	0.37

MATERIAL: Plywood

TEMPERATURE: 25°C

TEST NO.	TEST PERMEABILITY OVER RH RANGE: (% INSIDE CUP - % OUTSIDE CUP) $\bar{\mu} \times 10^{12}$			
	90-60	100-80	100-60	0-60
1	1.96	7.07	5.06	0.86
2	2.95	8.57	5.81	1.14
3	3.03	10.62	5.22	1.24
4	3.14	8.33	5.13	1.01
5	2.95	9.26	4.99	1.03
AVERAGE VALUE	2.81	8.77	5.24	1.06
ST. DEVIATION	0.48	1.30	0.33	0.14

MATERIAL: Plywood

TEMPERATURE: $20^{0}C$

TEST NO.	TEST PERMEABILITY OVER RH RANGE: (% INSIDE CUP - % OUTSIDE CUP) $\bar{\mu} \times 10^{12}$			
	90-60	0-80	100-80	100-60
1	2.98	0.97	10.1	5.16
2	2.72	1.26	8.64	5.28
3	3.14	0.97	8.88	5.7
4	3.67	0.9	8.27	5.15
5	3.03	1.06	8.0	5.41
6	2.64	1.32	9.03	5.34
7	2.61	0.81		
AVERAGE VALUE	2.97	1.04	8.82	5.34
ST. DEVIATION	0.37	0.19	0.73	0.20

MATERIAL: Plaster Board (Thin) TEMPERATURE: $20^{0}C$

TEST NO.	TEST PERMEABILITY OVER RH RANGE: (% INSIDE CUP - % OUTSIDE CUP) $\bar{\mu} \times 10^{11}$			
	0-60	100-60	100-80	90-60
1	2.13	2.57	2.94	2.41
2	2.07	2.61	2.93	2.32
3	2.13	2.72	3.09	2.21
4	2.20	2.64	3.04	2.32
5	2.10	2.74	3.17	2.28
6	2.12	2.54	3.04	2.34
7		2.58		2.43
AVERAGE VALUE	2.13	2.63	3.04	2.33
ST. DEVIATION	0.04	0.08	0.09	0.07

MATERIAL: Plaster Board (Thin) TEMPERATURE: $25^{0}C$

TEST NO.	TEST PERMEABILITY OVER RH RANGE: (% INSIDE CUP - % OUTSIDE CUP)			
	$\bar{\mu} \times 10^{11}$			
	100-60	100-80	0-60	89-60
1	2.36	2.73	2.07	2.32
2	2.36	2.71	2.11	2.27
3	2.48	2.87	2.19	2.18
4	2.45	2.84	2.10	2.25
5	2.52	2.92	1.90	2.83
6	2.46	2.85		
AVERAGE VALUE	2.44	2.82	2.07	2.37
ST. DEVIATION	0.07	0.08	0.11	0.26

MATERIAL: Plaster Board (Thick)

TEMPERATURE: $20^{0}C$

TEST NO.	TEST PERMEABILITY OVER RH RANGE: (% INSIDE CUP - % OUTSIDE CUP)			
	$\bar{\mu} \times 10^{11}$			
	60-0	100-80	100-60	93-60
1	2.41	3.47	3.26	2.87
2	2.31	3.68	3.40	2.91
3	2.37	3.39	3.22	2.86
4	2.37	3.67	3.28	2.83
5	2.40	3.39	3.16	3.04
6	2.40	3.81	3.30	2.86
7				2.85
AVERAGE VALUE	2.38	3.57	3.27	2.89
ST. DEVIATION	0.04	0.18	0.08	0.07

MATERIAL: Plaster Board (Thick)

TEMPERATURE: 25^{0}C

TEST NO.	TEST PERMEABILITY OVER RH RANGE: (% INSIDE CUP - % OUTSIDE CUP) $\bar{\mu} \times 10^{11}$			
	100-60	93-60	100-80	0-60
1	2.92	2.88	3.35	2.33
2	3.04	2.69	3.50	2.32
3	2.87	2.72	3.29	2.30
4	3.06	2.79	3.50	2.32
5	2.88	2.77	3.30	2.40
6	3.14	3.04	3.59	2.33
AVERAGE VALUE	2.99	2.82	3.42	2.33
ST. DEVIATION	0.11	0.13	0.11	0.03

MATERIAL: Wood

TEMPERATURE: $20^{0}C$

TEST NO.	TEST PERMEABILITY OVER RH RANGE: (% INSIDE CUP - % OUTSIDE CUP) $\bar{\mu} \times 10^{11}$			
	100-60	93 -60	0-60	100-80
1	1.57	1.16	0.18	2.46
2	1.34	1.20	0.17	2.18
3	1.39	1.26	0.19	2.27
4	1.44	1.10	0.20	2.36
5	1.43	1.05	0.20	2.28
6	1.34	1.11	0.18	2.23
AVERAGE VALUE	1.42	1.15	0.18	2.30
ST. DEVIATION	0.09	0.08	0.01	0.10

MATERIAL: Wood

TEMPERATURE: $25^{0}C$

TEST NO.	TEST PERMEABILITY OVER RH RANGE: (% INSIDE CUP - % OUTSIDE CUP) $\bar{\mu} \times 10^{11}$			
	100-60	93-60	0-60	100-80
1	1.36	0.96	0.17	2.16
2	1.19	0.98	0.14	1.87
3	1.12	0.94	0.16	1.85
4	1.31	0.91	0.17	2.15
5	1.31	0.93	0.14	2.18
6	1.38	0.96	0.16	2.23
AVERAGE VALUE	1.28	0.95	0.16	2.07
ST. DEVIATION	0.10	0.03	0.01	0.17

MATERIAL: Brick

TEMPERATURE: $20^{0}C$

TEST NO.	TEST PERMEABILITY OVER RH RANGE: (% INSIDE CUP - % OUTSIDE CUP) $\bar{\mu} \times 10^{12}$			
	100-60	93-60	0-60	100-80
1	2.38	1.34	0.66	3.43
2	1.98	1.03	0.72	2.74
3	2.59	1.51	0.67	3.51
4	2.28	1.27	0.73	2.91
5	2.21	1.52	0.82	3.54
6	1.84	1.35	0.80	2.97
AVERAGE VALUE	2.21	1.34	0.73	3.18
ST. DEVIATION	0.27	0.18	0.07	0.35

MATERIAL: Expanded Polystyrene

TEMPERATURE: $20^{0}C$

TEST NO.	TEST PERMEABILITY OVER RH RANGE: (% INSIDE CUP - % OUTSIDE CUP) $\bar{\mu} \times 10^{11}$			
	93-60	100-60	0-60	100-80
1	0.68	0.68	0.61	0.69
2	0.69	0.63	0.72	0.65
3	0.58	0.59	0.59	0.61
4	0.74	0.62	0.74	0.65
5	0.72	0.68	0.56	0.72
6	0.63	0.83	0.60	0.60
7	0.61	0.57	0.65	0.61
8	0.67	0.59	0.63	0.61
AVERAGE VALUE	0.67	0.65	0.64	0.64
ST. DEVIATION	0.05	0.08	0.06	0.04

MATERIAL: Expanded Polystyrene TEMPERATURE: $25^{0}C$

TEST NO.	TEST PERMEABILITY OVER RH RANGE: (% INSIDE CUP - % OUTSIDE CUP) $\bar{\mu} \times 10^{11}$			
	100-80	100-60	0-60	93-60
1	0.57	0.60	0.64	0.69
2	0.57	0.58	0.62	0.68
3	0.65	0.61	0.62	0.68
4	0.63	0.64	0.63	0.72
5	0.80	0.79	0.61	0.61
6	0.70	0.70	0.57	0.64
7	0.65	0.66	0.63	0.76
8	0.57	0.61	0.66	0.71
AVERAGE VALUE	0.64	0.65	0.62	0.69
ST. DEVIATION	0.08	0.07	0.03	0.05

MATERIAL: Extruded Polystyrene

TEMPERATURE: $23^{0}C$

TEST NO.	TEST PERMEABILITY OVER RH RANGE: (% INSIDE CUP - % OUTSIDE CUP) $\bar{\mu} \times 10^{11}$			
	0-50	80-60	93-60	100-60
1	2.405	1.860	2.619	2.319
2	2.736	2.124	2.857	2.423
3	2.399	1.770	2.856	2.399
4	2.532	2.517	2.068	1.814
5	1.543	1.936	1.959	1.871
6	2.058	2.424	2.652	1.883
AVERAGE VALUE	2.279	2.105	2.502	2.118
ST. DEVIATION	0.42	0.31	0.39	0.29

APPENDIX TWO

SECTION TWO

EQUILIBRIUM MOISTURE CONTENT RESULTS

TEST MATERIAL: Particle Board

TYPE OF ISOTHERM:	Absorption
EQUILIBRIUM TEMPERATURE:	23
TIME TO EQUILIBRIUM:	63 days

INITIAL R.H. (%)	EQUILIBRIUM R.H. (%)	NO. OF SAMPLES	AVERAGE EQUILIBRIUM WEIGHT (g)	AVERAGE DRY WEIGHT (g)	AVERAGE EQUILIBRIUM MOISTURE CONTENT (kg moisture/kg dry material)
0	32	8	90.602	85.448	0.0603
0	44	10	114.239	106.625	0.0714
0	58	9	103.638	95.195	0.0887
0	76	10	119.270	106.672	0.1181
0	93	9	113.340	95.591	0.1863
0	100	5	68.637	54.115	0.2684

TEST MATERIAL: Plywood

TYPE OF ISOTHERM:	Desorption
EQUILIBRIUM TEMPERATURE:	20
TIME TO EQUILIBRIUM:	25 days

INITIAL R.H. (%)	EQUILIBRIUM R.H. (%)	NO. OF SAMPLES	AVERAGE EQUILIBRIUM WEIGHT (g)	AVERAGE DRY WEIGHT (g)	AVERAGE EQUILIBRIUM MOISTURE CONTENT (kg moisture/kg dry material)
0	98	6	174.519	125.80	0.3873
98	80	6	160.354	125.80	0.2747
80	60	6	153.821	125.80	0.2227
60	40	6	149.558	125.80	0.1889
40	3	6	135.613	125.80	0.0780

TEST MATERIAL: Wood

TYPE OF ISOTHERM:	Desorption
EQUILIBRIUM TEMPERATURE:	20
TIME TO EQUILIBRIUM:	25 days

INITIAL R.H. (%)	EQUILIBRIUM R.H. (%)	NO. OF SAMPLES	AVERAGE EQUILIBRIUM WEIGHT (g)	AVERAGE DRY WEIGHT (g)	AVERAGE EQUILIBRIUM MOISTURE CONTENT (kg moisture/kg dry material)
0	98	6	148.136	104.87	0.4126
98	80	6	138.062	104.87	0.3165
80	60	6	131.963	104.87	0.2583
60	40	6	128.401	104.87	0.2244
40	3	6	115.430	104.87	0.1007

TEST MATERIAL: Brick

TYPE OF ISOTHERM:	Desorption
EQUILIBRIUM TEMPERATURE:	20
TIME TO EQUILIBRIUM:	75 days

INITIAL R.H. (%)	EQUILIBRIUM R.H. (%)	NO. OF SAMPLES	AVERAGE EQUILIBRIUM WEIGHT (g)	AVERAGE DRY WEIGHT (g)	AVERAGE EQUILIBRIUM MOISTURE CONTENT (kg moisture/kg dry material)
0	98	6	455.531	452.32	0.0071
98	80	6	454.265	452.32	0.0043
80	60	6	453.857	452.32	0.0034
60	40	6	453.315	452.32	0.0022
40	3	6	452.863	452.32	0.0012

TEST MATERIAL: Plaster Board (Thin)

TYPE OF ISOTHERM:		Absorption			
EQUILIBRIUM TEMPERATURE:		20			
TIME TO EQUILIBRIUM:		17 days			
INITIAL R.H. (%)	EQUILIBRIUM R.H. (%)	NO. OF SAMPLES	AVERAGE EQUILIBRIUM WEIGHT (g)	AVERAGE DRY WEIGHT (g)	AVERAGE EQUILIBRIUM MOISTURE CONTENT (kg moisture/kg dry material)
0	3	6	164.821	160.69	0.0257
3	40	6	165.828	160.69	0.0319
40	60	6	166.200	160.69	0.0343
60	80	6	167.032	160.69	0.0395
80	98	6	175.095	160.69	0.0897

TEST MATERIAL: Plaster Board (Thick)

TYPE OF ISOTHERM:			Absorption		
EQUILIBRIUM TEMPERATURE:			20		
TIME TO EQUILIBRIUM:			17 days		
INITIAL R.H. (%)	EQUILIBRIUM R.H. (%)	NO. OF SAMPLES	AVERAGE EQUILIBRIUM WEIGHT (g)	AVERAGE DRY WEIGHT (g)	AVERAGE EQUILIBRIUM MOISTURE CONTENT (kg moisture/kg dry material)
0	3	6	205.118	199.98	0.0257
3	40	6	206.287	199.98	0.0315
40	60	6	206.710	199.98	0.0337
60	80	6	207.724	199.98	0.0387
80	98	6	215.522	199.98	0.0777

TEST MATERIAL: Extruded Polystyrene

TYPE OF ISOTHERM:	Absorption				
EQUILIBRIUM TEMPERATURE:	23				
TIME TO EQUILIBRIUM:	10 days				
INITIAL R.H. (%)	EQUILIBRIUM R.H. (%)	NO. OF SAMPLES	AVERAGE EQUILIBRIUM WEIGHT (g)	AVERAGE DRY WEIGHT (g)	AVERAGE EQUILIBRIUM MOISTURE CONTENT (kg moisture/kg dry material)
0	3	16	10.689	10.581	0.0102
0	44	16	10.013	9.905	0.0109
0	58	16	10.810	10.689	0.0113
0	76	16	11.515	11.382	0.0117
0	93	16	11.593	11.439	0.0135
0	100	16	11.180	10.978	0.0184

TEST MATERIAL: Expanded Polystyrene

TYPE OF ISOTHERM:	Absorption
EQUILIBRIUM TEMPERATURE:	20
TIME TO EQUILIBRIUM:	10 days

INITIAL R.H. (%)	EQUILIBRIUM R.H. (%)	NO. OF SAMPLES	AVERAGE EQUILIBRIUM WEIGHT (g)	AVERAGE DRY WEIGHT (g)	AVERAGE EQUILIBRIUM MOISTURE CONTENT (kg moisture/kg dry material)
3	40	6	8.138	8.133	0.00061
40	60	6	8.140	8.133	0.00086
60	80	6	8.143	8.133	0.00123
80	98	6	8.166	8.133	0.00406

APPENDIX TWO

SECTION THREE

NON-ISOTHERMAL CUP TEST RESULTS

NON-ISOTHERMAL CUP TEST RESULTS FOR PARTICLE BOARD

TEST TEMPERATURE ^{0}C (inside cup - outside cup)	19.5-22.6	19.3-22.3	18.8-22.1	18.8-22.5
RELATIVE HUMIDITY % (inside cup - outside cup)	0-60	33-60	44-60	76-60
TEST NO.	PERMEABILITY $\bar{\mu}$ $x10^{12}$			
1	4.029	3.894	3.894	3.798
2	3.730	3.802	3.430	4.131
3	3.637	3.809	4.209	4.020
4	3.690	3.111	3.797	4.020
5	3.192	3.746	4.112	4.131
6	3.518	3.208	4.098	4.087
MEAN $\bar{\mu}$	3.633	3.595	3.923	4.031
ST. DEVIATION	0.275	0.342	0.286	0.125

NON-ISOTHERMAL CUP TEST RESULTS FOR EXTRUDED POLYSTYRENE

TEST TEMPERATURE ^0C (inside cup - outside cup)	16.0-22.4	16.4-22.4	16.3-22.4
RELATIVE HUMIDITY % (inside cup - outside cup)	0-60	44-60	76-60
TEST NO.	PERMEABILITY $\bar{\mu}$ x10^{12}		
1	1.51	1.70	2.47
2	2.21	1.49	1.68
3	2.87	1.85	2.88
4	1.49	2.25	1.63
5	1.46	1.64	2.58
6	2.28	2.21	
MEAN $\bar{\mu}$	1.97	1.86	2.25
ST. DEVIATION	0.58	0.31	0.56

APPENDIX THREE

BOUNDARY CONDITIONS APPLIED TO THE COMPUTER MODEL

APPENDIX THREE BOUNDARY CONDITIONS APPLIED TO THE COMPUTER MODEL

In chapter 5 a set of equations for heat and mass transfer was established. Appropriate experimental methods were then developed in chapter 6 to allow the required input data to be measured for different materials. However, these equations cannot be solved for a building structure without the specification of appropriate boundary conditions. Boundary conditions must be established for external surfaces, internal surfaces, and for the interface between the different elements of a structure.

A3.1 Boundary Conditions for Mass Transfer at Material Surfaces

Both external and internal wall surfaces will exchange mass with the ambient atmosphere by surface convection at the air side and at the material side by molecular diffusion as well as filtration flow, if a total pressure gradient exists. Designating superscript 0 for the air side and 1 for the material side, and assuming that there is no mass accumulation on the surface, then:

$$\sum j_i^0 = \sum j_k^1 \qquad i = 1,2; \quad k = 1,2$$

$$j_3^0 = j_3^1$$

As in previous chapters, subscript 1 denotes vapour, 2 liquid water and 3 inert gas (air).

A3.1.1 Vapour Transfer

At normal conditions when no surface wetting exists (i.e. from rain on the outside surface), moisture is transferred to the surface by convection on the air side.

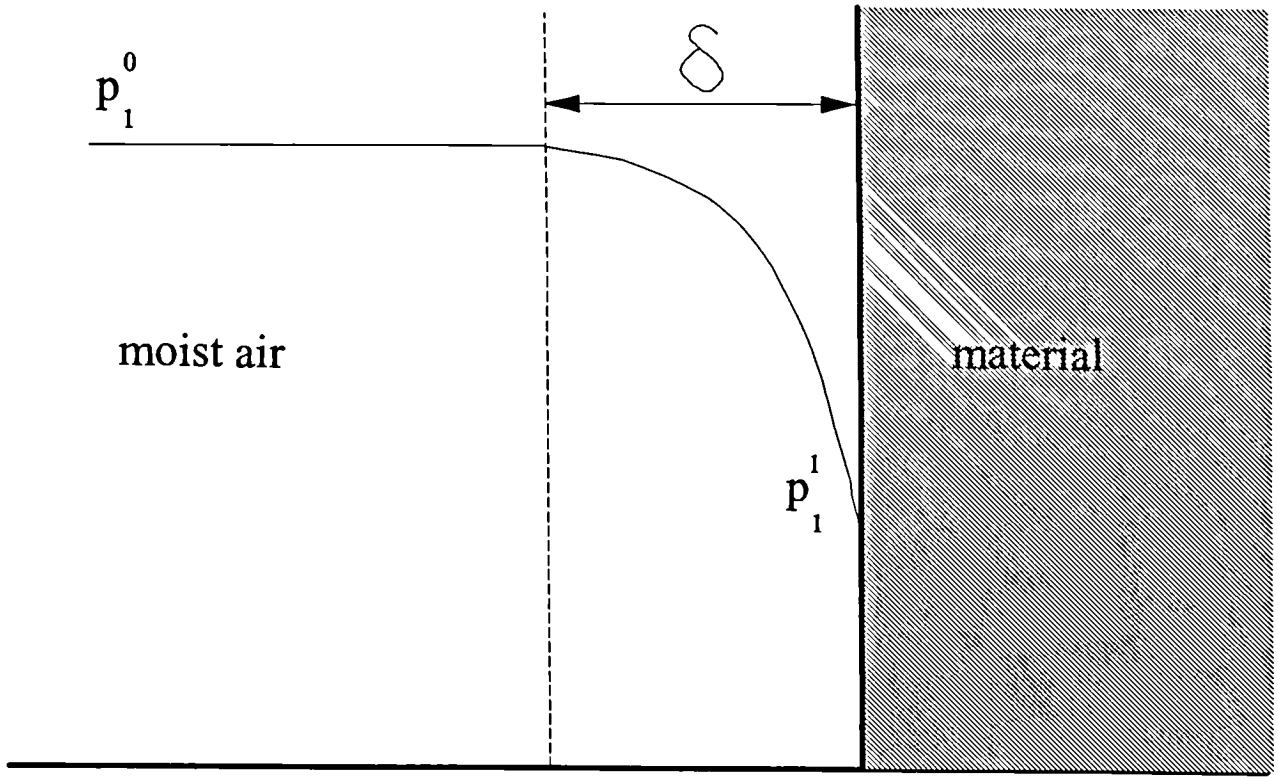

Fig.A3.1 Vapour Concentration Boundary Layer

Application of boundary layer theory allows the assumption that a concentration boundary layer will exist of thickness δ (Fig.A3.1). The magnitude of δ will depend on the mechanism of convection taking place - forced convection having a much smaller δ and hence enhanced transfer compared with natural convection. Within the boundary layer, flow can be either laminar or turbulent. The mass transfer, j_l^0, can be expressed using the following simplified relationship:[1][2][3]

$$j_l^0 = \beta \Delta \rho_l^0 \qquad (A3.1)$$

where β is the mass transfer coefficient, m/s.

The value of β will depend on the flow pattern within the boundary layer.

Unlike heat transfer, which has a considerable amount of data available on surface coefficients, little data is available in literature for the mass transfer coefficient, β, for different design situations. Assumptions must therefore be made to allow this coefficient to be evaluated.

As with the convection heat transfer coefficient H, the mass transfer coefficient is a function of the flow regime, the fluid properties and the geometric configuration of the surface. A convenient and widely-used method of approximating β is through

---

1KOHONON, R. 'A Method To Analyse The Transient Hygrothermal Behaviour of Building Materials and Components', PhD Thesis, Helsinki University of Technology, Otaniemi, Finland, Octobor 1984.

2ANN-CHARLOTTE ANDERSON 'Verification of Calculation Method for Moisture Transport in Porous Building Materials', D6:1985, Swedish Council for Building Research.

3PEDERSEN, C.R. 'Combined Heat and Mass Transfer in Building Constructions', Report No.214, Tech. Univ. of Denmark, 1990.

use of the analogy between the process of heat and mass transfer. On the basis of the Chilton-Colburn j-factor approach[1], this analogy is expressible in terms of H and β as:

$$\frac{H}{\beta \rho C p} = \left(\frac{\alpha}{D}\right)^{2/3} \qquad (A3.2)$$

where α is the thermal diffusivity, $\lambda / \rho C p$.

The ratio is referred to as the Lewis number. It is insentive to temperature variations and, for air-water mixture in the range of 0-20^{0}C, may be taken as approximately 0.85[2].The produce $\rho C p$ is the volumetric specific heat of moist air and varies with the ambient humidity and temperature. However, for environmental applications, a representative value of 1.2kJ/m^{3}K is acceptable with little error. For a temperature of 300K, D=0.000025m^2/s. Substituting these values into equation (A3.2):

$$\beta = 9.28 x 10^{-4} H \qquad (A3.3)$$

This relationship between the heat and vapour transfer coefficients can be considered valid for most situations encountered in building studies.

A3.1.2 Dry Air Transfer

Assuming that a uniform total pressure field exists within the material and across the thin, virtually stagnant, boundary (laminar) sub-layer next to the surface, the air flow must be such that it compensates for the pressure drop caused by vapour diffusion. Taking j^0_{1n} as the net flow of vapour diffusion and j^0_{3n} as the net dry air movement:

1SKELLAND, A.H.P. 'Diffusional Mass Transfer', Wiley, 1974.

2THRELKELD, J.L. 'Thermal Environmental Engineering', Prentice-Hall, 1962.

$$j^0_{3n} = -\frac{M_3}{M_1} j^0_{1n} \qquad (A3.4)$$

where M: the molecular weight.

In the above equation, j^0_{1n}depends upon the type of boundary condition on the air side. If it is of the first kind, as in the case of vapour pressure regulation with salt solutions:

$$\phi(t) = \phi_0$$
$$T(t) = T_0$$

where $\phi(t)$: function of relative humidity,

$T(t)$: function of temperature,

ϕ_0, T_0: constants

then $j^0_{1n} = 0$, because the amount of vapour diffused away is compensated by the vapour supply (the salt solution, for example). In this case, $j^0_3 = 0$, i.e. no net air diffusion. Under this condition, any tendency of air diffusion will be cancelled by the tendency of total pressure increase.

If the boundary condition has the initial form:

$$\phi|_{t=0} = \phi_0$$
$$T|_{t=0} = T_0$$

then $j^0_{1n} = j^0_1$. Air is diffused from or to the wall surface to compensate for the pressure drop by vapour transfer. Eventually this will lead to an equilibrium state of a uniform moisture field.

A3.1.3 Liquid Water Transfer

In the situation where driving rain is wetting a wall surface, the surface contacts pure liquid water and surface capillary suction occurs. In this circumstance, surfaces are firstly saturated with water and the water front then progresses further through the wall structure. If the time scale is long enough, the water front will eventually reach the other side of the wall, and within the structural materials liquid water will form a continuum phase. Investigation has shown that the distance of water front travel, ζ, and the mass increase by water capillary suction, m, follow exponential relationships with time[1][2][3][4]:

$$\zeta = C_1 t^{n1} \qquad (A3.5)$$

$$m = C_2 t^{n2} \qquad (A3.6)$$

where C_1, C_2, $n1$, $n2$ are constants. The values of $n1$ and $n2$ have been experimentally shown to be approximately 0.5.[1][2][3][4]

Experimental investigation of this effect is generally carried out by sealing the sample side faces and contacting one of its surfaces with liquid water, the opposite surface being exposed to moist air. A typical weight change of a sample is shown in Fig.A3.2.The sample weight increase follows a straight line against $\sqrt{t}$, the water front reaching the other side of the sample at time $\sqrt{t_0}$. After this the water suction decreases rapidly. The moisture content at capillary saturation is defined as the mean moisture content at t_0.

1KETTERNACKER, L. 'Ober die Fenchtigkeit von Manuern', GI 53 (1903) H.45, S.721-728.

2CAMMERER, W.F. 'Dia Kapillare Flussigkeitsbewegung in Porosen Korpen', VDI-forsch, H. 500 (1963).

3SCHWARZ, B. 'Die Kapillare Wasserantnahme von Baustoffen', GI 93 (1972), H.7, S.206-211.

4ANN-CHARLOTTE ANDERSON 'Verification of Calculation Method for Moisture Transport in Porous Building Materials', D6:1985, Swedish Council for Building Research.

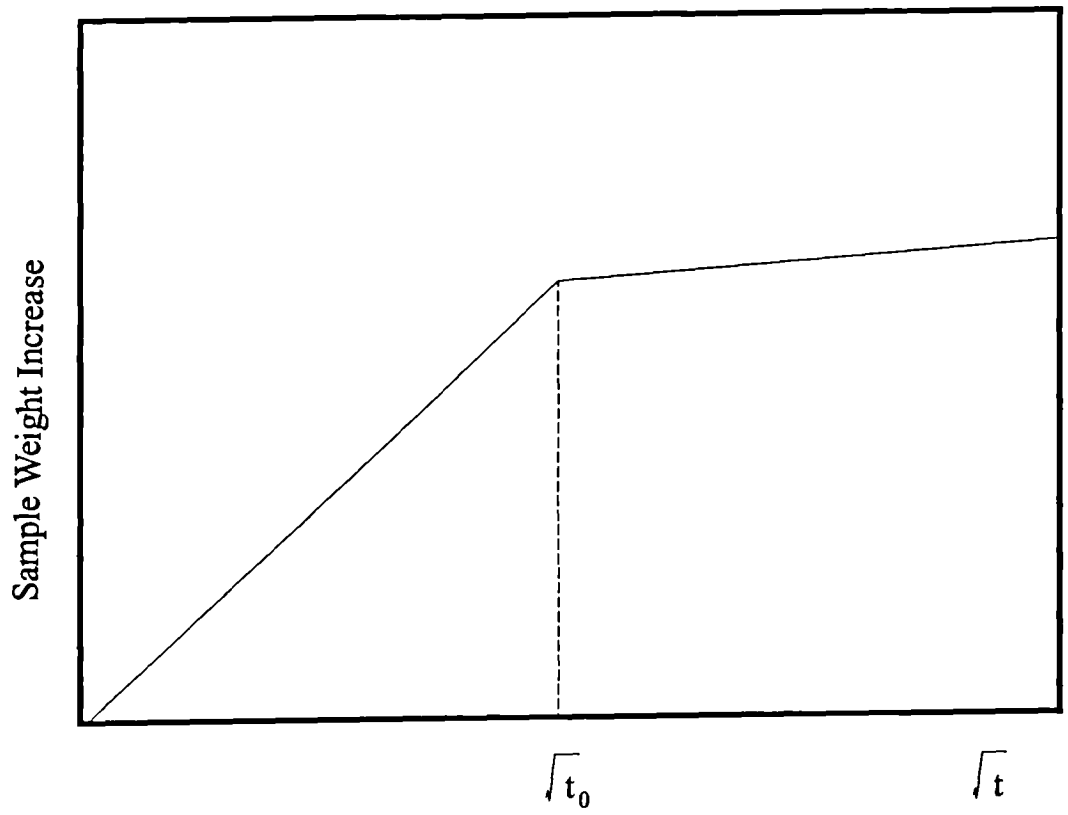

Fig.A3.2 Typical of Sample Weight Change in Capillary Suction

A3.2 Boundary Conditions for Energy Transfer at Material Surfaces

On the air side, energy is transferred to or from wall surfaces by the following mechanisms:

1) surface convection, q_c^0

2) mass transfer, $j_i^0 h_i$

3) radiation, q_r

On the material side, energy is transferred by conduction and moisture convection:

1) conduction, $q_{q\_cond}^1$

2) convection, $q_{q\_conv}^1 = j_i^1 h_i$

If no energy accumulation occurs at the surface:

$$q_c^0 + j_i^0 h_i + q_r = q_{q\_cond}^1 + q_{q\_conv}^1 \qquad (A3.7)$$

A3.2.1 Surface Convection

Energy transfer by surface convection takes the form of natural convection or forced convection. Natural convection occurs when the flow motion is caused by buoyancy forces. This type of convection is the primary process on the internal walls of building structures. Forced convection is the term used where the motion of the fluid arises from external forces - for instance, a fan, a blower or the wind. The external walls of a building are subject to wind driven forced convection. By the introduction of a heat transfer coefficient, H, the convection heat transfer, q_c^0, can be expressed as:

$$q_c^0 = H \Delta T \qquad (A3.8)$$

where ΔT: the temperature difference between the wall surface and the bulk air (K).

The heat transfer coefficient, H, greatly depends on the type of convection. Forced convection invariably has a much higher H than natural convection. The determination of values for H applicable to different situations is a major area of study in itself. In the following paragraph appropriate values are identified as being commonly used and accepted for the analysis of heat transfer in building structures.

Internal Walls with Natural Convection

The heat transfer coefficient, H, will depend on the orientation of the wall surface, the direction of heat flow and the temperature difference. Many correlations are available in terms of Nusselt number, Prandtl number and Grashof number[1][2][3][4]. However, for building designing purposes, typical values of the heat transfer coefficient have been suggested by the CIBSE GUIDE[5] as indicated in Table A3.1. These are typical values which are used in the United Kingdom by Building Services Engineers when estimating building heat loss.

1McADAM, W.H. 'Heat Transmission', 3rd Edition, McGraw-Hill, New York 1954.

2WARNER, C.Y., ARPARI, V.S. 'An Experimental Investigation of Turbulent Natural Convection in Air at Low Pressure Along A Vertical Heated Flat Plate', Int. J. Heat Mass Transfer, Vol.11, pp.397-406, 1968.

3FUJII, T., IMURA, H. 'Natural Convection From a Plate With Arbitrary Inclination', Int. J. Heat Mass Transfer, Vol.15, pp.755-767, 1972.

4RODGERS, G.G., SONSTER, C.G., PAGE, J.K. 'Development of An Interactive Computer Program SUN1', Rep. IRN BS28 (Sheefield: Sheffield Univ.)

5CHARTERED INSTITUTION OF BUILDING SERVICES ENGINEERS, GUIDE BOOK A, 1986.

External Walls with Forced Convection

External walls experience a much more complicated environment with the wind blowing in any possible direction and varying continually. McAdam[1] gives the following expression for heat transfer coefficient under forced convection:

$$H = 5.678\left[a + b\left(\frac{V}{0.3048}\right)^{n}\right] \qquad (A3.9)$$

where a, b and n are empirical values given in Table A3.2.

The CIBSE GUIDE[2] suggests the use of following equation for the prediction of H:

$$H = 5.8 + 4.1V_f \qquad (A3.10)$$

Pedersen quoted an expression by Jurges as[3]:

$$H = \begin{cases} 5.82 + 3.96V & V \leq 5m/s \\ 7.68V^{0.75} & V \geq 5m/s \end{cases} \qquad (A3.11)$$

Figure A3.3 shows the heat transfer coefficients predicted from the above correlations. These correlations show no great difference for velocities below 5m/s. Equation (A3.11) follows approximately the correlation proposed by McAdam for the smooth surface. The correlation given by the CIBSE overlaps equation (A3.9) when applied to a rough surface for wind speeds less than 10 m/s. At higher velocities the CIBSE equation deviates from the McAdam's equation to produce a prediction 20% higher at wind speeds of 30m/s.

1McADAM, W.H. 'Heat Transmission', 3rd Edition, McGraw-Hill, New York 1954.

2CHARTERED INSTITUTION OF BUILDING SERVICES ENGINEERS, GUIDE BOOK A, 1986.

3PEDERSEN, C.R. 'Combined Heat and Mass Transfer in Building Construction', Report No.214, Tech. Univ. of Denmark, 1990.

Table A3.1 Typical H Values (CIBSE GUIDE)

wall	3.0 W/m^{2}C
ceiling with upward heat flow	4.3 W/m^{2}C
floor with downward heat flow	1.5 W/m^{2}C

Table A3.2 Experimental coefficients in equation (A3.9)

Nature of surface	V < 4.88m/s			4.88 < V < 30.48m/s		
	a	b	n	a	b	n
Smooth	0.99	0.21	1	0	0.50	0.78
Rough	1.09	0.23	1	0	0.53	0.78

Fig.A3.3 Comparison of Correlations of Heat Transfer Coefficient

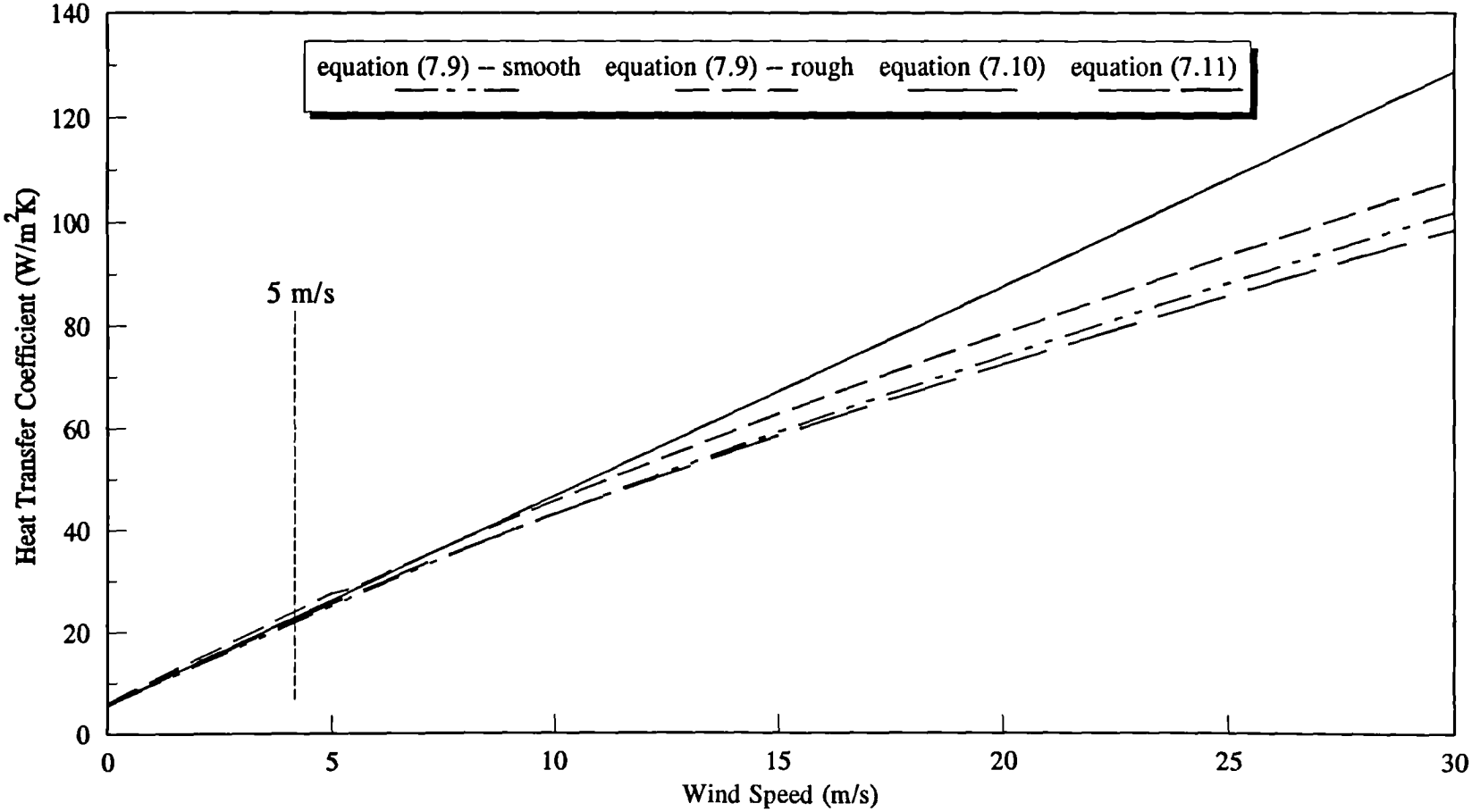

On the basis of the above it can been concluded that equation (A3.10) would be the most suitable equation for forced convection considering both simplicity and accuracy, and this equation has been incorporated in to the computer model.

A3.2.2 Radiation Exchange

When building structures are situated in a natural environment, energy transfer by direct absorption/emission of radiation should be considered. Radiation is generally divided into two regions: short-wave radiation with wavelengths less than 4μm (this region covers 99% of solar radiation energy); long-wave radiation with wavelengths greater than 4μm (this region is termed terrestrial radiation in the sense that it is the contribution from the solid and liquid of the earth's surface and atmosphere). External walls of building structures receive both short-wave and long-wave radiation. Internal walls, on the other hand, primarily exchange radiant heat as long-wave radiation.

Internal Walls

The radiant heat exchanged between an internal wall and other surfaces within a building can be simply expressed as:

$$q_{ri} = \epsilon_i H_{ri}(T_{ri} - T_{1i}) \qquad (A3.12)$$

where:
- H_{ri}: black body radiant heat transfer coefficient, W/m^{2}K
- ϵ_i: emissivity of internal walls
- T_{ri}: the radiant temperature of the other surfaces within the building, K. T_{ri} is generally not equal to the air temperature of the environment.
- T_{1i}: the temperature of internal wall surface, K.

When carrying out building thermal calculations this radiant heat transfer is often combined with surface convection to give the total heat transfer as:

$$q_i = q_{ci}^{0} + q_{ri}$$
$$= H(T_{0i} - T_{1i}) + \epsilon_i H_{ri}(T_{ri} - T_{1i}) \qquad (A3.13)$$

where T_{0i}: the air temperature, K.

In the United Kingdom the CIBSE use the concept of the environmental temperature, T_{ei}, to simplify the above equation to become[1][2]:

$$q_i = (H + H'_{ri})(T_{ei} - T_{1i}) \qquad (A3.14)$$

where $H'_{ri} = 1.2H_{ri}$[1]

The environmental temperature is a function of the air temperature T_{0i} and the area weighted mean surface temperature T_{0m}[1][2]:

$$T_{ei} = \frac{1}{3}T_{0i} + \frac{2}{3}T_{0m}$$

Typical values of H have already been discussed and are listed in Table A3.1. The value of H'_{ri} for a typical building structure is generally taken as 6.2W/m^{2}K[1][3].

1CHARTERED INSTITUTION OF BUILDING SERVICES ENGINEERS, GUILDE BOOK A, 1986.

2McLAUGHLIN, R.K., McLEAN, R.C., BONTHRON, W.J. 'Heating Service Design', Butterworths, 1981.

3WARNER, C.Y., ARPARI, V.S. 'An Experimental Investigation of Turbulent Natural Convection in Air at Low Pressure Along A Vertical Heated Flat Plate', Int. J. Heat Mass Transfer, Vol.11, pp.397-406, 1968.

External Walls

The concept of sol-air temperature is introduced both by CIBSE and ASHRAE as a convenient method of analysing total energy transfer for external walls of buildings. This temperature is the outside temperature which, in the absence of all radiation exchanges, would give the same temperature distribution and rate of heat transfer through the wall as exists with the actual combination of temperature differences and radiation. If H is designated as the outside convection heat transfer coefficient, T_{eo} as the sol-air temperature, and T_{oo} as the outside air temperature, then the total heat transfer rate of the outside wall including both the convection and radiation, q_o, is:

$$q_o = H(T_{eo} - T_{oo}) \qquad (A3.15)$$

Values of sol-air temperature are tabulated by CIBSE for different locations at different times of the year[1].

1CHARTERED INSTITUTION OF BUILDING SERVICES ENGINEERS, GUILDE BOOK A, 1986.

A3.3 Boundary Conditions for Material Interfaces

Within building structures, the contact of two adjacent material layers can be divided into two typical cases:

1) perfect hygrothermal contact

This kind of contact introduces no surface resistance and the driving potentials (vapour pressure and temperature) are continuous functions. However, it is worth noting here that the moisture content is not a continuous function from material to material due to the differences in material moisture capacity.

2) contact with surface resistance

This type of contact is what is almost always encountered in practice. There is in this case a potential gradient between the two adjacent surfaces.

Due to the lack of information for surface resistance within building structures, calculations are usually based on the assumption of a perfect hygrothermal contact between material surfaces.

The vapour pressure, temperature, density and liquid pressure are therefore all continuous functions across the surface.

A3.4 Air Gap

In air gaps diffusion/conduction and/or convection will occur, and the boundary balance equations become:

$$j_i^k = \beta_i(\rho_{is}^k - \rho_{ip}^1) \qquad (A3.16)$$

$$j_i^k h_i - \lambda_s^k \nabla T_s^k = H(T_s^k - T_p^1) + h_i \beta_i(\rho_{is} - \rho_{ip}) \qquad (A3.17)$$

where H: the heat transfer coefficient, kJ/m^2K.

In an air filled cavity, the radiation heat transfer is predominant and normally accounts for two thirds of the total heat transferred. The emissivity of the surface is therefore important and a substantial increase in the thermal resistance can be obtained by using low emissivity surfaces, such as aluminium foil in the case of a wall cavity. The heat transfer decreases with cavity thickness up to 20mm and thereafter remains constant. A horizontal cavity with heat flow downwards has a lower rate of heat transfer than similar cavities with upward heat flow or vertical cavities with horizontal flow.

When the cavity is ventilated, heat and mass are extracted from or added to that part of the structure directly. The heat extraction rate is dependent upon the air flow rate which in turn varies with wind speed and direction, temperature, and cavity configuration, and size of ventilation opening.

For design purposes, empirical values of the thermal resistance, $1/H$, are quoted in the CIBSE GUIDE[1] as listed in the Table A3.3 and Table A3.4.

1CHARTERED INSTITUTION OF BUILDING SERVICES ENGINEERS, GUIDE BOOK A, 1986.

Table A3.3 Thermal Resistance Quoted by CIBSE for Unventilated Airspace

Type of Air Space		Thermal Resistance (m^2K/W)		
Thickness	Surface Emissivity	Horizontal	Upward	Downward
5 mm	High	0.10	0.10	0.10
25 mm	Low	0.18	0.18	0.18
or more	High	0.18	0.17	0.22
	low	0.35	0.35	1.06
High emissivity plane and corrugated sheets in contact		0.09	0.09	0.11
Low emissivity multiple foil insulation with airspace on one side		0.62	0.62	1.76

Table A3.4 Thermal Resistance Quoted by CIBSE for Ventilated Airspace

Type of Airspace (thickness 25mm minimum)	Thermal Resistance (m^2K/W)
Airspace between asbestos cement or black metal cladding with unsealed joints, and high emotivity lining	0.16
Airspace between asbestos cement or black metal cladding with unsealed joints, and low emissivity surface facing airspace	0.30
Loft space between flat ceiling and unsealed asbestos cement sheets or black metal cladding pitched roof	0.14
Loft space between flat ceiling and pitched roof with aluminium cladding instead of black metal or low emissivity upper surface on ceiling	0.25
Loft space between flat ceiling and pitched roof lined with felt or building paper	0.18
Airspace between tiles and roofing felt or building paper	0.12
Airspace behind titles on tile-hung wall	0.12
Airspace in cavity wall construction	0.18

APPENDIX FOUR

COMPUTER PROGRAM LISTINGS

-- SECTION ONE: MICROSOFT FORTRAN COMPUTER ROUTINE FOR THE DETERMINATION OF MODEL 1 AND MODEL 2 TRANSFER COEFFICIENTS FROM ISOTHERMAL CUP TEST RESULTS

-- SECTION TWO: MAIN MICROSOFT FORTRAN COMPUTER MODEL FOR HEAT AND MASS TRANSFER THROUGH BUILDING STRUCTURES

APPENDIX FOUR

SECTION ONE

MICROSOFT FORTRAN COMPUTER ROUTINE FOR THE DETERMINATION OF MODEL 1 AND MODEL 2 TRANSFER COEFFICIENTS FROM ISOTHERMAL CUP TEST RESULTS

```
ccccccccccccccccccccccccccccccccccccccccccccccccccccccccccccccccccccccc
c     this program is to evaluate vapour and liquid transfer      c
c     coefficients predicted by both flow models mentioned in     c
c     chapter 5.                                                  c
c     the equations are in the forms:                             c
c                 model 1 : PERM = D1*area + D2*(RH**M)           c
c                 model 2 : PERM = D1 + D2*(RH**M)                c
ccccccccccccccccccccccccccccccccccccccccccccccccccccccccccccccccccccccc

      include 'fgraph.fi'
      include 'fgraph.fd'
      dimension rh1(10),rh2(10),perm(10),dif_rh(10),area(10)
      character*1 answer,material*30
      integer*1 model
      real mois(10)

      call clearscreen($GCLEARSCREEN)
      area=1.0
      write(6,10)
10    format(1x,'*************** Evaluation of Transfer Coefficients **
     1************'/)
      write(6,15)
15    format(1x,'Which Model to Use (1/2) ==> ',$)
      read(*,*) model
      write(6,'(a\)') ' Material name is: '
      read(5,'(a)') material
      if(model.eq.2) goto 17
      write(*,'(a\)') ' Enter Material Dry Density ==> '
      read(*,*) den
      write(*,'(a\)') ' Enter Material Porosity ==> '
      read(*,*) por
      write(*,'(a\)') ' Enter Water Density ==> '
      read(*,*) w_den
      write(*,'(a)') ' At Least Three Averaged Permeabilities, RHs and M
     +oisture Contents Needed'
```

```
      write(6,25)
      read(*,*) number
      write(*,'(a)') ' Enter RHs; Permeability and Moisture Contents...'
      do i=1,number
      write(6,16) i
16    format(1x,'No.',i1,' RH1 and RH2 (%), Perm. & Moist. Cont.==> ',$)
      read(5,*) rh1(i),rh2(i),perm(i),mois(i)
      rh1(i)=rh1(i)/100.0
      rh2(i)=rh2(i)/100.0
      dif_rh(i)=rh2(i)-rh1(i)
      area(i)=1.0-den*mois(i)/(w_den*por)
      end do
      goto 38

17    write(6,20)
20    format(1x,'At Least Three Averaged Permeabilities and its RHs are
     +Needed')
      write(6,25)
25    format(1x,'How Many Data Points Do You Have ==> ',$)
      read(*,*) number
      do i=1,number
      write(6,30) i
30    format(1x,'No.',i1,' RH1 and RH2 (%) and Permeability ==> ',$)
      read(5,*) rh1(i),rh2(i),perm(i)
      rh1(i)=rh1(i)/100.0
      rh2(i)=rh2(i)/100.0
      dif_rh(i)=rh2(i)-rh1(i)
      end do
```

```
38    write(6,40)
40    format(1x,'calulation in progress. please wait....')

      do 100 k=1,1900

      b=1.0+k*0.01

      sum_p=0.0
      sum_f=0.0
      sum_f2=0.0
      sum_pf=0.0
      sum_g=0.0
      sum_pg=0.0
      sum_h=0.0
      do i=1,number
      sum_p=sum_p+perm(i)/area(i)
      f1=(rh2(i)**b-rh1(i)**b)
      f=f1/(dif_rh(i)*area(i))
      sum_f=sum_f+f
      sum_f2=sum_f2+f*f
      sum_pf=sum_pf+f*perm(i)/area(i)
      g1=((rh2(i)**b)*log(rh2(i))-(rh1(i)**b)*log(rh1(i)))-f1/b
      g=g1/(dif_rh(i)*area(i))
      sum_g=sum_g+g
      sum_pg=sum_pg+perm(i)*g/area(i)
      sum_h=sum_h+f*g
      end do

      d2_b=(sum_pf-sum_p*sum_f/number)/(sum_f2-sum_f*sum_f/number)
      d1=(sum_p-d2_b*sum_f)/number
      eq_left=d1*sum_g+d2_b*sum_h
      eq_right=sum_pg
      errors=abs(eq_right/eq_left-1.0)
      if((k.gt.1).and.(e_min.le.errors) ) goto 100
```

```
      e_min=errors
      e_b=b
      e_d1=d1
      e_d2=d2_b*e_b
100   continue

      write(6,150)
150   format(1x,'calculation finished. ')
      write(6,160)
160   format(1x,'the closest solution found are:')
170   write(6,180) e_d1,e_d2,e_b-1.0
180   format(1x,'D1=',1p,e9.2,2x,'D2=',e9.2,2x,'m=',0p,f6.3)
      if(e_d1.GT.0.0.AND.e_d2.GT.0.0) GOTO 400
190   write(*,*) 'Coefficients less than zero.'
      write(*,*) 'May be caused by fluctuation of experimental values'
      write(*,*) 'It may suggest that the material is non-hygroscopic'
195   write(*,'(a\)') ' Calculation with assumption of non-hygroscopic '
      write(*,*) 'material...'
      e_b=2.0
      sum_p=0.0
      sum_f=0.0
      sum_f2=0.0
      sum_pf=0.0
      do i=1,number
      sum_p=sum_p+perm(i)/area(i)
      f=(rh2(i)+rh1(i))/area(i)
      sum_f=sum_f+f
      sum_f2=sum_f2+f*f
      sum_pf=sum_pf+perm(i)*f/area(i)
      end do
      e_d2=e_b*(sum_pf-sum_p*sum_f/number)/(sum_f2-sum_f*sum_f/number)
      e_d1=(sum_p-e_d2*sum_f/2.0)/number
      write(6,180) e_d1,e_d2,e_b-1.0
400   write(6,410)
```

```
410   format(1x,'want an output sheet ? (y/n) ',$)
      read(5,'(a)') answer
      if(answer.eq.'n'.or.answer.eq.'N') goto 2000
      open(1,file='out.dat',status='unknown')
      write(1,500)
500   format(1x,'******************************* Output Sheet ',$)
      write(1,'(a)') '*******************************'
      write(1,505) model
505   format(36x,'Model',i1)
      write(1,510) material
510   format(1x/,5x,'Material: ',a30/)
      write(1,520)
520   format(5x,'Relative Humidity Conditions',10x,
     +          'Experimental Permeabilities')
      do i=1,number
      write(1,530) rh1(i)*100.0,rh2(i)*100.0,perm(i)
530   format(10x,f5.1,' - ',f5.1,28x,1p,e9.2)
      end do
      write(1,540)
540   format(//5x,'Coefficients Evaluated:')
      write(1,550) e_d1
550   format(10x,'D1 = ',1p,e9.2)
      write(1,560) e_d2
560   format(10x,'D2 = ',1p,e9.2)
      write(1,570) e_b-1
570   format(10x,'m = ',0p,f5.2)
      write(1,580)
580   format(//5x,'Equation is:')
      select case(model)
      case(1)
      write(1,585) e_d1,e_d2,e_b-1
      case(2)
      write(1,590) e_d1,e_d2,e_b-1
      end select
```

```
585   format(10x,'PERM = ',1p,e9.2,'*t + ',e9.2,'*(RH**',0p,f5.2,')'/)
590   format(10x,'PERM = ',1p,e9.2,' + ',e9.2,'*(RH**',0p,f5.2,')'/)
      write(1,600)
600   format(5x,'Predicted Permeability for Experimental Conditions')
      write(1,610)
610   format(5x,'Relative Humidity Conditions',10x,
     +            'Predicted Permeabilities')
      do i=1,number
      p=e_d1*area(i)+e_d2*(rh2(i)**e_b-rh1(i)**e_b)
     + /(e_b*(rh2(i)-rh1(i)))
      write(1,530) rh1(i)*100.0,rh2(i)*100.0,p
      end do
      write(1,620)
620   format(//5x,'End of File.....End of File.....End of File.')
      close(1)
      write(*,*) 'Output sheet is stored in OUT.DAT'
      goto 2000
1000  write(*,*) 'No solution available for data entered'
2000  stop 'Program Finished'
      end
```

********** Output Sheet **********
Model1

Material: Particle Board

Relative Humidity Conditions	Experimental Permeabilities
3.0 - 60.0	3.66E-12
60.0 - 80.0	3.89E-12
60.0 - 93.0	5.59E-12
60.0 - 100.0	6.43E-12

Coefficients Evaluated:
D1 = 3.77E-12
D2 = 1.24E-11
m = 8.38

Equation is:
PERM = 3.77E-12*t + 1.24E-11*(RH** 8.38)

Predicted Permeability for Experimental Conditions

Relative Humidity Conditions	Predicted Permeabilities
3.0 - 60.0	3.57E-12
60.0 - 80.0	4.15E-12
60.0 - 93.0	5.32E-12
60.0 - 100.0	6.54E-12

End of File.....End of File.....End of File.

********** Output Sheet **********
Model2

Material: Particle Board

Relative Humidity Conditions	Experimental Permeabilities
3.0 - 60.0	3.66E-12
60.0 - 80.0	3.89E-12
60.0 - 93.0	5.59E-12
60.0 - 100.0	6.43E-12

Coefficients Evaluated:
D1 = 3.55E-12
D2 = 1.20E-11
m = 8.91

Equation is:
PERM = 3.55E-12 + 1.20E-11*(RH** 8.91)

Predicted Permeability for Experimental Conditions

Relative Humidity Conditions	Predicted Permeabilities
3.0 - 60.0	3.56E-12
60.0 - 80.0	4.17E-12
60.0 - 93.0	5.30E-12
60.0 - 100.0	6.54E-12

End of File.....End of File.....End of File.

APPENDIX FOUR

SECTION TWO

MAIN MICROSOFT FORTRAN COMPUTER MODEL FOR HEAT AND MASS TRANSFER THROUGH BUILDING STRUCTURES

DESCRIPTION OF PROGRAM CHMTBS

The Programme C(oupled) H(eat) and M(ass) T(ransfer) within B(uilding) S(tructures) consists of a core main programme and sixteen subroutines, as well as two function and two header files. This programme simulates the heat transfer and moisture movement of vapour and liquid water through building structures. The building structures can have up to ten layers of materials, including hygroscopic and non-hygroscopic materials and vapour barriers and air gaps. It outputs temperature, vapour pressure and moisture content for three points within each material (two near surfaces and one at the middle) and moisture flow rates for the two outmost surfaces.

Core Programme CHMTBS

The main programme CHMTBS does most of the interactions with the user. It determines the calculation time step required for stability and calls each individual subroutine as required. It follows the following steps:

1) calls FILE_READ to obtain material properties, initial conditions and boundary conditions
2) calls either MAN_MESH or AUTO_MESH for manual or automatic mesh generation
3) calculates the largest time step required for stability
4) starts simulation;
   a) calls boundary condition subroutines according their types
   b) calls HYGRO or NON_HYGRO for different materials
5) when all material layers finished
   a) re-calculates local properties by calling PROPERTY
   b) re-calculates local flow rates by calling FLOW_RATE
6) outputs results by calling OUT_PUT
7) stops when final time reached.

Subroutine HYGRO

This subroutine called by CHMTBS solves the set of governing equations for hygroscopic materials. It outputs the moisture content, temperature and vapour pressure for each mesh point at the next time step. It performs the following procedures:

1) calculates the divergence of flow rate
2) calculates the divergence of vapour flow rate
3) calculates the convection term in the energy equation
4) calculates the divergence of heat conduction
5) calculates the moisture content and temperature at the new time step
6) calculates the corresponding vapour pressure.
7) returns control back to CHMTBS

Subroutine NON_HYGRO

This subroutine called by CHMTBS solves the set of governing equations for non-hygroscopic materials. It outputs the moisture content, temperature and vapour pressure for each mesh point at the next time step. It performs the following procedures:

1) calculates the divergence of flow rate
2) calculates the coefficients in equation (4.22) for temperature and vapour pressure differentials vs time.
3) calculates the divergence of vapour and liquid water flow rate
3) calculates the convection term in the energy equation
4) calculates divergence of heat conduction
5) calculates the moisture content and temperature at the new time step
6) calculates the corresponding vapour pressure.
7) returns control back to CHMTBS

Subroutine M_A_BOUND

This subroutine called by CHMTBS solves the boundary conditions for outside surfaces: external and internal. Naming conventions for all the boundary condition routines are: M stands for Material; A for outside Air; G for air Gap; V for Vapour barrier and all names finished with _BOUND. Therefore M_A_BOUND means this subroutine relates to boundary conditions for materials facing air.

This subroutine solves the equations of mass and energy conservation across the surfaces as follows:

1) calculates which month the current time is in and utilise that months data accordingly
2) checks the surface type, external or internal, and uses the corresponding heat transfer coefficient
3) calculates the mass transfer coefficient
4) solves the mass and energy balance equations
5) converts vapour pressure and temperature to moisture content
6) returns control back to CHMTBS

Subroutine M_M_BOUND

This subroutine called by CHMTBS solves the boundary conditions for interfacial surfaces: material adjoining material. This subroutine solves the equations of mass and energy conservation across the surfaces as follows:

1) calculates permeabilities for the two adjacent materials
2) calculates individual terms in balance equations
3) solves the mass and energy balance equations
4) converts vapour pressure and temperature to moisture content
5) returns control back to CHMTBS

Subroutine M_G_M_BOUND

This subroutine called by CHMTBS solves the boundary conditions for interfacial surfaces: two materials enclosing an air gap. This subroutine solves the equations of mass and energy conservation across the surfaces as follows:

1) calculates permeabilities for the two material layers enclosing the air gap
2) calculates individual terms in balance equations
3) solves the mass and energy balance equations
4) converts vapour pressure and temperature to moisture content
5) returns control back to CHMTBS

Subroutine M_V_M_BOUND

This subroutine called by CHMTBS solves the boundary conditions for interfacial surfaces: material to vapour barrier and to another material. This subroutine solves the equations of mass and energy conservation across the surfaces as follows:

1) calculates permeabilities for the two relevant materials
2) calculates individual term in balance equations
3) solves the mass and energy balance equations
4) converts vapour pressure and temperature to moisture content
5) returns control back to CHMTBS

Subroutine M_V_G_BOUND

This subroutine called by CHMTBS solves the boundary conditions for interfacial surfaces: material to vapour barrier to air gap and to another material or material to air gap to vapour barrier and to another material. This subroutine solves the equations of mass and energy conservation across the surfaces as follows:

1) calculates permeabilities for the two relevant materials

2) calculates individual terms in balance equations

3) solves the mass and energy balance equations

4) converts vapour pressure and temperature to moisture content

5) returns control back to CHMTBS

Subroutine FILE_READ

This subroutine called by CHMTBS reads the data file and assigns material properties and boundary conditions to their corresponding variables. It has the following steps:

1) opens data file and checks for its existence

2) scans through the file until it finds the first data point

3) notes which layer is an air gap and which is a vapour barrier

4) reads in properties for each layer

5) reads in and calculates initial conditions

6) reads in boundary conditions: surface type, wind speed, ambient temperatures and relative humidities and the sol-air or environmental temperatures for 12 months. Each month has at present one data entry only.

6) returns control back to CHMTBS

Subroutine PROPERTY

This subroutine called by CHMTBS calculates properties for local mesh points. The properties include: thermal capacities, thermal conductivities, latent heat. They are evaluated for vapour, liquid water, total moisture and for moist materials.

Subroutine MAN_MESH

This subroutine called by CHMTBS generates mesh points for materials according to user requirements for each individual layer.

Subroutine AUTO_MESH

This subroutine called by CHMTBS generates mesh points for materials automatically according to the material's heat and mass transfer resistance. It tries to balance each cell of the materials involved such that they have the same resistance for heat and moisture transfer. However, if the calculation gives too few cells (<5) for each layer it will assume the minimum cell number of 5. On the other hand if the no. of cells exceeds 25 it will assume the maximum cell number of 25. It has the following steps:

1) asks for the total number of cells required for whole structure
2) calculates the combined heat and moisture transfer resistance for each material layer
3) allocates cells to each material according to their resistance
4) generates mesh
5) returns control back to CHMTBS

Subroutine FLOW_RATE

This subroutine called by CHMTBS calculates flow rates for each component: vapour, liquid water and air as followings:

1) calculates transfer coefficients and permeability for each material
2) calculates vapour pressure gradient
3) calculates flow rates
4) returns control back to CHMTBS

Subroutine PRES_TO_MOI

This subroutine utilises the sorption isotherm curve to convert vapour pressure to moisture content.

Subroutine MOI_TO_PRES

This subroutine uses the rearranged sorption isotherm to convert moisture content to vapour pressure.

Subroutine ERROR_HANDLE

This simple subroutine indicates the type of errors occurred during operation.

Subroutine OUT_PUT

This subroutine called by CHMTBS outputs temperature, vapour pressure and moisture content into different files as followings:

1) opens a number of files according to the number of material layers. Each file has the extension .PRN for compatibility with LOTUS FREELANCE for Windows
2) writes to files values of temperature, vapour pressure and moisture content
3) if final time is reached closes all files
4) returns control back to CHMTBS

Function SAT_PRES

This function calculates the saturation vapour pressure corresponding to any given temperature.

Function P_SAT_G

This function calculates the gradient of saturation vapour pressure vs temperature. This gradient is often required in the governing equations.

Header DEFINE.H1

This one line header file defines the dimensions of some important arrays

Header DEFINE.H2

This file defines six commonly used structured variable types. The six structures cover material properties, moisture transfer coefficients, sorption isotherms and boundary conditions.

Core Programe CHMTBS

```
      INCLUDE 'fgraph.fi'
      INCLUDE 'define.h1'
      INCLUDE 'fgraph.fd'
      INCLUDE 'define.h2'
      RECORD /buildings/ bld
      RECORD /boundary/ ext
      COMMON /wall/ bld
      COMMON /bound/ ext
      COMMON /mesh/node(dl),x_step(dl),x_coord(dl,dn)
      COMMON /var1/den_n(dl,dn),temp_n(dl,dn),pres_n(dl,dn),
     +            mois_n(dl,dn)
      COMMON /var2/den_o(dl,dn),temp_o(dl,dn),pres_o(dl,dn),
     +            mois_o(dl,dn)
      COMMON /prop/den2(dl,dn),cap(dl,dn,4),con(dl,dn,4),latent(dl,dn)
      COMMON /theory/model
      COMMON /time1/t_step
      COMMON /time2/actual_time
      COMMON /type/m_type(dl)
      INTEGER*1 error,type,type2,model,m_type
      INTEGER*2 bhr,bmin,bsec,b100th
      INTEGER*2 shr,smin,ssec,s100th,syr,smon,sday
      INTEGER*2 ehr,emin,esec,e100th,eyr,emon,eday
      INTEGER*2 hr,sec
      INTEGER*4 time,final_time,out_step,count
      REAL*8 mois_n,mois_o
      REAL m_end,latent
      DIMENSION day(10),nday(10)
      CHARACTER*1 answer,filename*30
```

```
      CALL gettim(bhr,bmin,bsec,b100th)
      CALL clearscreen($GCLEARSCREEN)
      WRITE(*,10)
10    FORMAT(23x,'Coupled Heat and Moisture Transfer')
      WRITE(*,20)
20    FORMAT(26x,'Through Building Structures'//)
      WRITE(*,'(A\)') ' Enter Data File Name ==> '
      READ(*,'(A)') filename
50    WRITE(*,'(A\)') ' Which Model to Use (1,2) ==> '
      READ(*,*,ERR=60) model

      SELECT CASE(model)
         CASE(1,2)
       CALL file_read(filename,error)
       CALL error_handle(error)
100          WRITE(*,'(A\)') ' Enter Mesh Manually (Y/N) ? '
       READ(*,'(A)') answer
       SELECT CASE(answer)
          CASE ('y', 'Y')
      CALL man_mesh
          CASE ('n','N')
       CALL auto_mesh
          CASE DEFAULT
       WRITE(*,'(A)') ' Input not recognized.'
       WRITE(*,'(A\)') ' Please Re_enter '
       GOTO 100
       END SELECT
       CALL pres_to_moi
       CALL property        !calculate physical properties of each mesh
       WRITE(*,'(A\)') ' Enter The Starting Month (1-12) ==> '
       READ(*,*) m_start
       WRITE(*,'(A\)') ' Enter Time Period (days) ==> '
       READ(*,*) m_end
```

```
CCCCCC
C     checking material type
CCCCCC
180          l_last=bld.n_layer
       DO i=1,l_last
       IF(m_type(i).GT.1) CYCLE
       expo=bld.walls(i).coef.r_exp
       IF(expo.EQ.1.0) m_type(i)=1
       END DO
CCCCCC
C     Now evaluate the biggest time step allowed.
CCCCCC

         DO i=1,l_last
       IF(m_type(i).GT.1) CYCLE            !not account for air gap or barrier
       den=bld.walls(i).prop.dens
       xstep=x_step(i)*x_step(i)
       extra=cap(i,1,4)/con(i,1,4)         !select values at first mesh point
       ratio=extra*xstep*den/4.0
       SELECT CASE(i)
         CASE(1)
      t_step=ratio
         CASE DEFAULT
      IF(t_step.GT.ratio) t_step=ratio
       END SELECT
       END DO
       final_time=int(m_end*3600.0*24.0/t_step)
      iday=3
      nday(1)=0
      nday(2)=int(final_time/2)
      nday(3)=final_time
      nday(4)=2.0*final_time
      WRITE(*,150)
```

```
150   FORMAT(1X,'This program outputs local values for three default
     +moments:')
      WRITE(*,155)
155   FORMAT(10X,'time=0, time=half of final time, time=final time')
      WRITE(*,160)
160   FORMAT(1X,'To change the three default moments (y/n)? ==> ',$)
      READ(*,'(A)') answer
      IF(answer.NE.'Y'.AND.answer.NE.'y') GOTO 190
      WRITE(*,162)
162   FORMAT(1X,'No. of moments ==> ',$)
      READ(*,*) iday
      WRITE(*,'(A\)') ' Which days ==> '
      READ(*,*) (day(i),i=1,iday)
      DO i=1,iday
      nday(i)=int(day(i)*3600*24/t_step)
      END DO
      nday(i)=2.0*final_time
CCCCCC
C     output points are fixxed to be 100
CCCCCC
190            out_step=int(final_time/100)
       IF(out_step.LT.1) out_step=1
       count=0
       GOTO 200
      END SELECT

60    WRITE(*,'(A)') 'Input NOT recognised'
      GOTO 50

200   CALL gettim(shr,smin,ssec,s100th)
      CALL getdat(syr,smon,sday)
      i_time=2+int(final_time/100)
```

```
      CALL flow_rate
      ii=1
      IF(nday(1).NE.0.0) goto 205
      CALL out_put(4)
      ii=2
      goto 206
205   CALL out_put(1)          !output initial conditions

206   DO 1000 time=1,final_time

      if(time.ne.i_time) goto 500

      CALL gettim(ehr,emin,esec,e100th)
      CALL getdat(eyr,emon,eday)
      eth=e100th-s100th
      IF(eth.LT.0.0) THEN
      eth=100+eth
      esec=esec-1
      END IF
      sec=esec-ssec
      IF(sec.LT.0.0) THEN
      sec=sec+60
      emin=emin-1
      END IF
      min=emin-smin
      ehr=ehr+(eday-sday)*24
      IF(min.LT.0.0) THEN
      min=min+60
      ehr=ehr-1
      END IF
      hr=ehr-shr
```

```
      total_t=(hr*3600.0+min*60.0+sec+eth/100.0)*1.667
      write(*,300) total_t
300   format(1x,'Need ',f8.1,' minutes to run this program...')

500   count=count+1
      actual_time=((time-1)*t_step/(24*3600))   !in days

      CALL m_a_bound(m_start,1)     !first boundary conditions
      CALL m_a_bound(m_start,2)
      DO i=1,l_last
      IF(i.EQ.l_last) CYCLE   !not for one layer wall
      type=m_type(i)
      IF(type.GT.1) CYCLE
      type2=m_type(i+1)
      SELECT CASE(type2)
          CASE(0,1)
       CALL m_m_bound(i)
          CASE(2)
       IF(m_type(i+2).LT.2) CALL m_g_m_bound(i)
       IF(m_type(i+2).EQ.3) CALL m_v_g_bound(i)
          CASE(3)
       IF(m_type(i+2).LT.2) CALL m_v_m_bound(i)
       IF(m_type(i+2).EQ.2) CALL m_v_g_bound(i)
       END SELECT
      END DO

      CALL flow_rate    !calculate individual flow rate of each mesh

      DO i=1,l_last
      type=m_type(i)
      IF(type.GT.1) CYCLE
      IF(type.EQ.0) CALL hygro(i)
      IF(type.EQ.1) CALL non_hygro(i)
      END DO
```

```
      den_o=den_n
      temp_o=temp_n
      pres_o=pres_n
      mois_o=mois_n

      CALL property        !calculate physical properties of each mesh


      IF(count.NE.out_step.AND.time.NE.final_time) CYCLE
      t_check=nday(ii)
      if(time.LT.t_check) THEN
      call out_put(0)
      ELSE
      call out_put(2)
      ii=ii+1
      END IF
      count=0
1000  END DO
      CALL out_put(100)
10000 CALL gettim(ehr,emin,esec,e100th)
      CALL getdat(eyr,emon,eday)
      WRITE(*,10010) bhr,bmin,bsec,b100th
10010 FORMAT('0Program Started at ',I2.2,1H:,I2.2,1H:,I2.2,1H:,I2.2)
      WRITE(*,10020) shr,smin,ssec,s100th
10020 FORMAT(1x,'Simulation Started at ',I2.2,1H:,I2.2,1H:,I2.2,1H:
     +                                                          ,I2.2)
      WRITE(*,10030) ehr,emin,esec,e100th
10030 FORMAT(1x,'Program Finished at ',I2.2,1H:,I2.2,1H:,I2.2,1H:
     +                                                          ,I2.2)
      sec=esec-ssec
      IF(sec.LT.0.0) THEN
      sec=sec+60
      emin=emin-1
```

```
      END IF
      min=emin-smin
      ehr=ehr+(eday-sday)*24
      IF(min.LT.0.0) THEN
      min=min+60
      ehr=ehr-1
      END IF
      hr=ehr-shr
      WRITE(*,10040) hr,min,sec
10040 FORMAT(1x,'Time Used for Simulation ',I2.2,1H:,I2.2,1H:,I2.2)
      STOP 'Simulation Completed'
      END
```

Subroutine HYGRO

```
      SUBROUTINE hygro(layer)
      INCLUDE 'define.h1'
      INCLUDE 'define.h2'
      RECORD /buildings/ bld
      COMMON /wall/ bld
      COMMON /mesh/node(dl),x_step(dl),x_cood(dl,dn)
                        !node ---> number of nodes in one layer
                        !x_step -> increment in x for each layer
                        !x_coord -> real coordinates of each node
      COMMON /var1/den_n(dl,dn),temp_n(dl,dn),pres_n(dl,dn),
     +             mois_n(dl,dn)
      COMMON /var2/den_o(dl,dn),temp_o(dl,dn),pres_o(dl,dn),
     +             mois_o(dl,dn)
      COMMON /rate/flow(dl,dn,4)
      COMMON /prop/den2(dl,dn),cap(dl,dn,4),con(dl,dn,4),latent(dl,dn)
      COMMON /time1/t_step
      COMMON /theory/model
      COMMON /var3/rh(dl,dn)
      COMMON /type/m_type(dl)
      REAL*8 mois_n,mois_o,m_now,m_past
      REAL j_g1, j1_g1,latent
      density=bld.walls(layer).prop.dens
      step=x_step(layer)
```

```
      uh_h=bld.walls(layer).sorp.uh
      a_a=bld.walls(layer).sorp.A
      a_n=bld.walls(layer).sorp.n
      DO i=2,node(layer)-1

      j_g1=(flow(layer,i+1,4)-flow(layer,i-1,4))/(2.0*step)
      m_past=mois_o(layer,i)
      m_now=m_past-t_step*j_g1/density
      mois_n(layer,i)=m_now
      tl=temp_o(layer,i-1)
      tm=temp_o(layer,i)
      tr=temp_o(layer,i+1)

      t_g1=(tr-tl)/(2.0*step)
      t_g2=(tr-2.0*tm+tl)/(step*step)

      heat=con(layer,i,4)*t_g2

      conv=0.0
      DO k=1,3
      conv=conv+flow(layer,i,k)*cap(layer,i,k)*t_g1
      END DO
      j1_g1=(flow(layer,i+1,1)-flow(layer,i-1,1))/(2.0*step)
      phase=latent(layer,i)*j1_g1
      t_past=temp_o(layer,i)
      t_now=t_past+t_step*(heat-conv+phase)/(cap(layer,i,4)*density)
      temp_n(layer,i)=t_now
CCCCC
C           convert moisture content to vapour pressure
CCCCC
      p_sat=sat_pres(t_now)
```

```
      term16=m_now/uh_h
      term17=(1.0-term16**(-a_n))
      term18=a_a*term17
      p_now=p_sat*exp(term18)
      r_h=p_now/p_sat
      IF(r_h.LT.1.0) GOTO 100
      r_h=1.0
      p_now=p_sat
100   rh(layer,i)=r_h
      pres_n(layer,i)=p_now
      den_n(layer,i)=p_now/(461.5*t_now)

      END DO

      RETURN
      END
```

Subroutine NON_HYGRO

```
      SUBROUTINE non_hygro(layer)

      INCLUDE 'define.h1'
      PARAMETER (r1=461.5)
      INCLUDE 'define.h2'
      RECORD /buildings/ bld
      COMMON /wall/ bld
      COMMON /mesh/node(dl),x_step(dl),x_cood(dl,dn)
                        !node ---> number of nodes in one layer
                        !x_step -> increment in x for each layer
                        !x_coord -> real coordinates of each node
      COMMON /var1/den_n(dl,dn),temp_n(dl,dn),pres_n(dl,dn),
     +             mois_n(dl,dn)
      COMMON /var2/den_o(dl,dn),temp_o(dl,dn),pres_o(dl,dn),
     +             mois_o(dl,dn)
      COMMON /rate/flow(dl,dn,4)
      COMMON /prop/den2(dl,dn),cap(dl,dn,4),con(dl,dn,4),latent(dl,dn)
      COMMON /time1/t_step
      COMMON /theory/model
      COMMON /var3/rh(dl,dn)
      COMMON /type/m_type(dl)

      REAL*8 mois_n,mois_o,m_now,m_past
      REAL latent,j_g1, j1_g1

      density=bld.walls(layer).prop.dens
      porosity=bld.walls(layer).prop.poro
      step=x_step(layer)
```

```
uh_h=bld.walls(layer).sorp.uh
a_a=bld.walls(layer).sorp.A
a_n=bld.walls(layer).sorp.n

DO i=2,node(layer)-1

j_g1=(flow(layer,i+1,4)-flow(layer,i-1,4))/(2.0*step)
m_past=mois_o(layer,i)
m_now=m_past-t_step*j_g1/density
mois_n(layer,i)=m_now

tl=temp_o(layer,i-1)
tm=temp_o(layer,i)
tr=temp_o(layer,i+1)

t_g1=(tr-tl)/(2.0*step)
t_g2=(tr-2.0*tm+tl)/(step*step)

heat=con(layer,i,4)*t_g2

conv=0.0
DO k=1,3
conv=conv+flow(layer,i,k)*cap(layer,i,k)*t_g1
END DO

j1_g1=(flow(layer,i+1,1)-flow(layer,i-1,1))/(2.0*step)
j2_g1=(flow(layer,i+1,2)-flow(layer,i-1,2))/(2.0*step)
enth1=(1.805*(tm-273.15)+2501.21)*1000
enth2=(4.1837*(tm-273.15)+0.11807)*1000
phase=enth1*j1_g1+enth2*j2_g1

eq_right=heat-conv-phase
```

```
      phi=rh(layer,i)
      p_sat=sat_pres(tm)
      ft_g=p_sat_g(tm)
      t2=uh_h*((1.0-log(phi)/a_a)**(-1.0-1.0/a_n))/(a_a*a_n)
cccccc
c     a_u_p1=(du/dT)_p1
cccccc
      a_u_p1=-t2*ft_g/p_sat
cccccc
c     a_u_T=(du/dp1)_T
cccccc
      pm=pres_o(layer,i)
      a_u_T=t2/pm
cccccc
c     a_k_T
cccccc
      aa1=cap(layer,i,4)*density
      aa2=-latent(layer,i)*porosity*pm/(r1*tm*tm)
      aa3=enth2*density*a_u_p1
      a_k_T=aa1+aa2+aa3
cccccc
c     a_k_p1
cccccc
      aa5=-aa2*tm/pm
      aa6=enth2*density*a_u_T
      a_k_p1=aa5+aa6
cccccc
c     coefficient of dT/dt
cccccc
```

```
      cct0=(m_past/uh_h)**(-a_n)
      cct1=exp(a_a*(1.0-cct0))
      cct2=a_k_T+a_k_p1*ft_g*cct1
CCCCCC
C     coefficient of du/dt
CCCCCC
      cct3=(m_now-m_past)
      cct4=a_k_p1*p_sat*a_a*a_n*cct0*cct1*cct3/m_past
      t_past=temp_o(layer,i)
      t_now=t_past+(t_step*eq_right-cct4)/cct2
      temp_n(layer,i)=t_now
CCCCC
C           convert moisture content to vapour pressure
CCCCC
      p_sat=sat_pres(t_now)
      term16=m_now/uh_h
      term17=(1.0-term16**(-a_n))
      term18=a_a*term17
      p_now=p_sat*exp(term18)
      r_h=p_now/p_sat
      IF(r_h.LT.1.0) GOTO 100
      r_h=1.0
      p_now=p_sat
100   rh(layer,i)=r_h
      pres_n(layer,i)=p_now
      den_n(layer,i)=p_now/(461.5*t_now)
      END DO

      RETURN
      END
```

Subroutine M_A_BOUND

```
      SUBROUTINE m_a_bound(m_start,side)
      INCLUDE 'define.h1'
      PARAMETER (r1=461.5)       !gas constant & H2O weight
      INCLUDE 'define.h2'
      RECORD /buildings/ bld
      RECORD /boundary/ ext
      COMMON /wall / bld
      COMMON /bound/ ext
      COMMON /mesh/node(dl),x_step(dl),x_coord(dl,dn)
      COMMON /var1/den_n(dl,dn),temp_n(dl,dn),pres_n(dl,dn),mois_n(dl,dn)
      COMMON /var2/den_o(dl,dn),temp_o(dl,dn),pres_o(dl,dn),mois_o(dl,dn)
      COMMON /var4/dp(dl,dn),dt(dl,dn)
      COMMON /prop/den2(dl,dn),cap(dl,dn,4),con(dl,dn,4),latent(dl,dn)
      COMMON /var3/rh(dl,dn)
      COMMON /rate/flow(dl,dn,4)
      COMMON /time1/t_step
      COMMON /time2/actual_time
      COMMON /theory/model
      DIMENSION m_day(12)
      INTEGER*1 model,side
      CHARACTER*1 chose
      REAL mass_coef,latent
      REAL*8 mois_n,mois_o

      DATA m_day /31,28,31,30,31,30,31,31,30,31,30,31/  !no. of days in each month

      day=actual_time
      IF(day.GT.365) day=day-365
      month_day=0
      DO month=m_start,12+m_start-1
```

```
mm=month
IF(month.GT.12) mm=mm-12
month_day=month_day+m_day(mm)
IF(day.le.month_day) EXIT
END DO

layer=ext.layers(side)

SELECT CASE(side)
      CASE(1)
            n_first=1
            next=2
            n_3=3
      CASE(2)
            n_first=node(layer)       !n_first is no. of the mesh on the surface
            next=n_first-1
            n_3=n_first-2
END SELECT

rh10=ext.r_h(side,mm)/100.0
tp10=ext.tempe(side,mm)
p10=rh10*sat_pres(tp10)
cons=r1*tp10
d10=p10/cons

t11=temp_o(layer,n_first)
t12=temp_o(layer,next)
t13=temp_o(layer,n_3)
p11=pres_o(layer,n_first)
p12=pres_o(layer,next)
p13=pres_o(layer,n_3)

st=x_step(layer)
```

```
d_p=dp(layer,n_first)
d_t=dt(layer,n_first)

chose=ext.f_type(side)
SELECT CASE(chose)
      CASE ('N','n')
           heat=3.0
      CASE ('F','f')
           heat=5.8+4.1*ext.wind(side)
END SELECT

mass_coef=heat*(9.53e-4)            !from the (7.3) UNIT:

chose=ext.w_type(side)

SELECT CASE(chose)
       CASE('I','i')
            tot_heat=heat+6.2       !6.2 is a typical value for
                                    !radient transfer coefficient
       CASE('E','e')
            tot_heat=heat           !for external walls the total
END SELECT                          !heat transfer coefficient is
                                    !the same as convection if the
                                    !sol-air temperature is applied
fl1=flow(layer,n_first,1)
fl2=flow(layer,n_first,2)
fl=fl1+fl2
energy0=fl*(1.805*(tp10-273.15)+2501.21)*1000
energy1=fl1*(1.805*(t11-273.15)+2501.21)*1000       !vapour->unit J/Kg, tem: C
energy2=fl2*(4.1837*(t11-273.15)+0.11807)*1000      !water->unit J/Kg, tem: C

tout=ext.a_e_temp(side,mm)
```

```
term3=con(layer,n_first,4)/st
term4=tot_heat*tout
term5=2.0*term3*t12
term6=-0.5*term3*t13
term7=energy0-energy1-energy2
IF(side.EQ.2) term7=-term7
term8=tot_heat+1.5*term3
t_now=(term4+term5+term6+term7)/term8
temp_o(layer,n_first)=t_now
temp_n(layer,n_first)=t_now


IF(side.EQ.1) THEN
      t_g1=(-3.0*t_now+4.0*t12-t13)/(2.0*st)
END IF
IF(side.EQ.2) THEN
      t_g2=(3.0*t_now-4.0*t12+t13)/(2.0*st)
END IF

term0=mass_coef*d10+d_p*(4.0*p12-p13)/(2.0*st)
term1=d_t*t_g1
term2=mass_coef/(r1*t11)+1.5*d_p/st
IF(side.EQ.2) term1=-term1

p_now=(term0+term1)/term2

pres_o(layer,n_first)=p_now
pres_n(layer,n_first)=p_now

p_sat=sat_pres(t_now)

d_now=p_now/(r1*t_now)
den_o(layer,n_first)=d_now
```

```
den_n(layer,n_first)=d_now
r_h=p_now/p_sat
rh(layer,n_first)=r_h

uh_h=bld.walls(layer).sorp.uh
a_a=bld.walls(layer).sorp.A
a_n=bld.walls(layer).sorp.n
t_m=uh_h*(1.0-log(r_h)/a_a)**(-1.0/a_n)
mois_n(layer,n_first)=t_m
mois_o(layer,n_first)=t_m

RETURN

END
```

Subroutine M_M_BOUND

```
      SUBROUTINE m_m_bound(layer)
      INCLUDE 'define.h1'
      PARAMETER (r1=461.5)
      INCLUDE 'define.h2'
      RECORD /buildings/ bld
      COMMON /wall/ bld
      COMMON /mesh/node(dl),x_step(dl),x_coord(dl,dn)
      COMMON /var1/den_n(dl,dn),temp_n(dl,dn),pres_n(dl,dn),mois_n(dl,dn)
      COMMON /var2/den_o(dl,dn),temp_o(dl,dn),pres_o(dl,dn),mois_o(dl,dn)
      COMMON /var3/rh(dl,dn)
      COMMON /var4/dp(dl,dn),dt(dl,dn)
      COMMON /rate/flow(dl,dn,4)
      COMMON /time1/t_step
      COMMON /time2/actual_time
      COMMON /theory/model
      COMMON /prop/den2(dl,dn),cap(dl,dn,4),con(dl,dn,4),latent(dl,dn)
      DIMENSION d_p(2),d_t(2),fl1(2),fl2(2),dis(2)
      DIMENSION s_con(2),t_next(2),t_3(2),p_next(2),p_3(2)
      DIMENSION energy(2)
      INTEGER*1 surf(2),dammy(2),next(2),n_3(2)
      REAL*8 mois_n,mois_o
      REAL latent

      dammy(1)=layer
      dammy(2)=layer+1
      surf(1)=node(dammy(1))
      surf(2)=1
      next(1)=surf(1)-1
```

```
next(2)=surf(2)+1
n_3(1)=surf(1)-2
n_3(2)=surf(2)+2

DO i=1,2
d_p(i)=dp(dammy(i),surf(i))
d_t(i)=dt(dammy(i),surf(i))
dis(i)=x_step(dammy(i))
t_next(i)=temp_o(dammy(i),next(i))
t_3(i)=temp_o(dammy(i),n_3(i))
p_next(i)=pres_o(dammy(i),next(i))
p_3(i)=pres_o(dammy(i),n_3(i))
s_con(i)=con(dammy(i),surf(i),4)
END DO

energy=0.0
t_c=temp_o(layer,node(layer))-273.15
ent1=(1.805*t_c+2501.21)*1000
ent2=(4.1837*t_c+0.11807)*1000
fl1(1)=flow(layer,node(layer),1)
fl2(1)=flow(layer,node(layer),2)
fl1(2)=flow(layer+1,1,1)
fl2(2)=flow(layer+1,1,2)
DO k=1,2
energy(k)=fl1(k)*ent1+fl2(k)*ent2
END DO

term4=s_con(1)/dis(1)
term5=s_con(2)/dis(2)
term6=energy(1)-energy(2)
term7=2.0*term4*t_next(1)-0.5*term4*t_3(1)
term8=2.0*term5*t_next(2)-0.5*term5*t_3(2)
term9=1.5*(term4+term5)
```

```
      t_now=(term6+term7+term8)/term9

      t1_g1=(3.0*t_now-4.0*t_next(1)+t_3(1))/(2.0*dis(1))
      t2_g1=(-3.0*t_now+4.0*t_next(2)-t_3(2))/(2.0*dis(2))

      term0=d_p(1)*(4.0*p_next(1)-p_3(1))/(2.0*dis(1))
      term1=d_p(2)*(4.0*p_next(2)-p_3(2))/(2.0*dis(2))
      term2=d_t(2)*t2_g1-d_t(1)*t1_g1
      term3=1.5*(d_p(1)/dis(1)+d_p(2)/dis(2))
      p_now=(term0+term1+term2)/term3

      d_now=p_now/(r1*t_now)

      p_sat=sat_pres(t_now)
      rrhh=p_now/p_sat
      IF(rrhh.LT.1.0) GOTO 100
      write(80,*) actual_time,dammy(i),i
      rrhh=1.0
      p_now=p_sat
      d_now=p_now/(r1*t_now)

100   den_o(layer,surf(1))=d_now
      den_n(layer,surf(1))=d_now
      den_o(layer+1,1)=d_now
      den_n(layer+1,1)=d_now
      temp_o(layer,surf(1))=t_now
      temp_n(layer,surf(1))=t_now
      temp_o(layer+1,1)=t_now
      temp_n(layer+1,1)=t_now
      pres_o(layer,surf(1))=p_now
      pres_n(layer,surf(1))=p_now
      pres_o(layer+1,1)=p_now
      pres_n(layer+1,1)=p_now
      rh(layer,surf(1))=rrhh
      rh(layer+1,1)=rrhh
```

```
DO i=1,2
uh1=bld.walls(dammy(i)).sorp.uh
a1=bld.walls(dammy(i)).sorp.A
a_n=bld.walls(dammy(i)).sorp.n

rrhh=rh(dammy(i),surf(i))
ttmm=uh1*((1.0-log(rrhh)/a1)**(-1.0/a_n))
mois_n(dammy(i),surf(i))=ttmm
mois_o(dammy(i),surf(i))=ttmm
END DO



RETURN
END
```

Subroutine M_G_M_BOUND

```
      SUBROUTINE m_g_m_bound(layer)

      INCLUDE 'define.h1'
      PARAMETER (v_dif=2.5e-5,r1=461.5)
      INCLUDE 'define.h2'
      RECORD /buildings/ bld
      COMMON /wall/ bld
      COMMON /mesh/node(dl),x_step(dl),x_coord(dl,dn)
      COMMON /var1/den_n(dl,dn),temp_n(dl,dn),pres_n(dl,dn),
     +            mois_n(dl,dn)
      COMMON /var2/den_o(dl,dn),temp_o(dl,dn),pres_o(dl,dn),
     +            mois_o(dl,dn)
      COMMON /var3/rh(dl,dn)
      COMMON /var4/dp(dl,dn),dt(dl,dn)
      COMMON /rate/flow(dl,dn,4)
      COMMON /time1/t_step
      COMMON /time2/actual_time
      COMMON /theory/model
      COMMON /prop/den2(dl,dn),cap(dl,dn,4),con(dl,dn,4),latent(dl,dn)
      DIMENSION p_1(2),p_2(2),p_3(2),t_1(2),t_2(2),t_3(2)
      DIMENSION rat_c(2),rat_m(2),energy(2)
      DIMENSION d_p(2),d_t(2),t_now(2),p_now(2),d_now(2)
      INTEGER*1 dammy(2),s_1(2),s_2(2),s_3(2)
      REAL*8 mois_o,mois_n
      REAL latent
```

```
      dammy(1)=layer
      dammy(2)=layer+2
      s_1(1)=node(layer)       !surface1 is surface of material
      s_1(2)=1                 !surface2 is surface of air
      s_2(1)=s_1(1)-1
      s_2(2)=s_1(2)+1
      s_3(1)=s_1(1)-2
      s_3(2)=s_1(2)+2

      DO i=1,2
      d_p(i)=dp(dammy(i),s_1(i))
      d_t(i)=dt(dammy(i),s_1(i))
      t_1(i)=temp_o(dammy(i),s_1(i))
      t_2(i)=temp_o(dammy(i),s_2(i))
      t_3(i)=temp_o(dammy(i),s_3(i))
      p_1(i)=pres_o(dammy(i),s_1(i))
      p_2(i)=pres_o(dammy(i),s_2(i))
      p_3(i)=pres_o(dammy(i),s_3(i))
      t=t_1(i)-273.15
      enth1=(1.805*t+2501.21)*1000
      enth2=(4.1837*t+0.11807)*1000
      energy(i)=enth1*flow(dammy(i),s_1(i),1)
     +                 +enth2*flow(dammy(i),s_1(i),2)
      rat_c(i)=bld.walls(dammy(i)).prop.cond/x_step(dammy(i))
      rat_m(i)=d_p(i)/x_step(dammy(i))
      END DO
CCCCCC
C     energy conservation first to get new temperature
CCCCCC
      term0=bld.walls(layer+1).prop.dens        !heat coefficient is stored here.
      term1=2.0*rat_c(2)*t_2(2)-0.5*rat_c(2)*t_3(2)-energy(2)
      term2=2.0*rat_c(1)*t_2(1)-0.5*rat_c(1)*t_3(1)+energy(1)
      term3=term0+1.5*rat_c(2)
```

```
      term4=(1.5*rat_c(1)+term0)*term3-term0*term0
      t_now(1)=(term0*term1+term3*term2)/term4
      t_now(2)=(term0*t_now(1)+term1)/term3

      t1_g1=(3.0*t_now(1)-4.0*t_2(1)+t_3(1))/(2.0*x_step(layer))
      t2_g1=(-3.0*t_now(2)+4.0*t_2(2)-t_3(2))/(2.0*x_step(layer+2))

      dtt1=d_t(1)*t1_g1
      dtt2=d_t(2)*t2_g1
CCCCCCC
C     now mass conservation
CCCCCCC
      resis_m=bld.walls(layer+1).prop.poro            !vapour resistance stored here
      term5=0.5*rat_m(2)*(4.0*p_2(2)-p_3(2))+dtt2
      term6=0.5*rat_m(1)*(4.0*p_2(1)-p_3(1))-dtt1
      term7=1.0+1.5*rat_m(2)*resis_m
      above=resis_m*(term5+term7*term6)
      term8=1.0+1.5*rat_m(1)*resis_m
      below=term8*term7-1.0
      p_now(1)=above/below
      d_now(1)=p_now(1)/(r1*t_now(1))

      p_now(2)=(p_now(1)+term5*resis_m)/term7
      d_now(2)=p_now(2)/(r1*t_now(2))


      DO i=1,2
      uh1=bld.walls(dammy(i)).sorp.uh
      a1=bld.walls(dammy(i)).sorp.A
      a_n=bld.walls(dammy(i)).sorp.n

      p_sat=sat_pres(t_now(i))
      rrhh=p_now(i)/p_sat
```

```
      IF(rrhh.LT.1.0) GOTO 100
      write(80,*) actual_time,dammy(i),i
      rrhh=1.0
      p_now(i)=p_sat
      d_now(i)=p_now(i)/(r1*t_now(i))
100   rh(dammy(i),s_1(i))=rrhh
      den_o(dammy(i),s_1(i))=d_now(i)
      den_n(dammy(i),s_1(i))=d_now(i)
      pres_o(dammy(i),s_1(i))=p_now(i)
      pres_n(dammy(i),s_1(i))=p_now(i)
      temp_o(dammy(i),s_1(i))=t_now(i)
      temp_n(dammy(i),s_1(i))=t_now(i)
      ttmm=uh1*((1.0-log(rrhh)/a1)**(-1.0/a_n))
      mois_o(dammy(i),s_1(i))=ttmm
      mois_n(dammy(i),s_1(i))=ttmm
      END DO

      RETURN
      END
```

Subroutine M_V_M_BOUND

```
      SUBROUTINE m_v_m_bound(layer)

      INCLUDE 'define.h1'
      PARAMETER (v_dif=2.5e-5,r1=461.5)
      INCLUDE 'define.h2'
      RECORD /buildings/ bld
      COMMON /wall/ bld
      COMMON /mesh/node(dl),x_step(dl),x_coord(dl,dn)
      COMMON /var1/den_n(dl,dn),temp_n(dl,dn),pres_n(dl,dn),mois_n(dl,dn)
      COMMON /var2/den_o(dl,dn),temp_o(dl,dn),pres_o(dl,dn),mois_o(dl,dn)
      COMMON /var3/rh(dl,dn)
      COMMON /var4/dp(dl,dn),dt(dl,dn)
      COMMON /rate/flow(dl,dn,4)
      COMMON /time1/t_step
      COMMON /time2/actual_time
      COMMON /theory/model
      COMMON /prop/den2(dl,dn),cap(dl,dn,4),con(dl,dn,4),latent(dl,dn)
      DIMENSION p_1(2),p_2(2),p_3(2),t_1(2),t_2(2),t_3(2)
      DIMENSION rat_c(2),rat_m(2),energy(2)
      DIMENSION d_p(2),d_t(2),t_now(2),p_now(2),d_now(2)

      INTEGER*1 dammy(2),s_1(2),s_2(2),s_3(2)
      REAL*8 mois_o,mois_n
      REAL latent

      dammy(1)=layer
      dammy(2)=layer+2
      s_1(1)=node(layer)       !surface1 is surface of material
      s_1(2)=1                 !surface2 is surface of air
      s_2(1)=s_1(1)-1
```

```
      s_2(2)=2
      s_3(1)=s_1(1)-2
      s_3(2)=3

      DO i=1,2
      d_p(i)=dp(dammy(i),s_1(i))
      d_t(i)=dt(dammy(i),s_1(i))
      t_1(i)=temp_o(dammy(i),s_1(i))
      t_2(i)=temp_o(dammy(i),s_2(i))
      t_3(i)=temp_o(dammy(i),s_3(i))
      p_1(i)=pres_o(dammy(i),s_1(i))
      p_2(i)=pres_o(dammy(i),s_2(i))
      p_3(i)=pres_o(dammy(i),s_3(i))
      t=t_1(i)-273.15
      enth1=(1.805*t+2501.21)*1000
      enth2=(4.1837*t+0.11807)*1000
      energy(i)=enth1*flow(dammy(i),s_1(i),1)
     +                +enth2*flow(dammy(i),s_1(i),2)
      rat_c(i)=bld.walls(dammy(i)).prop.cond/x_step(dammy(i))
      rat_m(i)=d_p(i)/x_step(dammy(i))
      END DO
CCCCCC
C     energy conservation first to get new temperature
CCCCCC
      term1=2.0*rat_c(2)*t_2(2)-0.5*rat_c(2)*t_3(2)-energy(2)
      term2=2.0*rat_c(1)*t_2(1)-0.5*rat_c(1)*t_3(1)+energy(1)
      term3=1.5*(rat_c(1)+rat_c(2))
      t_n=(term1+term2)/term3
      t_now(1)=t_n
      t_now(2)=t_n
```

```
      t1_g1=(3.0*t_now(1)-4.0*t_2(1)+t_3(1))/(2.0*x_step(layer))
      t2_g1=(-3.0*t_now(2)+4.0*t_2(2)-t_3(2))/(2.0*x_step(layer+2))

      dtt1=d_t(1)*t1_g1
      dtt2=d_t(2)*t2_g1
CCCCCCC
C     now mass conservation
CCCCCCC
      resis_m=bld.walls(layer+1).prop.thick          !vapour resistance stored here
      term5=0.5*rat_m(2)*(4.0*p_2(2)-p_3(2))+dtt2
      term6=0.5*rat_m(1)*(4.0*p_2(1)-p_3(1))-dtt1
      term7=1.0+1.5*rat_m(2)*resis_m
      above=resis_m*(term5+term7*term6)
      term8=1.0+1.5*rat_m(1)*resis_m
      below=term8*term7-1.0
      p_now(1)=above/below
      d_now(1)=p_now(1)/(r1*t_now(1))
      p_now(2)=(p_now(1)+term5*resis_m)/term7
      d_now(2)=p_now(2)/(r1*t_now(2))


      DO i=1,2
      uh1=bld.walls(dammy(i)).sorp.uh
      a1=bld.walls(dammy(i)).sorp.A
      a_n=bld.walls(dammy(i)).sorp.n
      p_sat=sat_pres(t_n)
      rrhh=p_now(i)/p_sat

      IF(rrhh.LT.1.0) GOTO 100
      write(80,*) actual_time,dammy(i),i
      rrhh=1.0
```

```
      p_now(i)=p_sat
      d_now(i)=p_now(i)/(r1*t_now(i))
100   rh(dammy(i),s_1(i))=rrhh
      den_o(dammy(i),s_1(i))=d_now(i)
      den_n(dammy(i),s_1(i))=d_now(i)
      pres_o(dammy(i),s_1(i))=p_now(i)
      pres_n(dammy(i),s_1(i))=p_now(i)
      temp_o(dammy(i),s_1(i))=t_now(i)
      temp_n(dammy(i),s_1(i))=t_now(i)
      ttmm=uh1*((1.0-log(rrhh)/a1)**(-1.0/a_n))
      mois_o(dammy(i),s_1(i))=ttmm
      mois_n(dammy(i),s_1(i))=ttmm
      END DO

      RETURN
      END
```

Subroutine M_V_G_BOUND

```
      SUBROUTINE m_v_g_bound(layer)

      INCLUDE 'define.h1'
      PARAMETER (v_dif=2.5e-5,r1=461.5)
      INCLUDE 'define.h2'
      RECORD /buildings/ bld
      COMMON /wall/ bld
      COMMON /mesh/node(dl),x_step(dl),x_coord(dl,dn)
      COMMON /var1/den_n(dl,dn),temp_n(dl,dn),pres_n(dl,dn),mois_n(dl,dn)
      COMMON /var2/den_o(dl,dn),temp_o(dl,dn),pres_o(dl,dn),mois_o(dl,dn)
      COMMON /var3/rh(dl,dn)
      COMMON /var4/dp(dl,dn),dt(dl,dn)
      COMMON /rate/flow(dl,dn,4)
      COMMON /time1/t_step
      COMMON /time2/actual_time
      COMMON /type/m_type(dl)
      COMMON /theory/model
      COMMON /prop/den2(dl,dn),cap(dl,dn,4),con(dl,dn,4),latent(dl,dn)
      DIMENSION p_1(2),p_2(2),p_3(2),t_1(2),t_2(2),t_3(2)
      DIMENSION rat_c(2),rat_m(2),energy(2)
      DIMENSION d_p(2),d_t(2),t_now(2),p_now(2),d_now(2)
      INTEGER*1 dammy(2),s_1(2),s_2(2),s_3(2),m_type,it
      REAL*8 mois_o,mois_n
      REAL latent
      dammy(1)=layer
      dammy(2)=layer+3
      s_1(1)=node(layer)        !surface1 is surface of material
      s_1(2)=1                  !surface2 is surface of air
      s_2(1)=s_1(1)-1
```

```
      s_2(2)=s_1(2)+1
      s_3(1)=s_1(1)-2
      s_3(2)=s_1(2)+2

      DO i=1,2
      d_p(i)=dp(dammy(i),s_1(i))
      d_t(i)=dt(dammy(i),s_1(i))
      t_1(i)=temp_o(dammy(i),s_1(i))
      t_2(i)=temp_o(dammy(i),s_2(i))
      t_3(i)=temp_o(dammy(i),s_3(i))
      p_1(i)=pres_o(dammy(i),s_1(i))
      p_2(i)=pres_o(dammy(i),s_2(i))
      p_3(i)=pres_o(dammy(i),s_3(i))
      t=t_1(i)-273.15
      enth1=(1.805*t+2501.21)*1000
      enth2=(4.1837*t+0.11807)*1000
      energy(i)=enth1*flow(dammy(i),s_1(i),1)
     +                +enth2*flow(dammy(i),s_1(i),2)
      rat_c(i)=bld.walls(dammy(i)).prop.cond/x_step(dammy(i))
      rat_m(i)=d_p(i)/x_step(dammy(i))
      END DO
CCCCCC
C     energy conservation first to get new temperature
CCCCCC
CCCCCC
C     only air gap has heat transfer resistance
CCCCCC
      it=m_type(layer+1)
      SELECT CASE(it)
            CASE(2)
              term0=bld.walls(layer+1).prop.dens      !heat resistance is stored here.
              resis_m1=bld.walls(layer+1).prop.poro           !vapour resistance stored here
              resis_m2=bld.walls(layer+2).prop.thick           !vapour resistance stored
```

```
here
            CASE(3)
              term0=bld.walls(layer+2).prop.dens
              resis_m1=bld.walls(layer+1).prop.thick          !vapour resistance stored
here
              resis_m2=bld.walls(layer+2).prop.poro           !vapour resistance stored
here
      END SELECT

      resis_m=resis_m1+resis_m2

      term1=2.0*rat_c(2)*t_2(2)-0.5*rat_c(2)*t_3(2)-energy(2)
      term2=2.0*rat_c(1)*t_2(1)-0.5*rat_c(1)*t_3(1)+energy(1)
      term3=term0+1.5*rat_c(2)
      term4=(1.5*rat_c(1)+term0)*term3-term0*term0
      t_now(1)=(term0*term1+term3*term2)/term4
      t_now(2)=(term0*t_now(1)+term1)/term3
      t1_g1=(3.0*t_now(1)-4.0*t_2(1)+t_3(1))/(2.0*x_step(layer))
      t2_g1=(-3.0*t_now(2)+4.0*t_2(2)-t_3(2))/(2.0*x_step(layer+3))

      dtt1=d_t(1)*t1_g1
      dtt2=d_t(2)*t2_g1
CCCCCCC
C     now mass conservation
CCCCCCC
      term5=0.5*rat_m(2)*(4.0*p_2(2)-p_3(2))+dtt2
      term6=0.5*rat_m(1)*(4.0*p_2(1)-p_3(1))-dtt1
      term7=1.0+1.5*rat_m(2)*resis_m
      above=resis_m*(term5+term7*term6)
      term8=1.0+1.5*rat_m(1)*resis_m
      below=term8*term7-1.0
      p_now(1)=above/below
      d_now(1)=p_now(1)/(r1*t_now(1))
```

```
      p_now(2)=(p_now(1)+term5*resis_m)/term7
      d_now(2)=p_now(2)/(r1*t_now(2))
      DO i=1,2
      uh1=bld.walls(dammy(i)).sorp.uh
      a1=bld.walls(dammy(i)).sorp.A
      a_n=bld.walls(dammy(i)).sorp.n
      p_sat=sat_pres(t_now(i))
      rrhh=p_now(i)/p_sat

      IF(rrhh.LT.1.0) GOTO 100
      write(80,*) actual_time,dammy(i),i
      rrhh=1.0
      p_now(i)=p_sat
      d_now(i)=p_now(i)/(r1*t_now(i))
100   rh(dammy(i),s_1(i))=rrhh
      den_o(dammy(i),s_1(i))=d_now(i)
      den_n(dammy(i),s_1(i))=d_now(i)
      pres_o(dammy(i),s_1(i))=p_now(i)
      pres_n(dammy(i),s_1(i))=p_now(i)
      temp_o(dammy(i),s_1(i))=t_now(i)
      temp_n(dammy(i),s_1(i))=t_now(i)
      ttmm=uh1*((1.0-log(rrhh)/a1)**(-1.0/a_n))
      mois_o(dammy(i),s_1(i))=ttmm
      mois_n(dammy(i),s_1(i))=ttmm
      END DO

      RETURN
      END
```

Subroutine FILE_READ

```
      SUBROUTINE file_read(filename,error)

      INCLUDE 'define.h1'
      PARAMETER (r1=461.5)
      INCLUDE 'define.h2'
      RECORD /buildings/ bld
      RECORD /boundary/ ext
      STRUCTURE /dummy/
            integer layer
            real    var(11,dl)
      END STRUCTURE
      RECORD /dummy/ reading

      EQUIVALENCE (bld,reading)

      COMMON /wall/ bld
      COMMON /bound/ ext
      COMMON /type/ m_type(dl)
      COMMON /var1/den_n(dl,dn),temp_n(dl,dn),pres_n(dl,dn),mois_n(dl,dn)
      COMMON /var2/den_o(dl,dn),temp_o(dl,dn),pres_o(dl,dn),mois_o(dl,dn)
      COMMON /var3/rh(dl,dn)
      INTEGER*1 check,position,error,m_type
      REAL*8 mois_n,mois_o
      CHARACTER*30 filename,file1,sub_file
      CHARACTER*80 line,file2
```

```
      m_type=0          !first assume all materials are hygroscopic
                        !nonhygroscopic materials will be assigned later
                        !from the value of moisture coefficient.

      OPEN(1,FILE=filename,STATUS='old',MODE='READ',ERR=1500)
10    READ(1,'(A)',END=1000) line
      DO i=1,80
      check=ICHAR(line(i:i))
      IF(check.GT.57.OR.check.LT.48) CYCLE
      file1=line(i:)
      READ(file1,20) reading.layer
20    FORMAT(i2)
      position=SCAN(file1,'Aa')
      IF(position.le.0) GOTO 30
      sub_file=file1(position+1:)
      READ(sub_file,20) position
      m_type(position)=2
30    position=SCAN(file1,'Bb')
      IF(position.le.0) GOTO 40
      sub_file=file1(position+1:)
      READ(sub_file,20) position
      m_type(position)=3
      GOTO 40
      END DO
      GOTO 10
40    DO 100 i=1,reading.layer
      DO 70 k=1,11
      IF(k.GT.1.AND.m_type(i).EQ.3) EXIT
      IF(k.GT.3.AND.m_type(i).EQ.2) EXIT
50    READ(1,'(A)',end=1000) line
```

```
      DO j=1,80
      check=ICHAR(line(j:j))
      IF(check.GT.57.OR.check.LT.48) CYCLE
      file1=line(j:)
      READ(file1,60) reading.var(k,i)
60    FORMAT(g20.3)
      GOTO 70
      END DO
      GOTO 50

70    CONTINUE

100   CONTINUE


C     read initial conditions
120   READ(1,'(A)',END=1000) line
      DO j=1,80
      check=ICHAR(line(j:j))
      IF(check.GT.57.OR.check.LT.48) CYCLE
      file1=line(j:)
      READ(file1,260) temperature
      GOTO 140
      END DO
      GOTO 120

140   READ(1,'(A)',END=1000) line
      DO j=1,80
      check=ICHAR(line(j:j))
      IF(check.GT.57.OR.check.LT.48) CYCLE
      file1=line(j:)
      READ(file1,260) r_humidity
      GOTO 160
      END DO
      GOTO 140
```

```
160   r_humidity=r_humidity/100.0
      temperature=temperature+273.15
      p_sat=sat_pres(temperature)
      v_pres=r_humidity*p_sat
      pres_n=v_pres
      den_n=v_pres/(r1*temperature)
      den_o=den_n
      pres_o=pres_n
      temp_n=temperature
      temp_o=temp_n
      rh=r_humidity

C     now read boundary conditions
      DO 500 i=1,2

C     first read wall no. that faces environment
200   READ(1,'(A)',END=1000) line
      DO j=1,80
      check=ICHAR(line(j:j))
      IF(check.GT.57.OR.check.LT.48) CYCLE
      file1=line(j:)
      READ(file1,210) ext.layers(i)
210   FORMAT(i2)
      GOTO 230
      END DO
      GOTO 200

C     secondly read in flow type
230   READ(1,'(A)',END=1000) line
      position=SCAN(line,'FfNn',.TRUE.)
      file1=line(position:)
      READ(file1,240) ext.f_type(i)
240   FORMAT(A1)
```

```
C     thirdly read in wind speed
250   READ(1,'(A)',END=1000) line
      DO j=1,80
      check=ICHAR(line(j:j))
      IF(check.GT.57.OR.check.LT.48) CYCLE
      file1=line(j:)
      READ(file1,260) ext.wind(i)
260   FORMAT(f10.3)
      GOTO 270
      END DO
      GOTO 250
C     last read in wall type, i.e. external or internal
270   READ(1,'(A)',END=1000) line
      position=SCAN(line,'EeIi',.TRUE.)
      file1=line(position:)
      READ(file1,240) ext.w_type(i)
C     THEN READ IN TEMPERATURE
290   READ(1,'(A)',end=1000) line
      DO j=1,80
      check=ICHAR(line(j:j))
      IF(check.GT.57.OR.check.LT.48) CYCLE
      file2=line(j:)
      READ(file2,300) (ext.tempe(i,k),k=1,12)
      DO k=1,12
      ext.tempe(i,k)=ext.tempe(i,k)+273.15
      END DO
300   FORMAT(12f5.1)
      GOTO 320
      END DO
      GOTO 290
```

```
C     AND READ IN RH
320   READ(1,'(A)',END=1000) line
      DO j=1,80
      check=ICHAR(line(j:j))
      IF(check.GT.57.OR.check.LT.48) CYCLE
      file2=line(j:)
      READ(file2,300) (ext.r_h(i,k),k=1,12)
      GOTO 350
      END DO
      GOTO 320
C     LAST READ IN SOL-AIR OR ENVIRONMENTAL TEMPERATURE
350   READ(1,'(A)',END=1000) line
      DO j=1,80
      check=ICHAR(line(j:j))
      IF(check.GT.57.OR.check.LT.48) CYCLE
      file2=line(j:)
      READ(file2,300) (ext.a_e_temp(i,k),k=1,12)
      DO k=1,12
      ext.a_e_temp(i,k)=ext.a_e_temp(i,k)+273.15
      END DO
      GOTO 500
      END DO
      GOTO 350
500   CONTINUE

      GOTO 2000
1000  error=1
      GOTO 2000
1500  error=2
2000  CLOSE(1)
      RETURN
      END
```

```
      SUBROUTINE property
      PARAMETER (pt=1e5)              !total pressure
      INCLUDE 'define.h1'
      INCLUDE 'define.h2'
      RECORD /buildings/ bld
      COMMON /wall/ bld
      COMMON /prop/den2(dl,dn),cap(dl,dn,4),con(dl,dn,4),latent(dl,dn)
      COMMON /mesh/node(dl),x_step(dl),x_coord(dl,dn)
      COMMON /var1/den_n(dl,dn),temp_n(dl,dn),pres_n(dl,dn),
     +            mois_n(dl,dn)
      COMMON /type/m_type(dl)
      COMMON /time1/t_step
      REAL*8 mois_n,mass2_1,mass2_2,mass2
      REAL latent
      INTEGER*1 m_type


      DO i=1,bld.n_layer
      IF(m_type(i).EQ.3) CYCLE
      den=bld.walls(i).prop.dens
      por=bld.walls(i).prop.poro
      DO j=1,node(i)
      tem=temp_n(i,j)-273.15
      tem2=tem*tem
      tem3=tem*tem2
      den2(i,j)=999.81+(5.232e-2)*tem-(7.267e-3)*tem2+(2.936e-5)*tem3
      cap(i,j,1)=1.87*1000
      sub=4.2114-(2.265e-3)*tem+(4.848e-5)*tem2-(3.012e-7)*tem3
      cap(i,j,2)=sub*1000
      cap(i,j,3)=(1.0037+(5.0e-5)*tem)*1000
      con(i,j,1)=(16.302+(7.994e-2)*tem-(3.717e-5)*tem2
     +                  +(1.19e-6)*tem3)*1e-3
```

```
con(i,j,2)=(569.04+1.82*tem-(4.996e-3)*tem2-(3.449e-5)*tem3)*1e-3
con(i,j,3)=(2.4144+(7.76e-3)*tem)*1e-2
latent(i,j)=(-2.3795*tem+2501.062)*1000

tem=temp_n(i,j)
u=mois_n(i,j)
mass2_1=u*den-pres_n(i,j)*den*por/(461.5*tem)
mass2_2=1.0-pres_n(i,j)/(461.5*tem*den2(i,j))
mass2=mass2_1/mass2_2
u2=mass2/den
u1=u-u2
IF(m_type(i).LE.1) THEN
   cap(i,j,4)=bld.walls(i).prop.capa+cap(i,j,1)*u1+cap(i,j,2)*u2
   con(i,j,4)=bld.walls(i).prop.cond+con(i,j,1)*u1+con(i,j,2)*u2
ELSE
      pm=pres_n(i,j)
      cap(i,j,4)=(cap(i,j,1)*pm+cap(i,j,3)*(pt-pm))/pt
END IF

END DO
END DO

RETURN
END
```

Subroutine MAN_MESH

```
      SUBROUTINE  man_mesh
      INCLUDE 'define.h1'
      INCLUDE 'define.h2'
      RECORD /buildings/ bld
      COMMON /wall/ bld
      COMMON /type/ m_type(dl)
      COMMON /mesh/node(dl),x_step(dl),x_coord(dl,dn)
      INTEGER*1 m_type

      WRITE(*,10) bld.n_layer
10    FORMAT(1x,'There are ', I2,' layers of walls')
      DO i=1,bld.n_layer
      SELECT CASE(m_type(i))
            CASE(0,1)
                  WRITE(*,50) i
50                FORMAT(1x,'Enter No. of Cell in Layer no.',I2,' '\)
                  READ(*,*) dum
                  node(i)=dum+1
                  x_step(i)=bld.walls(i).prop.thick/dum

                  start=0.0
                  IF(i.EQ.1) GOTO 200
                  DO k=1,i-1
                  IF(m_type(k).EQ.3) CYCLE
                  start=start+bld.walls(k).prop.thick
                  END DO

200               DO j=1,node(i)
                  x_coord(i,j)=start+x_step(i)*(j-1)
                  END DO
```

```
            CASE(2)
                  WRITE(*,250) i
250               FORMAT(1x,'Layer no.',I2,' is Air Gap')
            CASE(3)
                  WRITE(*,300) i
300               FORMAT(1x,'Layer no.',I2,' is Vapour Barrier')
      END SELECT

      END DO

      RETURN
      END
```

Subroutine AUTO_MESH

```
      SUBROUTINE  auto_mesh
      INCLUDE 'define.h1'
      PARAMETER (D_vapour=2.25e-5)          !vapour diffision coeffficient in air
      INCLUDE 'define.h2'
      RECORD /buildings/ bld
      COMMON /wall/ bld
      COMMON /mesh/node(dl),x_step(dl),x_coord(dl,dn)
      COMMON /var1/den_n(dl,dn),temp_n(dl,dn),pres_n(dl,dn),
     +             mois_n(dl,dn)
      COMMON /type/m_type(dl)
      COMMON /time1/t_step
      DIMENSION perm(dl),condu(dl),thi(dl),res(dl)
      INTEGER*1 m_type
      REAL*8 mois_n
      WRITE(*,'(A)') ' Generating mesh automatically.'
10    WRITE(*,'(A\)') ' Enter total number of mesh ==> '
      READ(*,*,ERR=20) n_total
      GOTO 50
20    WRITE(*,'(A)') 'Input NOT recognised. Re-enter Please.'
      GOTO 10
50    resistance=0.0
      DO i=1,bld.n_layer

      IF(m_type(i).GT.1) CYCLE            !vapour barrier is thin
      vc=bld.walls(i).coef.v_c
      wc=bld.walls(i).coef.w_c
      expo=bld.walls(i).coef.r_exp
      perm(i)=vc+wc*(0.5**expo)
      condu(i)=bld.walls(i).prop.cond
```

```
      thi(i)=bld.walls(i).prop.thick
      res(i)=thi(i)*thi(i)/(perm(i)*condu(i))
      resistance=resistance+res(i)

      END DO

      cell_res=resistance/n_total

      DO i=1,bld.n_layer
      IF(m_type(i).GT.1) CYCLE              !vapour barrier is thin
      node(i)=int(res(i)/cell_res)+1         !number of mesh point = cell + 1
      if(node(i).gt.50) node(i)=50
      if(node(i).lt.5) node(i)=5
      x_step(i)=bld.walls(i).prop.thick/(node(i)-1)

      start=0.0
      IF(i.EQ.1) GOTO 200
      DO k=1,i-1
      IF(m_type(k).EQ.3) CYCLE
      start=start+bld.walls(k).prop.thick
      END DO

200   DO j=1,node(i)
      x_coord(i,j)=start+x_step(i)*(j-1)
      END DO

      END DO
      RETURN
      END
```

Subroutine FLOW_RATE

```
      SUBROUTINE flow_rate
      INCLUDE 'define.h1'
      PARAMETER (r1=461.5)
      INCLUDE 'define.h2'
      RECORD /buildings/ bld
      COMMON /wall/ bld
      COMMON /var2/den_o(dl,dn),temp_o(dl,dn),pres_o(dl,dn),
     +            mois_o(dl,dn)
      COMMON /var4/dp(dl,dn),dt(dl,dn)
      COMMON /prop/den2(dl,dn),cap(dl,dn,4),con(dl,dn,4),latent(dl,dn)
      COMMON /mesh/node(dl),x_step(dl),x_coord(dl,dn)
      COMMON /time1/t_step
      COMMON /type/m_type(dl)
      COMMON /theory/model
      COMMON /var3/rh(dl,dn)
      COMMON /rate/flow(dl,dn,4)
                              ! 1 --> vapour
                              ! 2 --> water
                              ! 3 --> air
                              ! 4 --> moist air
      INTEGER*1 model,m_type
      REAL*8 mois_o
      REAL latent
```

```
      pressure=1e5

      DO i=1, bld.n_layer
      IF(m_type(i).GT.1) CYCLE
      density=bld.walls(i).prop.dens
      porosity=bld.walls(i).prop.poro
      d1=bld.walls(i).coef.v_c
      d2=bld.walls(i).coef.w_c
      expo=bld.walls(i).coef.r_exp

      num=node(i)
      st=x_step(i)

      DO j=1,num
      r_h=rh(i,j)
      IF(model.EQ.2) GOTO 100
      area=1.0-(density*mois_o(i,j))/(den2(i,j)*porosity)
      GOTO 200
  100 area=1.0
  200 d1t=d1*area
      d2t=d2*(r_h**expo)


      t_m=temp_o(i,j)
      t_l=temp_o(i,j-1)
      t_r=temp_o(i,j+1)
      p_m=pres_o(i,j)
      p_l=pres_o(i,j-1)
      p_r=pres_o(i,j+1)

      t_g1=(t_r-t_l)/(2.0*st)
      p_g1=(p_r-p_l)/(2.0*st)
```

```
IF(j.EQ.1) THEN
      t_g1=(-3.0*t_m+4.0*t_r-temp_o(i,3))/(2.0*st)
      p_g1=(-3.0*p_m+4.0*p_r-pres_o(i,3))/(2.0*st)
END IF
IF(j.EQ.num) THEN
      t_g1=(3.0*t_m-4.0*t_1+temp_o(i,j-2))/(2.0*st)
      p_g1=(3.0*p_m-4.0*p_1+pres_o(i,j-2))/(2.0*st)
END IF

p_t=p_m/t_m
term1=log(r_h)-latent(i,j)/(r1*t_m)
flow(i,j,1)=-d1t*(p_g1-p_t*t_g1)
flow(i,j,2)=-d2t*(p_g1+p_t*term1*t_g1)
flow(i,j,4)=flow(i,j,1)+flow(i,j,2)
flow(i,j,3)=-28.96*flow(i,j,1)/18.015

dp(i,j)=d1t+d2t
dt(i,j)=p_t*(d2t*term1-d1t)
END DO
END DO

RETURN
END
```

Subroutine PRES_TO_MOI

```
      SUBROUTINE pres_to_moi
      INCLUDE 'define.h1'
      INCLUDE 'define.h2'
      RECORD /buildings/ bld
      COMMON /wall/ bld
      COMMON /mesh/node(dl),x_step(dl),x_coord(dl,dn)
      COMMON /var2/den_o(dl,dn),temp_o(dl,dn),pres_o(dl,dn),
     +             mois_o(dl,dn)
      COMMON /var3/rh(dl,dn)
      COMMON /time1/t_step
      COMMON /type/m_type(dl)
      INTEGER*1 m_type
      REAL*8 mois_o

      DO i=1,bld.n_layer
      IF(m_type(i).GT.1) CYCLE            !exclude air gap and vapour barrier
      uh1=bld.walls(i).sorp.uh
      a1=bld.walls(i).sorp.A
      a_n=bld.walls(i).sorp.n

      DO j=1,node(i)
      p_sat=sat_pres(temp_o(i,j))
      p=pres_o(i,j)
      rh(i,j)=p/p_sat
100   mois_o(i,j)=uh1*((1.0-log(rh(i,j))/a1)**(-1.0/a_n))
      END DO

      END DO
```

```
RETURN
END
```

Subroutine MOI_TO_PRES

```
      SUBROUTINE moi_to_pres
      INCLUDE 'define.h1'
      INCLUDE 'define.h2'
      RECORD /buildings/ bld
      COMMON /wall/ bld
      COMMON /mesh/node(dl),x_step(dl),x_coord(dl,dn)
      COMMON /var2/den_o(dl,dn),temp_o(dl,dn),pres_o(dl,dn),
     +             mois_o(dl,dn)
      COMMON /var3/rh(dl,dn)
      COMMON /time1/t_step
      COMMON /type/m_type(dl)
      INTEGER*1 m_type
      REAL*8 mois_o

      DO i=1,bld.n_layer
      IF(m_type(i).GT.1) CYCLE      !exclude air gap and vapour barrier
      uh1=bld.walls(i).sorp.uh
      a1=bld.walls(i).sorp.A
      a_n=bld.walls(i).sorp.n

      DO j=1,node(i)
      p_sat=sat_pres(temp_o(i,j))
      term1=mois_o(i,j)/uh1
      term2=(1.0-term1**(-a_n))
      term3=a1*term2
      p1=p_sat*exp(term3)
```

```
pres_o(i,j)=p1
rh(i,j)=p1/p_sat
END DO

END DO

RETURN
END
```

Subroutine ERROR_HANDLE

```
SUBROUTINE error_handle(error)
INTEGER*1 error
SELECT CASE (error)
    CASE (1)
        WRITE(*,'(A)') 'End of File Error'
    CASE (2)
        WRITE(*,'(A)') 'Error in Opening File'
END SELECT

RETURN
END
```

Subroutine OUT_PUT

```
      SUBROUTINE out_put(k)
      INCLUDE 'define.h1'
      INCLUDE 'define.h2'
      RECORD /buildings/ bld
      COMMON /wall/ bld
      COMMON /mesh/node(dl),x_step(dl),x_coord(dl,dn)
      COMMON /var2/den_o(dl,dn),temp_o(dl,dn),pres_o(dl,dn),mois_o(dl,dn)
      COMMON /type/m_type(dl)
      COMMON /time2/ actual_time
      COMMON /rate/flow(dl,dn,4)
      DIMENSION tem(3),pres(3),moi(3),den(3)
      CHARACTER*3 base1(4),base2(4)*4
      CHARACTER*30 file(dl,4)
      INTEGER*1 k,m_type,channel,fl_ch
      REAL*8 mois_o,moi,c_m
      layer=bld.n_layer
      IF(k.NE.1.AND.k.NE.4) GOTO 100
            mt=0
            channel=29
            base1(1)='tem'
            base1(2)='pre'
            base1(3)='moi'
            base1(4)='den'
            DO i=1,layer
            IF(m_type(i).GT.1) CYCLE
            mt=mt+1
            DO j=1,4
            channel=channel+1
            base2(j)=base1(j)//CHAR(mt+48)
            file(mt,j)=base2(j)//'.prn'
            OPEN(channel,file=file(mt,j),status='unknown')
```

```
C     enter information on top of each file
CCCCC
            WRITE(channel,10) layer
10          FORMAT(1X,'Total No. of Layers ==> ',I2)
            WRITE(channel,20) i,node(i)
20          FORMAT(1X,'Layer No.',I2,' has ',I2,' mesh points')
            END DO
            END DO
            fl_ch=channel+1
            OPEN(fl_ch,file='flow.prn',status='unknown')
            OPEN(80,FILE='cond.prn',status='Unknown')
            write(80,'(a)') 'Condensation Information'
            write(80,1)
1           format(1x,'time',12x,'layer No.',3x,'surface')


100         if(k.eq.100) goto 300
            j1=2
            mt=0
            DO i=1,layer
            IF(m_type(i).GT.1) CYCLE
            mt=mt+1
            channel=30+(mt-1)*4
            j2=INT(node(i)/2.0+0.5)
            j3=node(i)-1
            tem(1)=temp_o(i,j1)-273.16
            tem(2)=temp_o(i,j2)-273.16
            tem(3)=temp_o(i,j3)-273.16
            pres(1)=pres_o(i,j1)
            pres(2)=pres_o(i,j2)
            pres(3)=pres_o(i,j3)
            moi(1)=mois_o(i,j1)
            moi(2)=mois_o(i,j2)
            moi(3)=mois_o(i,j3)
```

```
          den(1)=den_o(i,j1)
          den(2)=den_o(i,j2)
          den(3)=den_o(i,j3)
          WRITE(channel,250) actual_time,(tem(kt),kt=1,3)
          WRITE(channel+1,250) actual_time,(pres(kt),kt=1,3)
          WRITE(channel+2,255) actual_time,(moi(kt),kt=1,3)
          WRITE(channel+3,250) actual_time,(den(kt),kt=1,3)
250       FORMAT(1x,f13.5,3(5x,f13.5))
255       FORMAT(1X,F10.5,3(2X,F17.15))
          END DO
          fl1=flow(1,1,4)
          fl2=flow(layer,node(layer),4)
          WRITE(fl_ch,260) actual_time,fl1,fl2
260       FORMAT(1x,f13.5,2(5x,e13.5))
          IF(k.EQ.2.OR.k.EQ.4) THEN
          i_ch=fl_ch+1
          OPEN(i_ch,file='final.prn',status='unknown')
          WRITE(i_ch,*) 'Time is ',actual_time
270       format(1x,f8.4,f17.15,f8.2,f8.2,f13.5,e13.5)
          x=0.0
          do i=1,layer
          do j=1,node(i)
          x=x_coord(i,j)
          c_m=mois_o(i,j)
          p_v=pres_o(i,j)
          t_p=temp_o(i,j)-273.15
          d_v=den_o(i,j)
          f_l=flow(i,j,4)
          write(i_ch,270) x,c_m,p_v,t_p,d_v,f_l
          end do
          end do
          END IF
          IF(k.NE.100) RETURN
300       channel=29
```

```
      DO i=1,layer
      IF(m_type(i).GT.1) CYCLE
      DO j=1,4
      channel=channel+1
      CLOSE(channel)
      END DO
      END DO
      CLOSE(fl_ch)
      CLOSE(I_CH)
      CLOSE(80)
RETURN
END
```

```
Function SAT_PRES


CCCCCCCCCCCCCCCCCCCCCCCCCCCCCCCCCCCCCCCCCCCCCCCCCCCCCCCCCCCCCCCCCCCCCCC
C     This function calculates vapour saturation pressure          C
CCCCCCCCCCCCCCCCCCCCCCCCCCCCCCCCCCCCCCCCCCCCCCCCCCCCCCCCCCCCCCCCCCCCCCC
      REAL FUNCTION sat_pres(temperature)
      tem=temperature-273.16
      tem2=tem*tem
      tem3=tem*tem2
      sat_pres=540.225+78.992*tem-1.224*tem2+0.08782*tem3
      END


Function P_SAT_G


CCCCCCCCCCCCCCCCCCCCCCCCCCCCCCCCCCCCCCCCCCCCCCCCCCCCCCCCCCCCCCCCCCCCCCC
C     This function calculates vapour pressure gradient coefficient   C
CCCCCCCCCCCCCCCCCCCCCCCCCCCCCCCCCCCCCCCCCCCCCCCCCCCCCCCCCCCCCCCCCCCCCCC
      REAL FUNCTION p_sat_g(temperature)
      tem=temperature-273.16
      tem2=tem*tem
      p_sat_g=78.992-2.0*1.224*tem+3.0*0.08782*tem2
      END
```

```
      DEFINE.H1

      PARAMETER (dl=10,dn=50)


      DEFINE.H2

CCCCCCCCCCCCCCCCCCCCCCCCCCCCCCCCCCCCCCCCCCCCCCCCCCCCCCCCCCCCCCCCCCCCCCCCCC
C       This file defines some of the mostly used variables          C
C       used in the programmes.                                      C
CCCCCCCCCCCCCCCCCCCCCCCCCCCCCCCCCCCCCCCCCCCCCCCCCCCCCCCCCCCCCCCCCCCCCCCCCC

      STRUCTURE /properties/
      real thick         !wall layer thickness (for vapour barier
          !             thi is the vapour resistance)
      real dens          !density
      real poro          !material porosity
      real capa          !dry thermal capacity
      real cond          !dry thermal conductivity
      END STRUCTURE

      STRUCTURE /transfer_coefficient/
      real v_c          !vapour transfer coefficient
      real w_c          !water transfer coefficient
      real r_exp        !exponent for RH of water transfer terms
      END STRUCTURE

      STRUCTURE /sorption_isotherm/
      real uh
      real a
      real n
      END STRUCTURE

      STRUCTURE /material_properties/
      record /properties/ prop
```

```
record /transfer_coefficient/ coef
record /sorption_isotherm/ sorp
END STRUCTURE

STRUCTURE /buildings/
integer n_layer   !number of layers
record /material_properties/ walls(d1)
END STRUCTURE


STRUCTURE /boundary/
integer*1 layers(2)     !layer no.
character*1 w_type(2)  !wall type --> 'E': external wall
     !              'I': internal wall
character*1 f_type(2)  !flow type --> 'F': forced convection
     !              'N': natural convection
     !dimension 2 because there are two surfaces
real wind(2)           !wind speed for forced convection
real tempe(2,12)        !12 months ambient temperature
real r_h(2,12)          !12 months ambient rh
real a_e_temp(2,12)    !12 months ambient sol-air or
     !   enrironmental temperature
END STRUCTURE
```

EXAMPLE OF DATA BASE FOR TIMBER FRAMED WALL

==========
DATA BASE FOR PROGRAMME
==========

NO. OF MATERIAL LAYERS: 6, B2, A5

FIRST LAYER (Plaster Board):
LAYER THICKNESS: 0.015
MATERIAL DRY DENSITY: 846.0
MATERIAL POROSITY: 0.715
MATERIAL THERMAL CAPACITY: 840.0
MATERIAL CONDUCTIVITY: 0.16
VAPOUR TRANSFER COEFFICIENT: 24.0E-12
WATER TRANSFER COEFFICIENT: 20.6E-12
EXPONENT OF RELATIVE HUMIDITY: 5.66
SORPTION ISOTHERM CONSTANT uh: 0.19
SORPTION ISOTHERM CONSTANT A: 0.00075
SORPTION ISOTHERM CONSTANT n: 4.0
END OF FIRST LAYER.

SECOND LAYER (VAPOUR BARRIER)
VAPOUR RESISTANCE: 5.0E+011
END OF SECOND LAYER

THIRD LAYER (Insulation: Extruded Polystyrene):
LAYER THICKNESS: 0.05
MATERIAL DRY DENSITY: 36.0
MATERIAL POROSITY: 0.694
MATERIAL THERMAL CAPACITY: 1470.0
MATERIAL CONDUCTIVITY: 0.024
VAPOUR TRANSFER COEFFICIENT: 2.28E-12
WATER TRANSFER COEFFICIENT: 0.0
EXPONENT OF RELATIVE HUMIDITY: 1.0
SORPTION ISOTHERM CONSTANT uh: 0.0184
SORPTION ISOTHERM CONSTANT A: 0.00263
SORPTION ISOTHERM CONSTANT n: 10.65
END OF THIRD LAYER.

FOURTH LAYER (Plywood):
LAYER THICKNESS: 0.015
MATERIAL DRY DENSITY: 561.0
MATERIAL POROSITY: 0.79
MATERIAL THERMAL CAPACITY: 1214.0
MATERIAL CONDUCTIVITY: 0.115
VAPOUR TRANSFER COEFFICIENT: 1.15E-12
WATER TRANSFER COEFFICIENT: 17.8E-12
EXPONENT OF RELATIVE HUMIDITY: 8.96
SORPTION ISOTHERM CONSTANT uh: 0.3984
SORPTION ISOTHERM CONSTANT A: 0.309
SORPTION ISOTHERM CONSTANT n: 1.66
END OF FOURTH LAYER.

AIR GAP:
LAYER THICKNESS: 0.025
TOTAL HEAT TRANSFER COEFFICIENT: 5.6
VAPOUR RESISTANCE: 2.5E+8
END OF AIR GAP.

SIXTH LAYER (Brick):
LAYER THICKNESS: 0.103
MATERIAL DRY DENSITY: 1500.0
MATERIAL POROSITY: 0.237
MATERIAL THERMAL CAPACITY: 840.0
MATERIAL CONDUCTIVITY: 0.72
VAPOUR TRANSFER COEFFICIENT: 0.77E-12
WATER TRANSFER COEFFICIENT: 6.78E-12
EXPONENT OF RELATIVE HUMIDITY: 11.80
SORPTION ISOTHERM CONSTANT uh: 0.00773
SORPTION ISOTHERM CONSTANT A: 0.107
SORPTION ISOTHERM CONSTANT n: 1.91
END OF SIXTH LAYER.

INITIAL CONDITIONS:
INITIAL TEMPERATURE: 15.0
INITIAL RELATIVE HUMIDITY: 65.0
END OF INITIAL CONDITION.

BOUNDARY CONDITIONS:
FIRST BOUNDARY SURFACE AT LAYER: 1
FORCE CONVECTION OR NATURAL CONVECTION: F
WIND SPEED: 0.5
TYPE OF WALL SURFACE (EXTERNAL OR INTERNAL): E
AMBIENT TEMP: 15.0 15.0 15.0 15.0 15.0 15.0 15.0 15.0 15.0 15.0 15.0 15.0
AMBIENT RH: 65.0 65.0 65.0 65.0 65.0 65.0 65.0 65.0 65.0 65.0 65.0 65.0
SOL-AIR TEMP: 15.0 15.0 15.0 15.0 15.0 15.0 15.0 15.0 15.0 15.0 15.0 15.0

SECOND BOUNDARY SURFACE AT LAYER: 6
FORCE CONVECTION OR NATURAL CONVECTION: N
WIND SPEED: 0.0
TYPE OF WALL SURFACE (EXTERNAL OR INTERNAL): I
AMBIENT TEMP: 5.0 5.0 5.0 5.0 5.0 5.0 5.0 5.0 5.0 5.0 5.0 5.0
AMBIENT RH: 95.0 95.0 95.0 95.0 95.0 95.0 95.0 95.0 95.0 95.0 95.0 95.0
ENVIRON TEMP: 5.0 5.0 5.0 5.0 5.0 5.0 5.0 5.0 5.0 5.0 5.0 5.0